GIS Applications in the Studies of the Palaeozoic Graptolite Argillite and Landscape Change

SIGRID HADE

TALLINN UNIVERSITY OF TECHNOLOGY
Institute of Geology

This dissertation was accepted for the defence of the degree of Doctor of Philosophy in Earth Sciences on 25.06.2014.

Supervisor:

Prof. Alvar Soesoo, Institute of Geology at Tallinn University of Technology

Opponents:

Prof. Elena Panova, Faculty of Geology, Saint-Petersburg State University, Russia

Dr. Valter Petersell, Geological Survey of Estonia, Estonia

Defence of the thesis: August 8, 2014 at Tallinn University of Technology, Ehitajate tee 5, Tallinn, 19086, Estonia

Declaration: *Hereby I declare that this doctoral thesis, my original investigation and achievement, submitted for the doctoral degree at Tallinn University of Technology has not been submitted for doctoral or equivalent academic degree.*

Sigrid Hade

European Union
European Social Fund

Investing in your future

GIS meetodite rakendused Paleosoikumi graptoliit-argilliidi ja keskkonnaseisundi muutlikkuse uuringutes

SIGRID HADE

CONTENTS

LIST OF ORIGINAL PUBLICATIONS

This thesis is based on the following papers, referred to in the text with Roman numerals as listed below.

I HINTS, R., HADE, S., SOESOO, A., VOOLMA, M. 2014. Depositional framework of the East Baltic Tremadocian black shale revisited. *GFF*, 1–19.

II VOOLMA, M., SOESOO, A., HADE, S., HINTS, R., KALLASTE, T. 2013. Geochemical heterogeneity of Estonian graptolite argillite. *Oil Shale*, **30(3)**, 377–401.

III HADE, S., SOESOO, A. 2014a. Estonian graptolite argillites revisited: a future resource? *Oil Shale*, **31(1)**, 4–18.

IV SOESOO, A., HADE, S. 2012. Metalliferrous organic-rich shales of Baltoscandia – a future resource or environmental/ecological problem? *Archiv Euro Eco*, **2(1)**, 11–14.

V SOESOO, A., HADE, S. 2014. Black shale of Estonia: moving towards a Fennoscandian-Baltoscandian database. *Transactions of Karelian Research Centre, Russian Academy of Science*, **1**, 103–114.

VI HADE, S., SOESOO, A. 2014b. Public perception in monitoring environmental conditions using GIS methods. *International Journal of Research in Earth and Environmental Sciences*, **1(3)**, 11–16.

The co-authorship of the papers reflects that they are part of collaborative basic and applied research projects. The author was responsible for data collection, analysis and modelling, data interpretation and writing of the papers Nos. III & VI, and participated in data collection, interpretation, modelling (papers Nos. I, II, IV & V), and manuscript preparation in papers Nos. I, II, IV and V.

1. INTRODUCTION

The main aim of this thesis is to understand the spatial variation of metals in graptolite argillite (GA), the nature and position of this type of black shale in the Early Palaeozoic section in Estonia; and present a possible GIS-based application for assessment of environmental conditions. Thus, this PhD thesis includes two different applications of GIS methods: (1) the studies of the geology of the Estonian Palaeozoic graptolite argillite and its metal resources, and (2) assessment of public perception of landscape and environmental changes.

1.1. Black shale and the Estonian Palaeozoic graptolite argillite and its metal distributions

1.1.1. Shales and black shales

Shale is usually a fine-grained sedimentary rock containing organic matter and silt- and clay-size mineral grains that have accumulated together. Shale is characterized by fissility – it breaks along thin laminae, parallel layering or bedding texture that is less than one centimeter in thickness. Black shale commonly forms in anoxic or low oxygen conditions and it contains unoxidized carbon and iron sulfides such as pyrite. Minor amounts of authigenic carbonate minerals, either dispersed in cements or in concretions, are characteristic features of many black shale units. Most black shale is marine in nature and may have areal extents of thousands of square kilometers. It typically requires conditions that are conducive to the accumulation of large quantities of organic matter, as well as slow accumulation rates to prevent the dilution of the accumulating metals. Metals may be derived from seawater, either directly or via pre-concentration in planktonic organisms. Unusual circulation patterns and volcanic ash deposition may enhance metal enrichments. There is currently no consensus on the source of metals and genesis of black shale. It is plausible that several sources and mechanism may be responsible for different black shale formations. Black shale is common in many Palaeozoic and Mesozoic strata worldwide including Fennoscandia and Baltoscandia. Black shale commonly contains abundant heavy and other metals. Its units may have beds enriched in metals by factors much greater than 50 for Ag, for example, and greater than 10 for Mo (Krauskopf, 1955). Such increased concentrations of Ag, Mo, Zn, Ni, Cu, Cr, V, and less commonly Co, Se, and U are conspicuous features of only some black shales (Vine and Tourtelot, 1970). There are black shales that are quite enriched in uranium, for example, the Estonian graptolite argillites and Swedish alum shale are the main future resource of uranium for Europe.

1.1.2. Lower Paleozoic black shales

These occurrences of Middle Cambrian to Late Ordovician organic-rich black shale deposits in an extensive area of Sweden (alum shale; Andersson et al., 1985), the Oslo region (Henningsmoen, 1960), Bornholm (Poulsen, 1966), Estonia (known as graptolite argillite (Hints et al., 2014; Voolma et al., 2013; Hade & Soesoo, 2014a - PAPER I, II, III) or "Dictyonema shale" (Männil, 1966), and kukersite as proper oil shale), Poland (Szymariski, 1973) and northwest Russia (Baturin & Ilyin, 2013) have been known for a long time. The alum shale, as well as graptolite argillite, contains remarkably high concentrations of trace metals such as U, Mo, V and Ni, but may also be locally enriched with REE, Cd, Au, Sb, As, Pt (Voolma et al., 2013 – PAPER II; Hade & Soesoo, 2014a - PAPER III). The beds have historically been exploited for local uranium production in Sweden and Estonia. Kerogen in the black shale is of algal origin and the content of total organic carbon is mostly between 10-25 wt% (Andersson et al., 1985). The mineral matter of the black shale is dominated by clay minerals, illite-smectite and illite (Pukkonen & Rammo, 1992; Lindgreen et al., 2000). The high concentration of pyrite, which, together with kerogen, is thought to be the main carrier of some rare earth and other elements, is distinctive for black shale. The alum shale and graptolite argillite form patches over extensive areas in the outskirts of the Baltica palaeocontinent (Andersson et al., 1985) - Baltoscandia and Fennoscandia (Fig. 1). A possible spatial continuity of those complexes are the graphitic phyllites that are found in the tectonically disrupted allochtonous and autochtonous Caledonian complexes in central and northern Sweden and Norway (Sundblad & Gee, 1985). The metal-enriched phyllites exhibit similar geochemical signatures to the unmetamorphosed black shale of Baltoscandia (Sundblad & Gee, 1985). These geochemical similarities suggest that organic-rich mud might have accumulated over a wide geographic area and under fairly different depositional conditions – from pericratonic shallow marine settings to continental slope environments. The black shale of Fennoscandia and the graptolite argillite of Estonia can thus be treated as metal ore and a twofold energy source (including U and shale oil); the rocks have high scientific and significant economic value.
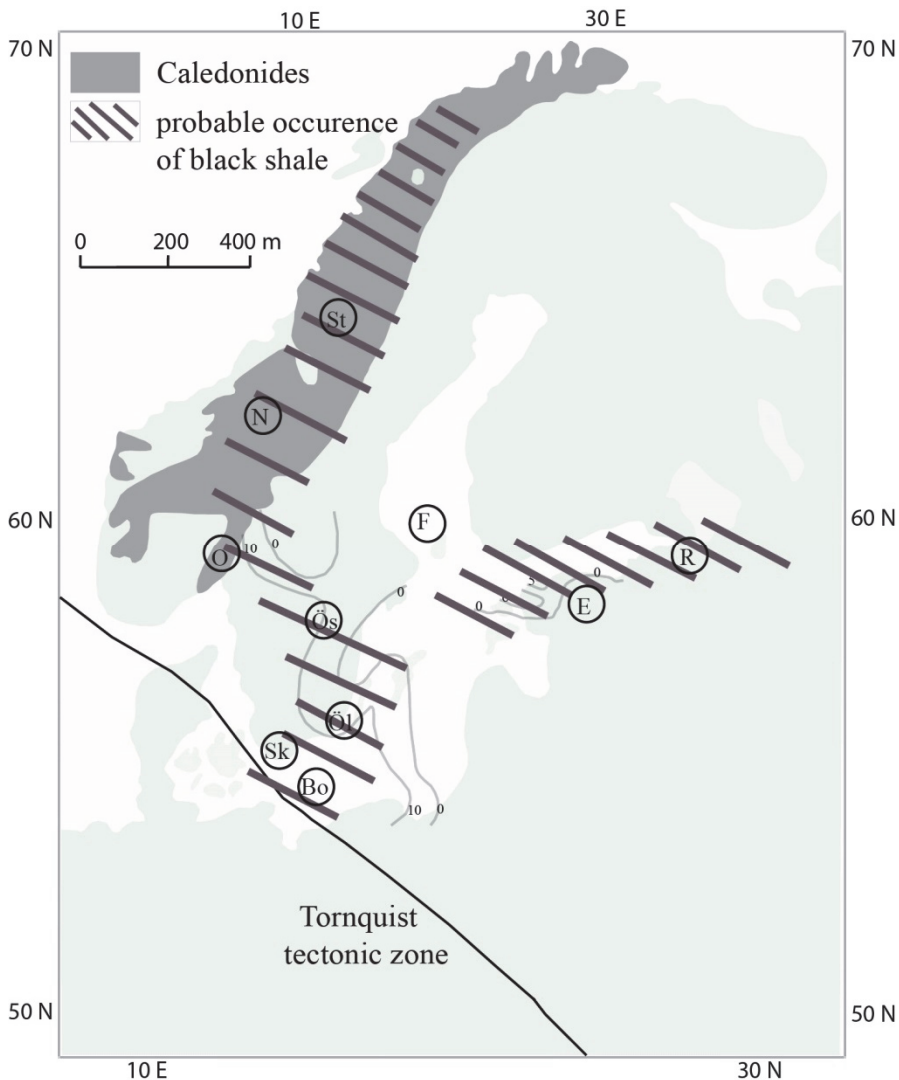
Fig.1. Lower Palaeozoic black shale (alum shale, graptolite argillite) occurrences in Fennoscandia and Baltoscandia. E – Estonia, R – Russia, F – Fasta Åland, St – Stepeniokk, N – Nordaunevoll, O – Oslo, Ös – Östersund, Öl – Öland, Sk – Skåne, Bo – Bornholm.

1.1.3. Black shale worldwide

There are many known Palaeozoic black shale deposits in various basins. The Silurian Zn-Pb deposits of Howards Pass (Canada) are also located in graptolite shale and contain in excess of 100×10^6 metric tonnes of ore (Gustavson & Williams, 1981). Devonian representatives are the well-known Zn-Pb deposits of Rammelsberg and Meggen in Germany and the Selwyn Basin Pb-Zn deposits in the Yukon Territory, Canada (Gardner & Hutcheon, 1985).

Some black shale is significantly enriched in noble metals, sometimes coupled with Mo- and Ni-bearing shale. For example, the Lower Cambrian black shale of southern China contains up to several hundred ppb's PGE's and Au in the strata deposited as individual, metal-rich sulfide layers, 2-15 cm thick (Grauch et al., 1991). Some of these elements in the Fennoscandian-Baltoscandian black shale may be of commercial value. In many Precambrian terrains metamorphosed sedimentary rocks, which were initially black shale, are known and also provide great economic interest.

Major base metal deposits in shale also occur in the Proterozoic of Australia, North America, and Africa. In Africa, the most prominent and best known are the deposits of the Zambian Copper Belt (Fleischer et al., 1976). In Australia, there are several Pb-Zn-Ag deposits hosted in Proterozoic shale, such as Mt. Isa, Hilton, McArthur River, and Lady Loretta (Gustavson & Williams, 1981). In North America, the known shale-hosted mineral deposits of Proterozoic age include the White Pine copper deposit in Michigan and the Sullivan Pb-Zn deposit in British Columbia (Gustavson & Williams, 1981).

1.1.4. Fennoscandian black shale resources

The Fennoscandian Shield provides several good examples of metamorphosed metal-rich black shale of the Precambrian age (Yudovich & Ketris, 1988; Arkimaa et al., 1999). A few are in active mining operation, several in exploration stage and many waiting to be discovered and exploited. The Talvivaara mine in Finland, with more than one-billion-ton resource, has been in production since 2008, by Talvivaara Mining Company Plc, and is the first mining operation collectively recovering NiCoCuZn(Mn)(U) by bioheapleaching polymetallic black shale. In the Viken area, Sweden, Continental Precious Minerals Inc. has estimated the uranium resource to be 1.05 billion lbs. of U_3O_8 in alum shale and large amount of other metals.

The Geological Survey of Finland has compiled a distribution map of Precambrian black shale in Finland, based on magnetic and apparent resistivity datasets (Arkimaa et al., 1999). An extensive study of on the Palaeozoic alum shale has previously been conducted in Sweden. The Geological Survey of Norway is compiling information about various aspects of black shale in the country. Russian scientists have also conducted drilling and studies of black shale (graptolite argillites) in the Leningrad oblast area. In Estonia, a compilation of existing and new geochemical studies has resulted in distribution maps of some element and elemental resource calculation (see Soesoo & Hade, 2014 – PAPER V; Voolma et al., 2013).

1.1.5. Alum shale and graptolite argillite of Fennoscandia as environmental concern

Apart from the commercial value of ore, there is another important aspect related to black shale – the environmental one. It has been known for a long time that the early mining in Sweden and Estonia has caused significant damage to environment and human health. However, mining is not the only cause of environmental impact. On or near the surface sedimentary black shale emanates radon, weathering of shale releases harmful elements into the soil and groundwater, and so on. It is only recently that we have started comprehending all the possible negative impacts related to this type of organic- and metal-rich shale. It is also important to note that metamorphosed Precambrian black shale also has an environmental impact -- even if it is not mined. This sulfide-rich black shale weathers more easily and thus releases more harmful elements than most of types of rock in the Fennoscandian Shield. For example, a study of a small lake in a black shale area in Finland indicated that it has been acidified for 9,000 years already (Loukola-Ruskeeniemi et al., 1998).

1.2. Public participation GIS

Environmental issues remain in focus of relationship between society and environment at present and in the future. Moreover, in modern societies sustainable development and clean environmental usage is a key issue to support growing wealth and population numbers. This in turn requires much better planning in landscape, natural resource and environment usage and better human population accommodation. The new approach should be able to grasp the relationship between a number of variables as a whole, taking into account the natural, historic, cultural, economic, and social factors, in conjunction with common human needs and environmental policies. A tool that allows matching qualitative and quantitative data with numerically immeasurable opinion of local people is called Public Participation Geographical Information System, or PPGIS (Sieber, 2006).

Relationships between people and their environment have been examined in several scientific disciplines in recent years in which the concept of land use and better planning has become central (Hade and Soesoo, 2014b – PAPER VI). New aspects and research methods are constantly introduced, and an integrated approach which includes examining the interchange between natural, physical, culture-historical and social factors and considers the social implications in environmental planning, has gained popularity (Cosgrove & Daniels, 1988; Jones, 1991; Bender, 1993; Duncan & Ley, 1994; Hirsh & O'Hanlon, 1995; Olwig, 1996; Cinderby, 1999; Granö, 2001; Peil, 2005; Hade et al., 2005; Brown, 2006; Couper & Miller, 2008; Brown & Weber, 2011; Brown, 2012).

The initial idea behind PPGIS was empowerment and inclusion of marginalized populations, who have little voice in the public arena, through geographic technology education and participation. PPGIS uses and produces digital maps, satellite imagery, sketch maps, and many other spatial and visual tools to change geographic involvement and awareness on a local level. With worldwide development of Internet, the Internet-based PPGIS becomes an affordable and accessible GIS tool for public engagement in many key issues of environmental planning. Here we briefly present a case study on the Pakri Peninsula, Northern Estonia, to show how PPGIS method can be used in assessment of landscape change, environmental pollution and recreational qualities of the area (Hade & Soesoo, 2014b).

2. MATERIAL AND METHODS

2.1. Estonian graptolite argillite data

Several publicly available graptolite argillite data sources and new geochemical data acquired by the workgroup at the Institute of Geology(TUT), have been used in this study, including Niin, Rammo & Saadre (2008; including digital map at a scale of 1:200 000); Pukkonen & Rammo (1992); Detkovski, Pukkonen & Rühko (1987), and Rühko & Pukkonen (1984).

In addition, selected data available from the Estonian geological base map (Estonian Land Board; www.maaamet.ee) has been used for layer thickness distribution analysis of underlying and overlying seams of GA. The Estonian graptolite argillite database (Niin, Rammo & Saadre, 2008; Geological Survey of Estonia; www.egk.ee) contains information on GA thickness, depths and elemental average concentrations of U, V, Mo, Zn and Pb in drill cores. In this database, 468 drill core total analyses are presented. For metal distribution and resource calculations, the database information has been evaluated and selected data were used in the calculations. For example, element concentration surfaces were modeled by the Kriging method using spherical distances (ESRI ArcGIS). For the distribution model of V the data from 297 drill cores were selected, for Mo 325, and for Pb 345 drill cores were used.

2.2. Geochemistry

In addition to the existing database, the Estonian graptolite argillites were studied in outrops (Paldiski, Saka) and in drill cores. Outcrops were sampled with 20-cm interval for geochemical analysis. Geochemical analysis was performed using X-ray fluorescence (XRF) and ICP-MS analysis at the Institute of Geology (TUT). XRF analysis was conducted with S4 Pioneer Spectrometer (Bruker AXS GmbH), using X-ray tube with a rhodium anode, which operated with the power of 3 kW. The samples were measured with a manufacturer's standard as MultiRes modification

(pre-calibrated standardless method). In-house standard ES-2 ("Dictyonema Shale") was used as reference material. ICP-MS analysis was conducted for rare earth elements (see details in Voolma et al., 2013).

The samples solutions for ICP-MS studies were prepared following the nitric acid, hydrofluoric acid, hydrochloric acid and boric acid digestion of a 0.250-g pulverized sample in Anton Paar MW3000 microwave oven. Some duplicate samples were analyzed at ACMELABS in Canada (see details in Voolma et al., 2013).

2.3. GIS software

In this work, ArcGIS Desktop ver. 9.3.1 & 10.1 with extensions of Spatial Analyst and 3D Analyst (Environmental Systems Research Institute, Inc., ESRI), and MapInfo Professional ver. 9.5 software were used. In some grid calculations Geochemistry for ArcGIS, Geosoft Inc., version 2.1 was additionally used.

The Natural Neighbour interpolation method in the ArcGIS Spatial Analyst software was used in the assessment for generating resource maps and computing resource volumes. The algorithm used by the Natural Neighbour interpolation tool finds the closest subset of input samples to a query point and applies weights to them based on proportionate areas to interpolate a value (Hade & Soesoo, 2014a). The value in an unsampled location is computed as a weighted average of the nearest neighbour values with weights dependent on areas or volumes rather than distances. It does not infer trends and will not produce peaks, pits, ridges, or valleys that are not already represented by the input samples. However, the surface grid and volume estimation results obtained by the Natural Neighbour interpolation method have been compared with other geo-statistical methods, such as Kriging (in ArcGIS Spatial Analyst, ESRI, and Geochemistry for ArcGIS, Geosoft Inc., version 2.1). Kriging is based on statistical models that include the statistical relationships among the measured points. The Kriging method assumes that the distance or direction between sample points reflects a spatial correlation that can be used to explain variation in the surface. Generally, Kriging is most appropriate when you know that there is a spatially correlated distance or directional bias in the data. It has been found that Kriging seems to be appropriate for phenomena with a very strong random component or for the estimation of statistical characteristics (uncertainty). However, most of the surfaces or volumes in the sedimentary environment are neither stochastic nor elastic media, but are a result of natural (e.g. sediment fluxes, deposition speed, hydromechanics, etc.) processes. Therefore, the Natural Neighbour interpolation method is thought to be more appropriate in case of the GA resource spatial/volume calculations in the present geological situation. In this case, the gridded GA thickness surface created by the Kriging method is slightly wider and calculated volumes are slightly higher (less than 1%; Hade & Soesoo, 2014a).

2.4. Public participation geographic information system method

The term Public Participation Geographical Information System (PPGIS) was conceived in 1996 at the meeting of the National Center for Geographic Information and Analysis (NCGIA) in the United States to describe how GIS technology could support public participation for a variety of applications with the goal of inclusion and empowerment of marginalized populations (Sieber, 2006). Since the 1990s, the range of PPGIS applications has been extensive, ranging from community and neighbourhood planning to environmental and natural resource management to mapping traditional ecological knowledge of indigenous people or local society (see Dunn, 2007; Brown, 2005; Sawicki & Peterman, 2002 for a review of PPGIS applications and methods). However, the formal definition of PPGIS remains still nebulous (Tulloch, 2007) with use of the term PPGIS emerging in the United States, Australia and developed country contexts while the term Participatory GIS (PGIS) emerged from participatory planning approaches in rural areas of developing countries, the result of a spontaneous merger of Participatory Learning and Action (PLA) methods with geographic information technologies (see Rambaldi et al., 2006). PGIS is often used to promote the goals of nongovernmental organizations, grassroots groups, and community-based organizations that may oppose official government policy, especially as pertaining to the rights of indigenous/local peoples and the current distribution of wealth and political power. In contrast, PPGIS may be sanctioned by government agencies, especially in Western democratic countries, as more effective means to engage in public participation and community consultation in land-use planning and decision-making.

The public participation is a vital part of environmental planning. It is not only dealing with deliberate hearings, but also seeking and facilitating public involvement in planning topics and the decision-making process (Goodspeed, 2008). Effective participation is a two-way process that includes sending information out to the publics and getting back their ideas, concerns and thoughts. The resulting "map of public positions, attitudes and wishes" is a good base for democratic and scientifically settled planning activities.

How the method works? Mapping of landscape and environment values, pollution and other spatial attributes can be achieved using a number of different data collection methods: paper maps through mail surveys, electronic maps through the Internet, and structured interviews or facilitated group processes such as workshops. Each approach has its inherent strengths and weaknesses. Even though the paper GIS method is the simplest method for collecting landscape value information from the general public, it may be not the cheapest and fastest. Following the instructions provided with a paper map, participants place sticker dots (or use other markers) on a study area. The respondent's data on the maps are then digitized into a GIS. Structured interviews or facilitated group meetings can be done with either paper or electronic maps, but considerable human effort is required to set up the interviews or meetings. Electronic mapping via the Internet can have the shortest turnaround time but has the disadvantage of requiring prospective participants to have access to both a

computer and the Internet. However, the internet questionnaire provides the participants an additional freedom of not disclosing his/her personality. The internet-based study can be implemented and completed using some digital map-based interface and data storing software. The Internet-based PPGIS method provides for rapid development and implementation of the studies at significantly reduced cost compared with a mail or workshop-based approach.

Once the spatial data are collected, the data can be analyzed using a variety of methods. The most useful starting point for analysis is to generate descriptive maps of topics under the question (landscape values, special place locations, pollution, etc.). The maps can be generated for each question/problem with different layers, if needed. The resulting maps can be analyzed by researchers and/or open for discussions by participants and other local society members for future elaborations and adequate decision-making. This is a good way to map the society's response to particular problems before the decisions are made.

The explosion in Internet mapping applications (including Google Maps and Google Earth) and virtual earth models has created an environment that should be favorable to the expansion of PPGIS methods in everyday life. However, the slow adoption of PPGIS methods by government agencies for regional and environmental planning does not appear technological but may reflect a lack of government commitment to public participation and two-directional consultation in general. The general lack of familiarity with PPGIS as a new consultation methodology and concerns with the accuracy and validity of lay knowledge in environmental decision processes serve to reinforce a propensity toward agency inertia.

3. RESULTS AND DISCUSSION

3. 1. Geology of the Estonian graptolite argillite

Organic-rich Early Ordovician marine metalliferous black shale -- graptolite argillite (GA) lies beneath most of northern Estonia (Fig. 2). Historically, it was called "Dictyonema shale", "Dictyonema argillite" or "alum shale." The word *dictyonema* came from the benthonic root-bearing *Dictyonema flabelliforme*, which subsequently turned into planktonic nema-bearing *Rhabdinopora flabelliformis* (Erdtmann, 1986). Here the term "graptolite argillite" is used, while "Dictyonema shale" is still used in Russian literature. However, general term "black shale" would be also appropriate to use in case of the Estonian graptolite argillite.
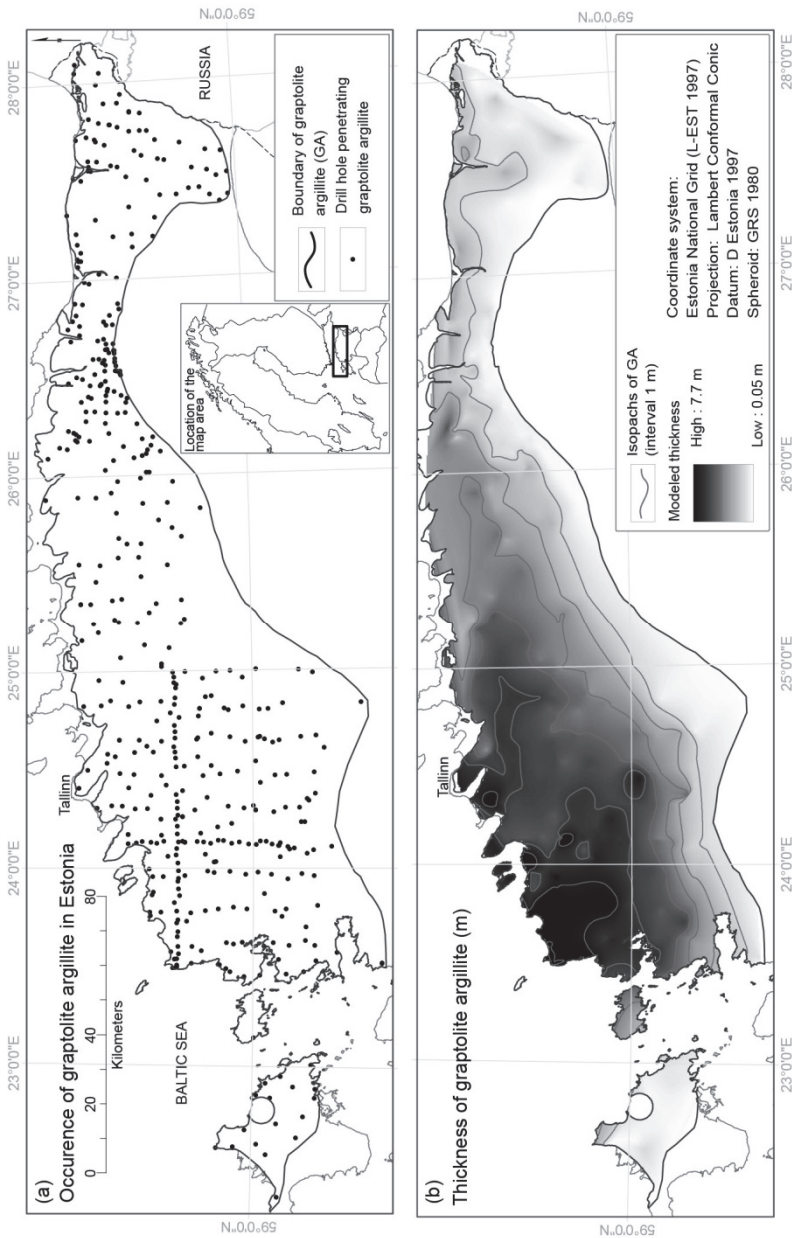
Fig. 2. A. Location map of the drill holes penetrating argillite layers (black dots) of the Estonian graptolite argillites (a) and the graptolite argillite thickness of model (b). The thickness of GA was modelled by ArcInfo 10.1, based on the studied drill holes. For creating the thickness grid, the Natural Neighbor interpolation method was used, and the grid cell size is 400 meters. Due to the location at the southern margin of the Precambrian Fennoscandian Shield GA layer is dipping southwards following the regional trend. Figure from Soesoo & Hade, 2014a.

The Estonian graptolite argillite is fine-grained, unmetamorphosed, (sub-)horizontally lying and undisturbed, organic-rich lithified clay (Türisalu Formation), which is commonly 0.5 to 6 m thick and belongs to the group of black shale of sapropelic origin (Petersell, 1997; Voolma et al., 2013; Hade & Soesoo, 2014a). The graptolite argillite is formed in the proximal settings of the Baltic palaeobasin in the Early Ordovician when Baltica was at approximately 40–50 degrees of southern latitudes (Cocks & Torsvik, 2005, Fig. 3).

Today, the graptolite argillite crops out in some places in Northern Estonia, in the klint area or in some narrow river valleys. Since the entire Estonian Lower Palaeozoic sedimentary section is inclined towards the south due to its geological position on the southern slope of Fennoscandian Shield (Soesoo et al., 2004), at the southwest end, the GA deposit lies at a depth of more than 250 meters (Fig. 3).

The shale of the Türisalu Formation, which contains fossilised fragments of early planktonic graptolites, is characterised by high OM content ranging from 8% to 20%, fine silt fraction dominating the composition and variable pyrite abundance (Kaljo & Kivimägi, 1970; Loog et al. 2001; Hade & Soesoo, 2014a, Hints et al., 2014). The OM of the Türisalu Formation is N-rich, highly aromatic and, according to previous studies, composed dominantly of transformation – condensation products of marine microbial matter (Klesment & Urov, 1980; Sumberg et al., 1990; Lille, 2003). From other biogenic components, early planktonic graptolites, fragments of phosphatic lingulid brachiopods, conodonts, acritarchs and polychaete jaws have been reported (e.g. Kaljo & Kivimägi, 1970; Kaljo et al., 1986; Paalits, 1995; Hints & Nõlvak, 2006). A characteristic feature of the Türisalu Formation is the absence of calcareous fossils.

Although the reserves of GA surpass those of Estonian kukersite (proper oil shale), it is of too poor quality for energy production at present. The GA calorific value ranges from 4.2–6.7 MJ/kg (Pukkonen & Rammo, 1992) and the Fischer Assay oil yield is 3–5% (e.g. for Estonian kukersite, it is about 30–47%; Veski and Palu, 2003). The moisture content of fresh GA ranges from 11.9 to 12.5%, while average composition of the combustible part is: C – 67.6%, H – 7.6%, O – 18.5%, N – 3.6% and S – 2.6% (Lippmaa & Maremäe, 2000). However, considering it is a low-grade oil source, its potential oil reserves are about 2.1 billion tonnes (Veski & Palu, 2003). The Fennoscandian black shale together with Estonian GA is considered to be a potential energy reserve for the future.

3.2. The environment of shale formation and lithology

Between Mid-Cambrian and Early Ordovician, the Baltica made through an anti-clockwise rotation. At the beginning of Tremadocian, Baltic palaeobasin was situated at western margins of the continent, facing the Iapetus Ocean in the west and the

Tornquist Sea in the south and south-west (Cocks & Torsvik, 2005). On a regional scale, the Türisalu Formation is part of a patchy but vast Mid-Cambrian – Lower Ordovician black shale belt in the Baltoscandian region, extending in the east – west dimension from Lake Onega to Jutland (Andersson et al., 1985; Kaljo et al., 1986). It accumulated in a large, flat-floored epicontinental sea (Nielsen & Schovsbo, 2011). Nielsen & Schovsbo (2006) considered the Estonian and Russian Tremadocian black shale to be a shallow-water tongue of the alum shale formation (in Sweden). In Estonia, the roughly flat-lying Türisalu Formation occurs within the tectonically undisturbed lower Palaeozoic sedimentary succession, and the entire Palaeozoic sedimentary complex is generally characterised by very low thermal maturity (Kirsimäe et al., 1999). Its distribution in Estonia and Russia has been considered one of the best examples of very shallow- marine near-shore Cambrian and Early Ordovician deposits with siliciclastic sedimentation (Kaljo et al., 1986; Mens & Pirrus, 1997; Artyushkov et al., 2000).
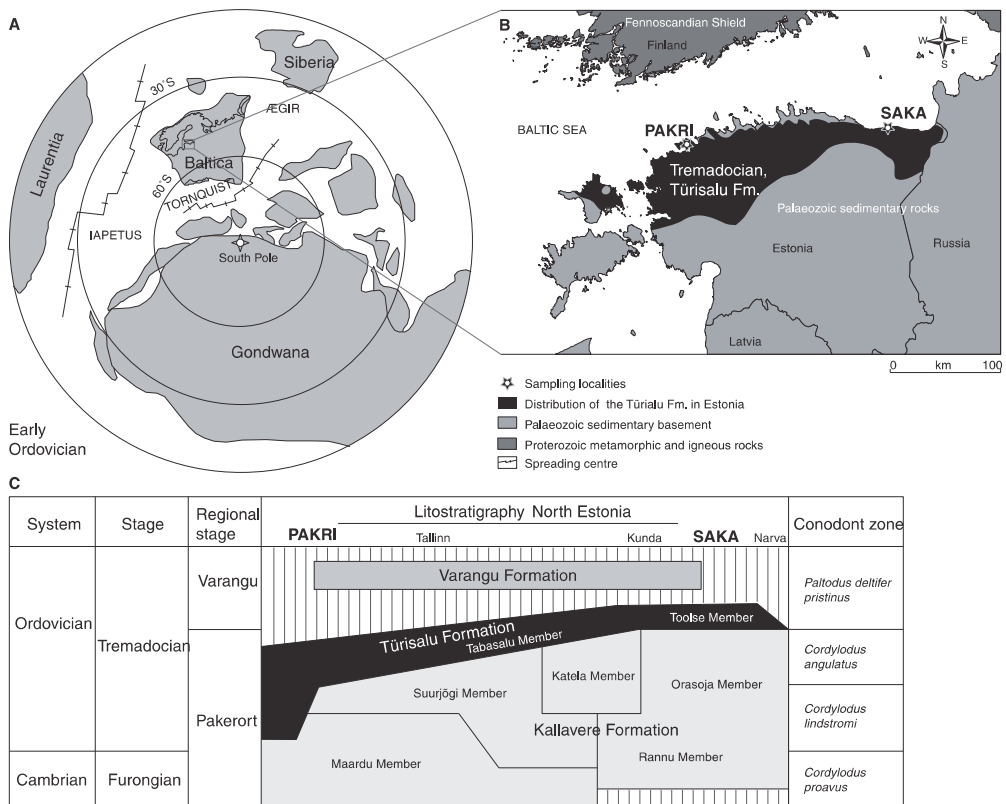

Fig. 3. A. Palaeogeography of Baltica continent in the Early Ordovician (after Cocks & Torsvik, 2005). B. Modern distribution of the Türisalu Formation and sampling localities Saka and Pakri on the Baltic klint. C. Lithostratigraphy of the Tremadocian deposits (Heinsalu et al., 2003) of Estonia. Figure from Hints et al. (2014).

The characteristic feature of the black shale is its high but spatially variable content of redox-sensitive trace elements, such as V, U and Mo, showing general positive covariance with OM abundance (Pukkonen & Rammo, 1992). The Türisalu Formation occurs on top of a complex of commonly cross-bedded siltstone and sandstone (Kallavere Formation; Fig. 4.) containing debris or rich coquinas of phosphatic brachiopods denoting a large-scale skeletal phosphorite accumulation episode during the Cambrian – Ordovician transition (Ilyin & Heinsalu, 1990; Hiller, 1993). These siliciclastic deposits also contain interbeds and lenses of black shales. In NW Estonia, a thick organic-rich mudstone bed caps a subaerial regional unconformity at the base of the transgressive Kallavere Formation (Nemliher & Puura, 1996). In NE Estonia, the black shale overlies the siliciclastic beds of the Kallavere Formation, presenting dense interfingerings of siltstone with phosphatic detritus and organic-rich mudstone beds (Heinsalu et al., 2003). The onset of accumulation of primary organic-rich muds of the Türisalu Formation across Estonia was not concurrent (Kaljo & Kivimägi, 1970) (Fig. 3). The older black shales in western Estonia belong to the Cordylodus lindstromi/angulatus conodont biozones (Pakerort Regional Stage). Eastwards the black shales become gradually younger, and in NE Estonia, the succession is assigned to the *Paltodus deltifer pristinus* conodont zone (Varangu Regional Stage; Kaljo et al., 1986; Heinsalu et al., 2003). The Varangu age generally denotes a major regressive episode in the region (e.g. Dronov et al., 2011). The upper boundary of the Türisalu Formation comprises a regional unconformity that is capped by organic-poor grey shales or glauconitic sandstones (Heinsalu, 1980) and marks a sea-level drop that terminated organic-rich mud accumulation in the proximal settings of the Baltic palaeobasin.

In western and north-central Estonia, the Türisalu Formation has been described as a considerably homogeneous black shale unit comprising laminated or massive lithologies (Tabasalu Member). The massive black shale varieties that are dominant in somewhat younger north-central Estonian settings have supposedly accumulated under more active hydrodynamic regime than the beds in the western settings (Pukkonen & Rammo, 1992). However, Heinsalu (1990) reported irregular encounters of cross- and wavy-lamination, trace fossils and minor ripple marks in older western Estonian black shales. In NE Estonia, the Türisalu Formation becomes thinner and more variable (Toolse Member). It embodies numerous silt intercalations that are regularly associated with authigenic carbonate or sulphide mineralisation, and the entire Türisalu Formation has been suggested to represent a shallower-water setting and a more variegated sedimentation environment than represented by the Tabasalu Member (Kaljo & Kivimägi, 1970; Kivimägi & Loog, 1972; Loog et al., 2001). For example, in the Toolse area, the Türisalu Formation was divided into four distinct intervals with different textural and structural characteristics and trace metal content (Kivimägi & Teedumäe, 1971). Furthermore, Heinsalu et al. (1994) suggested that the areas around Toolse and Rakvere (Rakvere Phosphorite Area) acted as a border zone between sub-environments with different hydrodynamic regimes in this proximal part of the palaeobasin during the Early Tremadocian and that subaerial highs likely existed in this shallow-water area before a main organic-rich mud accumulation episode (Fig. 3.).

In the rather homogenous mineral assemblages of the Türisalu Formation, K-feldspar has been found to dominate over quartz, illite-smectite and illite (Utsal et al., 1982; Kleesment & Kurvits, 1987; Loog & Petersell, 1995; Loog et al., 2001). High K-feldspar content is the characteristic feature of the Türisalu Formation, distinguishing the complex from the typical alum shale formation of Sweden in which K-rich clay minerals (illite and illite-smectite) tend to dominate in mineral assemblages, and which have been reported to present generally lower K_2O/Al_2O_3 molar ratio than Tremadocian black shales from Estonia (Snäll, 1988; Lindgreen et al., 2000; Schovsbo, 2003). It is remarkable that substantial amount of K-feldspar in the Türisalu Formation is likely authigenic in origin (Utsal et al., 1982; Loog et al., 2001; Hints et al., 2014). For quartz, a genetic link with primary biogenic silica has been suggested in NE Estonia, where lenticular intercalations of siliceous sponges are common (Müürisepp, 1964; Loog & Petersell, 1995).

Some geochemical indices, enrichment of redox-sensitive elements and high OM content seem to favour the idea that the primary mud formed in anoxic environment (Hints et al., 2014). In contrast, the observed traces of bioturbation and dynamic sedimentation features suggest oscillating redox conditions in the lower water column during primary mud accumulation. Metal sequestration in such environments could have been favoured by steep redox gradients at sediment–water interfaces covered by microbial mats.

As the Estonian GA is characterized by high to very high concentrations of U (up to 1200 ppm), Mo (1000 ppm), V (1600 ppm) Ni and other heavy metals, and is rich in N, S and O (Pukkonen & Rammo, 1992; Soesoo & Hade, 2012; Voolma et al., 2013) it may be of economic interest.. In this respect, the amount of metals and their spatial distributions can be modelled. The modelling approach is discussed below.

3.3. Estonian graptolite argillite as a metal resource

It has been long recognised that the Estonian graptolite argillite has high concentrations of a number metals. Most of the geological information on the Estonian GA is obtained from basement mapping and exploration projects conducted by the Geological Survey of Estonia, which started in the 1950s. The vast amount of detailed information on the GA lithology and geochemistry was collected when Estonia's phosphorite resources were prospected in the 1980s.

3.3.1. Tonnage of the Estonian graptolite argillite

The previous estimates of the graptolite argillite reserves in Estonia range from 60 (Petersell, 1997) to 70 billion tonnes (Veski & Palu, 2003) and little is known about the calculation methods and the initial data (number of drill cores etc.) that were used. Although practically no new data have been added during the last two decades, the

GIS-based methods now allow us to obtain better estimates of the total resource and metal distribution (see Hade & Soesoo, 2014a). The combined database of 468 drill cores (Geological Survey of Estonia & Estonian Land Board database, see at www.maaamet.ee) has been used as the initial data. The estimated area of the Estonian GA on the mainland and islands is 12 212.64 km^2, with a corresponding volume of 31.92 billion m^3 (Hade and Soesoo, 2014a). In order to calculate the total weight of the GA, the value of the specific gravity (density) is required. It is known (Petersell, 1997) that the density of the graptolite argillite varies to a great degree, mostly between 1 800 and 2 500 kg/m^3. So, assuming an average density of 1 800 kg/m^3, the total mass of GA is about 57.45 billion tonnes, while in case of 2 500 kg/m^3 the mass is 79.80 billion tonnes. Assuming the average density to be 2 100 kg/m^3, the total weight of GA is about 67 billion tonnes (Fig. 4), which is between the earlier estimates of 60 to 70 billion tonnes.
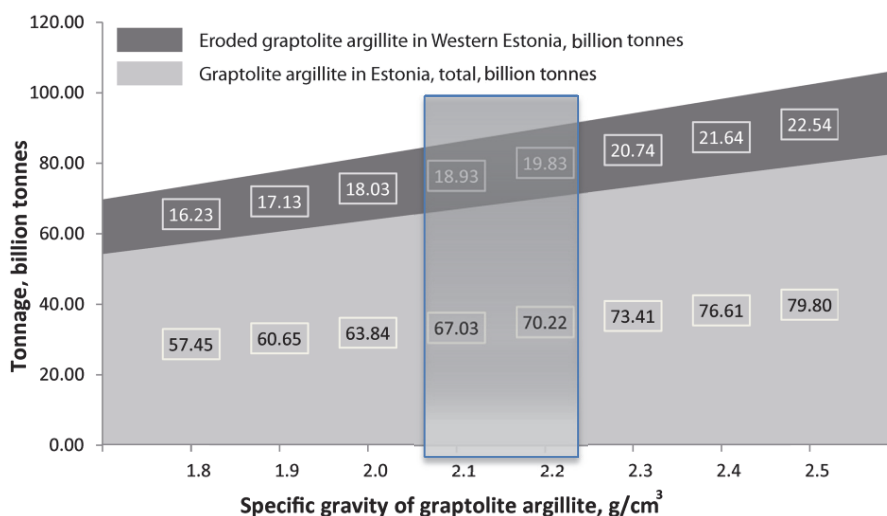
Fig. 4. Calculated volume and tonnage of Estonian GA (*in situ* and partly eroded area between the Estonian mainland and West-Estonian islands) as a function of specific gravity. Figure from Hade & Soesoo (2014a).

3.3.2. Metals in Estonian graptolite argillite

The Estonian GA is characterized by high to very high concentrations of U (up to 1200 ppm), Mo (1000 ppm), V (1600 ppm), Ni and other heavy metals, in addition to high N, S and O concentrations (Pukkonen & Rammo, 1992; Soesoo & Hade, 2012; 2014; Voolma et al., 2013). Locally, the shale is enriched in REE, Cd, Au, Sb, As, and Pt (Voolma et al., 2013).

The chemical composition of GA is definitely of great interest and its specificities have been known for nearly a century. Besides the high concentration of a number of

metals, its potassium and sulphur contents are much higher and the content of sodium and calcium lower than in average clays and shale. The concentration of K_2O in GA is higher than could be expected, based on the composition of known shale-forming minerals (Vaughan et al., 1989). With the increase in the volume of silt interlayers from the west to the east, the concentration of SiO_2, CaO and P_2O_5 increases, while that of Al_2O_3, K_2O and MgO decreases (Voolma et al., 2013). Based on previous geochemical exploration (Pukkonen & Rammo, 1992), three geochemical zones have been distinguished in the Estonian GA – Western, Central and Eastern. These zones differ mainly in the concentration of metals that are characteristic of GA – Mo, V, and U. However, based on recent studies (Voolma et al., 2014; Hade & Soesoo, 2014a) it appears that the distribution of metals in GA has a more complex pattern. Study by Voolma et al. (2014) dealt with two vertical sections of graptolite argillite (Pakri in North-Western and Saka in North-Eastern Estonia) and indicated the existence of pronounced fine-scale trace metal variability and the remarkably different behaviour of trace elements. The content of enriched elements was shown to change greatly over the examined sections. For example, an elevated abundance of a number of other trace metals, e.g. Pb, Zn, Cd, Cu, As and La, was detected in samples with an enhanced content of sulphur or phosphorus.

With respect to the standard values, such as PAAS and NASC, the Estonian GA is extremely rich in U and V. For example, the average U concentration in the Saka section (267 ppm) is a hundred times higher than the corresponding values for NASC (Voolma et al., 2013). In case of V, there is nine-fold difference between the concentrations in NASC and the average concentrations detected, for example, in the Saka section, in Eastern Estonia (1,190 ppm; Voolma et al., 2013). In general, the content of U in GA shows quite strong positive correlation with the organic matter content which most likely indicates early fixation via metal-organic complexes. At the same time, correlation of P_2O_5 with other enriched trace elements, such as U was not detected.

The high variability of the trace metal composition of GA, including heterogeneous REE patterns, may point to the polygenetic nature of metal compositions, apparently formed as the cumulative product of multistage evolution. However, our knowledge about metal distribution, and especially its origin, is still rather fragmentary and a multidisciplinary exploration is needed to adequately predict potential metal resources of GA in the future.

The distribution of U, Zn, Mo and V in the Estonian GA has been modelled and shown in studies by Voolma et al. (2013) and Hade & Soesoo (2014a). These elemental concentration data represent the average concentrations in the GA in the drill core. The central and western parts of the Eastern Zone show the highest concentrations for V and Mo, whereas V is also high in the southern part of the Eastern and Central Zones. Uranium shows the highest concentrations in the most easterly part of Estonia, while in Western Estonia the concentrations show medium values and the lowest values are characteristic of the Central Zone. Distribution of U has not been modelled on the Estonian islands due to the small number of analyses.

The high concentrations in the southwest corner may be an artefact of the model, since there are only a few drill cores available and those show locally high contents of U. Generally, it can be concluded that the concentration of most metals (except Zn) is relatively low in the Central Zone of the GA area (Hade & Soesoo, 2014a; Soesoo & Hade, 2014).

However, it is important to emphasize that the available chemical data is relatively unevenly distributed across the area and the present geochemical generalization is informative, but must be taken with caution. There is very little data on the southern margin of the GA area, so the concentrations may vary, but due to its limited thickness (less than 0.5 m) the total elemental amounts have not affected the calculations very much.

3.3.3. Tonnage of metals in the Estonian graptolite argillite

As average metal concentrations are very useful in indicating "poor" and "rich" deposits, the total content of a certain element depends on the thickness of the deposit layer. In order to calculate the total amount of the element/metal based on square meters, ESRI ArcGIS software was employed. As an example, the total concentration (tonnage) of uranium in the Estonian GA is shown on Fig. 6. This calculation is based:
- on the element/metal grid, which shows the element distribution in ppm (e.g. Fig. 5 for U);
- on an interpolated grid of the GA thickness, in meters;
- by assuming the average density of the GA to be 2 100 kg/m^3;
- since the element/metal and thickness grids were calculated with the cell size of 400 x 400 meters, the same cell size was used for the calculation of the total amount of an element/metal.

The results of U tonnage and market value within the cell of 400 m x 400 m (at the thickness of GA in the area) are presented in Hade & Soesoo (2014a). These calculations allow for the provision of a more realistic total amount for the metal in the Estonian GA (not just based on an average concentration value in ppm). For example, the calculated total weight of U is about 5.67 million tonnes (6.68 million tonnes as U_3O_8). Zn is as high as 16.53 million tonnes (20.58 million tonnes as ZnO) and for Mo is 12.76 million tonnes (19.15 million tonnes as MoO_3). The highest studied element amounts show a somewhat similar pattern – Western Estonia has the highest potential, especially for U and Mo. However, there are also distinctions between those elements. For example, the Central Zone where the enrichment is the lowest, still shows high amounts of Zn. The pure market value of these metals is high: about € 460 billion for the uranium, € 30 billion for the zinc and about € 350 billion for the molybdenum, considering the average market prices in April 2013 (Hade & Soesoo, 2014a; Soesoo & Hade, 2014). However, since a simple, environmentally friendly and economic technology has yet to be developed for the co-extraction of most of the enriched elements from GA, its economic value remains just theoretical.
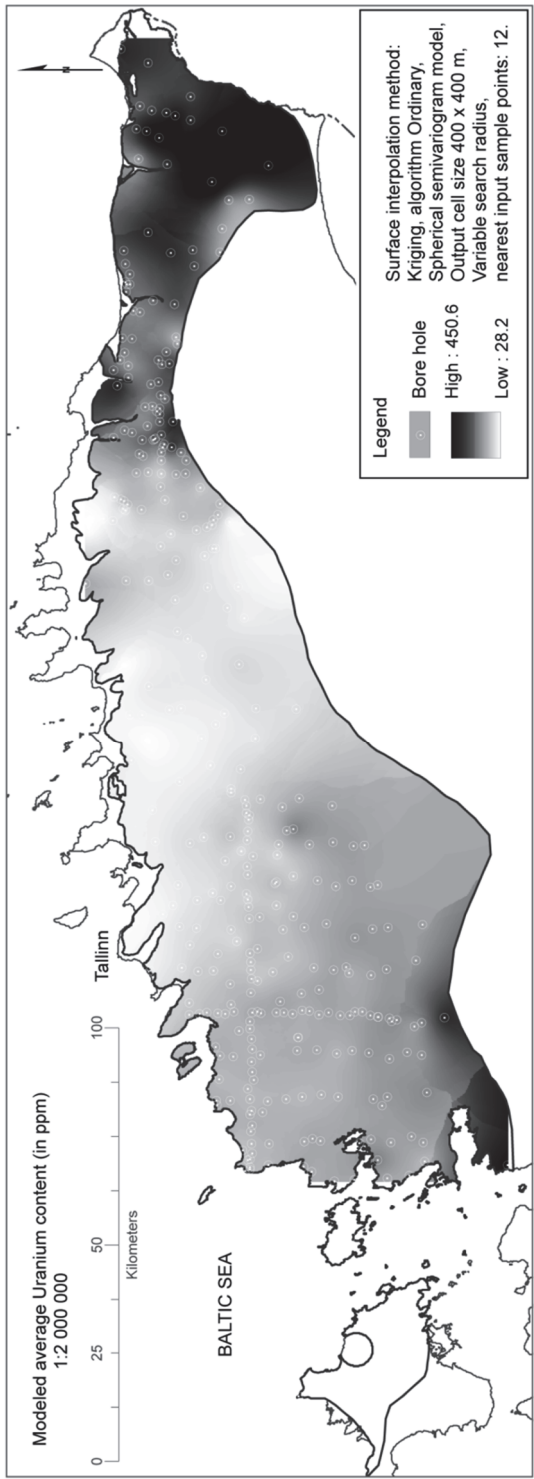
Fig. 5. Modelled uranium content in Estonian GA based on calculated average drill core analyses (data: Geological Survey of Estonia; Estonian Land Board - www.maaamet.ee; Institute of Geology at TUT). The element concentration surface is modelled by the Ordinary Kriging interpolation method.
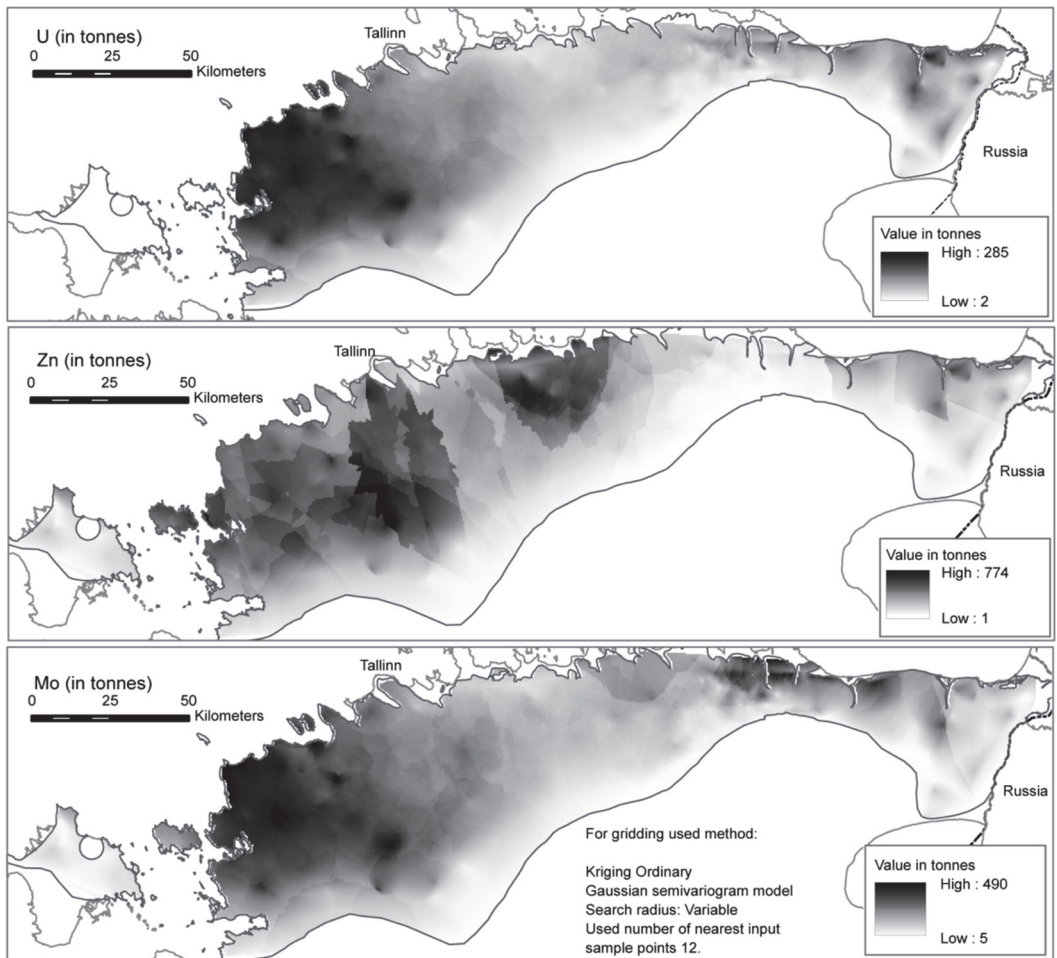
Fig. 6. U, Zn and V tonnage (in tonnes) model in the 400 m × 400 m cell at the modeled thickness of graptolite argillite.

3.3.4. Volume and tonnage of *in situ* and eroded graptolite argillite in Western and Northern Estonia.

In the similar way we can calculate the volume of eroded material between the Estonian mainland and Hiiumaa Island, and also in the northern extent. The calculation of the partly eroded and *in situ* GA material between the mainland and Hiiumaa Island is based on extrapolation of thickness data (Fig. 7B). Assuming the average specific gravity of 1 800 kg/m^3, the tonnage of the eroded GA is about 16.23 billion tonnes, while 2 500 kg/m^3 gives 22.54 billion tonnes and 2 100 kg/m^3 gives about 18.93 billion tonnes (Figs. 4 and 7B). It is more difficult to calculate the volume (presently totally eroded) of GA that occupied the area north of the present erosional line, towards the north of the North Estonian Klint (Fig. 7A). Assuming a

U-shaped depositional area, a minimum extension can be shown (see Fig. 7A). The volume of this hypothetical northern extension is about 8.80 billion m^3, which is in same order to the area between Estonian mainland and Hiiumaa Island. It is even more problematic to calculate the amount of metals in the eroded material. Extrapolating the average metal contents in the drill cores of the Western, Central and Eastern zones, with emphasis on the northern drill holes, the concentration values can be established. The estimated total amount of U is 1.8 million tonnes, Zn – 22 million, Mo – 4.4 and V – 13 million tonnes. These values are similar to those calculated for the Western part. However, it must be mentioned again that these values are hypothetical and must be considered as preliminary estimates.

Very little is known about the timing and cause of erosion in Northern and Western Estonia. The most prominent feature of this erosion is the North Estonian Klint. One hypothesis which explains the klint formation is related to a large, old, possibly Late Cenozoic, river system (Overeem et al., 2001; Soesoo & Miidel, 2007). A vast amount of terrigenous sediments is known to exist in the North Sea with an area of 100 000 km^2 (Overeem et al., 2001). The Eridanos River System, which drained most of North and North-Western Europe, developed during the Late Cenozoic as a result of the simultaneous uplift of the Fennoscandian Shield and the accelerated subsidence in the North Sea Basin. The erosion of the area to the north of the present mainland of Estonia and Western Estonia is most likely attributable to the Pra-Neva River, the tributary of the Eridanos.

It is well known that the fluvial deposits of Miocene to Early Pleistocene Age in Germany and the Netherlands were transported to the delta of the Eridanos River System (Rhebergen, 2009). However, the exact provenance of this sedimentary material continues to be a subject of discussion. Some of the sand from the Fennoscandian crystalline rocks, Ordovician terrigenous material, erratics with well-defined Ordovician fossils, which are similar to those in Northern Estonia and the St. Petersburg region (Russia) (Rhebergen, 2009), are known to exist within the sediments in the Eridanos fluvio-deltaic system in the North Sea area, the Netherlands and Germany. Most likely, the erosion of the Lower Palaeozoic sections in Western Estonia, including graptolite argillite, is related to those processes which generated the klint. The exact timing of those processes remains unknown; however, the original erosional processes were most likely active during the Late Miocene (some 20 to 5.332 million years ago) to Pliocene (5.332 to 2.588 million years ago). Some of the material may have been re-deposited during the Quaternary.

Assuming the volume and average chemical composition of the eroded graptolite argillite (Figs. 3 and 7), the amount of eroded, partly dissolved and re-deposited metals can be calculated. Based on the extrapolated GA thickness and average metal contents in the drill cores from the most westerly and northerly parts of Estonia, and from Vormsi and Hiiumaa islands, the minimum total amount of uranium (elemental U) that has been eroded and re-deposited reaches 1.80 million tonnes, zinc (Zn) 23.00 million tonnes, lead (Pb) 7 million tonnes, molybdenum (Mo) 4.58 million tonnes, and vanadium (V) 13.30 million tonnes.

As for volume, the contribution of graptolite argillite from Northern and Western Estonia to the Eridanos sedimentary budget is not high, considering the overall 62 000 km^3 of sediments in the Southern North Sea Basin alone (Overeem et al., 2001) versus 9 015 km^3 derived by erosion from Northern and Western Estonia. However, the metal contribution of GA to the overall Eridanos sedimentary budget is remarkable. The total amount of the elements that have now been re-deposited is extremely large. One can only imagine approximately 1.8 million tonnes of uranium and 13 million tonnes of vanadium (as minimum) incorporated into sediments somewhere below the Holocene sediments of the North Sea!
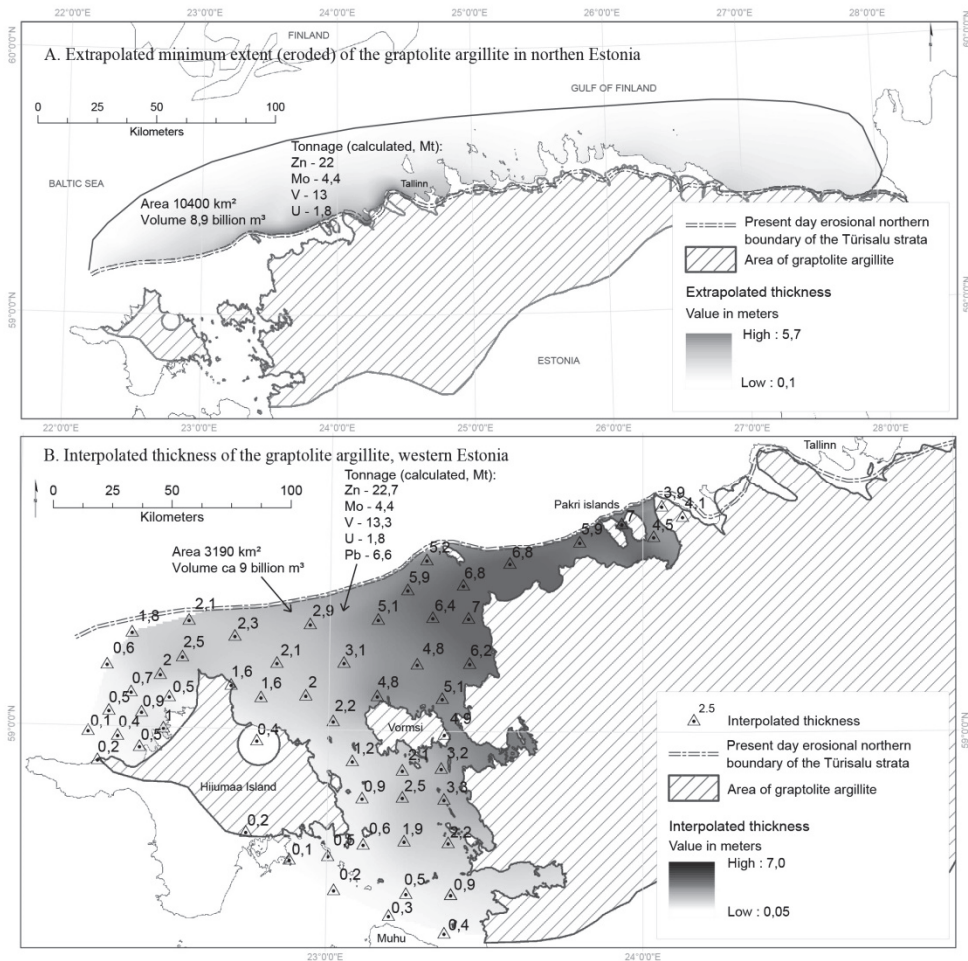

Fig. 7. Extrapolated extent, thickness, volume and metal tonnages of GA in Northern Estonia (A) and between Western Estonia and the islands (B). Modified figure from Hade & Soesoo (2014a).

3.4. Alum shale and graptolite argillite as health risk and environmental concern

Sedimentary, unmetamorphosed black shale has historically been used in Sweden and Estonia. In Sweden, the Cambrian and Lower Ordovician alum shale has been known for more than 350 years. Mining the shale for alum began in 1630s in Skåne. The alum shale was also recognized as a source of fossil energy and, toward the end of the 1800s, attempts were made to extract and refine hydrocarbons (Andersson et al., 1985). Before and during World War II, alum shale was retorted for its oil, but production ceased in 1966 owing to the availability of cheaper supplies of crude petroleum. During this period, about 50 million tonnes of shale was mined at Kinnekulle and Närke in Sweden.

For uranium production, a pilot plant built at Kvarntorp, Sweden, produced more than 62 tonnes of uranium between 1950 and 1961. A small uranium mill was constructed at Ranstad and went on-stream in 1965. The plant operated at reduced capacity for three years producing about 300 tonnes of yellowcake. The alum shale was also burned with limestone to manufacture "breeze blocks", a lightweight porous building block that was widely used in the Swedish construction industry. Production stopped when it was realized that the blocks were radioactive and emitted unacceptably large amounts of radon.

Just after World War II, due to the atomic bomb "competition", the Soviet Union started looking for uranium deposits. The nearest place where geologists found large quantities of uranium ore (graptolite argillite) was in Northeast Estonia and the first Soviet uranium processing facility was started in a small town called Sillamäe. A total of 22.50 tonnes of elemental uranium was produced from 272 000 tonnes of GA from an underground mine near Sillamäe (Veski & Palu, 2003; Soesoo & Hade, 2012). The plant operated as a top-secret Soviet institution until 1991.

3.4.1. Graptolite argillite as a co-product of phosphorite mining

In addition, graptolite argillite is also a co-product of phosphorite mining in Estonia, so the Maardu area near Tallinn is among the most polluted regions in Estonia (Jüriado et al., 2012). Between 1964 and 1991, approximately 73 million tonnes of GA was mined from a covering layer of phosphorite ore at Maardu, near Tallinn. It should be mentioned that the phosphorite in Estonia lies directly below the GA. The GA was mixed up with other overlying deposits, such as carbonate rocks, sandstone, glauconite sandstone, and Quaternary sediments, and piled into waste heaps. In 1989, opencast mining at Maardu was carried out on more than 6 km^2. Today, waste hills in Maardu contain about 73 million tonnes of GA, which contains, a minimum content of 30 ppm U, totally as much as 2.19 million kg of U (Jüriado et al., 2012). This waste leaches into the surface water and groundwater.

Under normal weathering conditions GA easily oxidizes, and spontaneous combustion can occur. In some places, for example at Maardu waste hills in Northern Estonia, the temperatures in the heap occasionally exceeded 500 ºC. It is interesting to note that spontaneous combustion can occur in heaps that are a few months or over
20 years old, which leads to the conclusion that some old heaps can still be dangerous. These processes lead to annual leaching of 1 500 tonnes of mineral matter per square kilometre of a waste dump and the waste-water being discharged into Lake Maardu. In 1990, at the average temperature of the heap, estimated 520.3×10^3 tonnes of oxygen was spent on oxidizing the rocks buried in the heap. The amount of gases emitted from burning shale was estimated as SO_2 - 10^4 tonnes and CO_2 - 73.3×10^3 tonnes (Pihlak, 2009). The effluent of the Maardu opencast mine and processing plant, which was directed into Muuga Bay (Gulf of Finland) delivered up to 20.18 million m^3 of water with varying levels of polluting elements each year. The amount of dissolved minerals delivered into the sea was estimated at up to 38.4×10^3 tonnes annually (Pihlak, 2009; Jüriado et al., 2012).

3.4.2. Graptolite argillite as a living environment

GA, if lying on or near to the surface, is also a major source for radon (Rn) in Estonia and elsewhere. Very high radon concentrations of up to 10 000 Bq/m^3 have been recorded at some natural outcrops of GA in the North Estonian Klint (Soesoo & Hade, 2012). Radon is a highly radioactive and carcinogenic element causing mutations, especially lung cancer.

In spite of the fact that the impact of black shale on a nation's health and biological environment is well recognized, little is being done to quantify these impacts in a real and reliable way. Moreover, only a small number of measures are being taken to avoid direct contamination of soil and groundwater and direct and indirect influences on the local people. Sometimes, contaminated black shale industrial areas are used as a political instrument in decision-making or for someone's commercial interest. In many cases, no real environmental improvement results from those decisions (Soesoo & Hade, 2014).

There are areas in Estonia, Sweden and elsewhere in Fennoscandia where black shale forms the surfaces where human live and conduct their everyday activities, thus directly influencing health and well-being. For example, there are a number of towns in Northern Estonia, which are located in area where graptolite argillite crops out or occurs in vicinity, including the capital Tallinn, Paldiski, Kunda, Aseri and others (Fig. 8). In Sweden, in the focus for the current interest in Alum shale mining is the Östersund area, where people have historically lived on the top of black shale. These influences need to be quantified and measures taken to minimize negative health and environmental impacts. However, as nations depend on mining and metal/electronics industries, the need for new resources cannot be neglected and a balance must be achieved between the nation's sustainable economic development, exploitation of

black shale resources and public health. A new, modern, science-based revision of black shale resources and related environments across Estonia – NW Russia – Sweden – Finland – Norway is proposed (Soesoo & Hade, 2014). This kind of data compilation will definitely foster a better understanding of the problem, and help to create an industrially and environmentally sound expert model of the Fennoscandian and Baltoscandian black shale potential (see Chapter 3.5).

Fig. 8. Areal extent of Estonian graptolite argillite and its possible environmental impact zone.

3.5. Towards a common Fennoscandian-Baltoscandian-scale black shale database

Creating regional, large-scale, cross-border databases is not uncommon in geology. Geological maps are the best and oldest form of such information compilation, which extend across political borders and continents. An initiative group on the Fennoscandia Metallogenic Map and Database, which involves specialists from the geological surveys and other organizations in Finland, Norway, Russia and Sweden, has been active for more than a decade. The work has resulted in well-compiled, cross-border database and a digital map (see http://en.gtk.fi/informationservices/databases/fodd/index.html).

The Fennoscandian Ore Deposit Database (FODD) is a comprehensive numerical database that includes the metallic mines, deposits and significant occurrences in Fennoscandian Shield, which could be part of the geological information compilation and standardization, and be very useful for future metal ore discoveries. The first FODD metallogenic map was published in 2009. An updated version became in August 2013. This database contains information on about 1 700 (June 2013) mines, deposits and significant occurrences in Fennoscandia. The map contains 168 major metallogenic areas, of which 46 are completely or partly in Finland, 40 in Norway, 41 in Russia, and 41 in Sweden. The map includes 24 areas that cross international border (http://en.gtk.fi/informationservices). The database and map contain information on the location, mining history, tonnage and commodity grades, with comments on data quality, geological setting, age, ore mineralogy, and types of mineralization, as well as genetic models and the primary sources of data. This range of information is also important in "mapping" black shale.

Since the Fennoscandian Shield and Palaeozoic Baltoscandia provide a large variety of black shale, with different genetic characteristics and metal, sulfur and carbon occurrences, and different environmental aspects, there is a need for a new and updated assessment and re-evaluation of this resource. Data should be gathered on both Palaeozoic black shale and Precambrian metamorphic black shale.

Compared to the Fennoscandian sedimentary and metamorphic black shale, the geological position and stratigraphic characteristics of Estonian black shale are very simple. Therefore, Estonia may be a good example on which to base the future Fennoscandian-wide compilation. At the moment, in Estonia, all available information is systemised and visualised from the point of metal concentrations and distributions. The environmental impact, however, has not been well studied and the real impacts need to be uncovered.

Our proposal is to compile the geological, geochemical and environmental information into the Fennoscandian-Baltoscandian Black Shale Database (FBSD) with browser-based visualization possibilities for thematic maps (Fig. 9).

1. The database should include both sedimentary and metamorphosed black shale from the Precambrian and Lower Palaeozoic ages. There will be some overlapping with FODD data concerning some Precambrian ores, which had formerly been black shale. However, compiling Fennoscandian Precambrian and Palaeozoic black shale data according to a common standard may even add some understanding of sulphide ore geology, and especially environmental conditions.

2. The data structure should include: a) location; b) geological setting and structure, body/deposit size; c) age; d) major and trace element geochemistry, calorific values; e) ore mineralogy, style of mineralization; f) tonnage and commodity grades with a comment on data quality; g) genetic models; h) groundwater and surface geology/soil and hydrogeological parameters; i) data on biological environment/harmful element assessment; j) infrastructure and population density; k) data source and l) mining history (Fig. 9).

3. The database should have GIS-based, easily browserable thematic layers allowing for the assessment of specific impacts as well as metal/element concentrations, additional resource (oil, gas, etc.) potential assessment and more.

This database can then be used by a number of specialists and officials including mineral explorers and local government decision-makers for preparing environmental impact assessments, as well as in infrastructure and social development planning. This information is also very useful for public health monitoring and development.

As far as the mineral resource part is concerned, the European Commission already has taken steps to improve the long-term availability of raw materials through the implementation of the Raw Material Initiative in 2008. The Initiative lists fourteen economically important metals and minerals labeled as critical, that are subject to a higher risk of supply interruption (e.g. REE, PGE, Co, etc.). As some of these metals have been concentrated in black shale, black shale too could be under consideration as a source of some of the EU's critical metals in near future. Thus, the FBSD initiative would fulfill several requirements at the EU and national levels, including resource, environment, public health and economy policies.
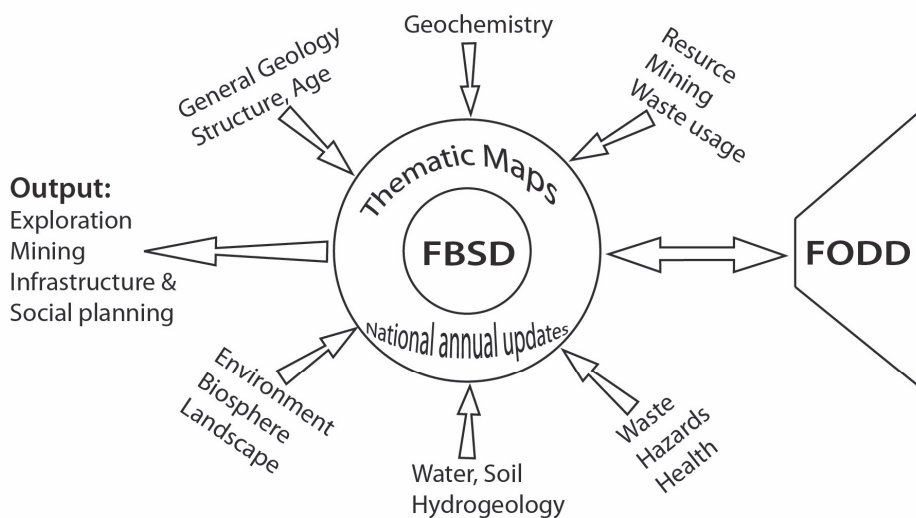
Fig. 9. Structure of a possible database (FBSD). Inputs and outputs of the Fennoscandian – Baltoscandian black shales database is shown. Tight interaction with the existing and still developing Fennoscandian Ore Deposit Database (FODD) is envisaged.

3.6. PP-GIS in studies of landscape and environmental changes

3.6.1 Environmental changes in a former military area: a case study, Paldiski Peninsula, North Estonia

The Pakri Peninsula was chosen for a pilot study because of its sensitive environment and very complex and ambiguous natural, cultural and social history, including major impacts on local landscapes during the two last centuries. Several projects have been launched on the Pakri Peninsula in recent years, but there is still lack of reliable and unified understanding how the recent changes affect local perception (Hade et al., 2005).

The Pakri Peninsula is situated in the north-western part of the Estonian mainland, Harjumaa County, between Lahepere and Paldiski Bays of the Baltic Sea. The length of the peninsula is about 12 km, the width is 5 km, and the area in total is ca 35 km^2. Geologically, the Pakri Peninsula is a plateau bordered by the Ordovician and Cambrian limestone and sandstone outcrops. The highest part of the limestone cliff on the Cape Pakri is about 25 m above the sea level. The relief of the peninsula is flat, with some ice-edge formations, like ridges and moraines. The Quaternary cover is mainly gravel, its thickness ranging from some centimeters to some meters. The Pakri peninsula is a colourful example of the North-Estonian Klint with its peculiar landscapes. The peninsula is edged by a klint escarpment, thus being one of the most

34

remarkable klint sections of the entire Baltic Klint (Soesoo & Miidel, 2007). The north-westward rising limestone plateau of the klint peninsula is nearly 25 m high at the northern tip of the peninsula (Cape Pakri) and as high is the bordering escarpment. From west of Paldiski, up to Kersalu in the east (18 km in total), the klint peninsula is bordered by a 2–24-m-high escarpment. Five separate coastal cliffs are differentiated here: Paldiski, Uuga, Pakerort, Leetse and Lahepere.

Historically, the deep and wind-sheltered Paldiski Bay has attracted seafarers already since the times of the Vikings. In the 17th century, the Swedes established a sea fortress. Peter the Great planned to build a giant military port of Rogerwiek here. Construction of the port started in 1716. Despite the efforts of thousands of convicts, the planned 2-km-long giant facility was not completed and later the completed part was quite soon destroyed by autumn storms. In 1762, Catherine II renamed the sea fortress of Rogerwiek to Baltiiski Port. The precipices and hills preserved from the fortress at the northern edge of the town are popularly known as the Peter's Fortress or Muula Hills. After the town came into the possession of Estonians, it was renamed as Paldiski in 1920. In May 1940, civilians were deported from both the Pakri Peninsula and Pakri Islands were to build Soviet military facilities here. In 1941, the area was occupied by the Germans, who burned down the town and the port at their withdrawal in 1944.

In the post-war period, the Pakri Peninsula and Paldiski town were the military sites of the Soviet Army. In 1962, Paldiski became a Soviet Navy nuclear submarine training center. Two PWR type nuclear reactors, 70 and 90 MW in output power, were used for training in safe operations of the nuclear Delta and Echo class submarine propulsion systems. With two land-based nuclear reactors, and employing some 16 000 people, it was the largest such facility in the Soviet Union. Because of its military importance, the whole town was closed off with barbed wire until the last Russian warship left in August 1994. Apart from two submarine hull sections, several other pollution-related facilities existed on the site, including liquid waste storage and treatment facilities.

The initial study was carried out in 2003 and followed by second study in 2010. The geographical map based questionnaire was used in both as printed and web-based forms. People living in Paldiski town and on the Pakri Peninsula were eligible to fill out the forms. Majority of local population preferred the web-based questionnaire. After anonymously defining person's sex, education and age, the participant moved to a set of maps where by using the paintbrush tool (in web-based version) or colour pencils (in paper version) he or she could answer the questions dealing with the extent of pollution, general landscape change and recreational possibilities on the Pakri Peninsula.

Separate maps were painted according to person's knowledge and preferences. Then the printed maps were digitised. In the Adobe Flash web-based interface the coordinates of painted sections were recorded and saved in MySQL backend database in the server with *php* scripts. By digitally summarizing all (answered) maps sheets,

the resulting maps showed in colour grades the topical perception of local people (see Fig. 10).

Figure 10 exemplifies the local perception of the question/problem – "Where has the landscape changed most during the last decade on the peninsula?" As seen, the drastic changes happened before year 2000 and in early 2000, while 2010 results show already diminishing impact on the landscape (Fig. 10). This is also true for other environmental changes, including pollution. These results show that the major landscape change and environmental impact was related to the period when the Soviet troops abandoned the area. However, the extent of environmental impact during the location of the Soviet military camp on the Pakri Peninsula is unknown because the area was closed and no such studies were conducted. Likely, the period of 10 to 15 years is minimum time to get first results on land and environment rehabilitation and, thus, change the perception of local people.
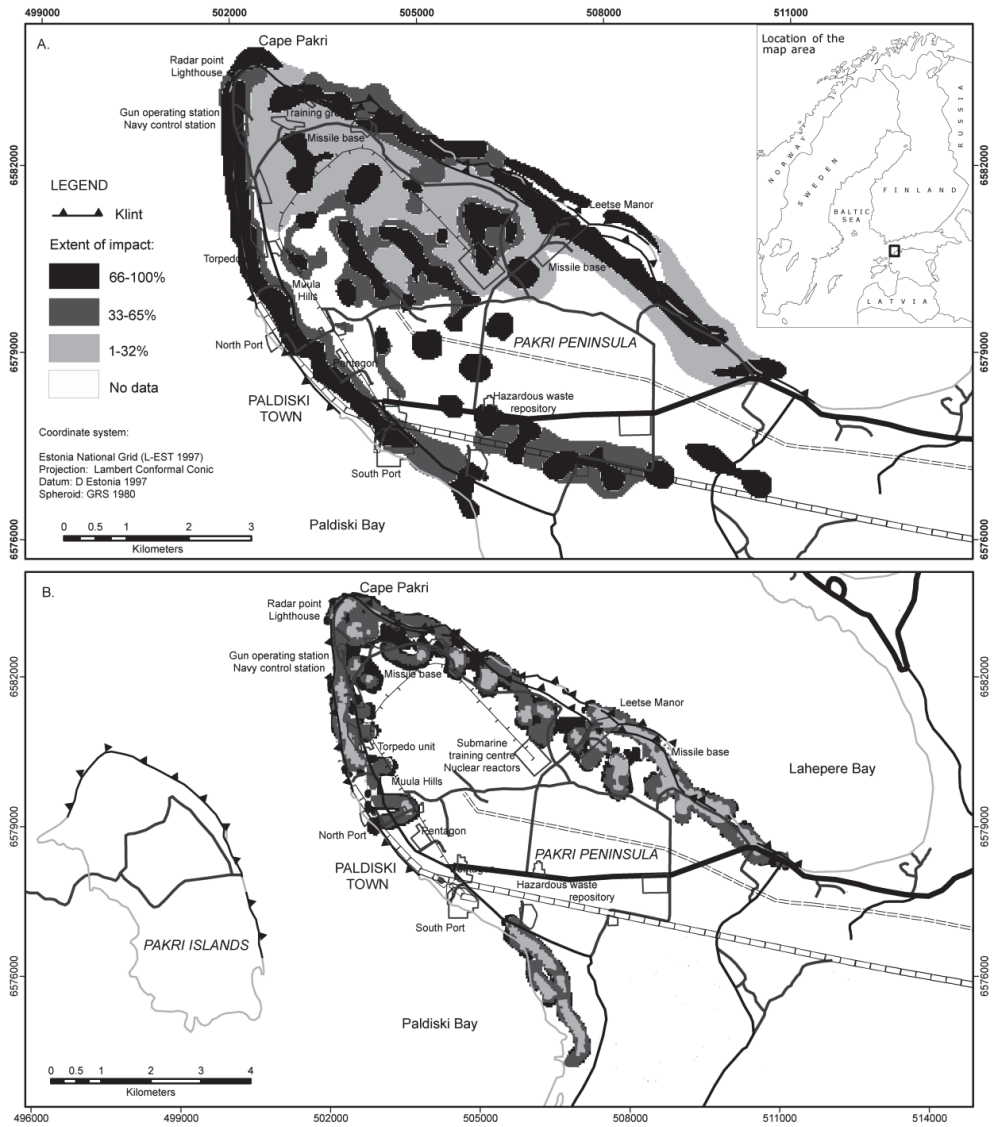
Fig. 10. Resulting sketch-map of the public geographical map-based questionnaire showing local people perception to the question "Where has the landscape most changed during the last decade on the peninsula?" The study was conducted in 2003 (A) and repeated in 2010 (B). Previous Soviet military sites are shown (presently not operational).

4. CONCLUSIONS

The occurrence of the Middle Cambrian to Upper Ordovician organic-rich black shale deposits in an extensive area of Baltoscandia has been known for a long time, but its economic and environmental impacts are not well understood. Alum shale as well as the Estonian graptolite argillite contains remarkably high concentrations of trace metals such as U, Mo, V and Ni, but may also be locally enriched with REE, Cd, Au, Sb, As and Pt.

The observed lithological characteristics of the Estonian graptolite argillite layers provide evidence that the sedimentary dynamics of the Türisalu Formation deposition time varied spatially and temporally, whereas intermittent accumulation with rapid short-term sedimentary fluxes prevailed. The cohesive sediment dispersal and deposition were mainly controlled by the near-bed storm-induced flows, which, besides causing the dynamic deposition of mud, also acted as eroding and reworking agents on muddy seafloor.

The combined database of 468 drill cores has been used as the initial data. The total estimated area (by GIS methods) of the Estonian GA on the mainland and islands is about 12 210 km^2, with the corresponding argillite volume of about 31.92 billion m^3. The estimated in situ and eroded area between the West-Estonian islands is about 3 190 km^2 with the corresponding eroded material volume of 9.02 billion m^3. The calculated total volume of Estonian GA extends up to 40 935 km^3. Assuming an average GA specific gravity of 2 100 kg/m^3, the amount of GA is about 67 billion tonnes. The amount of the material between the Estonian mainland and Hiiumaa Island is about 18.9 billion tonnes, while as minimum, the similar amount has been totally eroded in Northern Estonia.

These new thickness and element concentration models (the Estonian mainland and island, except under the sea) allow more realistic estimates of the total amount of metals in the Estonian GA (not just based on an average concentration value in ppm). For example, the calculated total weight of U is about 5.67 million tonnes (6.68 million tonnes as U$_3$O$_8$). Zn is as high as 16.53 million tonnes (20.58 million tonnes as ZnO) and for Mo is 12.76 million tonnes (19.19 million tonnes as MoO$_3$). The highest studied element amounts show somewhat similar pattern – Western Estonia has the highest potential, especially for U and Mo. However, there are also distinctions between those elements. For example, the Central Zone, where the enrichment is the lowest, still shows high amounts of Zn.

Using the thickness model, it can also be interpolated (cell size 400 X 400 m vs. thickness grid), the uranium tonnage in the region between the Estonian mainland and islands reaches 1.80 million tonnes (at an average content of 95 ppm), zinc (Zn) 22.70 million tonnes (average 1200 ppm), lead (Pb) 6.60 million tonnes (average 350 ppm), molybdenum (Mo) 4.50 million tonnes (average 235 ppm) and vanadium (V) 13.30 million tonnes (average 700 ppm). At least similar amounts have been eroded from

the northern part of Estonia (due to the Baltic Klint formation). Extrapolating the average metal contents in the drill cores of the Western, Central and Eastern zones, with emphasis on the northern drill holes, the concentration values in the eroded part can be established. The total amount of U is estimated 1.8 million tonnes, Zn – 22 million, Mo – 4.4 and V – 13 million tonnes. These values are similar to those of calculated for the Western part. However, it must be mentioned again, these values have to be considered as preliminary estimates. However, since a simple, environment-friendly and economic technology has yet to be developed for the co-extraction of most of the enriched elements from GA, its economic value remains theoretical.

Apart from being a future metal resource, the GA is also an environmental concern. During mining and re-deposition of GA, under normal weathering conditions GA oxidizes easily, and spontaneous combustion can occur. For example, in some places, for example at Maardu waste hills, in Northern Estonia, the temperatures in the heap occasionally exceeded 500 ºC. The GA, if lying on or near to the surface, is also a major source for radon. Very high radon concentrations of up to 10 000 Bq/m^3 have been recorded at some natural outcrops of GA in the North Estonian Klint. In spite of the fact that the impact of black shale on a nation's health and biological environment is well recognized, little is being done to quantify these impacts in a real and reliable way. Moreover, only a small number of measures are being taken to avoid direct contamination of soil and groundwater and direct and indirect influences on the local people. There are areas in Estonia, Sweden and elsewhere in Fennoscandia where black shale forms the surfaces where human live and conduct their everyday activities, thus directly influencing health and well-being. For example, there are a number of towns in northern Estonia, which are located in area where graptolite argillite crops out or occurs in the vicinity, including the capital Tallinn, Paldiski, Kunda, Aseri and others. These influences need to be quantified and measures taken to minimize negative health and environmental impacts.

A new, modern, science-based revision of black shale resources and related environments across Estonia – NW Russia – Sweden – Finland – Norway is proposed. This kind of data compilation will definitely foster a better understanding of the problem, and help to create an industrially and environmentally sound expert model of the Fennoscandian and Baltoscandian black shale potential. The proposed Fennoscandian-Baltoscandian-scale database should include (as minimum): a) geographical/stratigraphical position and resource/reserve estimate; b) metal/element distribution, calorific value etc.; c) environmental and health impact assessment, soil and groundwater impact. The compiled data should be put in a database and visualized in geographical space, and made accessible to the public.

Environmental issues remain in focus of relationship between the society and environment. A tool which allows matching qualitative and quantitative data with numerically immeasurable opinion of local people is called Public Participation Geographical Information System, or PPGIS. The Pakri Peninsula was chosen for a pilot study because of its sensitive environment and very complex and ambiguous

natural, cultural and social history, including major impacts on local landscapes during the last two centuries. The initial study was carried out in 2003 and followed by a second stage in 2010. The geographical map based questionnaire was used in both printed and web-based forms. The results were summarized as colour-graded maps showing perception of local people in environmental pollution, landscape change and recreational domains. The results show that the major landscape change and environmental impact was related to the period when Soviet troops abandoned the area. Likely, the period of 10 to 15 years is a minimum time to acquire first results on land and environment rehabilitation and, thus, change the perception of local people. This is a suitable GIS-based way to map the society's response to particular problems before making the local and regional decisions.

ACKNOWLEDGEMENTS

REFERENCES

ANDERSSON, A., DAHLMAN, B., GEE, D. G., SNÄLL, S. 1985. The Scandinavian Alum Shales. Sveriges Geologiska Undersökning, **56**, 1–50.

ARKIMAA, A., HYVÖNEN, E., LERSSI, J., LOUKOLA-RUSKEENIEMI, K., VANNE, J. 1999. Compilation of maps of black shales in Finland: Applications for exploration and environmental studies. In: S. Autio (ed.). Geological Survey of Finland. Spec. Paper, **27**, 113–116.

ARTYUSHKOV, E.V., LINDSTROM. M., POPOV, L.E. 2000. Relative sea-level changes in Baltoscandia in the Cambrian and early Ordovician: the predominance of tectonic factors and the absence of large scale eustatic fluctuations. Tectonophysics, **320**, 375–407.

BATURIN, N.G., ILYIN, A.V. 2013. Comparative Geochemistry of Shell Phosphorites and Dictyonema Shales of the Baltic. Geochemistry International, **51(1)**, 27–37.

BENDER B. 1993. (Ed.). Landscape: politics and perspectives. Oxford: Berg Publishers.

BROWN, G. 2012. An empirical evaluation of the spatial accuracy of public participation GIS (PPGIS) data. Applied Geography, **34**, 289–294.

BROWN, G., WEBER, D. 2011. Public Participation GIS: A New Method for Use in National Park Planning. Landscape and Urban Planning, **102(1)**, 1–15.

BROWN, G. 2006. Mapping Landscape Values and Development Preferences: A Method for Tourism and Residential Development Planning. International Journal of Tourism Research, **8(2)**, 101–113.

BROWN, G. 2005. Mapping Spatial Attributes in Survey Research for Natural Resource Management: Methods and Applications. Society & Natural Resources, **18(1)**, 1–23.

CINDERBY S. 1999. Geographic Information Systems for Participation: the future of environmental GIS? International Journal of Environment and Pollution, **11(3)**, 304–31.

COCKS, L.R.M., TORSVIK, T.H. 2005. Baltica from the late Precambrian to mid-Palaeozoic times: The gain and loss of a terrane's identity. Earth-Science Reviews, **72**, 39–66.

COSGROVE D., DANIELS S. 1988. (Eds.). The iconography of landscape: essays on the symbolic representation, design and use of past environments. Cambridge: Cambridge University Press, 318 p.

COUPER M.P., MILLER, P.V. 2008. Web survey methods introduction. Public Opinion Quarterly, **72(5)**, 831–835.

DETKOVSKI, S., PUKKONEN, E., RÜHKO, V. 1987. Eesti fosforiitide ja neid katvate setendite ainelise koostise uurimine ja metallisisalduse otsinguline hinnang aastatel 1985–1987. Report in Estonian Geological Foundation (in Russian).

DRONOV, A.V., AINSAAR, L., KALJO, D., MEIDLA, T., SAADRE, T., EINASTO, R. 2011. Ordovician of Baltoscandia: facies, sequences and sea-level changes. In:

J.C. Gutierrez-Marco, I. Rabano & D. Garcia-Bellido (eds.). Ordovician of the World, Instituto Geologico y Minero de España, Madrid, 143–150.

DUNCAN J.S., LEY D. 1993. (Eds.). Place/Culture/Representation. London, New York: Routledge. 341 p.

DUNN, C.E. 2007. Participatory GIS – A People's GIS? Progress in Human Geography, **31(5)**, 616–637.

ERDTMANN, B.-D. 1986. The planktonic nema-bearing *Rhabdinopora flabelliformis* versus benthonic root-bearing *Dictyonema Hall,* 1952. Proc. Acad. Sci. Estonian SSR, **35(3)**, 109–114.

FLEISCHER, V.D., GARLICK, W.G., HALDANE, R. 1976. Geology of the Zambian Copperbelt. Ed. K. H. Wolf. In: Handbook of Strata-Bound and Stratiform Ore Deposits. Elsevier, Amsterdam, **6**, 223–352.

GARDNER, H.D., HUTCHEON, I. 1985. Geochemistry, mineralogy, and geology of the Jason Pb-Zn deposits, Macmillan Pass, Yukon, Canada. Economic Geology, **80**, 1257–1276.

GOODSPEED, R.C. 2008. Citizen participation and Internet in urban planning. Master thesis, University of Maryland, 38 p.

GRANÖ O. 2001. The archipelago coast as a transitional zone between land and open sea – the origins and development of a research tradition grounded in the natural environment. Publicationes Instituti Geographici Universitatis Turkuensis, **164**, 11–25 (in Finnish).

GRAUCH, R.I., COVENEY, R. M. JR., MUROWCHICK, J.B., NANSHENG, C. 1991. Black shales as hosts for unconventional Platinum-Group-Element resources? Examples from China and Yukon, Canada, and implications for U.S. resources. In: U.S.G.S. Research on Mineral Resources, Seventh Annual V. E. McKelvey Forum on Mineral and Energy Resources, Reno, Nevada. U.S.G.S., Circular **1062**, 33 pp.

GUSTAVSON, L.B., WILLIAMS, N. 1981. Sediment-hosted stratiform deposits of copper, lead, and zinc. Ed. B. J. Skinner. In: Seventy-Fifth Anniversary Vol. The Economic Geology Publishing Co. Yale, 139–178.

HADE, S., SOESOO, A. 2014a. Estonian graptolite argillites revisited: a future resource? Oil Shale, **31(1)**, 4–18.

HADE, S., SOESOO, A. 2014b. Public perception in monitoring environmental conditions using GIS methods. International Journal of Research in Earth and Environmental Sciences, **1(3)**, 11–16.

HADE, S., PEIL, T., SOESOO, A. 2005. Maastikunägemus geoinfosüsteemi osana. Estonian Social Science Online 3: Special Issue of the Estonian Social Science V Annual Conference.

HEINSALU, H., KALJO, D., KURVITS, T., VIIRA, V. 2003. The stratotype of the Orasoja Member (Tremadocian, Northeast Estonia): lithology, mineralogy, and biostratigraphy. Proceedings of the Estonian Academy of Sciences, Geology, **52(3)**, 135–154.

HEINSALU, H., VIIRA, V., RAUDSEP, R. 1994. Environmental conditions of shelly phosphorite accumulation in the Rakvere phosphorite region, northern Estonia. Proceedings of the Estonian Academy of Sciences, Geology, **43**, 109–121.

HEINSALU, H. 1990. On the lithology and stratrigraphy of the late Tremadoc graptolitic argillites of North-West Estonia. Proceedings of the Estonian Academy of Sciences, Geology, **39(4)**, 142–151 (in Russian).

HEINSALU, H. 1980. On the facial relations of upper Tremadocian deposits in North Estonia. Proceedings of the Academy of Sciences of the Estonian SSR, Geology, **29(1)**, 1–7 (in Russian).

HENNINGSMOEN, G. 1960. Cambro-Silurian deposits of the Oslo region. Ed. A. Holtedahl. In: Geology of Norway. Norges geologiske undersmkelse, **208**, 130–150.

HILLER, N. 1993. A modern analogue for the Lower Ordovician Obolus conglomerate of Estonia. Geological Magazine, **130**, 265–267.

HINTS, O., NÕLVAK, J. 2006. Early Ordovician scolecodonts and chitinozoans from Tallinn, North Estonia. Review of Palaeobotany and Palynology, **139**, 189–209.

HINTS, R., HADE, S., SOESOO, A., VOOLMA, M. 2014. Depositional framework of the East Baltic Tremadocian marginal black shale revisited. *GFF*, 1–19.

HIRSH E., O'HANLON M. 1995. (Eds.). The anthropology of landscape: perspectives on place and space. Oxford: Clarendon Press, 280 p.

ILYIN, A.V., HEINSALU, H.N. 1990. Early Ordovician shelly phosphorites of the Baltic Phosphate Basin. In: A.J.G. Notholt & I. Jarvis (eds.). Phosphorite research and development. Geological Society of London Special Publication, **52**, 253–259.

JONES M. 1991. The elusive reality of landscapes. Concepts and approaches in landscape research. Norsk Geografisk Tidsskrift, **45**, 229–44.

JÜRIADO, K., RAUKAS, A., PETERSELL, V. 2012. Alum shales causing radon risks on the example of Maardu area, North-Estonia. Oil Shale, **29(1)**, 76–84.

KALJO, D., BOROVKO, N., HEINSALU, H., KHAZANOVICH, K., MENS, K., POPOV, L., SERGEJEVA, S., SOBOLEVSKAJA, R. 1986. The Cambrian-Ordovician boundary in the Baltic-Ladoga clint area (North Estonia and Leningrad Region, USSR). Proceedings of the Academy of Sciences of the Estonian SSR, Geology, **35(3)**, 97–108.

KALJO, D., KIVIMÄGI, E. 1970. On the distribution of graptolites in the Dictyonema shale of Estonia and the uncontemporaneity of its different facies. Proceedings of the Academy of Sciences of the Estonian SSR. Chemistry and Geology, **19(4)**, 334–341 (in Russian).

KIRSIMÄE, K., JØRGENSEN, P., KALM, V. 1999. Low-temperature diagenetic illite–smectite in Lower Cambrian clays in North Estonia. Clay Minerals, **34(1)**, 151–163.

KIVIMÄGI, E., LOOG, A. 1972. The main structural types of graptolitic argillites of the Toolse deposit. Proceedings of the Academy of Sciences of the Estonian SSR. Chemistry and Geology, **21(2)**, 143–147 (in Russian).

KIVIMÄGI, E., TEEDUMÄE, A. 1971. Results of a complex estimation of the rocks in the phosphorite deposit of Toolse. Proceedings of the Academy of Sciences of the Estonian SSR, Chemistry and Geology, **20(3)**, 243–250 (in Russian with English summary).

KLEESMENT, A., KURVITS, T. 1987. Mineralogy of Tremadoc graptolitic argillites of North Estonia. Oil Shale, **4(2)**, 130–138 (in Russian).

KLESMENT, I., UROV, K. 1980. Role of bacterial lipids in the formation of geolipids and kerogens. Proceedings of the Academy of Sciences of the Estonian SSR, Chemistry, **29(4)**, 241–245.

KRAUSKOPF, K.B. 1955. Sedimentary deposits of rare metals in Economic Geology. Ed. A. M. Bateman. Econ. Geol. 50th Anniversary Vol. 1905-1955, 411–463.

LILLE, U. 2003. Current knowledge on the origin and structure of Estonian kukersite kerogen. Oil Shale, **20(3),** 253–263.

LINDGREEN, H., DRITS, V.A., SAKHAROV, B.A., SALYN, A.L., DAINYAK, L.G. 2000. Illite-smectite structural changes during diagenesis of Lower Paleozoic black Alum Shales from the Baltic area. American Mineralogist, **85(9)**, 1223–1238.

LIPPMAA, E., MAREMÄE, E. 2000. Uranium production from the local Dictyonema shale in North-East Estonia. Oil Shale, **17(4)**, 387–394.

LOOG, A., KURVITS, T., ARUVÄLI, J., PETERSELL, V. 2001. Grain size analysis and mineralogy of the Tremadocian Dictyonema shale in Estonia. Oil Shale, **18(4)**, 281–297.

LOOG, A., PETERSELL, V. 1995. Authigenic siliceous minerals in the Tremadoc graptolitic argillite of Estonia. Proceedings of the Estonian Academy of Sciences, Geology, **44(1)**, 26–32.

LOUKOLA-RUSKEENIEMI, K., UUTELA, A., TENHOLA, M., PAUKOLA, T. 1998. Environmental impact of metalliferous black shales at Talvivaara in Finland, with indication of lake acidification 9000 years ago. Journal of Geochemical Exploration, **64**, 395–407.

MENS, K., PIRRUS, E. 1997. Vendian - Tremadocian clastogenic sedimentation basins. In: A. Raukas, A. Teedumäe (eds.). Geology and Mineral Resources of Estonia. Estonian Academy Publishers, Tallinn, 184–191.

MÄNNIL, R. 1966. Evolution of the Baltic basin during the Ordovician. Valgus, Tallinn, 1-200 (in Russian).

MÜÜRISEPP, K. 1964. Käsnläätsedest Pakerordi lademes. In: ENSV Teaduste Akadeemia Looduseuurijate Seltsi aastaraamat, Valgus, Tallinn, **56**, 17–24.

NEMLIHER, J., PUURA, I. 1996. Upper Cambrian basal conglomerate of the Kallavere Formation on the Pakri peninsula, NW Estonia. Proceedings of the Estonian Academy of Sciences, Geology, **45**, 1–8.

NIELSEN, A.T., SCHOVSBO, N.H. 2006. Cambrian to basal Ordovician lithostratigraphy in southern Scandinavia. Bulletin of the Geological Society of Denmark, **53**, 47–92.

NIELSEN, A.T., SCHOVSBO, N.H. 2011. The Lower Cambrian of Scandinavia: depositional environment, sequence stratigraphy and palaeogeography. Earth-Science Reviews, **107**, 207–310.

NIIN, M., RAMMO, M., SAADRE, T. 2008. Eesti maavarade kaart. Diktüoneemakilt (graptoliitargilliit).
Mõõtkava 1:400 000 (1:200 000). Kaart ja seletuskiri. Eesti Geoloogiakeskus, 2008.

OLWIG K.R. 1996. Recovering the substantive nature of landscape. Annals of the Association of American Geographers, **86(4)**, 630–53.

OVEREEM, I., WELTJE, G.J., BISHOP-KAY, C., KROONENBERG, S.B. 2001. The Late Cenozoic Eridanos delta system in the Southern North Sea Basin: a climate signal in sediment supply? Basin Res., **13(3)**, 293–312.

PAALITS, I. 1995. Acritarchs from the Cambrian-Ordovician boundary beds at Tõnismägi, Tallinn, North Estonia. Proceedings of the Estonian Academy of Sciences, Geology, **44(2)**, 87–96.

PEIL, T. 2005. Estonian heritage connection: people, past and place: The Pakri Peninsula. International Journal of Heritage Studies, **11**, 57–69.

PETERSELL, V. 1997. Dictyonema argillite. In: A. Raukas, A. Teedumäe (eds.). Geology and Mineral Resources of Estonia. Estonian Academy Publishers, Tallinn, 313–326.

PIHLAK, A.-T. 2009. On the history of investigation of self-burning processes and oxygen problems in Estonia. Infotrükk, Tallinn (in Estonian, with Russian summary).

POULSEN, V. 1966. Cambro-Silurian stratigraphy of Bornholm. Meddelelser fra Damk Geologisk Forening, **16**, 117–137.

PUKKONEN, E., RAMMO, M. 1992. Distribution of Molybdenum and Uranium in the Tremadoc Graptolite Argillite (Dictyonema Shale) of North-Western Estonia. Bulletin of the Geological Survey of Estonia, **2(1)**, 3–15.

RAMBALDI G., KWAKU KYEM, A.P., MBILE, P., MCCALL, M., WEINER, D. 2006. Participatory Spatial Information Management and Communication in Developing Countries. EJISDC, **25(1)**, 1–9.

RHEBERGEN, F. 2009. Ordovician sponges (Porifera) and other silicifications from Baltica in Neogene and Pleistocene fluvial deposits of the Netherlands and northern Germany. Est. J. Earth Sci., **58(1)**, 24–37.

RÜHKO, V., PUKKONEN, E. 1984. Fosforiite katvate kivimite (diktüoneemakiltade) geoloogilis-geokeemiline uuring. Report in Estonian Geological Foundation (in Russian).

SAWICKI, D.S., PETERMAN, D. R. 2002. Surveying the Extent of PPGIS Practice in the United States. In: W.J. Craig, T.M. Harris, D.M. Weiner (eds.). Community Participation and Geographic Information Systems. Taylor & Francis, London, 17–36.

SCHOVSBO, N.H. 2003. The geochemistry of Lower Paleozoic sediments deposited on the margins of Baltica. Bulletin of the Geological Society of Denmark, **50(1)**, 11–27.

SIEBER, R. 2006. Public Participation and Geographic Information Systems: A Literature Review and Framework. Annals of the American Association of Geographers, **96(3)**, 491–507.

SOESOO, A., HADE, S. 2014**.** Black shale of Estonia: moving towards a Fennoscandian-Baltoscandian database. Transactions of Karelian Research Centre, Russian Academy of Science, **1**, 103–114.

SOESOO, A., HADE, S. 2012. Metalliferous organic-rich shales of Baltoscandia – a future resource or environmental/ecological problem. Archiv Euro Eco, **2**, 11–14.

SOESOO, A., MIIDEL, A. 2007. North Estonian klint. Tallinn: Geoguide Baltoscandia, 32 p.

SNÄLL, S. 1988. Mineralogy and maturity of the alum shales of south-central Jämtland, Sweden. Sveriges Geologiska Undersökning, **C 818**, 1–46.

SUMBERG, A.I., UROV, K.E., AASMÄE, E.E. 1990. Characteristic of the Estonian Lower Ordovician fossil organic matter (Maardu member of the Pakerort horizon). Oil Shale, **7(3–4)**, 238–244 (in Russian with English summary).

SUNDBLAD, K., GEE, D.G. 1985. Occurrence of a uraniferous- vanadiniferous graphitic phyllite in the Köli Nappes of the Stekenjokk area, central Swedish Caledonides. GFF, **106**, 269–274.

SZYMARISKI, B. 1973. Osady Tremadoku i Arenigu na obszarze Biatowieiy. Institut Geologiczny, Prace, **69**, 1–92.

TULLOCH, D. 2007. Public Participation GIS (PPGIS). In: Encyclopedia of Geographic Information Science, SAGE Publications.

UTSAL, K., KIVIMÄGI, E., UTSAL, V. 1982. About method of investigating Estonian graptolithic argillite and its mineralogy. Acta et Commentationes Universitatis Tartuensis, Tartu, **527**, 116–136 (in Russian).

VAUGHAN, D.J., SWEENEY, M., DIEDEL, G.F.R., HARANCZYK, C. 1989. The Kupferschiefer: An overview with an appraisal of the different types of mineralization. Economic Geology, **84**, 1003–27.

VESKI, R., PALU, E. 2003. Investigation of Dictyonema oil shale and its natural and artificial transformation products by a vankrevelenogram. Oil Shale, **20(3)**, 265–281.

VINE, J.D., TOURTELOT, E. B. 1970. Geoghemistry of Black Shale Deposits – A Summary Report. Economic Geology, **65**, 253–272.

VOOLMA, M., SOESOO, A., HADE, S., HINTS, R., KALLASTE, T. 2013. Geochemical heterogeneity of the Estonian graptolite argillite. Oil Shale, **30(3)**, 377–401.

ЮДОВИЧ Я. Э., КЕТРИС М.П. 1988. Геохимия черных сланцев. Л.: Наука, 272 с.

ABSTRACT

This PhD thesis includes two different applications of GIS methods: (1) in the studies of the geology of the Estonian Palaeozoic graptolite argillite and its metal distribution, and (2) in public perception of landscape and environmental changes. It is previously known that the Estonian graptolite argillite (GA) contains remarkably high concentrations of trace metals such as U, Zr, Mo, V and Ni, however, the distribution characteristics of these metals as well total tonnage is not well known. The combined database of 468 drill cores has been used as the initial data to reconstruct layer thickness and elemental distribution models. The total area of the Estonian GA on the mainland and islands is about 12 210 km^2, with the corresponding argillite volume of about 31.92 billion m^3 and the GA amount of 67 billion tonnes (at specific gravity 2 100 kg/m^3). The estimated in situ and eroded area between the West-Estonian islands and the mainland is about 3 190 km^2 with the corresponding material volume of 9.02 billion m^3. The amount of the material between the Estonian mainland and Hiiumaa Island is about 18.9 billion tonnes, while as minimum, the similar amount has been totally eroded in the North Estonia possibly due to Pra-Neva erosional activity. These new thickness and element concentration models allow more realistic estimates of the total amount of metals in the Estonian GA. For example, the calculated total weight of U is about 5.67 million tonnes (6.68 million tonnes as U_3O_8); Zn is as high as 16.53 million tonnes (20.58 million tonnes as ZnO) and Mo – 12.76 million tonnes (19.15 million tonnes as MoO_3). The element amounts show a somewhat similar pattern – Western Estonia has the highest potential, especially for U and Mo. Using the thickness model, it can also be interpolated (cell size 400 X 400 m vs. thickness grid), the uranium tonnage in the region between the Estonian mainland and islands reaches 1.8 million tonnes (at an average content of 95 ppm), zinc (Zn) 22.7 million tonnes (average 1200 ppm), lead (Pb) 6.6 million tonnes (average 350 ppm), molybdenum (Mo) 4.5 million tonnes (average 235 ppm) and vanadium (V) 13.3 million tonnes (average 700 ppm). At least similar amounts are eroded from the northern part of Estonia (due to the Baltic Klint formation). Apart from being a future metal resource, the GA is also an environmental concern, especially due to high population density in the area where GA is lying at or close to the surface. In order to facilitate better economic and environmental assessment, a new, GIS-based spatial database of black shale resources and related environmental-social impacts across Estonia – NW Russia – Sweden – Finland – Norway is proposed.

As the environmental issues remain in focus of relationship between the society and environment, a GIS-based tool, which allows matching qualitative and quantitative data with numerically immeasurable opinion of local people, has been tested on the Pakri Peninsula. The results show that the major landscape change and environmental impact was related to the period when Soviet troops abandoned the area. Likely, the period of 10 to 15 years is minimum time to acquire first results on land and environment rehabilitation and, thus, change the perception of local people.

KOKKUVÕTE

Doktoritöö eesmärgiks on, kasutades GIS meetodeid, (1) hinnata Eesti Paleosoilise graptoliit-argilliidi (GA) kihi paksuse muutlikkust, sisalduvate metallide jaotust ja variatsiooni Eesti aladel ning (2) selgitada maastikulist ja keskkonna parameetrite muutlikkust läbi kohaliku elanikkonna nägemuse (PP-GIS).

Kambriumi kuni Vara-Ordoviitsiumi vanusega metalli- ja orgaanikarikkad settekivimid (tuntud kui alum-kildad, mustad kildad, graptoliit-argilliit) on teada laialdasel alal, mis kulgeb Leningradi oblastist üle Põhja-Eesti Lõuna-Rootsisse ja pöördub sealt põhja suunas kuni Põhja-Rootsi ning Põhja-Norra aladeni. Mitmete metallide (V, Zn, Mo jt.) kõrge sisaldus Eesti graptoliit-argilliidis on ammu teada. Vähem on teada elementide paigutus nii ruumiliselt kui läbilõigetes. Doktoritöös on kasutatud geokeemilist lähenemist ja GIS meetodeid, mis baseeruvad 468 puursüdamiku analüüsil, et koostada GA paksuse ja huvipakkuvate elementide ruumilised mudelid ning summaarselt hinnata GA massi kogu Eesti esinemisalal. Elemendilist variatsiooni on uuritud Saka (Ida-Eesti tsoon) ja Paldiski (Lääne-Eesti tsoon) läbilõigetes, mis tuvastasid kõrge elementide muutlikkuse olenemata kihi paksusest. Eesti GA hõlmab umbes 12 210 km² ala ja kivimi maht on 31,92 miljardit m³. GA kogumass, arvestades eritihedust 2 100 kg/m³ kohta, on 67 miljardit tonni. Sellele lisandub ligikaudu 18,9 miljardit tonni kivimit, mahuga 9,02 miljardit m³, mis paikneb (ja on põhjaosas kohati ära erodeeritud) umbes 3 190 km² alal Mandri- ja Lääne-Eesti saarte vahel. Ligikaudu samas mahus, minimaalselt vähemalt 19 miljardit tonni graptoliit-argilliiti on täielikult erodeeritud ja ümbersetitatud ning osaliselt lahustunud Põhja-Eesti rannikualalt Balti klindi tekkeperioodil seoses Ürg-Neeva tegevusega. Toetudes Eesti GA paksuse ja elementide kontsentratsioonide muutlikkuse mudelitele, on arvutatud elementide sisaldused kogu Eesti alal. Mudelis on kasutatud horisontaaltasapinnalist resolutsiooni 400 x 400 m. Näiteks, arvutatud elemendiline U sisaldus Eesti GA-s on 5,67 miljonit tonni (U_3O_8 sisaldus 6,68 miljonit tonni), Zn kogumass on 16,53 miljonit tonni (ZnO - 20,6 miljonit tonni), Mo 12,76 miljonit tonni (MoO_3 - 19,1 miljonit tonni). Minimaalselt 22 miljonit tonni Zn, 4,4 miljonit tonni Mo, 13 miljonit tonni V, 1,8 miljonit tonni U on ära erodeeritud ning ümbersetitatud Põhja-Eestist, Balti klindist põhja poole jäävatelt aladelt. Mudeli põhjal arvutatud metallide kogused Mandri-Eesti ja Lääne-Eesti saarte vahel on järgmised: U 1,8 miljonit tonni, Zn 22,7 miljonit tonni, Mo 4,5 miljonit tonni, V 13,3 miljonit tonni ja Pb 6,6 miljonit tonni. Lisaks sellele, et Eesti GA on mitmete metallide tulevikuressurss, on see kivim ka keskkonnaoht, eriti aladel, kus inimpopulatsiooni tihedus on kõrge ja kogukonnad paiknevad GA avamusalal. Et paremini hinnata Eesti GA, aga samuti Fennoskandia sarnase geneesiga mustade kiltade majanduslikku tähtsust ja keskkonnamõju, on töös välja pakutud Eesti, Venemaa, Rootsi, Soome ja Norra mustade kiltade ühisandmebaasi struktuur. Kasutajatele avatud brauseripõhine andmebaas annaks esmakordselt võimaluse hinnata mustade kiltade majanduslikke, sotsiaalseid ja keskkonnamõjusid koos.

Autori osalusel väljatöötatud GIS vahenditel baseeruvat internetipõhist rakendust (PP-GIS; Partner Participation GIS), mis lubab siduda keskkonna ja elanikkonnaga seonduvad kvalitatiivsed ja kvantitatiivsed muutujad ning mitte-numbriliselt mõõdetava kohalike elanike arvamuse, on katseliselt testitud Pakri poolsaarel. Rakenduse tulemused näitavad, et põhiline maastikuline muutus ja keskkonnamõju oli seotud perioodiga, mil Nõukogude Liidu väeosad lahkusid Pakri poolsaarelt. Uuringust järeldub, et 10 kuni 15 aastat on minimaalne aeg keskkonnamõjude rehabilitatsiooniks, mis kajastub otse ka kohalike elanike maastiku- ja keskkonnanägemuses.

ELULOOKIRJELDUS

Isikuandmed
Ees- ja perekonnanimi: Sigrid Hade
Sünniaeg ja -koht: 16.04.1973 Eestis
Kodakondsus: Eesti
E-posti aadress: sigrid.hade@ttu.ee

Hariduskäik
Tartu Ülikool, 1997, maastikuökoloogia ja loodusgeograafia eriala, MSc.

Keelteoskus
Inglise keel   kesktase
Vene keel   kesktase
Saksa keel   algtase

Teenistuskäik
1997–1999 Osula põhikool, õpetaja
1998–1999 Võru maavalitsuse keskkonnateenistus, looduskaitse peaspetsialist
1999–2000 Võru maavalitsus, arengu- ja planeeringu osakonna planeeringutalituse juhataja
2000–2007 Keskkonnaministeerium, Haanja looduspark, maa ja planeeringu spetsialist
2007–2012 Tallinna Tehnikaülikool, TTÜ Geoloogia Instituut; Projekti assistent (1.00)
2012– ... Tallinna Tehnikaülikool, TTÜ Geoloogia Instituut, Füüsikalise geoloogia õppetool; Assistent (1.00)

Teadustegevus ja juhendatud lõputööd
Teadustegevuse valdkonnaks on GIS analüüs ja rakendus Maateadustes, geoloogilistes ja geokeemilistes uuringutes, graptoliitargilliidi uuringud GIS meetoditega.
2008 Liiva geoloogiline uuring Kõpu poolsaarest loodes: kaardimaterjali koostamine, varude piiritlemine ja varuarvutus.
2010–2012 Jordaania põlevkivi uuringute projektis osalemine: kaardimaterjali koostamine ja ruumiline analüüs, geoloogilise kaardi koostamine.
2009–2012 Osalemine teadusteema "Fennoskandia ja Baltika litosfääri evolutsioon: geokeemia, geokronoloogia, paleokeskkond ja mineraalsed ressursid" koosseisus projekti täitjana.

CURRICULUM VITAE

Personal data
      Name: Sigrid Hade
      Date and place of birth: 16.04.1973 Estonia
      E-mail address: sigrid.hade@ttu.ee
      Nationality: Estonian

Education
      University of Tartu, 1997, Institute of Geography, specialising on landscape ecology and nature geography, MSc.

Language competence

English	average
Russian	average
German	basic skills

Professional employment
      1997–1999 Osula Primary School, teacher
      1998–1999 Võru County, leading specialist of natural protection
      1999–2000 Võru County, head of sub-department of development and planning
      2000–2007 Ministry of Environment, Haanja National Park, Specialist of natural planning
      2007–2012 Tallinn University of Technology , Institute of Geology at TUT; Project assistant (1.00)
      2012– ... Tallinn University of Technology , Institute of Geology at TUT, Chair of Physical Geology; Assistant (1.00)

Research activity and thesis supervised
      Main scientific interest: the Earth's crust geological variability studies applying the GIS techniques, including analysis of geochemical anomalies and the use of natural resources.
      2008 Geological study of sand deposites in Hiiumaa area: preparing of map material and resources calculations.
      2010–2012 Participation in Jordan oil shale research project: preparing of map material and spatial analyses, geological map compilation
      2009–2012 Participation in research topic "Evolution of the Fennoscandian-Baltic lithosphere: geochemistry, geochronology, paleoenvironments" as project participant.

PAPER I

HINTS, R., HADE, S., SOESOO, A., VOOLMA, M. 2014. Depositional framework of the East Baltic Tremadocian black shale revisited. *GFF*, 1 - 19.

Depositional framework of the East Baltic Tremadocian black shale revisited

RUTT HINTS, SIGRID HADE, ALVAR SOESOO and MARGUS VOOLMA

Abstract: This article presents a centimetre- to micrometre-scale study of sedimentary fabrics from Lower Ordovician metalliferous black shale from the Baltic palaeobasin. Two sections of the Türisalu Fm. NW and NE Estonia were analysed with light microscopy and scanning electron microscopy. This rock unit is characterised by mostly thin bedding ($< 10\,mm$), common occurrence of minor erosional features, and a large variety of sedimentary fabrics, including graded, cross-laminated and massive fabrics. Based on this, we suggest that dynamic sedimentation events, rather than commonly assumed slow net sedimentation, may be the dominant mechanism behind the accumulation of these beds. The storm-related near-bottom flows and the bed-load transport of mud particles were likely common distribution agents of organic-rich mud. The mud (re)distribution, mainly via near-bottom flows and controlled by flat seafloor topography and general clastic starvation, might explain the present lateral distribution and diachronous character of the Türisalu Fm. Documented traces of microbial mat growth and siliceous sponges in the NW Estonia indicate that in more sheltered settings, biogenic factors played a vital role in developing primary mud characteristics. The geochemical palaeoredox proxies, and high trace metal and organic matter content suggest that mud sedimentation could occur under anoxic conditions. The observed sedimentary fabrics and traces of bioturbation, however, favour prevailing oscillating redox conditions in the lower water column. The recorded heterogeneity of microfabrics indicates that dynamic transport and intermittent deposition together with biogenic factors likely forced the development of an array of unique (bio)geochemical microenvironments for syngenetic trace element sequestration.

Keywords: black shale; sedimentary fabrics; Türisalu Fm.; event sedimentation; microbial mat; trace elements.

Institute of Geology at Tallinn University of Technology, Ehitajate tee 5, 19086 Tallinn, Estonia; Rutt. Hints@ttu.ee, sigrid.hade@gmail.com, Alvar.Soesoo@gi.ee, Margus.Voolma@gi.ee

1. Introduction

Distal deep marine settings with stratified water columns were long considered a unique environment of black shale formation, and accumulation processes were envisioned as a slow, continuous net sedimentation of fine-grained organic and inorganic particles from a starved, persistently anoxic water column, which resulted in the formation of finely laminated mud intervals (Potter et al. 1980). Reports of shallow-water marginal black shales from many locations (e.g. Leckie et al. 1990; Schieber 1994; Wignall & Newton 2001), as well as the accumulation of a wealth of data in the modern marine research of organic-rich muds and their ancient analogues (e.g. Ganeshram et al. 1999; Lyons & Kashgarian 2005), in modern and ancient mud sedimentology and mudstone lithology (e.g. Traykovksi et al. 2000; Schieber et al. 2007; Macquaker et al. 2010a; Ghadeer & Macquaker 2011; Plint et al. 2012), advances in experimental mud research (e.g. Baas et al. 2011; Schieber 2011 and references there in) and in organic-rich mudstone geochemistry (e.g. Algeo & Maynard 2004), organic geochem-

istry (e.g. Blumenberg & Wiese 2012) and geobiology (e.g. Pacton et al. 2007) have revealed that many variable formation paths might have produced different black shales. Those discoveries indicate that organic-rich mud intervals might form under an agitated water column in shallow settings (e.g. Schieber 1994), and they in places contain event beds, erosion surfaces and other signs of a discontinuous sedimentary record (e.g. Schieber & Yawar 2009). Likewise, the occurrence of black shale does not necessarily reflect a permanently anoxic water column (e.g. Pedersen & Calvert 1990; Murphy et al. 2000; Schovsbo 2001; Egenhoff & Maletz 2012), and typical fossil black shales can contain various signs of benthic life (e.g. Kazmierczak et al. 2012).

The new discoveries allow us to revisit some of the controversial aspects of the sedimentary framework of the black shales that have long been known in Estonian Tremadocian succession. Those organic-rich and metalliferous black shales, formed in proximal settings of the vast

epicontinental sea of the Baltica palaeocontinent during an overall eustatic sea-level rise (Dronov et al. 2011), have been mainly described as shallow-water deposits (e.g. Scupin 1922; Kivimägi & Loog 1972), which accumulated in water depth near storm wave base (e.g. Heinsalu 1990; Artyushkov et al. 2000). In basinal scale, Schovsbo (2002) places Estonia within the inner-shelf environment of the Cambrian–Tremadocian black shales, i.e. to innermost and shallowest area of black shale formation in the Baltic palaeobasin. However, a considerably deeper water origin of more than 130 m has been suggested by some researchers for considered black shales (e.g. Pukkonen & Rammo 1992). The previous studies have indicated spatial regional-scale lithological heterogeneity and facies differences of the Türisalu Fm. between western and north-eastern Estonian settings, as well as the existence of small-scale lithological features, such as the random occurrence of cross-lamination, small ripple marks, irregular silt intercalations, traces of bioturbation and benthic sessile communities (Müürisepp 1964; Kaljo & Kivimägi 1970; Kivimägi & Teedumäe 1971; Kivimägi & Loog 1972; Heinsalu 1990; Pukkonen & Rammo 1992; Loog & Petersell 1995). However, the sedimentary framework behind those lithological features remains poorly understood. Recently, submillimetre- to millimetre-scale vertical lithological hetero-geneity has been recognised as a common feature in a wide variety of mudstones, including organic-rich mudstones (Aplin & Macquaker 2011 and references there in). In the case of the Türisalu Fm., the existence of pronounced spatial and subtle decimetre-scale vertical trace metal variability has been documented (Pukkonen & Rammo 1992; Soesoo & Hade 2012; Voolma et al. 2013). Whereas the syngenetic enrichment of redox-sensitive trace metals is a widely accepted pathway for metal sequestration in typical black shales (e.g. Algeo & Maynard 2004), the enrichment models are commonly based on the generalisation that sedimentation rates of primary mud remained constant over long periods, there suspension–redeposition of sediments and bioturbation are negligible according to their accumulation, and the physicochemical character of primary mud was not notably variable. Such simplifications, however, might not be appropriate for interpreting enrichment processes in shallow-water marginal black shales.

This article is based on the analysis of micrometre- to centimetre-scale fabrics of two sections from the Baltic Klint area, both representing the proximal settings of the Türisalu Fm. on Estonian territory. The aims of the study were to (1) document the vertical variability of small-scale sedimentary fabrics in the Türisalu Fm., (2) discuss a possible accumulation dynamics (physical factors) and the biogenic factors forming the observed fabrics, (3) outline the main features of sedimentary environment of ancient mud successions based on combined lithological and geochemical palaeoredox signals and (4) examine the possible influence of sedimentary dynamics and synsedimentary biogenic processes on organic matter (OM) and trace metal sequestration processes.

2. Geological background

The black shale of the Türisalu Fm. (historically known as *Dictyonema* shale or *Dictyonema* argillite, also the term "graphite argillite" is widely used in recent local literature) is an organic-rich black shale that formed in the proximal settings of the Baltic palaeobasin in the Early Ordovician (Männil 1966) when Baltica was at approximately 40–50° southern latitudes

(Fig. 1A and B) (Cocks & Torsvik 2005). Between Mid-Cambrian and Early Ordovician, the Baltica made through anti-clockwise rotation. At the beginning of Tremadocian, Baltic palaeobasin was situated at western margins of the continent, facing the Iapetus Ocean in the west and the Tornquist Sea in the south and south-west (Cocks & Torsvik 2005). On a regional scale, the Türisalu Fm. is part of a patchy (modern distribution) but vast Mid-Cambrian–Lower Ordovician black shale belt in the Baltoscandian region, extending in the east–west dimension from Lake Onega to Jutland (Andersson et al. 1985; Kaljo et al. 1986). It was accumulated in a large, exceptionally flat-floored epicontinental sea (Nielsen & Schovsbo 2011). Nielsen & Schovsbo (2006) considered the Estonian and Russian Tremadocian black shale to be a shallow-water tongue of the Alum Shale Fm. In Estonia, the almost flat-lying Türisalu Fm. occurs within the tectonically undisturbed lower Palaeozoic sedimentary succession, and the entire Palaeozoic sedimentary complex is generally characterised by very low thermal maturity (Kirsimäe et al. 1999). Its distribution in Estonia and Russia has been considered one of the best examples of very shallow-marine near-shore Cambrian and Early Ordovician deposits with siliciclastic sedimentation (Kaljo et al. 1986; Mens & Pirrus 1997; Artyushkov et al. 2000).

Dark-brown black shale of the Türisalu Fm., which contains fossilised fragments of early planktonic graptolites, is characterised by high OM content ranging from 10% to 20%, fine silt fraction dominating the composition and variable pyrite abundance (Kaljo & Kivimägi 1970; Loog et al. 2001). Another characteristic feature of the black shale is its high but spatially variable content of redox-sensitive trace elements, such as V, U and Mo, showing general positive covariance with OM abundance (Pukkonen & Rammo 1992). In Estonia, the thickness of the formation remains between 1 and 8 m, generally decreasing eastward and southward from the area of maximum thickness in north-western Estonia. The Türisalu Fm. occurs on top of a complex of commonly cross-bedded siltstone and sandstone (Kallavere Fm.) containing debris or rich coquinas of phosphatic brachiopods denoting a large-scale skeletal phos-phorite accumulation episode during the Cambrian–Ordovician transition (Ilyin & Heinsalu 1990; Hiller 1993). These siliciclastic deposits also contain interbeds and lenses of black shales. In NW Estonia, a thick organic-rich mudstone bed caps a subaerial regional unconformity at the base of the transgressive Kallavere Fm. (Nemliher & Puura 1996). In NE Estonia, the black shale overlies the siliciclastic beds of the Kallavere Fm., presenting dense interfingerings of siltstone with phosphatic detritus and organic-rich mudstone beds (Heinsalu et al. 2003). The onset of accumulation of primary organic-rich muds of the Türisalu Fm. across Estonia was not concurrent (Kaljo & Kivimägi 1970) (Fig. 1C). The older black shales in western Estonia belong to the *Cordylodus lindstromi/angulatus* con-odont biozones (Pakerort Regional Stage). Eastwards the black shales become gradually younger, and in NE Estonia, the succession is assigned to the *Paltodus deltifer pristinus* conodont zone (Varangu Regional Stage; Kaljo et al. 1986; Heinsalu et al. 2003). The Varangu age generally denotes a major regressive episode in the region (e.g. Dronov et al. 2011). The upper boundary of the Türisalu Fm. comprises a regional unconformity that is capped by organic-poor grey shales or glauconitic sandstones (Heinsalu 1980) and marks a sea-level drop that terminated organic-rich mud accumulation in the proximal settings of the Baltic palaeobasin.
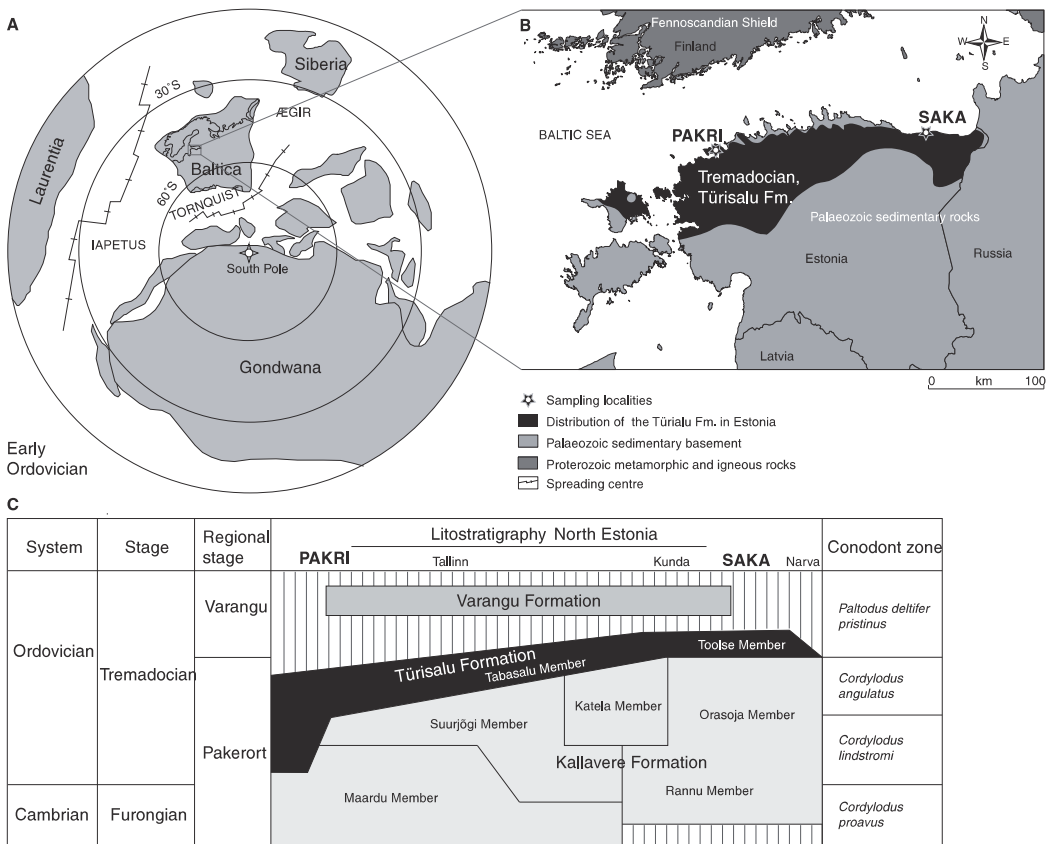
Fig. 1. **A**. Palaeogeography of Baltica in the Early Ordovician (after Cocks & Torsvik 2005). **B**. Modern distribution of the Türisalu Fm. and sampling localities on Baltic Klint. **C**. Lithostratigraphy of the Tremadocian deposits of Estonia (after Heinsalu et al. 2003).

Lithology and facies of the Türisalu Fm. have been targeted by several studies, including Müürisepp (1960), Kaljo & Kivimägi (1970), Kivimägi & Teedumäe (1971), Heinsalu (1980) and Heinsalu (1990). In western and north-central Estonia, the Türisalu Fm. has been described as a considerably homogeneous black shale comprising laminated or massive lithologies (Tabasalu Member). The massive black shale varieties that are dominant in somewhat younger north-central Estonian settings have supposedly accumulated under more active hydrodynamic regime than the beds in the western settings (Pukkonen & Rammo 1992). However, Heinsalu (1990) reported irregular encounters of cross- and wavy-lamination, trace fossils and minor ripple marks in older western Estonian black shales. In NE Estonia, the Türisalu Fm. becomes thinner and more variable (Toolse Member). It embodies numerous silt intercalations that are regularly associated with authigenic carbonate or sulphide mineralisation, and the entire Türisalu Fm. has been suggested to represent a shallower-water setting and a more variegated sedimentation environment than represented by the Tabasalu Mb. (Kaljo & Kivimägi 1970; Kivimägi & Loog 1972; Loog et al. 2001). For example, in the Toolse area, the Türisalu Fm. was divided into four distinct intervals with different textural

and structural characteristics and trace metal content (Kivimägi & Teedumäe 1971). Furthermore, Heinsalu et al. (1994) suggested that the areas around Toolse and Rakvere (Rakvere Phosphorite Area) acted as a border zone between subenvironments with different hydrodynamic regimes in this proximal part of the palaeobasin during the Early Tremadocian and that subaerial highs likely existed in this shallow-water area before a main organic-rich mud accumulation episode.

In the rather homogenous mineral assemblages of the Türisalu Fm., K-feldspar has been found to be dominant over quartz, illite−smectite and illite (Utsal et al. 1982; Kleesment & Kurvits 1987; Loog & Petersell 1995; Loog et al. 2001). High K-feldspar content is the characteristic feature of the Türisalu Fm., distinguishing the complex from the typical Alum Shale Fm. in which K-rich clay minerals (illite and illite−smectite) tend to dominate in mineral assemblages, and which have been reported to present generally lower K_2O/Al_2O_3 molar ratio than Tremadocian black shales from Estonia (Snäll 1988; Lindgreen et al. 2000; Schovsbo 2003). It is remarkable that substantial amounts of K-feldspar in the Türisalu Fm. is likely authigenic in origin (Utsal et al. 1982; Loog et al. 2001; unpublished data). For quartz, a genetic link with primary biogenic silica has been
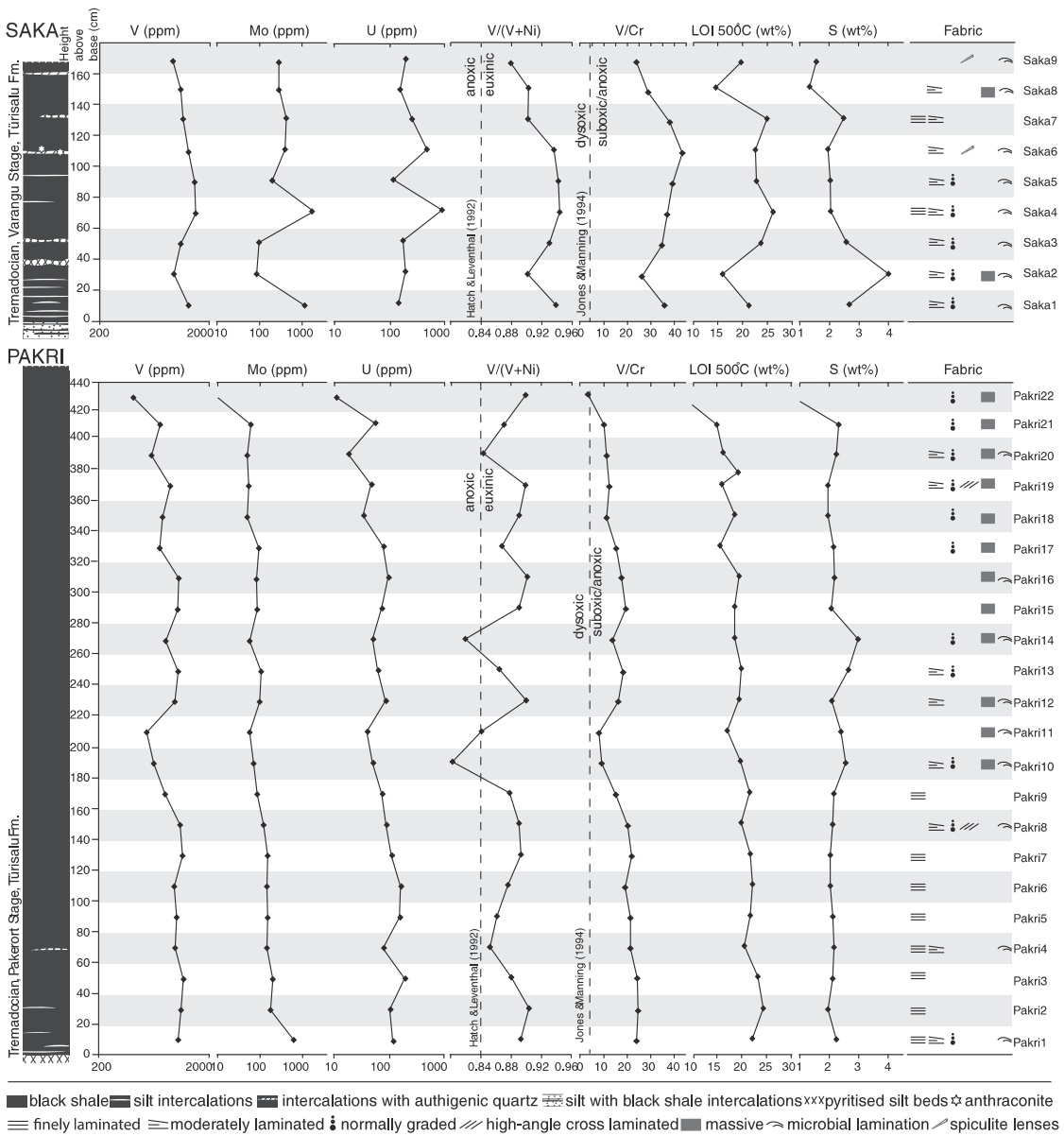
Fig. 2. The cross-section of the Saka and Pakri sections, with sampling intervals, vertical profiles of redox-sensitive trace elements, palaeoredox proxies (after Hatch & Leventhal 1992; Jones & Manning 1994), environmental indices based on data by Voolma et al. (2013) and observed sedimentary fabrics.

suggested in NE Estonia, where lenticular intercalations of siliceous sponges are common (Müürisepp 1964; Loog & Petersell 1995). The OM of the Türisalu Fm. is N-rich, highly aromatic and, according to previous studies, composed dominantly of transformation–condensation products of marine microbial matter (Klesment & Urov 1980; Sumberg et al. 1990;

Lille 2003). From other biogenic components, early planktonic graptolites, fragments of phosphatic lingulid brachiopods, conodonts, acritarchs and polychaete jaws have been reported (e.g. Kaljo & Kivimägi 1970; Kaljo et al. 1986; Paalits 1995; Hints & Nõlvak 2006). A characteristic of the Türisalu Fm. is the absence of calcareous fossils.

3.   Materials and methods

This study is based on two sections of the Türisalu Fm. from the Saka Cliff (59.4419°N, 27.2150°E) and the Pakri Peninsula Uuga Cliff (59.3766°N, 24.0364°E). Thick and rather homogeneous Pakri section (Pakerort Stage, Türisalu Fm. and Tabasalu Member (after Mens et al. 1996)) represents transitional black shale setting between western Estonian considerably organic- and metal-rich and the more massive and trace metal poor northern central Estonian settings (cf. Heinsalu 1990; Pukkonen & Rammo 1992). The lithologically more variable Saka section is part of the heterogeneous NE Estonian Toolse Member (Varangu Stage, Türisalu Fm. and Toolse Member (after Heinsalu et al. 2003)) and is known to contain abundant lenses of siliceous spicules and small anthraconites (Müürisepp 1964).

For this study, the Pakri and Saka sections were sampled at 20-cm intervals. From each collected field sample, approximately half was crushed and homogenised for major and trace element analyses (Voolma et al. 2013). The rest was used for lithological study. For fabric analysis presented in this article, five to seven subsamples from every field sample were selected randomly, cut perpendicular to bedding and roughly polished. The polished surfaces of the subsamples were scanned with a high-resolution flatbed scanner and studied with a light microscopy (Leica M205 A) to establish small-scale fabrics and stacking successions. In selected subsamples, the morphology of bedding planes was also studied on surfaces that were fractured parallel to bedding. Microfabric study and microanalyses of selected samples from both sections were carried out with a scanning electron microscopy (SEM) (Zeiss EVO MA15) equipped with EDS (Oxford INCA) at the Institute of Geology at Tallinn University of Technology. Fig. 2 presents schematic sections of both study locations, sampling intervals together with enriched trace metal profiles, and some commonly used geochemical palaeoredox and environmental indices based on data of Voolma et al. (2013). Note that the geochemical data are results of analyses of homogenised whole-rock samples, each representing average chemical composition of 20 cm long interval of studied sections. The presented loss on ignition (LOI, at 500°C) values can be used as rough estimates of the OM content. Fig. 2 also summarises the main fabric types recorded in both sections. The studied samples and data are deposited at the Institute of Geology at Tallinn University of Technology.

4.   Observations

4.1   Small sedimentary fabrics

The examination of samples from the Pakri and Saka sections demonstrated the existence of submillimetre-to-centimetre range vertical in homogeneity of the black shale. Based on variations in bed thickness and continuity, lamination and bedding boundary characteristics, and the existence of grading and biogenic features, a number of distinct black shale varieties with dominant sedimentary–fabric types were distinguished. However, the listed varieties do not cover the complete array of encountered fabrics, as in several cases beds with mixed characteristic features, or the later overprinting (e.g. diagenetic growth of carbonate concretions and secondary gypsum) of primary fabrics was observed. The samples from both sections were mostly organised into rather thin beds with a common thickness of less than 10 mm. The bed boundaries were traceable by thin silt intercalations or by colour, fabric or macrocomponent contrast between the beds. The thicker

average bed sizes of up to 5 cm (and rarely more) were encountered in the upper portion of the Pakri section, in the part dominated by massive varieties.

4.2   Beds with laminated fabrics

Fig. 3A demonstrates black shale samples with millimetre-scale laminated planar fabric, a characteristic of the lowest organic-rich part of the Pakri section, but encountered also at some levels of the Saka section. Those beds were fine grained and well sorted. The lamination appeared as an alteration of darker, more organic-rich, and lighter, less organic containing thin continuous laminae. However, many finely laminated beds from the studied sections appear to present subtle discontinuous lamination with minor asymmetric mud lenses and uneven bedding surfaces (Fig. 3B). Furthermore, in the case of somewhat less sorted samples, low-angle cross-lamination was observed, showing curved down-dipping laminae or inclined non-parallel bedding surfaces (Fig. 3B–D). Few bedding planes of finely laminated beds from the lower part of the Pakri section revealed poorly preserved remains of *Rhabdinopora* sp. (Pakri 2 and 4).

4.3   Graded beds

In addition to laminated fabrics, graded black shale varieties were regularly encountered in the studied sections. The upward-fining beds recorded in the Türisalu Fm. had typical average thicknesses between 0.5 and 5 mm and were invariably sharp-based with flat or rough basal surfaces, the latter presenting common scour-like structures. The normal graded fabrics were widespread in the Saka section and in the upper part of the Pakri section. The beds with well-pronounced normal grading (Fig. 4A–D) comprised either couplets of silt- or organic-rich lamina sets or, in some cases, exhibited a triplet motive similar to that described by Macquaker et al. (2010a). In some intervals, the lower lamina sets of such graded beds presented distinct curved ripple-laminated fabrics. The proportion of graded beds from the upper part of the Pakri section and a few subsamples from the middle and upper part of the Saka section showed more gradational changes. In those cases, the grading appeared as a decrease in grain size or in the marine detritus content and as a colour shift from light brown to darker brown, indicating an increase in organic fraction in upper part of beds (Fig. 4E). Sharp and flat lower contacts were the characteristics for such beds.

4.4   Cross-laminated beds with soft sediment deformation structures

High-angle cross-laminated black shales with ripple sets were encountered in distinct intervals of the Pakri section (Pakri 8 and 19; Fig. 5A and B). The curved bedding surfaces, as well as abundant soft sediment deformation features, such as load structures, were typical for such beds, indicating sediment loading on uncompacted and water-enriched mud.

4.5   Beds with massive fabrics

The examination of the upper portion of the Pakri section revealed several intervals dominated by massive and thick beds compared with the rest of the section. The observed lithologies varied from isotropic massive fabric to poorly sorted irregular varieties (Fig. 5C and D), the latter containing detritus of phosphatic brachiopods. The other typical features were the absence of erosional features at the bed base, sharp bedding
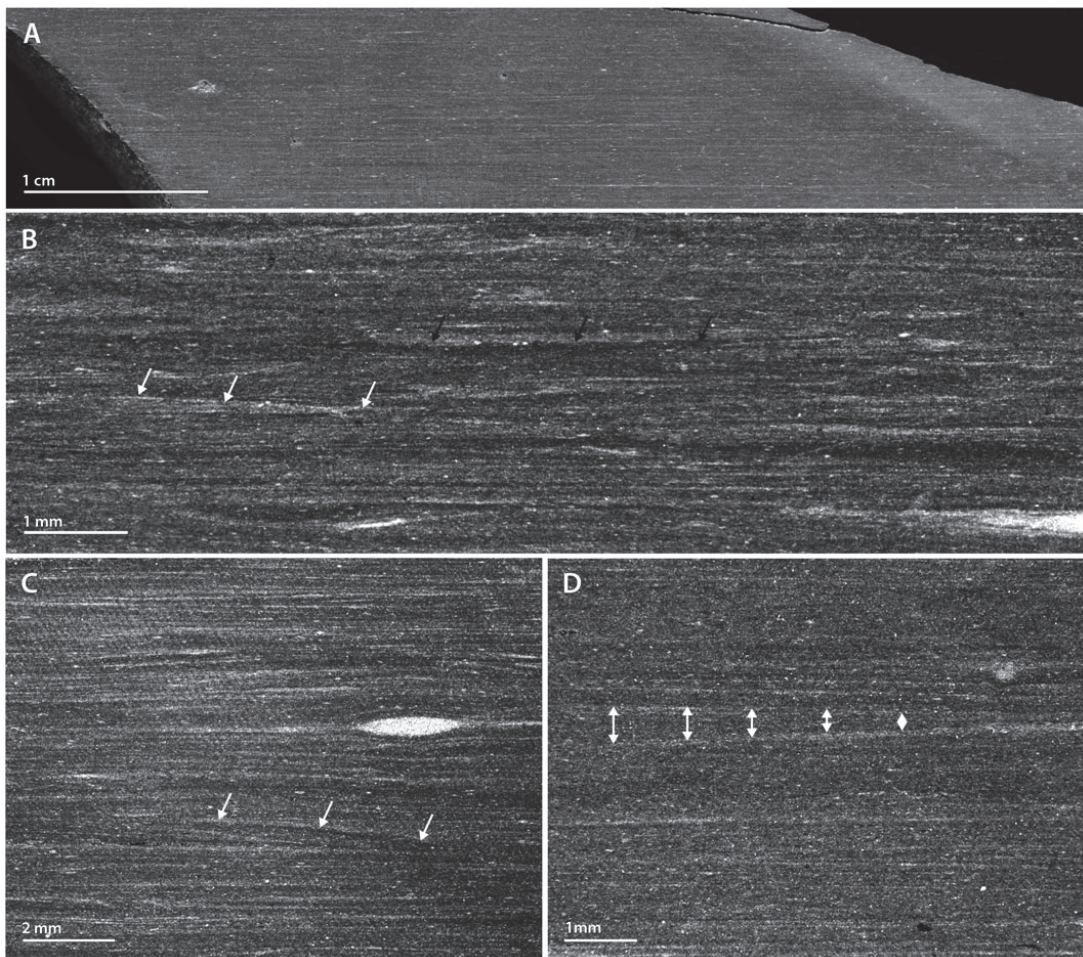
Fig. 3. Scanned image (A) and micrographs (B–D) of small-scale laminated fabrics. **A**. Subsample Pakri 4-1 with finely laminated planar fabric. **B**. Laminated fabric (Pakri 2-1) with subtle non-parallel lamina geometry showing thin, discontinuous black shale laminae (white arrows) and eroded uneven bedding surfaces (black arrows). **C**. Pakri 4-2 exhibits discontinuous fine lenticular lamination; arrows mark down-dipping surface of the possible ripple lamina. **D**. Pakri 9-1 with inclined non-parallel planar bedding boundaries.

boundaries and the irregular thickness distribution of intimately stacked beds. Some massive beds from the middle part of the Pakri section presented different characters with indistinct bedding boundaries and halo zones (see also section on biogenic fabrics).

4.6   Siliciclastic intercalations

The siliciclastic intercalations and lenses with thickness of a few grains to several centimetres were recorded throughout both sections, whereas their frequency was higher in the Saka section. In both sections, the thickest intercalations were confined to the lowermost ∼ 60 cm of the Türisalu Fm. Siliciclastic intercalations were sharp-based and regularly with scoured lower contacts. In addition to angular to subrounded quartz, the thicker studied

intercalation contained variegated sulphide paragenesis, rare glauconitic grains and marine detritus including phosphatic brachiopods and conodonts. Rather typical for the siliciclastic beds of the lower part of the Saka section was the occurrence of well-preserved, coarse euhedral muscovite. In the lower part of the same section, thin silty laminae were occasionally observed on the top of gradational upper contact of black shales beds, whereas grain sizes of silt particles matched with those from the underlying strata.

4.7   Beds with biogenic fabrics (biolamination, spiculite lenses and bioturbation)

The studied sections revealed a number of fabrics, which were likely formed by biogenic factors. Throughout the Saka section
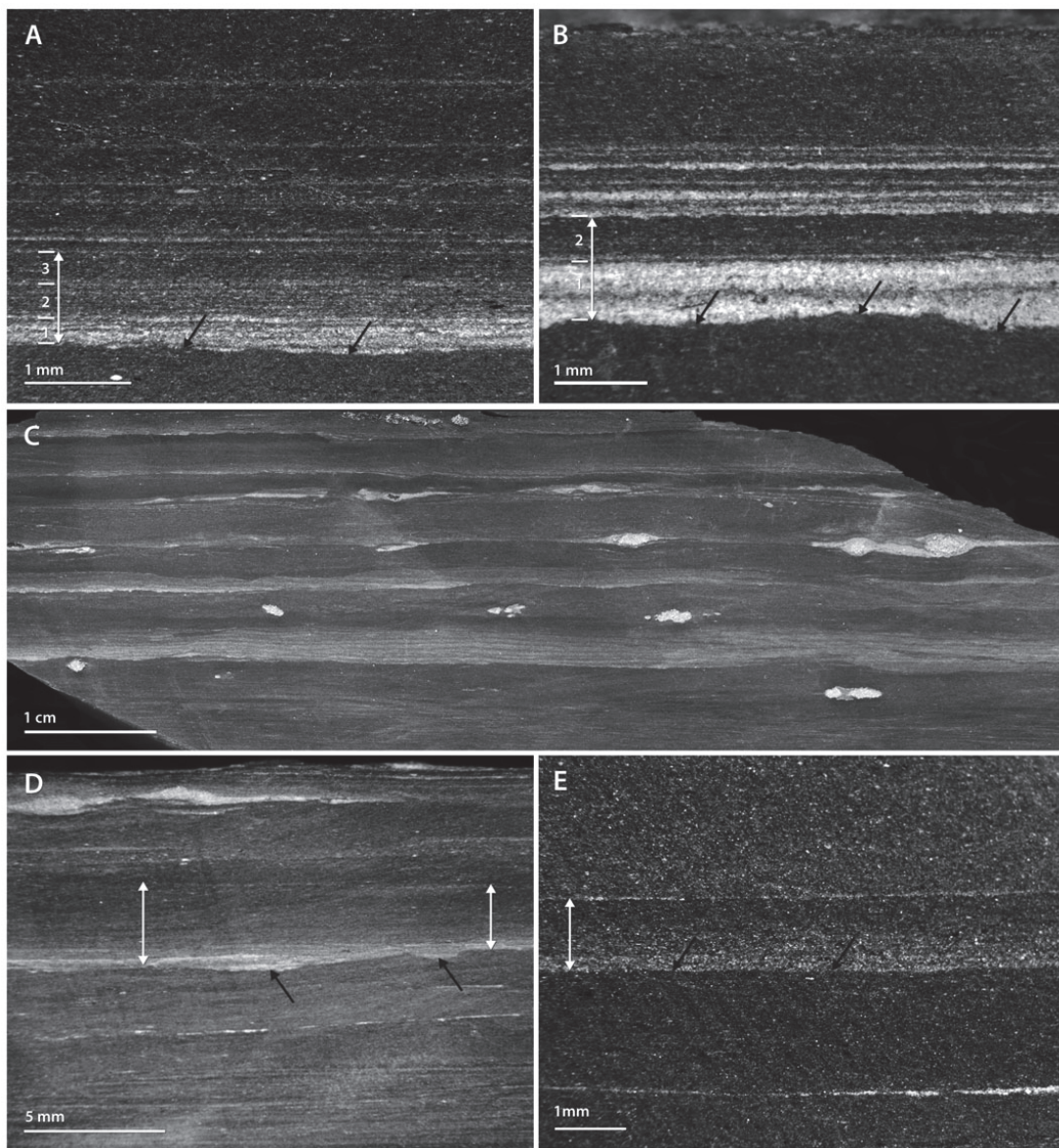
Fig. 4. Micrographs (A, B, D and E) and scanned image (C) of the studied black shales with normal graded fabrics. **A**. Pakri 10-1 presents sharp grading with triple fabric (individual lamina sets of single bed marked by numbers) comprising a lower silt-rich, an intercalated silt-rich and an organic/clay-rich lamina set and upper organic/clay-rich lamina set. Note the irregular surface below the bed (black arrows). **B**. Saka 1-1 presents fabric with a graded appearance, with silt-rich lower and dark organic-rich upper lamina sets (individual lamina sets marked by numbers). Black arrows mark the irregular bedding boundary. **C**. Succession of graded beds of sample OM8-105 from the uppermost half metre of the Pakri section; the lower silt-rich lamina set shows small-scale hummocky cross-lamination. **D**. Pakri 13-1 with graded fabric and scour structures (black arrows) at bedding surface; note the irregular thickness of the graded bed. **E**. Gradually graded bed of Saka 4-1 with smooth lower contact.

and in some intervals of the Pakri section, beds with wavy-crinkly lamination were observed (Fig. 6C–E). They appeared as very dark brown to black, dense, subparallel curved laminae,

best visible at the top lamina set of beds, or as wavy crinkly intercalations in silt interlayers. A different type of supposed biolamination was encountered in some intervals of the Pakri
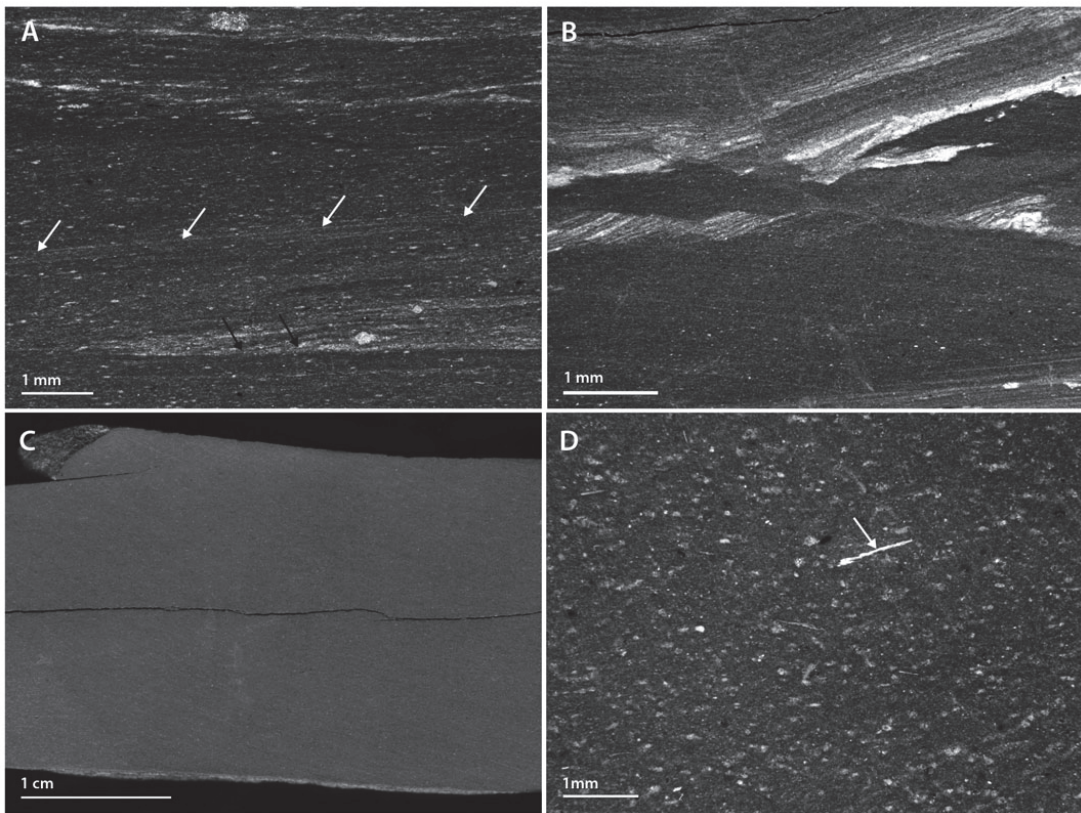
Fig. 5. Micrographs (A, B and D) and scanned image (C) of the black shales with high-angle cross-laminated and massive fabrics. **A**. Subsample Pakri 8-1 exhibits cross-lamination, grading and curved bedding boundaries. Note inclined laminae (white arrows) and down dipping of laminae to the basal surface (black arrow). **B**. Black shale (Pakri 19-1) with ripple sets, grading, curved bedding boundaries and flame structures. **C**. Well-sorted black shale (Pakri 19-2) with featureless massive fabric. **D**. Black shale with massive fabric from Pakri 17-1, white arrow marks the randomly oriented platy fragments in the poorly sorted bed.

section, where firm organic-rich filaments comprised an irregular web in black shale and presented features such as coated mineral grains and vertically oriented filaments (Fig. 6A and B). The additional features of probable biolaminated beds were mica flakes at wavy bed surfaces and the layer-specific distribution of pyrite. In the Saka section, distinctive cross-laminated fabrics were encountered in two intervals in which the thoroughly cross-laminated nature of the beds was traceable thanks to inclined lenses of spicules and quartz (Fig. 7A and B). It is noteworthy that such cross-laminated spicule-rich fabrics occur in an organic-rich and rather metalliferous part of the section (Fig. 2). In the upper part of the Saka section (starting from sample Saka 4), the intercalations commonly comprised rather poor microcrystalline quartz, which is probably a recrystallisation product of biogenic silica (cf. Loog & Petersell 1995). Furthermore, various traces of horizontal bioturbation throughout the studied black shale sections were observed (Fig. 7C−F). At bedding boundaries of finely laminated organic-rich beds of the Pakri section, the pyritised horizontal flattened tubular traces up to a few millimetres thick were occasionally

recorded. The features of the traces resemble those of ichnofossil *Planolites* (e.g. Egenhoff & Fishman 2013). More silty laminated beds and some massive beds in the Pakri section showed discontinuous indistinct lamination, halo zones, partly destroyed probable biolamination, diffused surface boundaries and, less commonly, mottled appearances (see also the massive fabric section). Those fabric elements were likely a product of homogenisation by bioturbation (Fig. 7C and D). In discrete intervals, the Saka section (Saka 6 and 9) yielded rare vertical traces with height of up to a few centimetres, and mottled fabrics, in both cases visible due to the mixing of organic-rich mud, spicules and quartz (Fig. 7E). The observed vertical traces may represent "escape traces" of zoobenthos.

4.8   Microfabrics by SEM

SEM observations were conducted to study how the above-described centimetre- to millimetre-scale features are connected to the micrometre-scale morphology of the deposit. It appears that finely laminated samples (Fig. 8A) are characterised
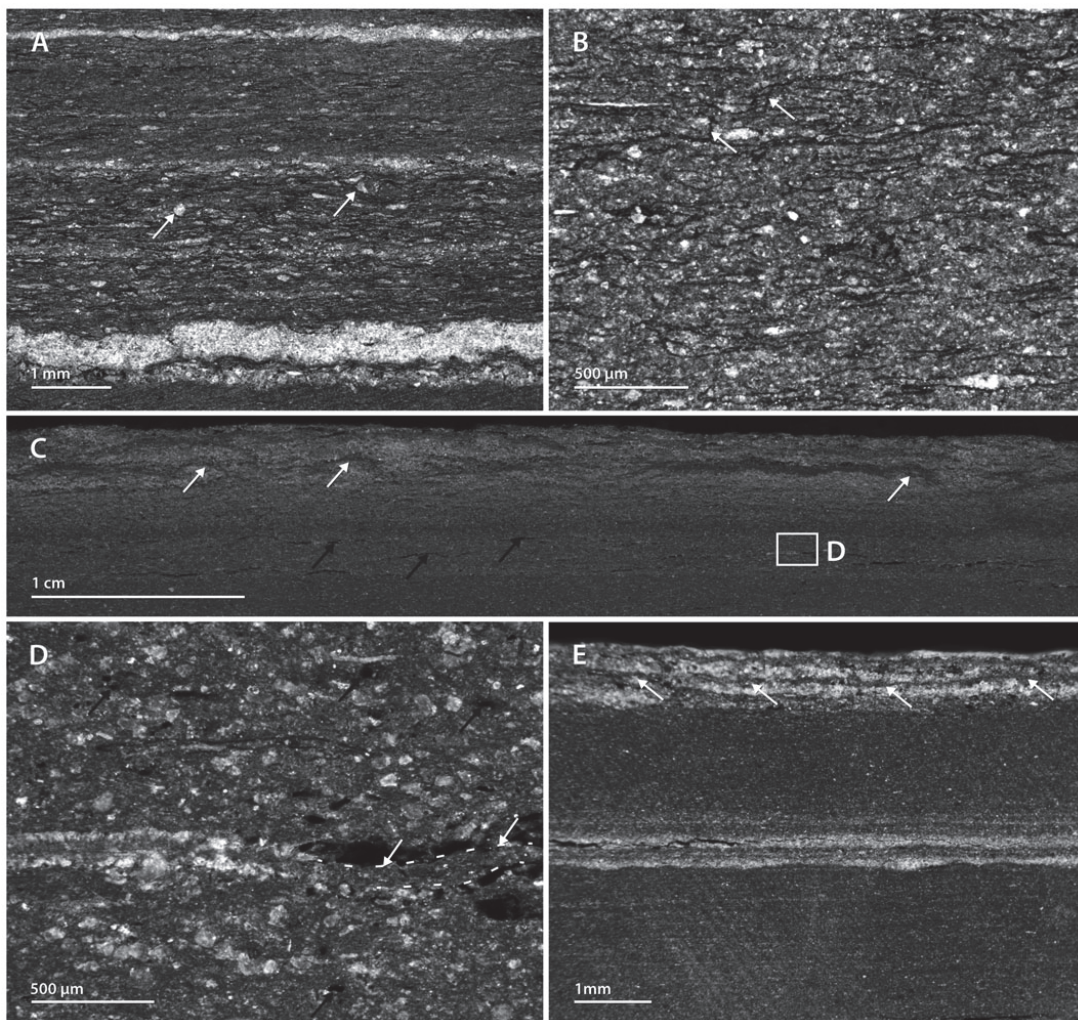
Fig. 6. Micrographs (A, B, D and E) and scanned images (C) of samples with probable biolaminated microfabrics. **A**. Fabric with a dense network of organic-rich laminae in black shale (Pakri 14-1). Arrows mark the grains coated by organic-rich filaments. **B**. Higher magnification micrograph of fabric of Pakri 14-1. Note the widespread occurrence of vertically oriented organic-rich filaments (arrows). **C**. Scanned slab of probable biolaminated fabric of Saka 3-1, with thick wavy slightly upward convex dark organic-rich bands (white arrows) within a lighter matrix. The black arrows mark the elongated pores in less contrast parts of subsample. **D**. Higher magnification micrograph of Saka 3-1. Wavy-crinkly organic-rich lamina (white arrows, dotted lines) in black shale. Note the rather granular character of fabric and large open pores (black arrows). **E**. Series of wavy organic-rich laminae on the top of black shale bed, Saka 4-2.

by anisotropic microfabric with a preferred orientation of platy minerals and bioclastic compounds and evenly distributed regular-size elongated small interparticle micropores (micropores $>0.75\,\mu m$; pore size classification after Loucks et al. 2009). By contrast, in samples with massive morphology (Fig. 8B), the observed isotropic microfabrics presented a random orientation of mineral platelets and detritus in the matrix and randomly distributed closed interparticle micropores. The probable biolaminated fabrics from the Saka section revealed

heterogeneous and highly porous microfabrics (Fig. 8C) with loosely packed and randomly oriented grains and a connected network of large irregularly shaped micropores. SEM studies of supposed biolaminated samples also indicated the presence of abundant curved, convoluted, folded organic-rich filaments, with thicknesses from less than 1 to several tens of microns (Fig. 8D–F). Some samples revealed convoluted homogenous laminae, or few micrometre-thick layers with laminar structures that most likely are remnants of palynomorphs. The presence of
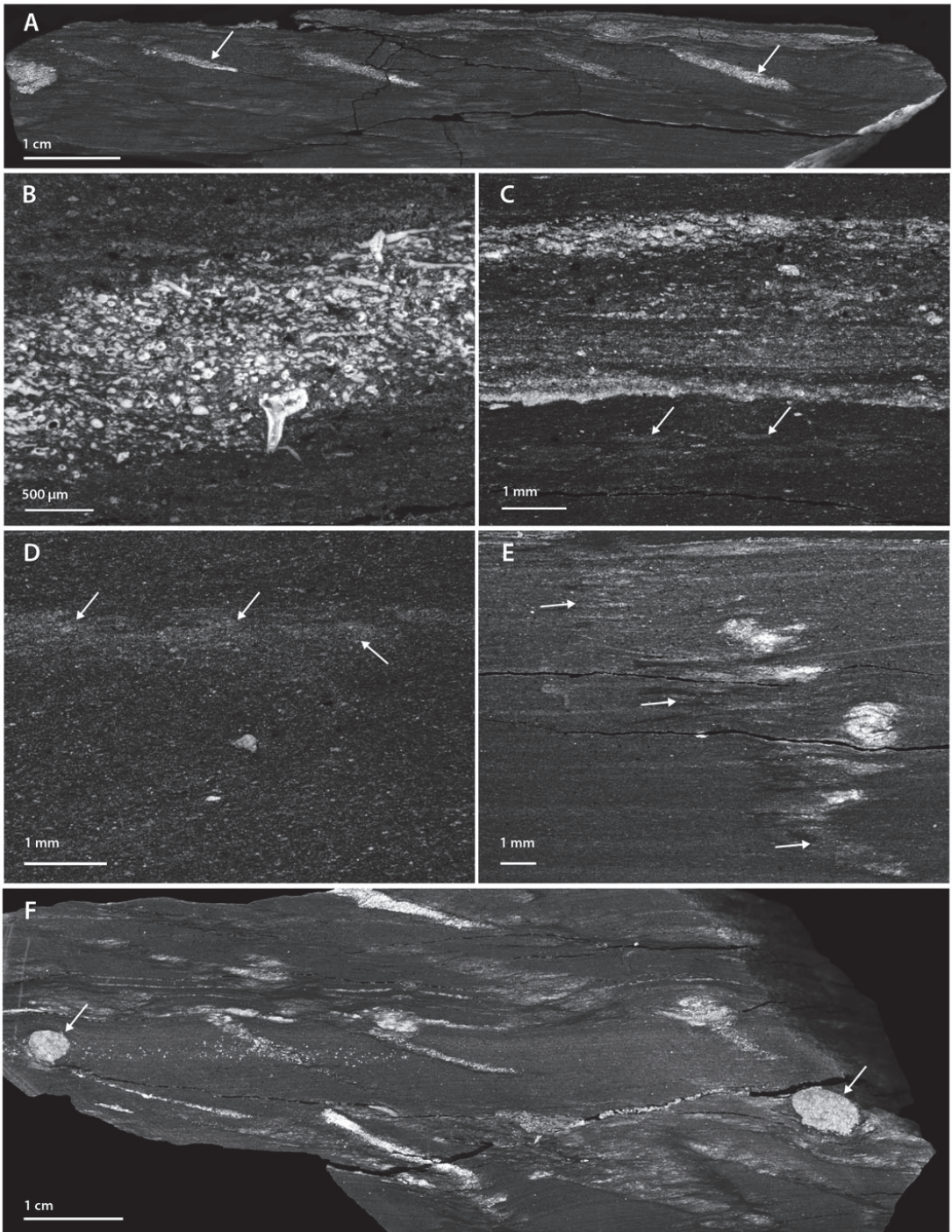
thicker heterogeneous laminae with bumpy surfaces and uneven thickness distribution was also rather a characteristic for biolaminated samples. The conducted SEM–EDS analysis of such filaments suggested a high carbon content and the presence of Si, Fe, S and Al. Similar organic-rich sheaths, commonly partly mineralised by silica or Fe–Al silicates, have been recognised from different siliciclastic rocks, including black shales, and interpreted as fossilised remnants of microbial mats (e.g. Noffke et al. 2001; Gorin et al. 2009; Kazmierczak et al. 2012).

5.   Interpretation of sedimentary fabrics

The finely laminated fabrics in mudstones are traditionally interpreted as products of slow deposition of fine, loose particles or organomineralic aggregates from a generally stagnant water column (Potter et al. 1980) and widely recognised as a characteristic of black shales. Occurrence of finely laminated beds with discontinuous inclined laminae in the Türisalu Fm., however, suggests that such beds were not formed simply by gravitational settling. Similar low-angle cross-laminated fabrics have been recently recognised in several black shales and interpreted as a product of lateral mud accumulation by near-seabed flows (Schieber et al. 2007; Macquaker et al. 2010a; Ghadeer & Macquaker 2011). The flume experiments by Schieber (2011) demonstrated that flocculated clay–silt particles could sustain integrity under high flow speeds and that such flocs could actually move by bed-load transport. Compaction of water-enriched mud ripples has been shown to result in the formation of microlaminated beds, very similar to those found in black shales (Schieber & Yawar 2009). Moreover, research of modern mud dynamics has revealed many quick dispersal mechanisms, some of which could form widespread "event mud blankets", even in the case of low topographic gradient (e.g. Traykovski et al. 2000). Such mechanisms may involve the formation of sediment-laden unidirectional near-bed flows – eroding, dispersing and depositing the sediments during one and the same flow event (e.g. Macquaker et al. 2010a). Wider acknowledgement that dynamically deposited muds could have been voluminously important in the geologic history of shallow seas has been achieved because of several recent studies of ancient low-gradient mud dominated settings. These investigations indicate that the cross-shelf drift of fine cohesive particles in various settings could have been partly or dominantly driven by short-lived sediment-laden currents (Macquaker et al. 2010a; Plint et al. 2012). The encounter of stacked successions of finely parallel and subtle lenticular laminated fabric in the lower part of the Pakri section indicates that the intermittent advective transport-controlled deposition of mud was likely one of the major mechanisms behind laminated mud accumulation. However, the same interval is also characterised by the high content of OM (LOI 500°C) and V, Mo and U (Voolma et al. 2013; Fig. 2), which designate that the sedimentary environment

should have been favourable for accumulating and preserving biogenic matter and redox-sensitive trace metal enrichment. Based on the recorded fabric characteristics, it is difficult to adequately differentiate the role of suggested dynamic sedimentation and that of slow background suspension settling in the formation of finely laminated muds. Overall, however, the finely laminated beds likely represent a subenvironment with the lowest hydrodynamic energy among the observed black shale varieties of the Türisalu Fm.

Also, other fabrics observed in the Türisalu Fm., such as normally graded and high angle cross-laminated beds, support organic-rich mud formation by sediment-laden flows. Appearance of grading in marine sedimentary record is typically interpreted as deposition in environment where the speed of sediment-loaded current changes over time (e.g. the formation of tempestites). The occurrence of normal grading with distinct lamina sets in studied section of the Türisalu Fm., together with erosional features on the lower bedding surfaces, suggests that those elements are likely products of the same turbulent near-bed flow event (e.g. Macquaker et al. 2010a). Furthermore, the occurrence of ripple-laminated lamina sets in the lower silt-rich lighter part of graded beds clearly points to the bed-load transport of mud particles. Macquaker et al. (2010a) interpreted normally graded beds composed of three distinct lamina sets as products of wave-enhanced sediment gravity flows. Importantly, such combined flows do not require steep slopes like typical turbidites, but can progress in low-gradient shallow settings thanks to energy derived from orbital motion of surface waves, which help to maintain sediment in suspension (Traykovski et al. 2000; Macquaker et al. 2010a). Dynamically deposited mudbeds with thicknesses comparable to those observed in the Türisalu Fm. have been attributed to low-density diluted flows with sediment loads of 1–10 g/l (Mackay & Dalrymple 2011). On the other hand, the absence of erosional features below beds with more gradational grading also observed in the Türisalu Fm., coupled with mostly rather silty composition of such beds, could indicate that the primary mud settled from a suspended sediment (storm) cloud during considerably short time intervals. The observed high-angle cross-laminated fabrics in the Türisalu Fm. unequivocally point to high-energy sedimentation event most likely controlled by surface storm waves. The accompanying soft sediment deformation features in such beds suggest rapid sediment loading on seabed, whereas resistance of those fabrics to later compaction indicates the general grain supported nature of the primary sediments.

Deciphering of formation of observed massive fabrics is more problematic as different pathways and sedimentary settings can lead to formation of massive fabrics in mudstones. Massive varieties could appear as products of the simple gravitational settling of fluidised mud, deposition from fluid mud flows, products of settling from a suspended sediment cloud in slack shallow-water settings (e.g. Traykovski et al. 2000; Baas & Best 2002; Ichaso & Dalrymple 2009; Mackay & Dalrymple 2011) or as products of post-sedimentary homogenisation by bioturba-

Fig. 7. Micrographs (B, C, D and E) and scanned image (A and F) of beds with lenses of spiculite and traces of bioturbation. **A**. Thorough cross-lamination of the black shale (Saka 6-1) is traceable thanks to inclined lenses of spicules of siliceous sponges (white arrow). **B**. Close-up of Saka 6-1 presenting the detail of spicule-rich lens. **C**. Black shale (Pakri 16-1) shows low-contrast burrow mottled fabric in its lower part (arrows). **D**. Massive bed of Pakri 12-1 with a lighter halo zone (arrows). **E**. Vertical trace (arrows) in subsample Saka 6-2. **F**. Black shale (Saka 9-2) with composite spicules cross-laminated and partly bitoturbated fabric with pyritised traces (arrows).
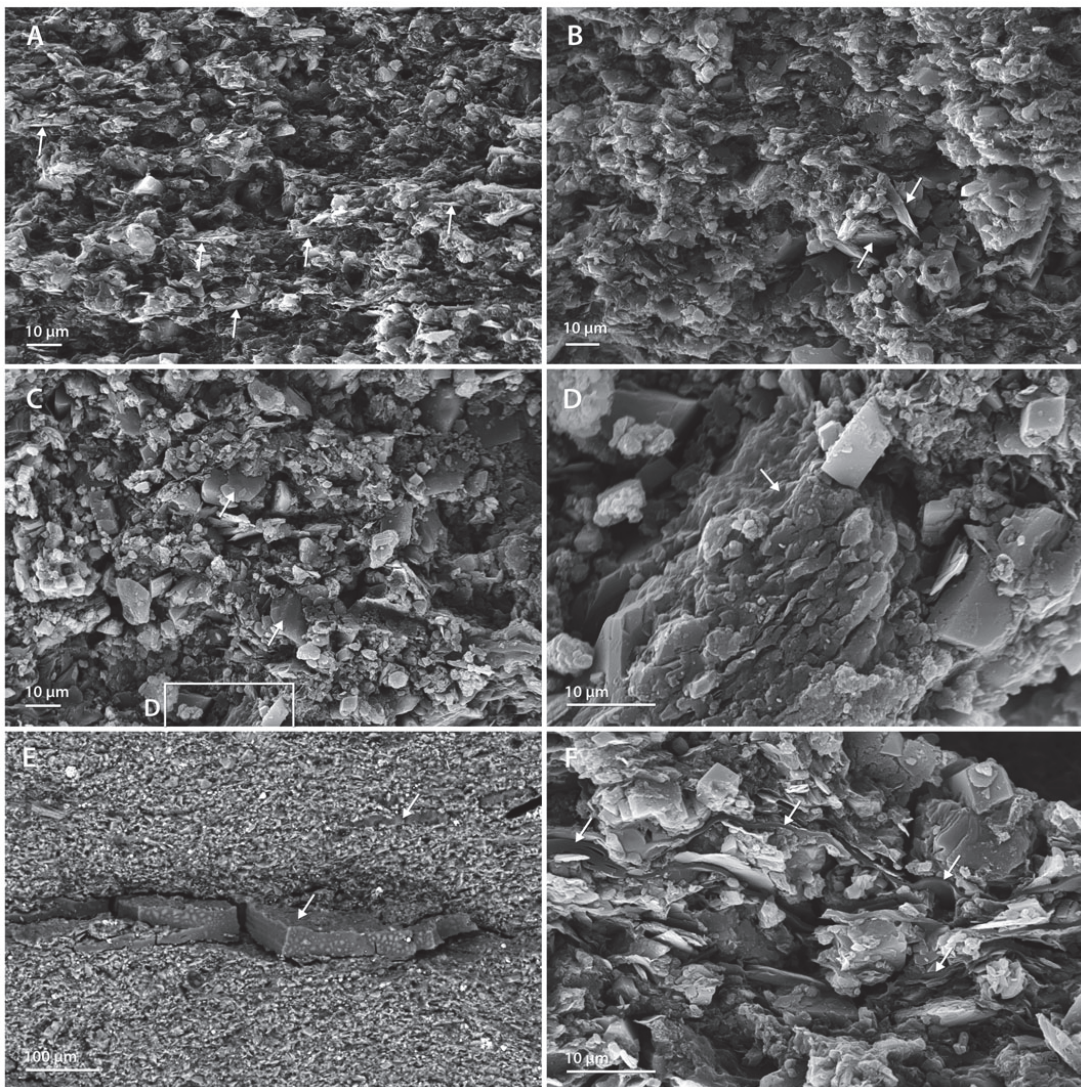
Fig. 8. Representative secondary (A–D and F) and backscattered electron (E) images of microfabrics. **A**. Microfabric of finely laminated bed (Pakri 4). Note the preferred planar parallel orientation of platy particles (arrows). **B**. Microfabric of massive black shale (Pakri 20) presents irregular orientation of large platy mineral particles (arrows). **C**. Biolaminated microfabric (Saka 3) with random orientation of mineral grains (white arrows) and OM laminae. **D**. Detail from image C with thick partly mineralised organic-rich lamina in the centre (white arrow). **E**. Microfabric of black shale (Saka 2) presenting thick partly mineralised organic-rich laminae (arrows) interpreted as remnants of microbial mat. **F**. Thin organic-rich convoluted laminae (arrows) of problematic biogenic origin (Saka 3).

tion. The preservation of sharp bedding surfaces in studied black shale samples suggests that the major part of observed massive fabrics in the Türisalu Fm. are likely primary sedimentary features and might thus reflect an accumulation of mud in an environment that was shallow enough to support surficial mud fluidisation by storm waves. However, as shown by studies of modern muddy shallow-marine areas like the Eel river shelf

(Traykovski et al. 2000; Macquaker et al. 2010a), the massive fabrics in mud might be as well produced by deposition from dense fluid mud flows, which on the Eel river shelf act as the major agents of offshore transport of cohesive flood sediments. In the case of the Türisalu Fm., considerably immature siliciclastic fresh input into palaeobasin and proximity of terrestrial feeding systems of sediment supply could be argued

based on the heterolithic character of Lower Tremadocian successions and by the abundance of both mica flakes and subangular quartz in siliciclastic intercalations in the studied black shale sections. Those intercalations are traditionally considered to be products of distal storm flows, which very infrequently disturbed the otherwise tranquil environment of black shale accumulation (e.g. Heinsalu 1990). However, as suggested by our study, both siliciclastic intercalations and shale beds likely originated from sediment-laden wave-aided flows, which plausibly controlled cohesive sediment dispersal in the inner-shelf settings of the Tremadocian epicontinental palaeo-basin. Gradational silty upper contact of black shale beds observed in the Saka section suggests that additionally to deposition by the storm flows, the winnowing of surface mud by bottom currents could also cause the formation of the observed silty laminae.

Besides physical factors which controlled the accumulation of black shales of the Türisalu Fm., biogenic processes had considerable role on the final character of those beds. Carbon-rich wrinkled structures, similar to those observed in the Saka section have been documented in different siliciclastic rocks including mudstones (e.g. Schieber 1999) starting from Archean (e.g. Noffke 2009). These features have been interpreted as recalcitrant remnants of benthic microbial mats, supposedly produced by phototrophic bacteria, encapsulated into thick films of extracellular polymeric substances (EPSs) or by more complex multitrophic microbial consortia (e.g. Gorin et al. 2009). EPS is a general term for sticky substances composed dominantly of polysaccharides and secreted by different types of microorganisms (e.g. Decho 1990). The EPS-rich microbial mats are found to be typical for high-energy well-lit shallow-water environments, whereas EPS has a considerable role in biostabilisation of mat-covered seabed (e.g. Noffke 2009). The somewhat different types of supposed biolamination recorded in the Pakri section with vertical organic-rich filaments were probably formed as the result of an upward migration of the microbial mat during its life cycle (Noffke et al. 2001). Synsedimentary detrital grain trapping by sticky mat surfaces and the benthic community-controlled subsurface sulphate reduction could be suggested based on common encounters of abundant mica flakes at wavy mat surfaces and the observed layer-specific distribution of pyrite in biolaminated samples (e.g. Schieber 1999).

The influence of zoobenthos is conventionally considered to be negligible in the case of typical laminated black shales (Wignall 1994); however, our research as well as previous studies (Heinsalu 1990) report traces of bioturbation throughout the Türisalu Fm. Furthermore, recent investigations of Lower Ordovician black shales in Scandinavia have suggested that black shales might actually present abundant traces of bioturbation even in levels rich in graptolite fossils. This is in contrast to commonly upheld notion that such beds should have accumulated in anoxic environment (Egenhoff & Maletz 2012). Although a detailed study of benthic communities in the Türisalu Fm. is beyond the scope of this article, the observed traces of bottom colonisation (bioturbation and sponge spicules) suggest the availability of free oxygen at the sediment–water interface regularly, or at least episodically, throughout the accumulation history of the Türisalu Fm. However, the heterogeneity of the observed biogenic fabrics denotes that the conditions for benthic life varied through time.

The comparison of microfabrics of black shales showed that notable difference exists between samples with distinct small-

scale sedimentary features. General feature of all studied black shale varieties was the large volume of micropores and a low level of compaction, which is consistent with low diagenetic maturity and silt-fraction dominated size fractions of the deposit. SEM observations also confirmed profound effect of biogenic processes, such as in situ formation of microbial mats, on the development of microfabrics of black shales by supporting the formation of highly heterogeneous, porous and relatively fragile varieties. The ripped up cohesive fragments of such microbial mats (e.g. Schieber 1999) could have been the source of the convoluted organic-rich fragments that were commonly observed in the matrix of the Saka and the Pakri samples.

The results of this research demonstrate that vertical sections of the Türisalu Fm. are lithologically heterogeneous, even in intervals dominated by well-laminated beds. We suggest that the observed fabric variability with elements such as ripple and high-angle cross-lamination, grading, common microbial lamination, lenticular intercalations of siliceous sponges, submarine erosional surfaces, silty massive fabrics with marine detritus and traces of bioturbation indicate a shallow-water surface-wave-controlled sedimentary environment of primary mud accumulation. The interpretation of a shallow-water origin is consistent with the conclusion that was previously made by numerous studies (e.g. Scupin 1922; Heinsalu 1990). However, accumulation pathways of primary mud in those settings were obviously much more variable than the commonly assumed "slow suspension settling in stagnant water column inferred by rather infrequent storm events" (e.g. Heinsalu 1990). In their landmark paper, Rine & Ginsburg (1985) demonstrated, based on studies of modern equatorial Atlantic mud shore faces, that siliciclastic mud deposits can form in high-energy dynamic shallow-water environment. Furthermore, their study hinted that actual mud- or sand-dominated facies distribution in shallow-water settings can be rather different from traditional sandy near-shore–muddy offshore facies zonation.

The well-documented occurrence of typical marine fauna in the Türisalu Fm. such as early planktic graptolites *Rhabdinopora* sp. (Kaljo et al. 1986) designates that inner-shelf organic-rich muds deposited under normal marine conditions with non-restricted surface circulation. The documented fabric successions of the Pakri black shale shows general change from the laminated fabrics-dominated lower part to massive varieties-dominated upper part. This could possibly reflect a major shift in the character of sediment-laden flows during the accumulation of studied black shale section, from diluted turbulent flows to more dense fluid mud flows. According to Baltoscandian sea-level reconstruction of Nielsen (2004), the initial Early Ordovician transgression, which reached to its maximum in *Rhabdinopora* spp. interval (lower part of the Pakerort Stage), was followed by shallowing at the base of the *Adelographus hunnebergensis* graptolite zone and then by more moderate sea-level rise, which culminated during the *Kiaerograptus* Drowning Event (lower part of the Varangu Stage). Thus, the shift from more laminated to massive fabrics observed in the Pakri section could be related to eustatic sea-level fall. A limited occurrence of massive fabrics and widespread biogenic fabrics in the stratigraphically younger Saka section suggests that, besides water depth control, different sediment accumulation patterns and related hydrodynamic and sediment supply regimes were dominant in the two studied localities. The Saka section most likely represented a more sheltered shallow-marine setting, protected from storm waves by submerged sand bars or ridges between the Vihula and Toolse

areas as proposed by Heinsalu et al. (1994). Such sheltered, but not stagnant environments favoured an increase in benthic biogenic factors, including the development of benthic microbial mats and abundant shallow-water sponges.

6.   Discussion

6.1   Sedimentary framework of organic-rich mud accumulation

In the early Palaeozoic, the considered marginal area of the Baltic palaeobasin was situated in the interior of the palaeocontinent, hundreds of kilometres away from deep water settings, facing the Iapetus Ocean and the Tornquist Sea, and hosting the Alum Shale Fm. For Alum Shale, which was deposited from the Mid-Cambrian to the early Tremadocian, the average net accumulation rate of 1–10 mm/1000 years has been suggested (Thickpenny 1987; Schovsbo 2001). Based on the available biostratigraphic framework and the latest time-scale calibration, black shales of the Türisalu Fm. deposited within a maximum time frame of ~5 My (Cooper & Sadler 2012). Thus, the average net accumulation rates stayed very low both in the deeper basin and in the marginal settings. The very low level of terrestrial input into the primary sedimentary environment was controlled by the peneplained nature of the main input area – low-altitude Proterozoic hard rock terrain of the Fennoscandian Shield in the present day north and northeast (Utsal et al. 1982; Artyushkov et al. 2000). Furthermore, a drop in fluvial particulate input into more distal settings at the start of the organic-rich mud accumulation was apparently supported by the sea-level rise and trapping riverine fluxes in back-stepping estuarine-coastal systems (e.g. Wignall 1991; Nielsen & Schovsbo 2011). At the time of high sea level (Nielsen 2004; Dronov et al. 2011) in early Tremadocian, the Finland–Russian part of the Fennoscandian Shield (adjacent to the accumulation area of the Türisalu Fm.) likely remained the main terrestrial source area of siliciclastic input for this part of the palaeobasin, as indicated by the occurrence of relatively immature siliciclastic deposits in Estonian settings (e.g. Heinsalu et al. 2003). The encounter of regular small-scale erosional features and the bedded character of the studied black shale successions indicate that the Türisalu Fm. is not a condensed deposit *sensu stricto* but presents evidence of intermittent dynamic sedimentation and reworking.

Formation of cohesive sediment-laden flows (as well as sediment storm clouds) in the accumulation environment of the Türisalu Fm. could have either been connected with the reactivation of muds that were trapped in coastal/estuarine settings, with the resuspension of seabed muds or alternatively with "fresh" fine sediment load into the basin from extensive flooding events (e.g. Arthur & Sageman 2005). The rivers of the pre-vegetational era were likely far more prone to the generation of sediment surges during flooding events compared with modern rivers (Davies & Gibling 2010). On other hand, the storm wave activity at dynamic estuaries (supposedly rather typical for pre-Devonian rivers according to Davies & Gibling (2010)) or in related coastal systems most likely had a higher potential for triggering the formation of long-travelling sediment-laden flows and for causing the dispersal of fine sediments.

In the early Palaeozoic, the study area was characterised by high tectonic and sedimentary facies zone stability (Männil 1966; Jaanusson 1976). In settings with very flat seabed, additional wave energy was needed to allow the progression of

sediment-laden flows over long distances (e.g. Plint et al. 2012). Such seabed topography was not probably favourable for the formation and progression of sediment-laden density currents in water depth below storm wave base. Furthermore, the innermost shelf position also meant that the Estonian area was situated far from strong currents and upwelling systems at the continental margins, which thus had likely minor influence on sediment dispersal. The flow deposition features observed in the Türisalu Fm. together with palaeogeographic position therefore favour shallow-water storm-wave-controlled deposition rather than a deeper water origin of primary muds. Several general features in the architecture of the Türisalu Fm. indicate a tight supply–transport–accommodation space-controlled nature of the black shale distribution: (1) the belt of the Estonian–Russian Tremadocian black shales (e.g. Heinsalu 1986) along the supposed terrestrial areas, (2) diachronous accumulation in different localities, (3) the gradual thinning towards the most distal (southern) part with respect to supposed terrestrial sources and (4) the gradual thinning and decrease in age towards more shallow-water settings in the NW Estonia (Fig. 9). The intimate association of black shales with the peritidal shell phosphorite-containing Kallavere Fm. has been commonly considered as a strong evidence for a shallow-water origin of the Türisalu Fm. (e.g. Scupin 1922; Heinsalu 1990). Furthermore, the Türisalu Fm. is set within the limits of shallow-water North Estonian facies belt in terms of post-Tremadocian Ordovician carbonate sedimentary basin being absent in the deeper water settings of the Livonian Tongue facies belt (Jaanusson 1976). Thus, based on the thickness distribution of the Kallavere and Türisalu formations (and the absence of evidence on major tectonic movements in the considered setting in the Tremadocian), the migration of the sedimentation locus towards near-shore settings during sea-level rise and diminished clastic input is suggested. Alternatively, however, the absence of organic-rich Tremadocian sediments in presumably deeper water settings in southern Estonia could be related to post-Tremadocian erosion of mudbeds (Mens & Pirrus 1997). Nevertheless, the rather irregular thickness of the Kallavere Fm., juxtaposed with the established litho- and bio-stratigraphy of the Türisalu Fm., suggest that the sedimentary architecture of the primary organic-rich mud was strongly influenced by inherited seafloor topography, i.e. drowning of complex sets of sand–silt bed forms formed during the previous stages of transgression (cf. Heinsalu et al. 1994).

Previous studies by Heinsalu (1990) and Artyushkov et al. (2000) have suggested that the black shales of the Türisalu Fm. should have been deposited at a depth near storm-wave base (40–60 m). The results of this research, however, indicate that the accumulation of primary mud could also probably occur in shallower depths depending on the local physiography, material supply and patterns of wind-forced storm waves. Thus, spatial and stratigraphic changes in the lithology within the Türisalu Fm. cannot be directly interpreted in terms of water depth, but reflect an interlinked effect of proximity to hinterlands, the volume and type of distributed sediment, seafloor gradients, seafloor morphology and variegated hydrodynamic energy patterns (e.g. Macquaker et al. 2010a). We suggest that storm-induced sediment dispersal and sedimentation characteristic of the later Early Ordovician sedimentary record in the north Estonian shelf (Dronov et al. 2002), dominated also in the Tremadocian and storm-wave-
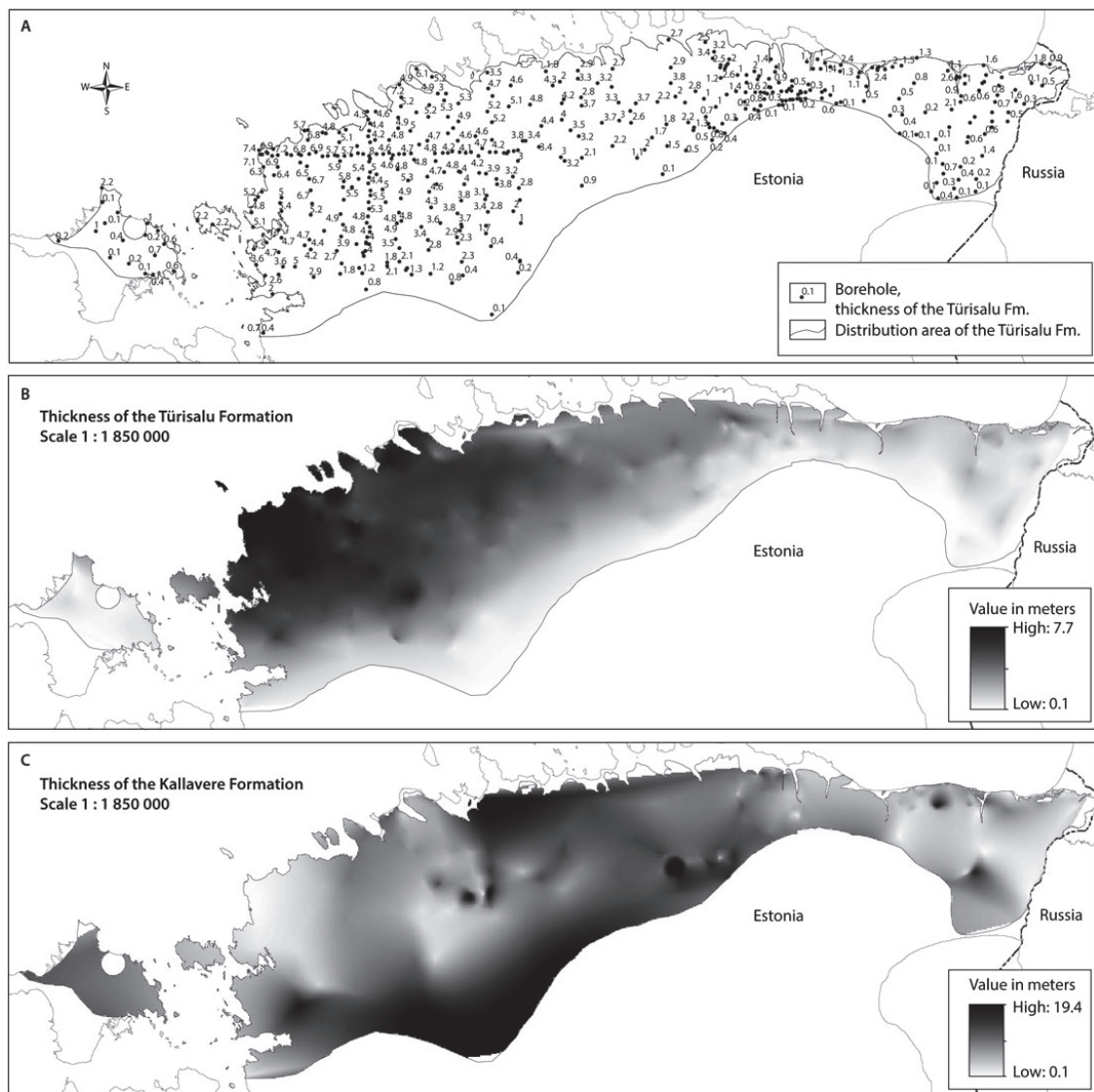
Fig. 9. Thickness of the Türisalu and Kallavere Fm. **A**. Location of drill cores used for thickness calculations and representative thicknesses of the Türisalu Fm. Data of Geological Survey of Estonia (Niin et al. 2008). **B**. Scheme of interpolated thicknesses of Türisalu Fm. **C**. Scheme of interpolated thicknesses of the Kallavere Fm. Note that only thicknesses within the distribution area of the Türisalu Fm. are provided on the scheme.

aided near-bed flows, acted as major agents of mud reworking, dispersal and accumulation in the studied black shale localities.

6.2 Sequestration of OM and trace metals in the context of dynamic deposition

Evidence of physical and biogenic mixing of precursor muds of the Türisalu Fm. suggests a shallow-water hydrodynamically

variegated marine environments and makes permanent anoxia (euxinia) in the lower water column questionable. However, an O_2 deficit has been shown to be a critical factor for the preservation of labile marine OM and trace metal enrichment in black shales (e.g. Algeo & Maynard 2004). Both studied sections presented a high content of redox-sensitive elements such as V, Mo and U (recorded maximum content: V = 1500 ppm, Mo = 1800 ppm, U = 800 ppm; Voolma et al.

2013). The average concentration of those metals was detected to be considerably higher in the Saka section (enrichment factor V = 1.2, U = 2.95, Mo = 3.9 respective to the average content in the Pakri section; Voolma et al. 2013). Widely used geochemical palaeoredox proxies, such as V/(V + Ni) and V/Cr (Fig. 2; Hatch & Leventhal 1992; Jones & Manning 1994), suggest that the studied organic-rich mud deposit is formed under anoxic (euxinic) conditions. Thus, lithologically more heterogeneous and an average more metalliferous, the Saka section yielded results varying from anoxic to euxinic conditions. Somewhat less anoxic conditions were deduced for the Pakri section. The few element-based indices might have, however, limited value for interpreting the palaeoredox situation without a detailed knowledge of the local geological situation (e.g. Tribovillard et al. 2006). Schovsbo (2001) calibrated the combined V/(V + Ni) and sulphur values in the Alum Shale Fm. against trilobite and brachiopod occurrence data. According to this classification, most of the Türisalu Fm. belong to an upper dysoxic zone, where V enrichment was favoured by advective transport of the trace elements (Schovsbo 2001). The latter author also suggested crucial role of advective transport by U enrichment of the near-shore Cambrian Alum Shale Fm. and Tremadocian black shales.

Global-scale processes, such as the development of a strongly stratified ocean with anoxic deep waters, are commonly seen as the triggers of widespread contemporary black shale development (Schlanger & Jenkyns 1976). The Upper Cambrian part of the metalliferous Alum Shale Fm. in deeper basinal settings of the Baltic palaeobasin could have been linked to one such ocean anoxic event in the Late Cambrian (Gill et al. 2011). Wilde et al. (1989) suggested a build-up of strong upwelling at the western margin of Baltica in the Tremadocian and a transgression of deep anoxic nutrient-rich waters to the shelf. However, Schovsbo (2001) argued that at the beginning of the Ordovician, less oxygen-depleted conditions and better circulation had been restored in the Baltic palaeobasin compared with the Upper Cambrian marine environments. Despite the uncertainty about deep water redox conditions, it is evident that the primary muds of the Türisalu Fm. accumulated well within the photic zone (e.g. Chester 2003). In present-day seas, photic zone anoxia can be found under specific conditions that are related to strongly stratified water column limiting the O_2 supply and/or high bioproduction–decomposition rates and is confined to closed or barred marine to brackish water bodies (e.g. Yao & Millero 1995) and/or to environments with high anthropogenic nutrient input fuelling eutrophication (e.g. Rabalais et al. 2002). In mid-latitude epicontinental shallow seas, such as the Baltic palaeobasin in the Tremadocian, strong thermohaline stratification could possibly develop because of a combined effect of high freshwater fluxes and seasonal temperature variations. However, modern and ancient analogues suggest that such stratification most likely had temporal character because large seasonal climate variation at mid-latitudes also supports perturbation and regular mixing of the water column, thus favouring oscillatory redox conditions (cf. Murphy et al. 2000). Another critical factor of black shale development is bioproduction. The formation of rich skeletal phosphorite complexes during the initial stage of the Late Cambrian–early Tremadocian transgression suggests enhanced bioproductivity in considered marginal settings of the Baltic palaeobasin (Ilyin & Heinsalu 1990). The primary OM of the Türisalu Fm. was likely produced by cyanobacteria and possibly by green sulphur bacteria (Klesment & Urov 1980;

Lille 2003). Both those groups contain species capable of fixing N_2. The dominance of nitrogen-fixing primary production pathways during the accumulation of Tremadocian black shales in Estonia has been lately proposed by Kiipli & Kiipli (2013) based on low $\delta^{15}N$ values. Blumenberg & Wiese (2012) suggested that high bioavailable P loading versus bioavailable N could have been the main trigger of black shale formation in shallow seas during late phases of Cenomanian/Turonian ocean anoxic event. The rather low P content (average P_2O_5 concentration of the studied section remains less than 0.5 wt%) in the studied black shale sections versus the high OM content (Voolma et al. 2013) could indicate the effective recycling of this element in a primary marine environment. This process was likely supported by the anoxic conditions in the sediment column, seasonal mixing of water masses, but possibly also by constant reworking and lateral transport of sediments (e.g. Emeis et al. 2000). Consequently, the deposition of primary organic-rich muds of the Türisalu Fm. might have been controlled by a feedback loop to the supply of biolimiting elements (most importantly bioavailable P) to the marginal photic settings, enhanced bioproductivity and build-up of strong P bioproduction–regeneration cycling (e.g. Tribovillard et al. 2006; Blumenberg & Wiese 2012).

The role of bioproduction and the OM incorporation into primary mudbeds of the Türisalu Fm. are nevertheless rather poorly understood. The herein documented occurrence of microbial mats is the first direct evidence of the existence of microbial consortia at the sediment–water interface of primary organic-rich muds and suggests that microbial mats could have been major primary producers of OM of the Türisalu Fm. (cf. Gorin et al. 2009). Buchardt et al. (1997) proposed that widespread thick algal mats could have been the source of OM in the Alum Shale Fm. The oxygen production by benthic photosynthesising microbes in the photic zone and the degradation of the OM below mat surface could support the formation of steep redox gradients at sediment–water interface (e.g. Kazmierczak et al. 2012). On the other hand, several recent studies have implied a crucial role of the formation of organomineral aggregates in the water column (e.g. during phytoplankton blooms) and the related quick sequestration of OM into sediments (Macquaker et al. 2010b). Inside such aggregates, and also in benthic microbial mats, the OM could be protected by EPS (Pacton et al. 2007) or by physicochemical interactions with mineral particles (Salmon et al. 2000), thus supporting selective OM preservation in generally oxygenated environments. Consequently, the aggregation of organic and mineral matter might explain the preservation of the organic fraction in dynamic sedimentary processes in shallow-water oxic settings. Event deposition could also promote the preservation of OM by increasing episodic burial rates and limiting the residence time of OM at sediment–water interface (Macquaker et al. 2010b; Ghadeer & Macquaker 2012). Studies of microfabrics in the Saka section hinted that rather different physicochemical (biological) conditions of primary mud layers (including permeability, diffusion and microbially mediated processes) possibly developed in those settings compared with the Pakri section. Higher porosity and simultaneous supposedly steep redox gradients at the sediment–water interface braced fluxes of redox-sensitive elements between mudbeds and marine water (cf. Schovsbo 2001). The development of high trace metal heterogeneity in the Türisalu Fm. (Voolma et al. 2013) has thus been partly forced by variegated fabric characteristics of the

primary mud. We suggest that during the accumulation of primary mud of the Türisalu Fm., the lower water column was characterised by oscillating redox systems with H_2S-rich conditions mostly confined below the sediment−water interface. The OM supply, intermittent deposition, contact time of mud with seawater and heterogeneity of mud fabrics and porosity likely had a profound influence on trace metal enrichment processes in the examined settings. Not less importantly, advective transport and redeposition of particulate and colloidal matter most likely acted as major controllers of element cycling, including P recycling and trace element supply.

7. Conclusions

The results of this research are consistent with previous studies on the shallow-water origin of the Türisalu Fm., further suggesting that the water depth remained above the storm wave base within the photic zone throughout the deposition of the studied proximal complexes. The observed lithological characteristics provide evidence that the sedimentary dynamics of the Türisalu Fm. varied spatially and temporally, whereas intermittent accumulation with rapid short-term sedimentary fluxes prevailed. The cohesive sediment dispersal and deposition were mainly controlled by the near-bed storm-induced flows, which, besides causing the dynamic deposition of mud, also acted as eroding and reworking agents on muddy seafloor.

The rather shallow-water organic-rich mud settings in NE Estonia were protected from storm wave action by a complex set of drowned transgressive sand bodies that favoured the formation and preservation of more mosaic fabric patterns in primary mud successions, including common biogenic fabrics. This study is the first to report the occurrence of fossilised microbial mats in these settings of the Türisalu Fm.

Some geochemical indices, enrichment of redox-sensitive elements and high OM content seems to favour the idea that the primary mud formed in anoxic environment. In contrast, the observed traces of bioturbation and dynamic sedimentation features suggest oscillating redox conditions in the lower water column during primary mud accumulation. Metal sequestration in such environments could have been favoured by steep redox gradients at sediment−water interfaces covered by microbial mats.

This work suggests that a thorough understanding of syngenetic metal sequestration pathways in the Türisalu Fm. requires further studies on sedimentary environments. In particular, we need to learn more about (1) variability of accumulation rates, (2) proximity to fluvial sources, (3) sediment transport routes within the basin, (4) element cycling because of redeposition, (5) OM production and preservation, (6) supply of dissolved and colloidal species to sediment−water interface, (7) chemocline character, (8) the physicochemical character of primary mudbeds, (9) benthic microbial consortiums and (10) the role of diagenetic overprinting.

References

Algeo, T.J. & Maynard, J.B., 2004: Trace element behavior and redox facies in core shales of Upper Pennsylvanian Kansas-type cyclothems. *Chemical Geology 206*, 289−318.

Andersson, A., Dahlman, B., Gee, D.G. & Snäll, S., 1985: The Scandinavian Alum Shales. *Sveriges Geologiska Undersökning Serie Ca 56*, 1−50.

Aplin, A.C. & Macquaker, J.H.S., 2011: Mudstone diversity: origin and implications for source, seal and reservoir properties in petroleum systems. *AAPG Bulletin 95 (12)*, 2031−2059.

Arthur, M.A. & Sageman, B.B., 2005: Sea level control on source rock development: perspectives from the Holocene Black Sea, the mid-Cretaceous Western Interior Basin of North America, and the Late Devonian Appalachian Basin. *In* N.B. Harris & B. Pradier (eds.): *The Deposition of Organic Carbon-rich Sediments: Models, Mechanisms and Consequences. SEPM Special Publication 82*, 35−59.

Artyushkov, E.V., Lindstrom, M. & Popov, L.E., 2000: Relative sea-level changes in Baltoscandia in the Cambrian and early Ordovician: the predominance of tectonic factors and the absence of large scale eustatic fluctuations. *Tectonophysics 320*, 375−407.

Baas, J.H. & Best, J.L., 2002: Turbulence modulation in clay-rich sediment-laden flows and some implications for sediment deposition. *Journal of Sedimentary Research 72*, 336−340.

Baas, J.H., Best, J.L. & Peakall, J., 2011: Depositional processes, bedform development and hybrid bed formation in rapidly decelerated cohesive (mud-sand) sediment flows. *Sedimentology 58*, 1953−1987.

Blumenberg, M. & Wiese, F., 2012: Imbalanced nutrients as triggers for black shale formation in a shallow shelf setting during the OAE 2 (Wunstorf, Germany). *Biogeosciences 9 (10)*, 4139−4153.

Buchardt, B., Nielsen, A.T. & Schovsbo, N.H., 1997: Alun skiferen i Skandinavien. *Geologisk Tidsskrift 3*, 1−30.

Chester, R., 2003: *Marine Geochemistry*. Blackwell Publishing, London. 506 pp.

Cocks, L.R.M. & Torsvik, T.H., 2005: Baltica from the late Precambrian to mid-Palaeozoic times: the gain and loss of a terrane's identity. *Earth-Science Reviews 72*, 39−66.

Cooper, R.A. & Sadler, P.M., 2012: Chapter 20. The Ordovician Period. *In* F.M. Gradstein, J.G. Ogg, M.D. Schmitz & G.M. Ogg (eds.): *The Geological Time Scale 2012*, 489−523. Elsevier, Amsterdam.

Davies, N.S. & Gibling, M.R., 2010: Cambrian to Devonian evolution of alluvial systems: the sedimentological impact of the earliest land plants. *Earth-Science Reviews 98*, 171−200.

Decho, A.W., 1990: Microbial exopolymer secretions in ocean environments: their role(s) in food webs and marine processes. *Oceanography & Marine Biology, Annual Review 28*, 73−154.

Dronov, A.V., Ainsaar, L., Kaljo, D., Meidla, T., Saadre, T. & Einasto, R., 2011: Ordovician of Baltoscandia: facies, sequences and sea-level changes. *In* J.C. Gutierrez-Marco, I. Rabano & D. Garcia-Bellido (eds.): *Ordovician of the World*, 143−150. Instituto Geologico y Minero de España, Madrid.

Dronov, A.V., Mikuláš, R. & Loginova, M., 2002: Trace fossils and ichnofabrics across the Volkhov depositional sequence (Ordovician, Arenigian of St. Petersburg Region, Russia). *Journal of the Czech Geological Society 47 (3-4)*, 133−146.

Egenhoff, S.O. & Fishman, N.S., 2013: Traces in the dark-sedimentary processes and facies gradients in the upper shale member of the Upper Devonian−Lower Mississippian Bakken Formation, Williston Basin, North Dakota, USA. *Journal of Sedimentary Research 83*, 803−824.

Egenhoff, S.O. & Maletz, J., 2012: The sediments of the Floian GSSP: depositional history of the Ordovician succession at Mount Hunneberg, Västergötland, Sweden. *GFF 134 (4)*, 237−249.

Emeis, K.C., Struck, U., Leipe, T., Pollehne, F., Kunzendorf, H. & Christiansen, C., 2000: Changes in the C, N, P burial rates in some Baltic Sea sediments over the last 150 years − relevance to P regeneration rates and the phosphorus cycle. *Marine Geology 167*, 43−59.

Ganeshram, R.S., Calvert, S.E., Pedersen, T.F. & Cowie, G.A., 1999: Factors controlling the burial of organic carbon in laminated and bioturbated sediments off NW Mexico: implications for hydrocarbon preservation. *Geochimica et Cosmochimica Acta 63*, 1723−1734.

Ghadeer, S.G. & Macquaker, J.H.S., 2011: Sediment transport processes in an ancient mud-dominated succession: a comparison of processes operating in marine offshore settings and anoxic basinal environments. *Journal of the Geological Society 168*, 1121−1132.

Ghadeer, S.G. & Macquaker, J.H.S., 2012: The role of event beds in the preservation of organic carbon in fine-grained sediments: analyses of the sedimentological processes operating during deposition of the Whitby Mudstone Formation (Toarcian, Lower Jurassic) preserved in northeast England. *Marine and Petroleum Geology 35 (1)*, 309−320.

Gill, B.C., Lyons, T.W., Young, S.A., Kump, L.R., Knoll, A.H. & Saltzman, M. R., 2011: Geochemical evidence for widespread euxinia in the Later Cambrian ocean. *Nature 469*, 80−83.

Gorin, G., Fiet, N. & Pacton, M., 2009: Benthic microbial mats: a possible major component of organic matter accumulation in the Lower Aptian oceanic anoxic event. *Terra Nova 21*, 21−27.

Hatch, J.R. & Leventhal, J.S., 1992: Relationship between inferred redox potential of the depositional environment and geochemistry of the Upper Pennsylvanian (Missourian) Stark Shale Member of the Dennis Limestone, Wabaunsee County, Kansas, U.S.A. *Chemical Geology 99*, 65−82.

Heinsalu, H., 1980: On the facial relations of upper Tremadocian deposits in North Estonia. *Proceedings of the Academy of Sciences of the Estonian SSR, Geology 29 (1)*, 1−7 (in Russian).

Heinsalu, H., 1986: The lithofacial zonality of Early Tremadoc deposits in the East-European Platform. *Proceedings of the Academy of Sciences of the Estonian SSR, Geology 35 (3)*, 115−121 (in Russian with English summary).

Heinsalu, H., 1990: On the lithology and stratigraphy of the late Tremadoc graptolitic argillites of North-West Estonia. *Proceedings of the Estonian Academy of Sciences, Geology 39* (4), 142–151 (in Russian with English summary).

Heinsalu, H., Kaljo, D., Kurvits, T. & Viira, V., 2003: The stratotype of the Orasoja Member (Tremadocian, Northeast Estonia): lithology, mineralogy, and biostratigraphy. *Proceedings of the Estonian Academy of Sciences. Geology 52* (3), 135–154.

Heinsalu, H., Viira, V. & Raudsep, R., 1994: Environmental conditions of shelly phosphorite accumulation in the Rakvere phosphorite region, northern Estonia. *Proceedings of the Estonian Academy of Sciences, Geology 43* (3), 109–121.

Hiller, N., 1993: A modern analogue for the Lower Ordovician Obolus conglomerate of Estonia. *Geological Magazine 130*, 265–267.

Hints, O. & Nõlvak, J., 2006: Early Ordovician scolecodonts and chitinozoans from Tallinn, North Estonia. *Review of Palaeobotany and Palynology139*, 189–209.

Ichaso, A.A. & Dalrymple, R.W., 2009: Tide- and wave generated fluid mud deposits in the Tilje Formation (Jurassic), offshore Norway. *Geology 37*, 539–542.

Ilyin, A.V. & Heinsalu, H.N., 1990: Early Ordovician shelly phosphorites of the Baltic Phosphate Basin. *In* A.J.G. Notholt & I. Jarvis (eds.): *Phosphorite research and development.Geological Society of London Special Publication 52*, 253–259.

Jaanusson, V., 1976: Faunal dynamics in the Middle Ordovician (Viruan) of Balto-Scandia. *In* M.G. Bassett (ed.): *The Ordovician system. Proceedings of the Palaeontological Association*, 301–326. University of Wales Press, Cardiff.

Jones, B. & Manning, D.A.C., 1994: Comparison of geochemical indices used for the interpretation of palaeoredox conditions in ancient mudstones. *Chemical Geology 111*, 111–129.

Kaljo, D., Borovko, N., Heinsalu, H., Khazanovich, K., Mens, K., Popov, L., Sergejeva, S., Sobolevskaja, R. & Viira, V., 1986: The Cambrian–Ordovician boundary in the Baltic-Ladoga Clint area (North Estonia and Leningrad Region, USSR). *Proceedings of the Academy of Sciences of the Estonian SSR, Geology 35* (3), 97–108.

Kaljo, D. & Kivimägi, E., 1970: On the distribution of graptolites in the Dictyonema shale of Estonia and the uncontemporaneity of its different facies. *Proceedings of the Academy of Sciences of the Estonian SSR. Chemistry and Geology 19* (4), 334–341 (in Russian with English summary).

Kazmierczak, J., Kremer, B. & Racki, G., 2012: Late Devonian marine anoxia challenged by benthic cyanobacterial mats. *Geobiology 10*, 371–383.

Kiipli, E. & Kiipli, T., 2013: Nitrogen isotopes in kukersite and black shale, implying Ordovician–Silurian seawater redox conditions. *Oil Shale 30* (1), 60–75.

Kirsimäe, K., Jørgensen, P. & Kalm, V., 1999: Low-temperature diagenetic illite-smectite in Lower Cambrian clays in North Estonia. *Clay Minerals 34* (1), 151–163.

Kivimägi, E. & Loog, A., 1972: The main structural types of graptolitic argillites of the Toolse deposit. *Proceedings of the Academy of Sciences of the Estonian SSR. Chemistry and Geology 21* (2), 143–147 (in Russian with English summary).

Kivimägi, E. & Teedumäe, A., 1971: Results of a complex estimation of the rocks in the phosphorite deposit of Toolse. *Proceedings of the Academy of Sciences of the Estonian SSR. Chemistry and Geology 20* (3), 243–250 (in Russian with English summary).

Kleesment, A. & Kurvits, T., 1987: Mineralogy of Tremadoc graptolitic argillites of North Estonia. *Oil Shale 4* (2), 130–138 (in Russian with English summary).

Klesment, I. & Urov, K., 1980: Role of bacterial lipids in the formation of geolipids and kerogens. *Proceedings of the Academy of Sciences of the Estonian SSR. Chemistry29* (4), 241–245.

Leckie, D.A., Singh, C., Goodarzi, F. & Wall, J.H., 1990: Organic-rich, radioactive marine shale: a case study of a shallow-water condensed section, Cretaceous Shaftesbury Formation, Alberta, Canada. *Journal of Sedimentary Petrology 60*, 101–117.

Lille, U., 2003: Current knowledge on the origin and structure of Estonian kukersite kerogen. *Oil Shale 20* (3), 253–263.

Lindgren, H., Drits, V.A., Sakharov, B.A., Salyn, A.L. & Dainyak, L.G., 2000: Illite–smectite structural changes during metamorphism in black Cambrian Alum Shales from the Baltic area. *American Mineralogist 85*, 1223–1238.

Loog, A., Kurvits, T., Aruväli, J. & Petersell, V., 2001: Grain size analysis and mineralogy of the Tremadocian Dictyonema shale in Estonia. *Oil Shale 18* (4), 281–297.

Loog, A. & Petersell, V., 1995: Authigenic siliceous minerals in the Tremadoc graptolitic argillite of Estonia. *Proceedings of the Estonian Academy of Sciences. Geology 44* (1), 26–32.

Loucks, R.G., Reed, R.M., Ruppel, S.C. & Jarvie, D.M., 2009: Morphology, Genesis, and Distribution of Nanometer-Scale Pores in Siliceous Mudstones of the Mississippian Barnett Shale. *Journal of Sedimentary Research 79*, 848–861.

Lyons, T.W. & Kashgarian, M., 2005: Paradigm lost, paradigm found. The Black Sea-black shale connection as viewed from the Anoxic Basin Margin. *Oceanography 18*, 86–99.

Mackay, D.A. & Dalrymple, R.W., 2011: Dynamic mud deposition in a tidal environment: the record of fluid-mud deposition in the Cretaceous Bluesky Formation, Alberta, Canada. *Journal of Sedimentary Research 81*, 901–920.

Macquaker, J.H.S., Bentley, S.J. & Bohacs, K.M., 2010a: Wave enhanced sediment-gravity flows and mud dispersal across continental shelves: reappraising sediment transport processes operating in ancient mudstone successions. *Geology 38*, 947–950.

Macquaker, J.H.S., Keller, M.A. & Davies, S.J., 2010b: Algal blooms and "Marine snow": mechanisms that enhance preservation of organic carbon in ancient fine-grained sediments. *Journal of Sedimentary Research 80*, 934–942.

Männil, R., 1966: *Evolution of the Baltic basin during the Ordovician*. Valgus, Tallinn. 201 pp (in Russian).

Mens, K., Heinsalu, H., Jegonjan, K., Kurvits, T., Puura, I. & Viira, V., 1996: Cambrian–Ordovician boundary beds in the Pakri Cape section, NW Estonia. *Proceedings of the Estonian Academy of Sciences. Geology 45*, 9–21.

Mens, K. & Pirrus, E., 1997: Vendian - Tremadocian clastogenic sedimentation basins. *In* A. Raukas & A. Teedumäe (eds.): *Geology and Mineral Resources of Estonia*, 184–191.

Murphy, A.E., Sageman, B.B., Hollander, D.J., Lyons, T.W. & Brett, C.E., 2000: Black shale deposition and faunal overturn in the Devonian Appalachian basin: clastic starvation, seasonal water-column mixing and efficient biolimiting nutrient recycling. *Paleoceanography 15*, 280–291.

Müürisepp, K., 1960: Die Lithostratigraphie der Packerort-Stufe nach den Angaben der Aufschlüsse in der Estnischen SSR. In *ENSV TA Geoloogia Instituudi uurimused 5*, 37–44. ENSV Teaduste Akadeemia, Tallinn. (in Russian with German summary).

Müürisepp, K., 1964: Käsnläätsedest Pakerordi lademes. In *ENSV Teaduste Akadeemia Looduseuurijate Seltsi aastaraamat 56*, 17–24. Valgus, Tallinn.

Nemliher, J. & Puura, I., 1996: Upper Cambrian basal conglomerate of the Kallavere Formation on the Pakri peninsula, NW Estonia. *Proceedings of the Estonian Academy of Sciences.Geology 45*, 1–8.

Nielsen, A.T., 2004: Sea-level changes – a Baltoscandian perspective. *In* B.D. Webby, F. Paris, M.L. Droser & I.G. Percival (eds.): *The Great Ordovician Biodiversification Event*, 84–93. Columbia University Press, New York.

Nielsen, A.T. & Schovsbo, N.H., 2006: Cambrian to basal Ordovician lithostratigraphy in southern Scandinavia. *Bulletin of the Geological Society of Denmark 53*, 47–92.

Nielsen, A.T. & Schovsbo, N.H., 2011: The Lower Cambrian of Scandinavia: depositional environment, sequence stratigraphy and palaeogeography. *Earth-Science Reviews 107*, 207 – 310.

Niin, M., Rammo, M. & Saadre, R., 2008: Eesti Maavarade kaart. V etapp. 1:400 000 (1:200 000). Diktüoneemakilt (graptoliitargilliit). Seletuskiri. Eesti Geoloogiakeskus, Tallinn.

Noffke, N., 2009: The criteria for the biogeneicity of microbially induced sedimentary structures (MISS) in Archean and younger, sandy deposits. *Earth-Science Reviews 96* (3), 173–180.

Noffke, N., Gerdes, G., Klenke, T. & Krumbein, W.E., 2001: Microbially induced sedimentary structures: a new category within the classification of primary sedimentary structures. *Journal of Sedimentary Research 71* (5), 649.

Paalits, I., 1995: Acritarchs from the Cambrian–Ordovician boundary beds at Tõnismägi, Tallinn, North Estonia. *Proceedings of the Estonian Academy of Sciences. Geology 44* (2), 87–96.

Pacton, M., Fiet, N. & Gorin, G., 2007: Bacterial activity and preservation of sedimentary organic matter: the role of exopolymeric substances. *Geomicrobiology Journal 24*, 571–581.

Pedersen, T.F. & Calvert, S.E., 1990: Anoxia vs. productivity: what controls the formation of organic-carbon-rich sediments and sedimentary rocks? *AAPG Bulletin 74* (4), 454–466.

Plint, A.G., Macquaker, J.H.S. & Varban, B.L., 2012: Bedload transport of mud across a wide, storm-influenced ramp: Cenomanian–Turonian Kaskapau Formation, Western Canada Foreland Basin. *Journal of Sedimentary Research 82* (11), 801–822.

Potter, P.E., Maynard, J.B. & Pryor, W.A., 1980: *Sedimentology of Shale. Study Guide and Reference Source*. Springer-Verlag, New York. 303 pp.

Pukkonen, E. & Rammo, M., 1992: Distribution of molybdenum and uranium in the Tremadoc Graptolite Argillite (Dictyonema Shale) of North-Western Estonia. *Bulletin of the Geological Survey of Estonia 2* (1), 3–15.

Rabalais, N.N., Turner, R.E. & Scavia, D., 2002: Beyond science into policy: Gulf of Mexico hypoxia and the Mississippi River. *Bioscience 52*, 129–142.

Rine, J.M. & Ginsburg, R.N., 1985: Depositional facies of a mud shoreface in Suriname, South America: a mud analogue to sandy, shallow-marine deposits. *Journal of Sedimentary Research 55*, 633–652.

Salmon, V., Derenne, S., Lallier-Vergès, E., Largeau, C. & Beaudoin, B., 2000: Protection of organic matter by mineral matrix in a Cenomanian black shale. *Organic Geochemistry 31*, 463–474.

Schieber, J., 1994: Evidence for high-energy events and shallow water deposition in the Chattanooga Shale, Devonian, central Tennessee, USA. *Sedimentary Geology 93*, 193–208.

Schieber, J., 1999: Microbial mats in terrigenous clastics: the challenges of identification in the rock record. *Palaios 14*, 3–12.

Schieber, J., 2011: Reverse engineering Mother Nature–shale sedimentology from an experimental perspective. *Sedimentary Geology 238*, 1–22.

Schieber, J., Southard, J.B. & Thaisen, K., 2007: Accretion of mudstone beds from migrating floccule ripples. *Science 318*, 1760–1763.

Schieber, J. & Yawar, Z., 2009: A new twist on nud deposition—mud ripples in experiment and rock record. *The Sedimentary Record 7 (2)*, 4–8.

Schlanger, S.O. & Jenkyns, H.C., 1976: Cretaceous oceanic anoxic events: causes and consequences. *Geologie en Mijnbouw 55*, 179–184.

Schovsbo, N.H., 2001: Why barren intervals? A taphonomic case study of the Scandinavian Alum Shale and its faunas. *Lethaia 34*, 271–285.

Schovsbo, N.H., 2002: Uranium enrichment shorewards in black shales: a case study from the Skandinavian Alum Shale. *GFF 124*, 107–115.

Schovsbo, N.H., 2003: The geochemistry of Lower Paleozoic sediments deposited on the margins of Baltica. *Bulletin of the Geological Society of Denmark 50 (1)*, 11–27.

Scupin, H., 1922: Ist der Dictyonemaschiefer eine Tiefseeablagerung? *Zeitschrift Deutschen Geologischen Gesellschaft 73 (6/7)*, 153–155.

Snäll, S., 1988: Mineralogy and maturity of the alum shales of south-central Jämtland, Sweden. *Sveriges Geologiska Undersökning Serie C 818*, 1–46.

Soesoo, A. & Hade, S., 2012: Metalliferous organic-rich shales of Baltoscandia - a future resource or environmental/ecological problem. *Archiv Euro Eco 2*, 11–14.

Sumberg, A.I., Urov, K.E. & Aasmäe, E.E., 1990: Characteristic of the Estonian Lower Ordovician fossil organic matter (Maardu member of the Pakerort horizon). *Oil Shale 7 (3–4)*, 238–244 (in Russian with English summary).

Thickpenny, A., 1987: Palaeooceanography and depositional environment of the Scandinavian Alum shales: sedimentological and geochemical evidence. *In* J. K. Leggett & G.G. Zuffa (eds.): *Marine Clastic Sedimentology–Concepts and Case Studies*, 156–171. Graham & Trotman, London.

Traykovski, P., Geyer, W.R., Irish, J.D. & Lynch, J.F., 2000: The role of wave-induced density-driven fluid mud flows for cross-shelf transport on the Eel River continental shelf. *Continental Shelf Research 20*, 2113–2140.

Tribovillard, N., Algeo, T.J., Lyons, T.W. & Riboulleau, A., 2006: Application of trace metals as paleoredox and paleoproductivity proxies. *Chemical Geology 232*, 12–32.

Utsal, K., Kivimägi, E. & Utsal, V., 1982: About method of investigating Estonian graptolithic argillite and its mineralogy. *Acta et Commentationes Universitatis Tartuensis 527*, 116–136. Tartu Riiklik Ülikool, Tartu (in Russian with English summary).

Voolma, M., Soesoo, A., Hade, S., Hints, R. & Kallaste, T., 2013: Geochemical heterogeneity of the Estonian graptolite argillite. *Oil Shale 30 (3)*, 377–401.

Wignall, P.B., 1991: Model for transgressive black shales? *Geology 19*, 167–170.

Wignall, P.B., 1994: *Black Shales. Geology and Geophysics Monographs 30*. Oxford University Press, Oxford. 130 pp.

Wignall, P.B. & Newton, R., 2001: Black shales on the basin margin: a model based on examples from the Upper Jurassic of the Boulonnais, northern France. *Sedimentary Geology 144*, 335–356.

Wilde, P., Quinby-Hunt, M.S., Berry, W.B.N. & Orth, C.J., 1989: Palaeo-oceanography and biogeography in the Tremadoc (Ordovician) Iapetus Ocean and the origin of the chemostratigraphy of *Dictyonema flabelliforme* black shales. *Geological Magazine 126*, 19–27.

Yao, W. & Millero, F.J., 1995: The chemistry of anoxic waters in the Framvaren Fjord, Norway. *Aquatic Geochemistry 1 (1)*, 53–88.

PAPER II

VOOLMA, M., SOESOO, A., HADE, S., HINTS, R., KALLASTE, T. 2013. Geochemical heterogeneity of Estonian graptolite argillite. *Oil Shale*, **30(3)**, 377–401.

GEOCHEMICAL HETEROGENEITY OF ESTONIAN GRAPTOLITE ARGILLITE

MARGUS VOOLMA[*], ALVAR SOESOO, SIGRID HADE, RUTT HINTS, TOIVO KALLASTE

Institute of Geology, Tallinn University of Technology, Ehitajate tee 5, 19086 Tallinn, Estonia

Abstract. *This paper describes vertical fine-scale geochemical heterogeneity of Estonian graptolite argillite (GA). GA samples from Pakri and Saka outcrop sections were collected at 20 cm intervals for chemical analysis of major and trace elements, including rare earth elements. The study indicates GA enrichment in U, V, Mo and Pb with respect to the average black shales and thus confirms the formerly reported data on GA geochemistry in general. However, the content of enriched elements and other trace metals was recorded to vary greatly across the sequences suggesting that trace metal distribution in GA is notably more heterogeneous than previously assumed. The origin of the observed complex distribution of trace elements was likely controlled by the interplay of different primary metal supply-sequestration factors/processes, such as synsedimentary redox-driven sequestration of redox sensitive elements, the provenance of clastic input, the post-sedimentary redistribution, etc.*

Keywords: graptolite argillite, black shale, geochemistry, trace metals, REE, Estonia.

1. Introduction

The Estonian graptolite argillite (GA), Tremadoc in age, is distributed in northern Estonia and on Vormsi and Hiiumaa islands. It belongs to the Türisalu Formation and is overlain by glauconitic sandstones and clays of the Varangu Stage and underlain by the phosphatic quartzose sandstone of the Kallavere Formation [1]. The GA is an argillaceous rock enriched with organic matter [2] and is characterized by high concentrations of a number of trace elements, including U, V and Mo. The thickness of GA reaches 7.4 m in NW Estonia and decreases towards the east and south. On a regional scale, GA belongs to the wide but patchy belt of Middle Cambrian

---

[*] Corresponding author: e-mail *voolma@gi.ee*

to Lower Ordovician black shales extending from Lake Onega district in the east to the Caledonian front, Oslo region and Jutland Peninsula in the west [3–6].

There are numerous studies conducted on various metalliferous black shale/oil shale deposits worldwide – black shale deposits in North America [7–12], China [13, 14], central Europe [15], and alum shale in Scandinavia [3, 16–20] – focusing on the general characteristics and different aspects of metallogenesis in those assemblages. Also, a series of investigations have been targeted on the general geochemistry and trace element distribution of Estonian GA [21–30].

The metalliferous nature of GA was well known already in the first half of the last century. A more systematic picture of GA outside its outcrop area near the Baltic Klint, however, was gathered thanks to the extensive geological mapping of basement, drilling and geochemical investigations, which started in the 1950s and were conducted by the Geological Survey of Estonia. The vast amount of detailed information on the GA lithology and geochemistry was collected during the prospecting of Estonian phosphorite resources, e.g. [23, 31, 32]. The previous investigations have allowed depicting general trends of trace element enrichment and lateral distributions within GA, demonstrating at the same time high trace metal heterogeneity of those deposits [26, 28, 29]. Still, relatively little is known about the source of metals and the mechanism that caused metal enrichment in many black shale deposits worldwide, including GA. Although several investigations have been conducted during the past decades [25–30], the origin of metals is still unclear, as why their content is so heterogeneous laterally and also vertically through the GA complex.

Based on previous geochemical investigations [26] three geochemical zones have been distinguished in Estonian GA: Western, Central and Eastern zones (Fig. 1). The zones differ mainly in concentration of metals which are characteristic of GA – Mo, V, U. However, based on the present study it will be shown that the distribution of metals in GA has a more complex pattern. This paper describes the vertical bed-to-bed variation of metals, with emphasis on two vertical cross-sections, and discusses some possible critical factors that may stand behind the trace metal enrichment and heterogeneity in those complexes. Samples for the study were collected from Pakerort cliff on Pakri Peninsula, NW Estonia and Saka cliff, NE Estonia (Fig. 1), selected to represent GA complex in different geochemical zones. According to biostratigraphic studies GA in those localities does not represent strictly coeval sedimentation: GA from Western Estonia is assigned to the Pakerort Stage, whereas GA within the Eastern Zone belongs to the younger Varangu Stage [33, 34].
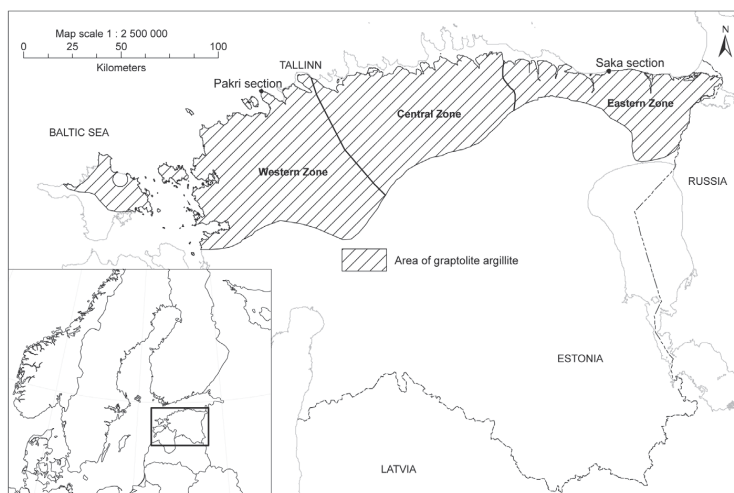
Fig. 1. Map of the location of GA and sampled outcrop sections.

2. Material and methods

Two outcrops, Pakri and Saka, were sampled at 20 cm intervals for geochemical analysis. Twenty-one fresh GA samples from Pakri and nine samples from Saka were collected from the outcrop sections of 4.2 m and 1.8 m, respectively. The weight of samples was approximately 2 kg. The samples were cleaned, dried, crushed and homogenized for chemical analysis. The sample powders were analyzed for major and trace element composition, including rare earth elements, in order to determine the geochemical changes across the section and general rock composition. Geochemical analysis was performed using X-ray fluorescence (XRF) and ICP-MS analysis.

XRF analysis was conducted at the Institute of Geology, Tallinn University of Technology (TUT), with an S4 Pioneer Spectrometer (Bruker AXS GmbH, Germany), using an X-ray tube with a rhodium anode, which operated with a power of 3 kW. The samples were measured with a manufacturer's standard as MultiRes modification (pre-calibrated standardless method). The in-house standard ES-2 ("Dictyonema Shale") was used as reference material [34]. Loss on ignition (LOI) was determined from 1 g of sample material at 500 °C and 920 °C. ICP-MS analysis was conducted at the Institute of Geology, TUT. Rare earth elements of Pakri samples were determined from solutions which were prepared following the nitric, hydrofluoric, hydrochloric and boric acids digestion of a 0.250 g pulverized sample in an Anton Paar MW3000 microwave oven. A set of samples from

Pakri and Saka were additionally re-analyzed for trace elements, including rare earths, at ACMELABS in Canada.

Mineralogical analysis of selected whole rock powdered samples was conducted using an X-ray diffractometry apparatus (HZG4 diffractometer) at the Institute of Geology, TUT. XRD analysis was performed using a Fe-filtered Co radiation (35 kV and 25 mA) and scintillation detector. The range from 5–45°2Θ was scanned with a step of 0.04°2Θ. For selected samples complementary scanning electron microscope (SEM) analysis was used. SEM examination of uncoated rough and flat unpolished GA samples was carried out at the Institute of Geology, TUT, with a Zeiss EVO MA15 scanning electron microscope.

3. Mineralogy of graptolite argillite

GA is a fine-grained kerogen-rich siliceous deposit characterized by high content of organic matter (15–20%) and pyrite (2.4–6.0%) [2], and very low thermal maturity. The mineral assemblage of GA is according to previous studies dominated by K-feldspars, quartz and clay minerals [35, 36]. In the lateral as well as vertical dimension the contents of major rock-forming minerals show slight but pronounced variation patterns [35, 37, 36]. The average content of quartz in GA gradually rises eastward with the corresponding clay mineral decrease. In NE Estonia, the argillite complex is intercalated with numerous quartzose silt beds [30]. From authigenic sulfides, the occurrence of pyrite, marcasite, sphalerite and galena has been documented. In outcrops and drill cores secondary gypsum and jarosite commonly appear. In general, a higher degree of sulfide mineralization within GA is associated with the occurrence of silt interbeds. Those interbeds might also host a higher amount of other minor authigenic compounds typical for GA – phosphates (mainly apatite as biogenic detritus and nodules), carbonates (calcite and dolomite as cement and concretions), barite and glauconite. Besides the highly resistant terrigenic accessory phases, considerable abundance of micas in GA beds has been documented [35, 37].

Detailed mineralogical study is beyond the scope of the present paper. However, in order to record general mineralogical outline, XRD analysis of selected GA samples from the Pakri outcrop was performed. The study confirmed the presence of K-feldspar (sanidine), illite (illite-smectite, micas), quartz, pyrite, marcasite, apatite, calcite, dolomite, galena and chlorite. The analysis with SEM revealed high micrometer-scale morphological heterogeneity in the examined samples. The dominance of finely disseminated microcrystalline euhedral K-feldspar and quartz in argillite suggests that these minerals in GA are commonly authigenic in origin. The multistage development of syngenetic-diagenetic mineral assemblages and importance of redistribution processes in GA are suggested by the

occurrence of a high variety of pyrite crystal forms within the argillite matrix as well as in sulfide enriched interbeds.

4. Results and discussion on the geochemistry of the Estonian graptolite argillite

Detailed vertical geochemical heterogeneity in the GA has not been studied previously. There is little understanding of the scale of heterogeneity and distribution pattern of elements. Moreover, detailed lateral geochemical changes across the GA unit are unknown. As an example of elemental distribution, V, Mo and Pb within the Estonian GA unit are displayed in Figure 2. The initial data were selected from the database of the Geological
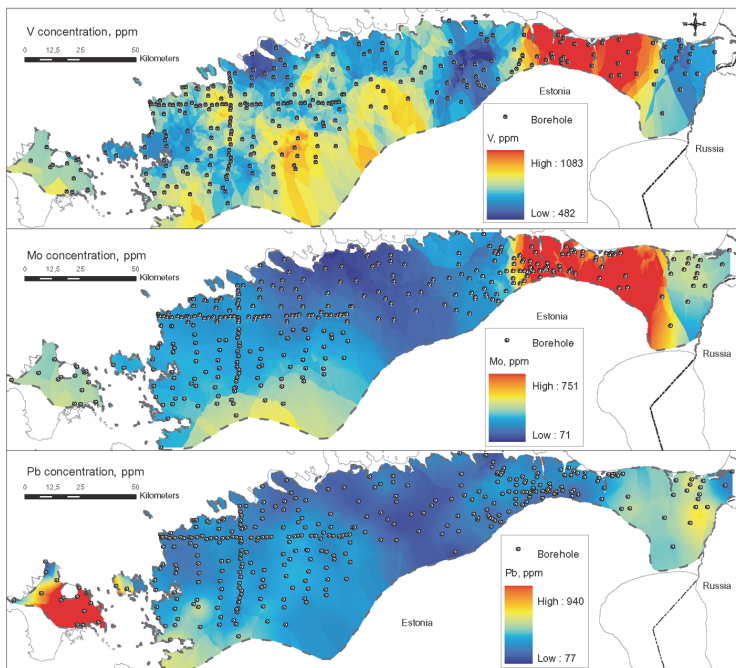

Fig. 2. V, Mo and Pb concentrations in Estonian GA as modeled using calculated average drill core analyses (data: Geological Survey of Estonia, 2008). Element concentration surfaces were modeled by the kriging method using spherical distances (ESRI ArcGIS). For distribution model of V data from 297 drill cores were selected, for Mo 325 and for Pb 345 drill cores were used.

Survey of Estonia. These elemental concentration data represent the calculated average concentration in the GA in the drill core. The central and western parts of the Eastern Zone show the highest concentrations for V and Mo (Figs. 2, 1). Generally, it can be concluded that the concentration of most of the metals is relatively low in the Central Zone (Figs. 2, 1). Pb shows the highest concentrations on Hiiumaa Island. It must be emphasized that the available data is relatively unevenly distributed, especially the southern margin of the GA bed. Therefore, geochemical generalizations of this kind are informative but must be taken with precaution. More drilling material and studies of the vertical geochemical change of elements in GA are needed to define spatial geochemical patterns.

4.1. Major elements

The bed-to-bed study performed on geochemical variation from Saka and Pakri sections show that major elements vary relatively little across the examined GA sequences (Table 1). Analyses indicate that the GA assemblage is siliceous, high-K, Mn-poor and with variable Fe and S contents.

The SiO_2 abundance in examined GA sections varies from 45.74 to 55.11 wt% and shows a general increase towards the upper part of the GA complex. The observed distribution pattern agrees with previously described lithological changes – general increase of the silt/clay ratio from bottom to top of the beds in Estonian GA sequences [37, 36]. Besides, there is an inverse correlation between LOI 500 °C (reflecting organic matter content in GA) and SiO_2. The Al_2O_3 content varies between 10.9 and 14.49 wt% and its average concentration is somewhat higher in GA from the Pakri locality. Titanium behavior shows a strong correlation with aluminum suggesting a possible detrital origin. The distinct feature of the Estonian GA is its elevated potassium content, in Pakri and Saka GA sequences K_2O ranges from 6.59 to 8.44 wt%. The high potassium content is likely connected with the abundance of authigenic K-feldspar in those beds, thus differentiating Estonian GAs from the Scandinavian alum shale, where clay minerals occur as the dominant K-rich phases [38]. Pronounced potassium enrichment is also evident when the detected chemical composition of GA is compared with the compositions of widely used standard shale compilations such as PAAS (Post Archaean Australian Shale) [39], and NASC (North American Shale Composite) [40] (Fig. 3). On the other hand, a number of major element compounds, such as MnO, Na_2O, CaO, MgO, appear to be considerably depleted with respect to the "standard shale" composition. The content of all those elements in the studied GA sequences is consistently well below 1.5 wt%.

The invariably low manganese content of Cambrian-Tremadoc black shales of the Baltoscandian region was interpreted by Wilde et al. [10] as an indicator of persistently euxinic environment during accumulation of the

Table 1. Major elements in GA samples from Pakri and Saka sections

Interval, cm		Sample	GI XRF %												%	GI %	
From	To		SiO_2	TiO_2	Al_2O_3	Fe_2O_3	MnO	MgO	CaO	Na_2O	K_2O	P_2O_5	Cl	S	SUM	LOI500°C	LOI920°C
0	20	Pakri1	46.10	0.72	13.91	4.89	0.020	1.31	0.25	0.07	8.00	0.15	0.019	2.23	99.48	22.10	24.05
20	40	Pakri2	45.74	0.71	13.60	4.01	0.020	1.33	0.22	0.07	7.77	0.11	0.020	1.96	99.69	24.46	26.09
40	60	Pakri3	46.83	0.70	13.55	4.29	0.019	1.30	0.20	0.07	7.73	0.12	0.026	2.11	99.69	23.27	24.86
60	80	Pakri4	48.77	0.72	13.66	4.33	0.020	1.27	0.23	0.06	7.95	0.14	0.022	2.16	99.16	20.46	21.99
80	100	Pakri5	48.01	0.72	13.60	4.44	0.020	1.26	0.13	0.06	7.82	0.12	0.025	2.11	99.54	21.77	23.33
100	120	Pakri6	47.57	0.72	13.38	4.07	0.019	1.22	0.12	0.06	7.85	0.10	0.023	2.02	98.87	22.21	23.73
120	140	Pakri7	48.37	0.73	13.65	4.13	0.018	1.22	0.11	0.07	7.92	0.12	0.029	2.03	99.59	21.69	23.22
140	160	Pakri8	49.91	0.75	13.85	4.36	0.019	1.23	0.10	0.07	8.02	0.12	0.023	2.12	99.87	19.79	21.42
160	180	Pakri9	48.25	0.73	13.85	4.28	0.018	1.23	0.12	0.06	8.12	0.09	0.024	2.16	99.99	21.59	23.22
180	200	Pakri10	49.63	0.70	13.45	4.95	0.017	1.17	0.16	0.06	7.88	0.14	0.018	2.56	99.54	19.73	21.36
200	220	Pakri11	51.35	0.75	13.94	4.97	0.017	1.18	0.15	0.07	8.25	0.18	0.020	2.39	99.70	16.96	18.83
220	240	Pakri12	49.71	0.75	13.65	4.25	0.018	1.19	0.13	0.07	8.12	0.14	0.023	2.08	99.03	19.30	20.99
240	260	Pakri13	49.09	0.74	13.67	5.22	0.019	1.25	0.14	0.07	7.77	0.13	0.017	2.64	100.03	19.95	21.92
260	280	Pakri14	49.41	0.74	13.88	6.08	0.018	1.25	0.21	0.07	7.72	0.19	0.017	2.98	99.98	18.45	20.40
280	300	Pakri15	49.61	0.76	14.06	4.38	0.019	1.30	0.18	0.07	8.20	0.13	0.018	2.06	99.02	18.60	20.29
300	320	Pakri16	48.97	0.75	14.00	4.44	0.018	1.24	0.10	0.07	8.15	0.13	0.019	2.18	99.15	19.50	21.27
320	340	Pakri17	52.43	0.68	13.21	4.25	0.019	1.16	0.60	0.07	7.91	0.48	0.015	2.14	98.18	15.40	17.35
340	360	Pakri18	50.03	0.79	14.49	4.21	0.021	1.33	0.18	0.07	8.44	0.14	0.017	1.95	100.12	18.58	20.40
360	380	Pakri19	51.69	0.80	14.41	4.42	0.021	1.33	0.23	0.07	8.42	0.17	0.013	1.95	99.20	15.83	17.62
380	400	Pakri20	51.87	0.78	14.12	4.72	0.020	1.23	0.18	0.07	8.32	0.11	0.014	2.23	99.33	16.10	17.89
400	420	Pakri21	51.59	0.79	14.09	5.02	0.022	1.27	0.43	0.08	8.16	0.27	0.015	2.41	99.49	15.30	17.76
0	20	Saka1	49.73	0.73	11.94	4.21	0.009	0.72	0.25	0.06	7.23	0.37	0.020	2.68	99.99	21.28	24.73
20	40	Saka2	51.75	0.64	11.00	6.00	0.008	0.64	1.08	0.06	6.59	1.08	0.019	4.00	99.29	16.03	20.43
40	60	Saka3	48.28	0.64	11.27	4.20	0.009	0.67	0.18	0.05	6.90	0.54	0.028	2.57	99.05	23.70	26.29

Table 1 (continuation)

	Interval, cm			GI XRF %												%	GI %	
From	To	Sample	SiO$_2$	TiO$_2$	Al$_2$O$_3$	Fe$_2$O$_3$	MnO	MgO	CaO	Na$_2$O	K$_2$O	P$_2$O$_5$	Cl	S	SUM	LOI500°C	LOI920°C
60	80	Saka4	46.54	0.68	11.84	3.93	0.012	0.87	0.11	0.06	7.17	0.25	0.021	2.05	99.91	26.19	28.43
80	100	Saka5	49.95	0.70	11.55	3.78	0.012	0.87	0.13	0.05	7.29	0.29	0.030	2.03	99.84	22.83	25.19
100	120	Saka6	52.02	0.67	10.90	3.81	0.011	0.78	0.13	0.05	6.90	0.24	0.020	1.95	99.77	22.61	24.25
120	140	Saka7	48.01	0.65	11.01	4.97	0.012	0.82	0.19	0.05	6.85	0.20	0.022	2.48	99.80	24.96	27.02
140	160	Saka8	55.11	0.75	12.38	4.82	0.018	0.98	0.25	0.06	7.51	0.23	0.019	1.34	99.38	14.63	17.24
160	180	Saka9	48.86	0.64	10.91	4.95	0.033	0.82	1.24	0.06	6.79	1.33	0.020	1.57	99.29	19.71	23.63
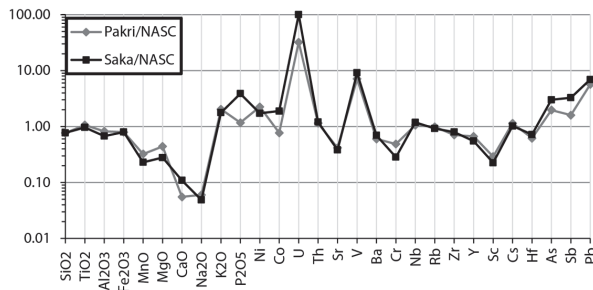
Fig. 3. Major and trace elements of GA samples normalized to NASC (North American Shale Composite) after [40].

black shale complexes. Typically for the organic-rich deposits formed under oxygen deficient environment, the Estonian GA suggests efficient sequestration of sulfur and iron. The content of these elements is, however, highly variable in different samples investigated. The content of Fe_2O_3 in the examined samples varied between 3.79 and 6.08 wt%. The sulfur concentration changed from 1.34 to 4 wt%. The strong correlation between the abundances of sulfur and iron in the Pakri GA sequence indicates that most of the sulfur is incorporated into iron sulfides rather than into organic matter. In the Saka section the correlation between the behaviors of sulfur and iron is less apparent, partly probably due to formation of secondary sulfates and phosphates. P_2O_5 and CaO, whose abundance in GA is generally low, are mainly included in apatite, as suggested by the covariance of those elements in the GA samples. Nevertheless, the detailed variance patterns of phosphorus in Saka and Pakri sequences reveal that on the background of generally monotonous phosphorus content some GA intervals (e.g. Saka2, Saka9, Pakri17) present anomalously high concentrations of P_2O_5. Elevated phosphorus values might be due to the higher level of mixing with phosphatic detritus, suggested by the considerable abundance of phosphatic bioclastic fragments in these GA levels or due to the formation of diagenetic apatite.

If the two GA sequences under study are compared on the basis of major element composition, differences appear to be moderate – the Pakri samples have a slightly higher content of K_2O, Al_2O_3, TiO_2 and MgO and a lower content of CaO and P_2O_5. In general, the relatively homogeneous major element distribution gives limited clues for predicting the highly inhomogeneous trace element enrichment patterns and for unraveling the processes behind enrichment.

4.2. Trace elements

Trace metal enrichment in black shales is mostly explained by two alternative theories: 1) synsedimentary sequestration of metals under oxygen-deficient conditions from marine water, e.g. [41, 12, 20], or 2) flushing of the sediments by metal-enriched syngenetic brines or contemporaneous exhalation of such brines into marine basin, e.g. [42, 14, 43, 25, 30]. However, these theories are challenged by works that underline the influence of source rocks and particulate precursor material on the final character of metal enrichment in black shales, e.g. [44], or the crucial role of diagenetic redistribution processes induced by late diagenetic brines, e.g. [8, 45].

In general, U-Mo-V-Pb enriched trace metal association with sporadically elevated concentrations of some other trace elements was detected in GA from Saka and Pakri sections (Table 2). For assessing the degree of enrichment of particular trace metals in GA, the detected average trace element abundances were compared with average shale and black shale standard compilations. With respect to PAAS and NASC values the GA appears to be extremely enriched in U and V (Fig. 3). For example, the average U concentration in the Saka section (267 ppm) is a hundred times higher than the corresponding values for NASC. There is a nine-fold difference in V concentration between NASC and Saka GA section (average 1190 ppm). If compared with the minimum enrichment values (m.e.v.) for metalliferous black shales (suggested by Vine and Tourtelot [7] on the basis of generalized data of numerous North-American black shales), the studied samples and the Estonian GA in general could be considered enriched with U (m.e.v. 30 ppm), Mo (m.e.v. 200 ppm), V (m.e.v. 1000 ppm), Pb (m.e.v. 100 ppm) and Co (m.e.v. 30 ppm; only in Saka samples) [28].

All previously listed enriched trace metals of GA as well as other abundant trace elements, like As, Sb, Ni, Cu, Re, belong to the group of redox sensitive and/or stable sulfide-forming metals and might undergo considerable partitioning in marine geochemical and biochemical cycles. As indicated by the studies of trace elements in modern marine environments, e.g. [46–48], the redox sensitive elements mostly occur as soluble species under oxidizing conditions. Under the oxygen-depleted conditions, however, the redox sensitive elements are typically present as insoluble species (metal-organic complexes, sulfides, metal oxyhydrates) and thus tend to sequester into sediments. The whole metal trapping process is strongly linked with organic matter breakdown and sulfate reduction processes, which inhibit the crystallization of sulfides. In addition to the redox sensitive trace elements, other elements like Fe and Mn found commonly enriched in black shales, are essential recyclers in redox partitioning in marine systems [49]. Consequently, based on numerous comparative studies of trace element accumulation in modern and ancient organic rich sediments, e.g. [50, 51], it has been suggested that oxygen availability in sedimentary environment could have had sole control over development of enriched trace metal associations in different black shales, e.g. [12].

Table 2. Trace elements in GA samples from Pakri and Saka sections

Interval, cm		Lab	Acme									GI XRF	Acme		GI XRF			Acme	GI XRF					Acme		
														PPM												
From	To	Sample	Mo	Cu	Pb	Zn	Ni	Co	As	U	Th	Sr	Sb	V	Ba	Cr	Se	Ga	Nb	Rb	Zr	Y	Sc	Be	Li
0	20	Pakri1	639	146	105	45	130	18	55	126	13	62	5.4	1081	398	45	3.7	17.8	13.6	128	129	23	3.3	1.8	17.3
20	40	Pakri2	181	115	75	40	124	16	39	108	12	65	4.3	1166	395	48	3.1	15.6	13.5	127	128	19	3.5	1.6	18.0
40	60	Pakri3	203	134	101	49	166	33	56	206	13	65	5.0	1223	381	51	3.5	15.7	13.0	127	133	19	4.5	2.3	18.8
60	80	Pakri4	148	133	98	845	178	27	51	82	13	63	3.9	1025	384	48	3.3	14.2	12.5	121	134	27	4.5	2.1	16.4
80	100	Pakri5	155	143	116	138	170	24	56	164	14	62	4.2	1061	369	50	3.7	15.0	17.2	125	132	18	5.0	2.3	18.7
100	120	Pakri6	151	133	98	134	144	15	52	172	13	64	4.4	1015	399	54	3.3	15.2	19.5	124	138	17	3.8	2.0	15.3
120	140	Pakri7	157	148	105	42	147	22	55	117	15	63	4.0	1229	347	57	4.1	14.9	15.2	125	136	20	4.8	2.0	17.1
140	160	Pakri8	126	151	193	39	141	21	52	93	15	64	3.3	1144	381	57	4.5	14.0	14.0	126	142	18	4.6	1.3	16.3
160	180	Pakri9	88	162	143	39	115	18	47	78	14	61	2.6	827	374	54	3.1	15.6	14.3	124	131	13	4.4	1.4	15.3
180	200	Pakri10	74	152	135	38	160	22	59	52	14	56	2.5	652	388	71	4.1	14.6	11.9	113	137	24	4.2	1.6	14.5
200	220	Pakri11	61	151	135	60	107	15	72	41	16	57	2.4	563	376	72	3.8	14.5	12.8	117	144	17	4.2	1.3	14.6
220	240	Pakri12	102	129	132	50	115	16	54	91	14	57	3.0	1040	387	65	4.7	12.9	12.6	125	144	21	n.a.	n.a.	n.a.
240	260	Pakri13	110	161	152	40	172	19	68	65	15	55	4.4	1096	318	60	7.7	16.8	13.9	115	139	21	4.7	1.7	15.6
260	280	Pakri14	60	162	174	37	185	21	118	52	14	54	5.2	839	344	62	5.8	12.5	10.7	105	140	31	4.2	2.0	14.6
280	300	Pakri15	92	131	103	40	133	21	52	76	14	59	3.1	1081	408	57	4.3	15.0	14.0	128	140	21	4.5	1.2	16.1
300	320	Pakri16	85	144	117	42	120	17	54	102	15	56	3.5	1096	358	63	4.0	16.2	15.9	128	138	13	4.6	1.0	15.4
320	340	Pakri17	96	120	105	38	113	35	63	82	16	67	3.3	739	377	48	3.7	13.9	10.6	118	148	73	5.0	1.3	14.9
340	360	Pakri18	53	141	103	41	96	17	45	35	14	54	2.2	781	377	70	2.9	16.7	13.2	131	142	21	4.9	1.2	16.7
360	380	Pakri19	57	129	100	42	104	15	53	49	16	54	2.7	925	429	73	4.8	16.5	12.7	128	150	23	4.7	1.0	16.4
380	400	Pakri20	52	125	94	40	116	17	55	19	14	48	2.0	622	393	56	2.6	15.9	12.3	121	153	21	4.1	1.0	14.6
400	420	Pakri21	65	101	88	36	99	17	65	57	14	55	2.1	745	369	74	3.6	13.7	13.4	119	157	40	n.a.	n.a.	n.a.
0	20	Saka1	1143	76	193	14	82	44	64	137	13	62	9.1	1266	390	36	5.3	15.0	16.0	120	168	9	2.8	0.5	3.9
20	40	Saka2	85	85	187	10	103	102	76	182	16	56	5.3	946	409	36	5.7	12.0	10.0	92	171	31	3.6	0.6	3.1

Table 2 (continuation)

| Interval, cm		Lab	Acme									Gl XRF	Acme	Gl XRF			Acme		Gl XRF				Acme		
			PPM																						
From	To	Sample	Mo	Cu	Pb	Zn	Ni	Co	As	U	Th	Sr	Sb	V	Ba	Cr	Se	Ga	Nb	Rb	Zr	Y	Sc	Be	Li
40	60	Saka3	97	134	152	14	82	62	86	169	15	52	4.5	1093	406	32	5.3	16.0	17.0	108	155	12	3.2	0.8	4.1
60	80	Saka4	1844	176	101	25	89	31	72	805	16	51	9.9	1497	438	41	5.5	16.0	19.0	141	165	6	4.8	1.2	9.1
80	100	Saka5	202	122	135	22	89	43	54	111	16	49	5.5	1453	435	38	5.1	15.0	14.0	116	163	11	3.1	0.7	7.1
100	120	Saka6	408	106	124	21	88	25	57	433	14	47	5.7	1288	441	30	4.3	13.0	16.0	122	160	9	3.0	0.7	6.9
120	140	Saka7	413	108	137	36	127	28	50	239	14	50	7.2	1165	390	31	4.1	13.0	21.0	114	135	16	2.7	0.5	8.1
140	160	Saka8	279	116	125	116	118	51	75	145	16	56	6.5	1096	421	38	5.6	11.0	16.0	121	173	23	3.8	0.9	9.8
160	180	Saka9	299	148	95	23	125	53	236	184	15	66	8.0	908	650	38	7.1	10.0	10.0	102	149	57	3.2	0.8	7.8
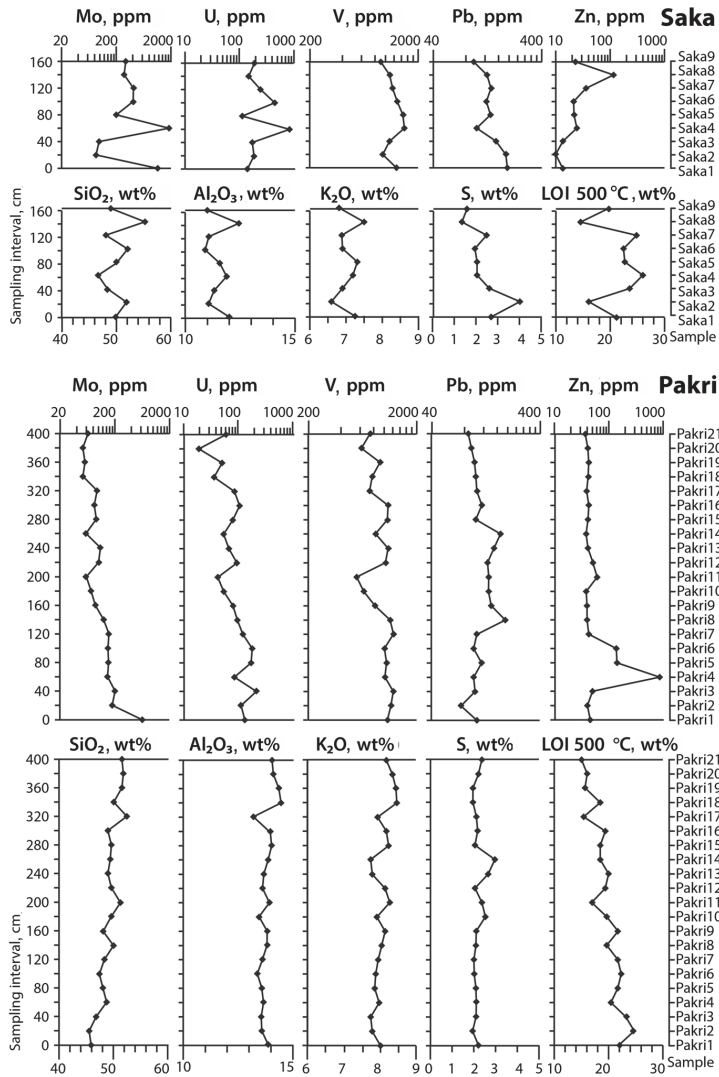
Fig. 4. Vertical distribution profiles of major compounds SiO_2, Al_2O_3, K_2O, S, and LOI 500 °C and enriched trace metals from Saka and Pakri GA sections.

The performed geochemical investigations revealed that the studied sequences present pronounced vertical variations in U, V, Mo and Zn con-

centrations (Fig. 4). The listed trace elements do not show completely matching variance patterns and the maximum (and minimum) enrichment intervals of different components mostly do not overlap. In case of the Pakri GA sequence one can separate about 1.3 m thick lower part, which is enriched with some trace metals like Mo, U and Sb, and also contains more organic matter as indicated by higher LOI 500 °C values. While Mo is gradually decreasing towards the upper part of the Pakri sequence, U and V contents are somewhat more erratic. The thinner GA complex from Saka, which on average contains more Mo, U and V than the Pakri GA, is also characterized by the larger variance of those elements. In Saka samples, no clear vertical distribution trends of Mo and U can be followed, the concentrations fluctuate on a large scale and very high values alternate with low ones. For example, in samples Saka1 and Saka4 the Mo content is 1143 and 1843 ppm, respectively, while between these samples it only varies between 85 and 97 ppm. In general, Mo and U contents in the Saka section show quite a strong positive covariance with organic matter content (LOI 500 °C). The sample Saka4, which presents anomalously high values of these elements, also yielded the highest LOI 500 °C value. These results agree with the observation that the contents of V, U and Mo in black shales typically correlate with the abundance of organic matter [7], likely indicating early fixation via metal-organic complexes. However, in case of V, which shows considerably high values throughout both studied GA sequences, the correlation with organic matter is less expressed.

The average content of Pb is similar in both investigated sections and its vertical distribution is rather homogeneous. Lead shows a positive covariance with elements presumably related with sulfides – Fe_2O_3, S, Cu, Se, Ag, Hg in Pakri samples, while in Saka there is a positive correlation with S and Ta, and a negative one with Cu, Li, Re, Sn. Zn generally demonstrates an opposite trend to internally enriched elements such as U, V, Mo. Its abundance is two times higher in Pakri samples compared to Saka ones. However, the elevated concentrations of Zn in the Pakri section (up to 761 ppm in Pakri4) are limited to the well-defined interval 60–120 cm from the bottom, whereas the rest of the sequence is characterized by a monotonous Zn concentration near 40–60 ppm. In the Saka section the content of Zn is very low in the lower part of the section, but shows a general increase toward the upper part of the complex. The pronounced positive covariance of Cd with Zn in the studied sequences likely indicates a coeval trapping of those phases during sphalerite formation.

U positive covariance with P_2O_5 was not detected in the samples under study. Trace metal partitioning into phosphates has been suggested by some studies [52] as a process responsible for the higher general concentration of U in the GA of NE Estonia.

In general, the dominance of common marine redox sensitive elements among enriched metals in GA favors syngenetic enrichment as the major process of trace metal sequestration. On the other hand, the remarkably high

concentration of enriched elements in GA and the variable covariance patterns imply that element sequestration solely from seawater due to Eh gradients is likely an insufficient model for explaining the observed large-scale trace metal heterogeneity in GA. Furthermore, the current data (Tables 2, 3) as well as previous studies [2] indicate that besides the elements, for which partitioning in marine systems is well known, GA sporadically presents elevated levels of some minor elements, e.g. PGE and W, characterized by generally very low abundance in average crust and modern marine sediments. The accumulation of such minor compounds in GA underlines the role of internal input of metals into the sedimentary or diagenetic environment.

The closeness of probable denudation areas (the peneplain of Proterozoic crystalline rocks in Southern Finland) to the sedimentary setting where GA accumulated hints that the trace elemental composition of sea water in these areas likely bore a distinct terrestrial signature, similarly to recent coastal marine environments [49]. Moreover, recent studies in Caledonian Nappe complexes, e.g. [53], suggest the existence of subduction zone related volcanic arc complexes within the Iapetus Ocean near the western border of the Baltica paleocontinent in the Late Cambrian and Tremadoc. The associated volcanic activity in these areas could supply overlying waters with extra trace metal budgets and modify regional marine trace metal signals enhancing, for example, Zn and V content of marine water. Then again, the likely introduction of the particulate volcanic matter to the sedi-mentary basin during the times of GA formation is suggested by clay mineral studies. According to Utsal et al. [35] the widespread occurrence of authigenic illite-smectite in GA indicates that at least 10% of its primary sedimentary matter was made up of volcanic ash.

The differences in trace element composition of GA might thus in some instances reflect variations in source material fluxes. First of all this relates to non-reactive elements with negligible solubility in surface environments transported to the sedimentary basin mainly in the composition of terrigenic (volcanic) matter such as residual heavy minerals, secondary weathering products or volcanic ash. According to Vine and Tourtelot [7], the detrital fraction of most black shales is characterized by the elements Al, Ti, Zr, Ga, Sc, and may also commonly include Be, B, Ba, Na, K, Mg, and Fe. Additional elements generally considered insensitive to secondary processes include Nb, Y, Th, Ta, Hf, and the REEs [39].

On the La-Al and La-Ti diagrams (Figs. 5A, 5B) the distribution of Al and Ti shows a similar pattern with respect to the lanthanum behavior. The Pakri samples with higher alumina and silica values and somewhat higher Ti content have enhanced La values as compared to Saka samples. The covariance of La with typical detrital compounds suggests that La may be dominantly bounded by detrital phases. However, the abnormally high La content detected in three phosphorus-rich samples may suggest a possible synsedimentary incorporation into the biogenic detritus or diagenetic
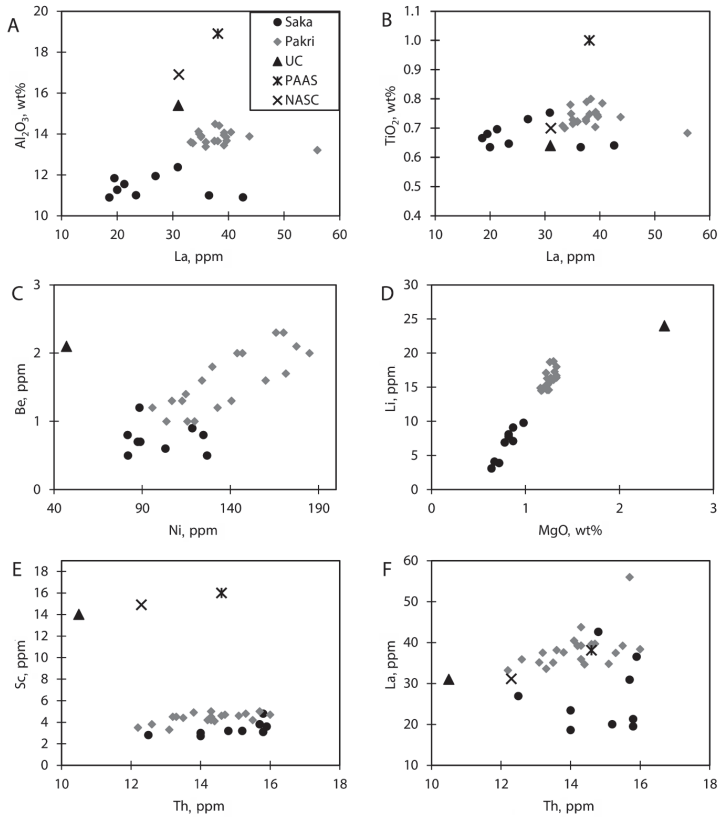
Fig. 5. Relationships between trace elements in graptolite argillite. UC = Upper Continental Crust [55]; PAAS = Post Archaean Australian Shale [39]; NASC = North American Shale Composite [40].

mobility of La. Be and Ni abundances in the Pakri section demonstrate a two-line positive covariance trend (Fig. 5C). Such a distribution pattern of two elements with generally different geochemical behavior in surface systems might reflect the terrigenic (volcanogenic) flux into the sedimentary environment from a distinct source during the initial period of accumulation of the GA or specific sedimentary conditions supporting Ni enrichment. The terrigenic flux controlled abundance is suggested also for Li and Mg (Fig. 5D). Both elements show a very well defined positive correlation, suggesting that Li and Mg are likely bonded into the crystal structure of micas and/or clay minerals. Figures 5E and 5F present the relations of Sc, Th,

and La, widely exploited for discriminating different magmatic rock types and settings. Numbers of studies have employed these variations to track possible precursor rocks of ancient shale and black shale complexes [39, 54]. On the Th-Sc graph the Pakri and Saka samples present anomalously low Sc and high Th/Sc content (Fig. 5E), thus suggesting a generally felsic upper crustal precursor for GA. The La/Th ratios of the analyzed GA samples demonstrate considerably higher scattering. As mentioned above, however, the enhanced La values in phosphorus-rich samples suggest that precursor rock signal had been in some cases evidently obscured by the synsedimentary incorporation or posterior redistribution of La.

In general, the clustering of non-reactive trace element data into the two fields may suggest that two different dominant source areas were involved in the supply of detrital material to the localities where organic-rich muds once accumulated.

4.3. Rare earth element variations

The REE patterns recorded for post-Archaean shales (PAAS) show striking similarity worldwide: they are light REE enriched, with a negative Eu anomaly and relatively flat heavy REEs [55, 39]. Samples from Pakri show chondrite-normalized (CN) REE patterns (Fig. 6C) generally similar to those recorded for PAAS, being considerably enriched in light rare earth elements (LREEs) with respect to heavy rare earth elements (HREEs). The main difference from the average shale compilations appears in content of MREEs (Fig. 6B). Like PAAS, all the studied samples exhibit negative Eu anomaly. The La_{CN}/Yb_{CN} ratio ranges from 6.65 to 10.26, staying thus well below the upper crust's La_{CN}/Yb_{CN} ratio. The Gd_{CN}/Yb_{CN} ratio varies from 1.09 to 2.22 with an average of 1.44 which is close to the PAAS value. The PAAS-normalized REE patterns of the examined GA samples show generally flat shape (Figs. 6A, 6B). In respect of the considerably monotonous REE variations, three samples from the Pakri locality exhibit distinct behavior. Pakri21 and Pakri14 have similar REE fractionation patterns with a somewhat elevated content of MREEs compared to PAAS. A unique hat-shape REE shale-normalized pattern was recorded for Pakri17 sample, which also presents a clearly elevated absolute REE concentration and strong MREEs enrichment. Compared to the Pakri sequence the REE patterns for Saka samples show higher fractionation and variation in the content of REEs (Figs. 6A, 6C). The La_{CN}/Yb_{CN} ratio is similar to that in Pakri samples, except in Saka1 and Saka4 where it reaches 15.56 and 14.27, respectively. The Gd_{CN}/Yb_{CN} ratios show high variation from 0.66 to 2.76, being the highest in samples Saka2 and Saka3. The MREE pattern shows higher variation than in Pakri samples. The PAAS-normalized REE patterns of Saka1, Saka4, Saka5, and Saka6 show low REE absolute abundances, but are characterized by distinctive concave shape patterns with considerably enriched HREEs (Tm-Yb) with respect to depleted MREEs (Ce-Er). Remarkably, these samples have the lowest content of Fe_2O_3 and the highest

contents of Mo, U and V (though high contents of these trace elements also occur in other samples). The hat-shaped (similar to that of Pakri17), MREE enriched patterns characterize Saka2 and Saka3 samples. The REE patterns of samples Saka7, Saka8, and Saka9 are more flat-shaped, similar to a typical Pakri pattern.
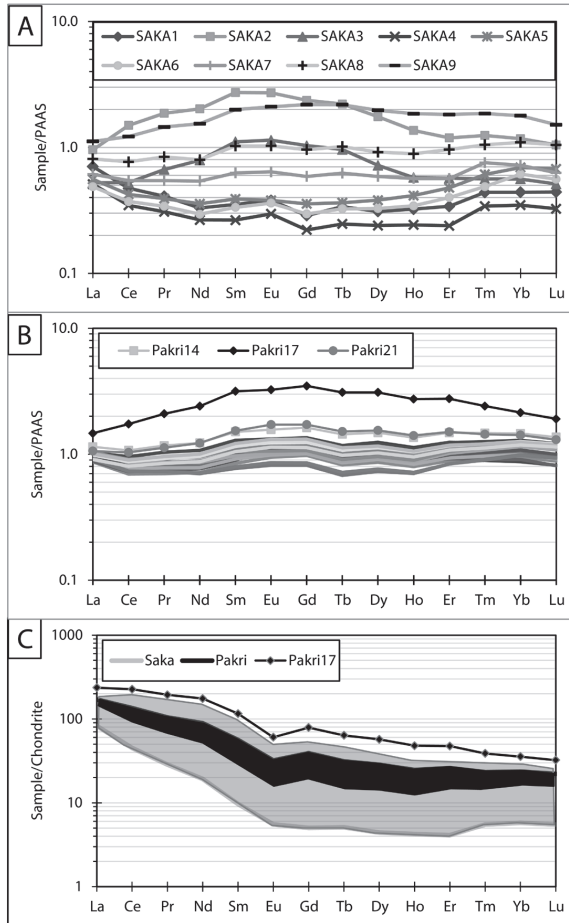

Fig. 6. Rare earth element patterns of GA samples normalized to PAAS (A; B) [39] and chondrite (C).

Table 3. Rare earth elements in GA samples from Pakri and Saka sections, ppm

Lab	Sample	La	Ce	Pr	Nd	Sm	Eu	Gd	Tb	Dy	Ho	Er	Tm	Yb	Lu
GI; Acme	Pakri1	35.1	58.5	6.5	26.0	5.0	1.14	5.07	0.70	4.22	0.83	2.51	0.37	2.46	0.35
GI; Acme	Pakri2	33.2	55.4	6.2	24.2	4.7	1.02	4.56	0.63	4.03	0.79	2.53	0.37	2.67	0.38
GI	Pakri3	33.6	57.7	6.6	26.1	5.3	1.12	4.92	0.70	4.43	0.85	2.63	0.37	2.56	0.35
GI	Pakri4	37.5	68.6	8.1	32.5	6.6	1.38	6.28	0.90	5.81	1.12	3.54	0.50	3.48	0.49
GI	Pakri5	35.9	62.4	7.2	28.1	5.6	1.16	5.11	0.72	4.62	0.89	2.85	0.42	2.90	0.41
GI; Acme	Pakri6	35.9	61.0	6.9	26.5	5.1	1.07	4.70	0.66	4.25	0.82	2.66	0.40	2.81	0.40
GI	Pakri7	37.5	65.8	7.6	29.6	5.8	1.17	5.09	0.72	4.54	0.88	2.83	0.42	3.05	0.43
GI	Pakri8	39.6	68.1	7.6	29.2	5.5	1.09	4.80	0.67	4.36	0.87	2.90	0.44	3.24	0.46
GI	Pakri9	35.1	58.5	6.4	23.8	4.3	0.88	3.81	0.52	3.42	0.70	2.38	0.37	2.79	0.41
GI	Pakri10	39.2	76.0	9.1	36.4	7.2	1.43	6.30	0.90	5.67	1.10	3.51	0.52	3.63	0.52
GI	Pakri11	39.2	72.4	8.3	31.5	5.9	1.14	4.98	0.70	4.49	0.89	2.99	0.46	3.40	0.50
GI; Acme	Pakri12	38.1	70.0	8.2	31.9	6.2	1.23	5.41	0.77	4.93	0.96	3.15	0.47	3.37	0.49
GI	Pakri13	39.7	71.8	8.3	32.3	6.2	1.25	5.45	0.78	5.00	0.98	3.21	0.49	3.48	0.50
GI	Pakri14	43.8	85.4	10.3	41.7	8.4	1.69	7.57	1.11	6.93	1.34	4.22	0.60	4.12	0.59
GI	Pakri15	39.2	72.0	8.4	33.2	6.6	1.36	5.91	0.84	5.28	1.01	3.23	0.48	3.40	0.48
GI	Pakri16	34.8	58.0	6.4	24.1	4.5	0.93	3.99	0.55	3.57	0.71	2.39	0.37	2.76	0.40
GI	Pakri17	56.0	138.2	18.4	81.6	17.7	3.51	16.23	2.38	14.48	2.71	7.86	0.99	6.04	0.82
GI	Pakri18	37.6	69.3	8.1	32.6	6.5	1.35	5.83	0.83	5.26	1.03	3.33	0.50	3.55	0.52
GI	Pakri19	38.4	71.6	8.4	33.9	6.8	1.42	6.13	0.87	5.44	1.05	3.36	0.49	3.51	0.51
GI	Pakri20	34.6	63.9	7.4	29.5	5.9	1.23	5.25	0.75	4.78	0.94	3.07	0.46	3.34	0.49
GI; Acme	Pakri21	40.4	82.3	9.9	41.5	8.6	1.86	8.01	1.17	7.23	1.39	4.29	0.59	4.01	0.56
Acme	Saka1	26.9	37.7	3.6	11.2	2.0	0.41	1.34	0.26	1.45	0.32	0.97	0.18	1.24	0.19
Acme	Saka2	36.5	119.0	16.4	68.6	15.3	2.93	11.00	1.70	8.19	1.35	3.39	0.51	3.30	0.45
Acme	Saka3	20.0	41.7	5.9	26.8	6.2	1.23	4.81	0.74	3.37	0.57	1.62	0.23	1.58	0.22
Acme	Saka4	19.5	27.6	2.7	9.0	1.5	0.32	1.03	0.19	1.12	0.24	0.68	0.14	0.98	0.14
Acme	Saka5	21.3	33.7	3.5	12.1	2.2	0.41	1.66	0.28	1.78	0.41	1.36	0.25	1.95	0.29
Acme	Saka6	18.6	29.6	3.0	10.0	1.9	0.39	1.38	0.25	1.53	0.34	1.14	0.20	1.73	0.24
Acme	Saka7	23.4	43.4	4.8	18.3	3.5	0.69	2.74	0.48	2.75	0.56	1.61	0.31	2.03	0.27
Acme	Saka8	30.9	61.1	7.4	27.0	5.7	1.11	4.47	0.78	4.29	0.88	2.74	0.43	3.09	0.45
Acme	Saka9	42.6	97.0	12.8	52.2	11.2	2.27	10.17	1.68	9.21	1.83	5.20	0.76	5.03	0.65

The observed large-scale variations in REE patterns – the encounter of normal flat shape as well as hat and concave like patterns – could be explained by variations in detrital input, e.g. variations in accessory mineral associations. However, alternatively it might point to the possibility that in most samples of the Saka sequence and in some intervals of Pakri the source rock inherited REE signals have been masked or obscured by the synsedimentary, diagenetic, hydrothermal or weathering induced redistribution-enrichment of REEs. The recent studies of black shales have indicated that authigenic phases such as sulfides, phosphates and carbonates as well as organic matter may host elevated REEs and their presence might influence

the absolute abundances of REEs as well as the fractionation patterns, e.g. [56]. Cruse et al. [57] interpreted the intermittent occurrence of hat and con-cave shape shale-normalized REE patterns in authigenic phosphate-rich and low-phosphate black shales as the evidence of an early diagenetic redistribu-tion of REEs formed as the result of a preferential uptake of MREE in apatite and simultaneous depletion of phosphate-poor host shale beds. A similar enrichment process could be hypothesized for the MREE enriched samples of Saka and Pakri GA, all characterized by elevated phosphorus content compared to the rest of the samples under study. This agrees with high REE values detected by SEM analysis of authigenic as well as bio-clastic phosphates in the studied sequences. Lev et al. [58] demonstrated the importance of post-/syn-depositional mineralizing fluid induced disturbance in REE-systems together with redistribution of U in black shales. Con-sequently, the encountered REE fractionation patterns could theoretically indicate also the influence of short-term low temperature brines. In case of GA the possible influence of deep source brines on the formation of its mineral assemblage has been suggested previously by sulfur isotope studies of pyrite [25]. However, the influence of deep brines on the Estonian Lower Paleozoic sedimentary assemblage is problematic as the whole complex is thermally almost unaltered. On the other hand, Somelar et al. (2010) [59] suggested intrusion of low temperature K-rich brines as the mechanism behind the illitization of Estonian Ordovician K-bentonites, pointing to the possible wide-scale influence of alkaline brines on the region in the Late Silurian.

Nevertheless, despite the lack of knowledge of the precise formation mechanism of the observed variability of REEs, it might suggest REE mobility in sedimentary or diagenetic environments. One could also speculate that the co-appearance of MREE depleted patterns and enhanced U, V and Mo abundances in GA from the Saka outcrop might indicate that those enriched elements were affected by the same redistribution processes which resulted in the formation of MREE depleted patterns.

5. Conclusions

The studies of two vertical sequences of graptolite argillite (GA) show the existence of pronounced fine-scale trace metal variability in GA. The examined samples were detected to be enriched in U, V, Mo and Pb with respect to average black shales, the obtained results thus agreeing with pre-viously published data on the geochemistry of GA. The content of enriched elements was, however, recorded to change greatly over the examined sequences, suggesting a notably more complex nature of trace metal dis-tribution in GA than previously assumed. Redox sensitive metals U and Mo, and also V to a lesser extent, showed loose covariance with organic matter content (LOI 500 °C), apparently indicating their trapping mainly via

organic matter tied species, and the enrichment primary linked to organic matter sequestration. The elevated abundance of a number of other trace metals, e.g. Pb, Zn, Cd, Cu, As and La, was detected in samples with an enhanced content of sulfur or phosphorus. The remarkably different behavior of the listed elements in two examined GA sequences could suggest that somewhat different sets of metal sequestration driving processes were responsible for the development of trace elemental assemblages in E and NW Estonian settings. As the trace element composition of GA is dominated by common marine redox sensitive and/or stable sulfide forming metals, the syngenetic trapping of metals from sea and interstitial water in redox boundary zones probably had first rate control over the development of trace element enrichment patterns. However, the observed high variability in the trace metal composition of GA, including heterogeneous REE patterns, points to the polygenetic nature of metal assemblages, apparently formed as the cumulative product of multistage evolution. On the whole, the study demonstrates that the knowledge base about metal distribution in GA is still rather fragmentary and that detailed geochemical, as well as multi-disciplinary investigations are essential for adequately predicting potential metal resources of GA in the future.

Acknowledgements

REFERENCES

1. Heinsalu, H., Viira, V. Pakerort Stage. In: *Geology and Mineral Resources of Estonia* (Raukas, A., Teedumäe, A., eds.). Estonian Academy Publishers, Tallinn, 1997, 52–58.
2. Petersell, V. Dictyonema argillite. In: *Geology and Mineral Resources of Estonia* (Raukas, A., Teedumäe, A., eds.). Estonian Academy Publishers, Tallinn, 1997, 313–326.
3. Andersson, A., Dahlman, B., Gee, D. G., Snäll, S. The Scandinavian Alum Shales. *Sveriges Geologiska Undersökning* (*SGU*), 1985, **56**, 1–50.
4. Kaljo, D., Borovko, N., Heinsalu, H., Khazanovich, K., Mens, K., Popov, L., Sergeeva, S., Sobolevskaya, R., Viira, V. The Cambrian-Ordovician boundary in the Baltic-Ladoga clint area (North Estonia and Leningrad Region, USSR). *Proc. Acad. Sci. Estonian SSR, Geology*, 1986, **35**(3), 97–108.
5. Heinsalu, H., Bednarczyk, W. Tremadoc of the East European Platform: Lithofacies and palaeogeography. *Proc. Est. Acad. Sci. Geol.*, 1997, **46**(2), 59–74.

6. Buchardt, B., Nielsen, A. T., Schovsbo, N. H. Alum shale in Scandinavia (Alun skiferen i Skandinavien). *Geologisk Tidsskrift*, 1997, 3, 1–30 (in Danish).
7. Vine, J. D., Tourtelot, E. B. Geochemistry of black shale deposits – a summary report. *Econ. Geol.*, 1970, **65**, 253–272.
8. Coveney, R. M. Jr., Leventhal, J. S., Glascock, M. D., Hatch, J. R. Origins of metals and organic matter in the Mecca Quarry Shale Member and stratigraphically equivalent beds across the Midwest. *Econ. Geol.*, 1987, **82**, 915–933.
9. Quinby-Hunt, M. S., Wilde, P., Orth, C. J., Berry, W. B. N. Elemental geochemistry of black shales – statistical comparison of low-calcic shales with other shales. In: *Metalliferous Black Shales and Related Ore Deposits* (Grauch, R. I., Leventhal, J. S., eds.), US Geological Survey Circular, 1989, No. **1037**, 8–15.
10. Wilde, P., Quinby-Hunt, M. S., Berry, W. B. N., Orth, C. J. Palaeo-oceanography and biogeography in the Tremadoc (Ordovician) Iapetus Ocean and the origin of the chemostratigraphy of *Dictyonema flabelliforme* black shales. *Geol. Mag.*, 1989, **126**(1), 19–27.
11. Hatch, J. R., Leventhal, J. S. Relationship between inferred redox potential of the depositional environment and geochemistry of the Upper Pennsylvanian (Missourian) Stark Shale Member of the Dennis Limestone, Wabaunsee County, Kansas, U.S.A. *Chem. Geol.*, 1992, **99**(1–3), 65–82.
12. Algeo, T. J., Maynard, J. B. Trace-element behavior and redox facies in core shales of Upper Pennsylvanian Kansas-type cyclothems. *Chem. Geol.*, 2004, **206**, 289–318.
13. Steiner, M., Wallis, E., Erdtmann, B.-D., Zhao, Y. L., Yang, R. D. Submarine-hydrothermal exhalative ore layers in black shales from South China and associated fossils – insights into a Lower Cambrian facies and bio-evolution. *Palaeogeogr. Palaeocl.*, 2001, **169**(3–4), 165–191.
14. Jiang, S. Y., Yang, J. H., Ling, H. F., Chen, Y. Q., Feng, H. Z., Zhao, K. D, Ni, P. Extreme enrichment of polymetallic Ni- Mo-PGE-Au in Lower Cambrian black shales of South China: an Os isotope and PGE geochemical investigation. *Palaeogeogr. Palaeocl.*, 2007, **254**(1–2), 217–228.
15. Vaughan, D. J., Sweeney, M., Diedel, G. F. R., Haranczyk, C. The Kupfer-schiefer: An overview with an appraisal of the different types of mineralization. *Econ. Geol.*, 1989, **84**, 1003–1027.
16. Sundblad, K., Gee, D. G. Occurrence of a uraniferous-vanadiniferous graphitic phyllite in the Köli Nappes of the Stekenjokk area, central Swedish Caledonides. *Geol. Foren. Stock. For.*, 1984, **106**(3), 269–274.
17. Berry, W. B. N., Wilde, P., Quinby-Hunt, M. S., Orth, C. J. Trace element signatures in Dictyonema shales and their geochemical and stratigraphic significance. *Norsk Geol. Tidsskr.*, 1986, **66**, 45–51.
18. Leventhal, J. S. Comparative geochemistry of metals and rare earth elements from the Cambrian alum shale and kolm of Sweden. *Sp. Publ. Int.*, 1990, **11**, 203–215.
19. Leventhal, J. S. Comparison of organic geochemistry and metal enrichment in two black shales: Cambrian Alum Shale of Sweden and Devonian Chattanooga Shale of United States. *Miner. Deposita*, 1991, **26**, 104–112.
20. Schovsbo, N. H. Uranium enrichment shorewards in black shales: A case study from the Scandinavian Alum Shale. *Geol. Foren. Stock. For.*, 2002, **124**(2), 107–115.

21. Loog, A. Geochemistry of Lower Ordovician of Estonia. In: *Studies of the Institute of Geology, ESSR Academy of Sciences*. Tallinn, 1962. No. 10, 273–291 (in Russian).
22. Baukov, S. S. General characteristics of dictyonema shale. In: *Geology of Coal and Oil Shale Deposits of the USSR*, **11**. Nedra, Moscow, 1968, 145–148 (in Russian).
23. Petersell, V., Mineyev, D., Loog, A. Mineralogy and geochemistry of obolus sandstones and dictyonema shale of North Estonia. *Acta et Commentationes Universitatis Tartuensis*, No. 561, Tartu, 1981, 30–49 (in Russian).
24. Loog, A. On the geochemistry of postsedimentary mineral formation in the Tremadoc graptolitic argillites of North Estonia. *Acta et Commentationes Universitatis Tartuensis*, No. 527, Tartu, 1982, 44–49 (in Russian).
25. Petersell, V. H., Zhukov, F. I., Loog, A. R., Fomin, Y. A. Origin of Tremadoc kerogenous-bearing siltstones and argillites of North Estonia. *Oil Shale*, 1987, **4**(1), 8–13 (in Russian).
26. Pukkonen, E. M. Major and minor elements in Estonian graptolite argillite. *Oil Shale*, 1989, **6**(1), 11–18 (in Russian).
27. Kallaste, T., Pukkonen, E. Pyrite varieties in Estonian Tremadocian argillite (Dictyonema shale). *Proc. Est. Acad. Sci. Geol.*, 1992, **41**(1), 11–22.
28. Pukkonen, E., Rammo, M. Distribution of molybdenum and uranium in the Tremadoc graptolitic argillite (Dictyonema shale) of North-Western Estonia. *Bulletin of the Geological Survey of Estonia*, 1992, **2**(1), 3–15.
29. Loog, A., Petersell, V. The distribution of microelements in Tremadoc graptolitic argillite of Estonia. *Acta et Commentationes Universitatis Tartuensis*, No. 972, Tartu, 1994, 57–75.
30. Loog, A., Petersell, V. Authigenic siliceous minerals in the Tremadoc graptolitic argillite of Estonia. *Proc. Est. Acad. Sci. Geol.*, 1995, **44**(1), 26–32.
31. Heinsalu, H. Lithostratigraphical subdivision of Tremadoc deposits of North Estonia. *Proc. Acad. Sci. Estonian SSR, Geology*, 1987, **36**(2), 66–78 (in Russian).
32. Raudsep, R. Ordovician. Pakerort Stage. Ceratopyge Stage. In: *Geology and mineral resources of the Rakvere phosphorite-bearing area* (Puura, V., ed.). Valgus, Tallinn, 1987, 29–39 (in Russian).
33. Kaljo, D., Kivimägi, E. On the distribution of graptolites in the Dictyonema shale of Estonia and the noncontemporaneity of its different facies. *Proc. Acad. Sci. Estonian SSR, Chem., Geol.*, 1970, **19**(4), 334–341 (in Russian).
34. Kiipli, T., Batchelor, R. A., Bernal, J. P., Cowing, C., Hagel-Brunnström, M., Ingham, M. N., Johnson, D., Kivisilla, J., Knaack, C., Kump, P., Lozano, R., Michiels, D., Orlova, K., Pirrus, E., Rousseau, R. M., Ruzicka, J., Sandström, H., Willis, J. P. Seven sedimentary rock reference samples from Estonia. *Oil Shale*, 2000, **17**(3), 215–223.
35. Utsal, K., Kivimägi, E., Utsal, V. About the method of investigating Estonian graptolitic argillite and its mineralogy. *Acta et Commentationes Universitatis Tartuensis*, No. 527, Tartu, 1982, 116–136 (in Russian).
36. Loog, A., Kurvits, T., Aruväli, J., Petersell, V. Grain size analysis and mineralogy of the Tremadocian Dictyonema shale in Estonia. *Oil Shale*, 2001, **18**(4), 281–297.
37. Kleesment, A.-L., Kurvits, T. U. Mineralogy of Tremadoc graptolitic argillites of North Estonia. *Oil Shale*, 1987, **4**(2), 130–138 (in Russian).

38. Snäll, S. Mineralogy and maturity of the alum shales of south-central Jämtland, Sweden. *Sveriges Geologiska Undersökning* (*SGU*), 1988, Serie C, **818**, 1–46.

39. Taylor, S. R., McLennan, S. M. *The Continental Crust: its Composition and Evolution*. Blackwell Scientific Publication, Oxford, 1985.

40. Gromet, L. P., Dymek, R. F., Haskin, L. A., Korotev, R. L. The "North American shale composite": its compilation, major and trace element characteristics. *Geochim. Cosmochim. Ac.*, 1984, **48**, 2469–2482.

41. Holland, H. D. Metals in black shales – A reassessment. *Econ. Geol.*, 1979, **74**, 1676–1680.

42. Coveney, R. M. Jr., Glascock, M. D. A review of the origins of metal-rich Pennsylvanian black shales, central U.S.A., with an inferred role for basinal brines. *Appl. Geochem.*, 1989, **4**(4), 347–367.

43. Yu, B., Dong, H., Widom, E., Chen, J., Lin, C. Geochemistry of basal Cambrian black shales and cherts from the Northern Tarim Basin, Northwest China: Implications for depositional setting and tectonic history. *J. Asian Earth Sci.*, 2009, **34**(3), 418–436.

44. Leventhal, J. S., Hosterman, J. W. Chemical and mineralogical analysis of Devonian black-shale samples from Martin County, Kentucky; Carroll and Washington counties, Ohio; Wise County, Virginia; and Overton County, Tennessee, U.S.A. *Chem. Geol.*, 1982, **37**(3–4), 239–264.

45. Peacor, D. R., Coveney, R. M. Jr., Zhao, G. Authigenic illite and organic matter: the principal hosts of vanadium in the Mecca Quarry shale at Velpen, Indiana. *Clay. Clay Miner.*, 2000, **48**(3), 311–316.

46. Calvert, S. E., Pedersen, T. F. Geochemistry of recent oxic and anoxic marine sediments: Implications for the geological record. *Mar. Geol.*, 1993, **113**(1–2), 67–88.

47. Nameroff, T. J., Balistrieri, L. S., Murray, J. W. Suboxic trace metal geochemistry in the Eastern Tropical North Pacific. *Geochim. Cosmochim. Ac.*, 2002, **66**(7), 1139–1158.

48. Morford, J. L., Emerson, S. The geochemistry of redox sensitive trace metals in sediments. *Geochim. Cosmochim. Ac.*, 1999, **63**(11–12), 1735–1750.

49. Chester, R. *Marine Geochemistry*. Blackwell, London, 2000.

50. Nijenhuis, I. A., Bosch, H.-J., Sinninghe Damsté, J. S., Brumsack, H.-J., De Lange, G. J. Organic matter and trace element rich sapropels and black shales: a geochemical comparison. *Earth Planet. Sc. Lett.*, 1999, **169**(3–4), 277–290.

51. Brumsack, H.-J. The trace metal content of recent organic carbon-rich sediments: implications for Cretaceous black shale formation. *Palaeogeogr. Palaeocl.*, 2006, **232**(2–4), 344–361.

52. Kochenov, A. V., Baturin, G. N. The paragenesis of organic matter, phosphorus and uranium in marine sediments. *Lithology and Mineral Resources*, 2002, **37**(2), 107–120.

53. Grimmer, J. C., Greiling, R. O. Serpentinites and low-K island arc metavolcanic rocks in the Lower Köli Nappe of the central Scandinavian Caledonides: Late Cambrian – early Ordovician serpentinite mud volcanoes in a forearc basin? *Tectonophysics*, 2012, **541–543**, 19–30.

54. Quinby-Hunt, M. S., Wilde, P., Orth, C. J.,Berry, W. B. N. The provenance of low-calcic black shales. *Miner. Deposita*, 1991, **26**(2), 113–121.

55. Rudnick R. L., Gao, S. Composition of the continental crust. In: *Readings from the Treatise on Geochemistry* (Holland, H. D., Turekian, K. K., eds.). Elsevier, Amsterdam, 2010, 131–198.

56. Lev, S. M., McLennan, S. M., Hanson, G. N. Mineralogic controls on REE mobility during black-shale diagenesis. *J. Sediment. Res.*, 1999. Vol. 69. P. 1071–1082.

57. Cruse, A. M., Lyons, T. W., Kidder, D. L. Rare-earth element behavior in phosphates and organic-rich host shales: An example from the Upper Carboniferous of Midcontinent North America. In: *Marine Authigenesis: From Global to Microbial* (Glenn, C. R., Prévôt-Lucas, L., Lucas, J., eds.), SEPM Special Publication, 2000, **66**, 445–453.

58. Lev, S. M., Filer, J. K., Tomascak, P. Orogenesis vs. Diagenesis: Can we use organic-rich shales to interpret the tectonic evolution of a depositional basin? *Earth Sci. Rev.*, 2008, **86**(1–4), 1–14.

59. Somelar, P., Kirsimäe, K., Hints, R., Kirs, J. Illitization of Early Paleozoic K-Bentonites in the Baltic Basin: decoupling of burial- and fluid-driven processes. *Clay. Clay Miner.*, 2010, **58**(3), 388–398.

PAPER III

HADE, S., SOESOO, A. 2014a. Estonian graptolite argillites revisited: a future resource? *Oil Shale*, **31(1)**, 4 - 18.

ESTONIAN GRAPTOLITE ARGILLITES REVISITED: A FUTURE RESOURCE?

SIGRID HADE[*], ALVAR SOESOO

Institute of Geology, Tallinn University of Technology, Ehitajate tee 5, 19086 Tallinn, Estonia

Abstract. *The occurrence of Cambrian to Ordovician organic-rich black shale deposits has been known in Baltoscandia, including Estonia, for a long time. The Estonian graptolite argillite (GA) shows high to very high concentrations of U (800 ppm), Mo (1000 ppm), V (1600 ppm), Ni and other heavy metals, and are rich in N, S and O, unlike normal shale. The present study provides a new estimate of the total GA tonnage in Estonia, including estimates for U, Zn and Mo. The total preserved volume of GA is about 31.92 billion m^3, while about 9.02 billion m^3 has been eroded between the Estonian mainland and western islands. The total mass of GA is about 67 billion tonnes at a specific gravity of 2.1 g/cm^3. About 18.93 billion tonnes of GA has been eroded and re-deposited, including 1.8 million tonnes of U, 22.7 million tonnes of Zn, 6.6 million tonnes of Pb, 4.4 million tonnes of Mo and 13.3 million tonnes of V. In Estonian GA the total U_3O_8 reaches 6.7 million tonnes, ZnO 20.6 million tonnes and MoO_3 19.1 million tonnes as calculated using a cell size of 400 m.*

Keywords: *graptolite argillite, black shale, metals, resource, Estonia.*

1. Introduction

The occurrence of Middle Cambrian to Late Ordovician organic-rich black shale deposits in an extensive area of Sweden (alum shale [1]), the Oslo region [2], Bornholm [3], Estonia (known as graptolite argillite, "Dictyonema shale" [4], and kukersite as proper oil shale), Poland [5] and North-West Russia [6] has been known for a long time.

Alum shale, as well as graptolite argillite, contains remarkably high concentrations of trace metals such as U, Mo, V and Ni, but may also be locally enriched with rare earth elements (REE), Cd, Au, Sb, As, Pt [7]. The beds have historically been exploited for uranium production in Sweden and Estonia. Also, a high content of potassium, sulphur and organic matter is

---

[*] Corresponding author: e-mail *sigrid.hade@ttu.ee*

characteristic of those beds. Kerogen in black shale is of algal origin and the content of total organic carbon is mostly between 10 and 25 wt% [1]. The mineral matter of black shale is dominated by clay minerals – illite-smectite and illite [8, 9]. Distinctive of black shale is its high concentration of pyrite, which, together with kerogen, is thought to be the main carrier of some rare elements. Alum shale and graptolite argillite form patches over extensive areas in the outskirts of the Baltica palaeocontinent [1]. Possible spatial continuities of those complexes are graphitic phyllites, which are found in the tectonically disrupted allochthonous and autochthonous Caledonian complexes in central and northern Sweden and Norway. The metal-enriched phyllites exhibit similar geochemical signatures to the unmetamorphozed black shale of Baltoscandia [10]. These geochemical similarities suggest that the organic-rich muds might have accumulated over a wide geographic area and under fairly different depositional conditions – from pericratonic shallow marine settings to continental slope environments. The Fennoscandian black shale and Estonian graptolite argillite (GA) can thus be treated as metal ore and a twofold source of energy (including U and shale oil), the rocks have a high scientific and significant economic value.

Despite the long history of exploration and exploitation of Baltoscandian black shale and graptolite argillite [1, 11–14], the origin of high metal concentrations of the beds has remained controversial. Also, the volume of shale and argillite and the distribution pattern of metals are not well known.

Previous estimates of the graptolite argillite tonnage in Estonia range from 60 billion [15] to 70 billion tonnes [16]. GA occurs throughout Northern Estonia in an area covering about 11,000 km^2 (Fig. 1). However, large quantities of GA have been eroded away in the northern and north-western parts of Estonia. The extent of GA towards the north is unknown, but the amount of the eroded material can be interpolated and calculated between the Estonian mainland and Hiiumaa Island.

The present study provides a new estimate, based on calculations using ESRI ArcInfo software, of the total GA resource in Estonia, and of the GA that has been eroded away between the Estonian mainland and Hiiumaa. Also, based on the new estimates, some total metal amounts have been calculated, and the GA thickness and metal concentration dynamics shown.

2. Geological overview of Estonian graptolite argillite

The Lower Ordovician organic-rich marine metalliferous black shale – graptolite argillite (GA) lies beneath most of Northern Estonia (Fig. 1). Earlier it was called „Dictyonema shale", „Dictyonema argillite" or „alum shale". The name *dictyonema* came from the benthonic root-bearing *Dictyonema flabelliforme*, which afterward turned to planktonic nema-bearing *Rhabdinopora flabelliformis* [17]. In this study, the term *graptolite argillite* is used. Graptolite argillite is fine-grained, unmetamorphosed,

(sub)horizontally lying organic-rich (8–20%) lithified clay and argillite (Türisalu Formation) belonging to the group of black shales of sapropelic origin [15]. GA is characterized by high to very high concentrations of U (up to 1200 ppm; unpublished data by A. Soesoo; database of the Institute of Geology, Tallinn University of Technology (TUT)), Mo (1000 ppm), V (1600 ppm), Ni and other heavy metals, and is rich in N, S and O [18, 19, 20], unlike normal sedimentary shales. High concentrations of certain elements may be potentially useful or hazardous. During the Soviet era, GA was mined for uranium production at Sillamäe, in North-East Estonia, between 1948 and 1952 [16]. A total of 22.5 tonnes of elemental uranium was produced from 271,575 tonnes of GA from an underground mine near Sillamäe. Between 1964 and 1991 approximately 73 million tonnes of GA was mined from the covering layer of phosphorite ore at Maardu, near Tallinn. GA was mixed up with other overlying deposits, such as carbonate rocks, sandstone, glauconite sandstone, and Quaternary sediments, and piled in waste heaps.

Although the tonnage of GA surpasses that of kukersite, its quality is poor for energy production purposes. The calorific value of GA ranges from 4.2 to 6.7 MJ/kg [18], and the Fischer Assay oil yield is 3–5% (for Estonian kukersite it is about 30–47%, for example [16]). The laboratory moisture content of fresh GA ranges from 11.9 to 12.5 %, while the average composition of the combustible part is as follows: C 67.6%, H 7.6%,
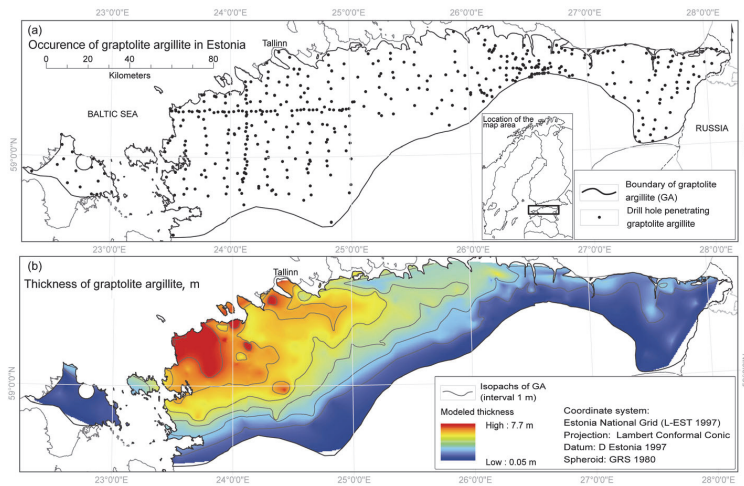

Fig. 1. (a) Location map of Estonian GA and location of the drill holes penetrating the graptolite argillite layers. (b) Modeled thickness of GA based on the studied drill holes (thickness grid created by the Natural Neighbour interpolation method, grid cell size 400 m).

O 18.5%, N 3.6% and S 2.6% [21]. However, considering it is a low-grade oil source, its potential oil yields are about 2.1 billion tonnes [16]. Scandinavian black shale together with Estonian GA is considered to be a potential energy reserve for the future.

The specific gravity of GA mostly varies between 1.8 and 2.5 g/cm^3 [15] (see also Fig. 2). The pyrite content of GA is also highly variable, from 1.5 to 9.0%, but mainly from 2.4 to 6%. Pyrite forms fine-crystalline disseminations, thin interlayers and concretions with different forms and sizes. The diameter of concretions is usually 2–3 cm. Some concretions are complex in structure and contain crystals of galenite, sphalerite and calcite. Sometimes pyrite comprises marcasite. Under atmospheric conditions, this part of pyrite is rapidly replaced by jarosite and anhydrite.

The mineral composition of GA is dominated by K-feldspars, quartz and clay minerals. In the lateral as well as vertical dimension the contents of major rock-forming minerals show slight, but pronounced variation patterns [20]. GA also contains light-brown phosphatic ooids. The rock contains accessory amounts of zircon, tourmaline, garnet, rutile, calcopyrite and glauconite, whereas corundum, amphiboles and disthen have been preserved in Western Estonia [22]. In general, the higher degree of sulphide mineralization within GA is associated with the occurrence of silt interbeds. Those interbeds might also contain a higher amount of other minor authigenic compounds typical of GA – phosphates (mainly apatite as biogenic detritus and nodules), carbonates (calcite and dolomite as cement and concretions), barite and glauconite. Carbonate minerals occur sporadically. They cement the terrigenous material in patches or form concretions: calcite occurs in the western sections and dolomite in the eastern ones. The occurrence of phosphatic cement, or even lumps of the earlier formed chemogeneous phosphatic layer, is characteristic of some silt interlayers [23]. Besides the highly resistant accessory terrigenic phases, a considerable abundance of micas in the GA beds has been documented [23, 20, 24]. Rare apatite, titanite, alkali amphibole (aegirine), baryte and diopside have also been found in GA [25].

Some sections of GA, especially in Eastern Estonia, contain small lense- or nest-shaped silica interlayers. The interlayers contain white or grey porous silica and terrigeneous quartz with the grain size of fine sand [23]. The average quartz content of GA gradually rises eastward with the corresponding decrease in clay minerals. In North-East Estonia, the argillite complex is intercalated with numerous quartzose silt beds [23].

Organic matter (OM), constituting about 15–20% of GA, is sapropelic in origin [8] and rich in N, S and O. The ratio of C to H in OM is about 9. OM is fine-dispersed and spread rather evenly. The OM concentration is the lowest in those parts of the sections where the interlayers of carbonate minerals or silt are high. The concentration of S ranges between 2 and 6%, of which 0.6–0.8% is comprised of OM, ca. 0.3% is sulphatic, and the remaining part is sulphitic S [13].

Recently, an XRD analysis of selected GA samples from the Pakri outcrop was performed [20]. The study confirmed the presence of K-feldspar (sanidine), illite (illite-smectite, micas), quartz, pyrite, marcasite, apatite, calcite, dolomite, galena and chlorite. The SEM analysis revealed high micrometer-scale morphological heterogeneity in the examined samples.

The chemical composition of GA is definitely of great interest and its specificities have been known for nearly a century. Besides the high concentration of a number of metals, its potassium and sulphur contents are much higher and the content of sodium and calcium lower than in average clays and shale. The concentration of K_2O in GA is higher than could be expected, based on the composition of known shale-forming minerals [15]. With the increase in the volume of silt interlayers from the west to the east, the concentration of SiO_2, CaO and P_2O_5 increases, while that of Al_2O_3, K_2O and MgO decreases. Based on previous geochemical exploration [18, 20], three geochemical zones have been distinguished in the Estonian GA − Western, Central and Eastern zones. These zones differ mainly in the concentration of metals that are characteristic of GA − Mo, V, U. However, based on a recent study [20] it was shown that the distribution of metals in GA has a more complex pattern. The study dealt with two vertical sections of graptolite argillite (Pakri in North-Western and Saka in North-Eastern Estonia) and indicated the existence of pronounced fine-scale trace metal variability and the remarkably different behaviour of trace elements. The content of enriched elements was shown to change greatly over the examined sections [20]. For example, an elevated abundance of a number of other trace metals, e.g. Pb, Zn, Cd, Cu, As and La, was detected in samples with an enhanced content of sulphur or phosphorus. The high variability of the trace metal composition of GA, including heterogeneous REE patterns, may point to the polygenetic nature of metal compositions, apparently formed as the cumulative product of multistage evolution. Currently, our knowledge about metal distribution, and especially its origin, is rather fragmentary and a multidisciplinary exploration is needed for adequately predicting potential metal resources of GA in the future.

3. Resource estimate of Estonian graptolite argillite

Most of the geological information on GA is obtained from basement mapping and exploration projects conducted by the Geological Survey of Estonia, which started in the 1950s. The vast amount of detailed information on the GA lithology and geochemistry was collected during the prospecting of Estonia's phosphorite resources [15]. The previous estimates of the graptolite argillite resource in Estonia range from 60 billion [15] to 70 billion tonnes [16] and little is known about the calculation methods and initial data (number of drill cores, etc.) used. Although there has practically been no new data during the last two decades, the GIS-based methods now

allow us to obtain more precise estimates of the total resource and metal distribution.

In this work, a new estimate of the GA resource in Estonia is presented. The Natural Neighbour interpolation method in the ArcGIS Spatial Analyst (Environmental Systems Research Institute, Inc. (ESRI), versions 9.3.1 and 10.1) software was used in the present assessment for generating resource maps and computing resource volumes. The algorithm used by the Natural Neighbour interpolation tool finds the closest subset of input samples to a query point and applies weights to them based on proportionate areas to interpolate a value [26]. The value in an unsampled location is computed as a weighted average of the nearest neighbour values with weights dependent on areas or volumes rather than distances. It does not infer trends and will not produce peaks, pits, ridges, or valleys that are not already represented by the input samples. However, the surface grid and volume estimation results obtained by the Natural Neighbour interpolation method have been compared with other geo-statistical methods, such as Kriging (in ArcGIS Spatial Analyst, ESRI, and Geochemistry for ArcGIS, Geosoft Inc., version 2.1). Kriging is based on statistical models that include the statistical relationships among the measured points. The Kriging method [27, 28] assumes that the distance or direction between sample points reflects a spatial correlation that can be used to explain variation in the surface. Generally, Kriging is most appropriate when you know that there is a spatially correlated distance or directional bias in the data. Kriging seems to be appropriate for phenomena with a very strong random component or for the estimation of statistical characteristics (uncertainty). However, most of the surfaces or volumes in the sedimentary environment are neither stochastic nor elastic media, but are the result of natural (e.g. sediment fluxes, deposition speed, hydromechanics, etc.) processes. Therefore, the Natural Neighbour interpolation method is thought to be more appropriate in case of the GA resource spatial/volume calculations in the present geological situation. In this case, the gridded GA thickness surface created by the Kriging method is slightly wider and calculated volumes are slightly higher (less than 1%).

On the other hand, average metal concentrations in sedimentary sections may be more stochastic, and there may not be a clear special relationship between the element concentrations as well as between the elements. In the given case, the metal concentrations in the initial data represent the average of the entire drill core. As seen from the calculated thickness map (Fig. 1), there is quite a large variation in the thickness of GA, ranging mostly from 0.5 m to 6 m. The large variability in the thickness of GA thus excludes making a direct comparison of elemental averages between the drill cores. This is the reason why metal concentration grids are calculated using the Kriging method.

As initial data, the combined database of 468 drill cores (Geological Survey of Estonia and Estonian Land Board database, see at www.maaamet.ee) has been used. A vast amount of GA has been eroded and

carried away between the West-Estonian islands (Figs. 1 and 3). An attempt has been made to calculate the volume and tonnage of this eroded material by an extrapolation of GA thickness data. In this extrapolation, the northern boundary has been fixed at the current erosional line of the Türisalu strata, as no knowledge exists about the northern extension of the Estonian-(Russian) graptolite argillite basin.

The estimated area of Estonian GA on the mainland and islands is about 12,210 km^2, with the corresponding volume of 31.92 billion m^3 (Fig. 2). The estimated eroded area between the West-Estonian islands (Fig. 3) is about 3,190.4 km^2 with the corresponding volume of 9.02 billion m^3. The calculated total volume of Estonian GA (on the mainland and in the eroded part in Western Estonia) extends up to 40,935 km^3 with an area of more than 15,400 km^2. For instance, Estonian oil shale – kukersite occupies an area of 2,884 km^2, and its reserves (active and passive) in 2012 were about 4.774 billion tonnes [29]. In order to calculate the tonnage of GA, the value of specific gravity is needed. It is known [15] that the specific gravity of graptolite argillite varies to a great degree, mostly between 1.8 and 2.5 g/cm^3. So, assuming an average specific gravity of 1.8 g/cm^3, the tonnage of GA is about 57.45 billion tonnes, while in case of 2.5 g/cm^3 the mass is 79.80 billion tonnes (Fig. 2). Assuming the average specific gravity to be 2.1 g/cm^3, the tonnage of GA is about 67 billion tonnes, which is in between the earlier estimates of 60 to 70 billion tonnes.

In a similar way we can calculate the tonnage of eroded material, in between the Estonian mainland and Hiiumaa Island. Assuming the average specific gravity of 1.8 g/cm^3, the tonnage of the eroded GA is about 16.23 billion tonnes, while 2.5 g/cm^3 gives 22.54 billion tonnes and 2.1 g/cm^3
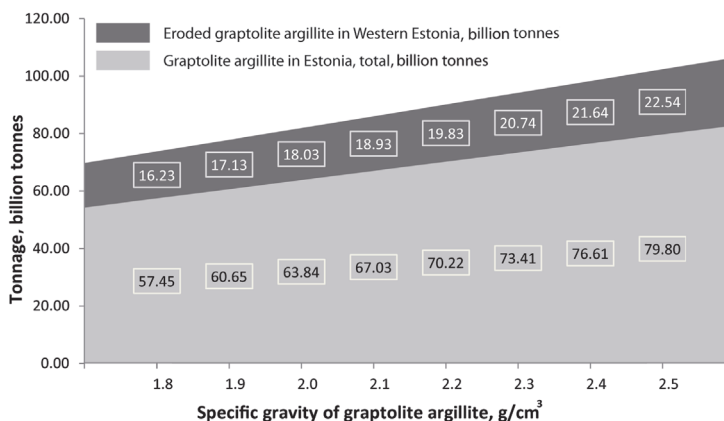

Fig. 2. Calculated volume and tonnage of Estonian GA (in situ and in an eroded area between the Estonian mainland and West-Esonian islands) as a function of specific gravity.
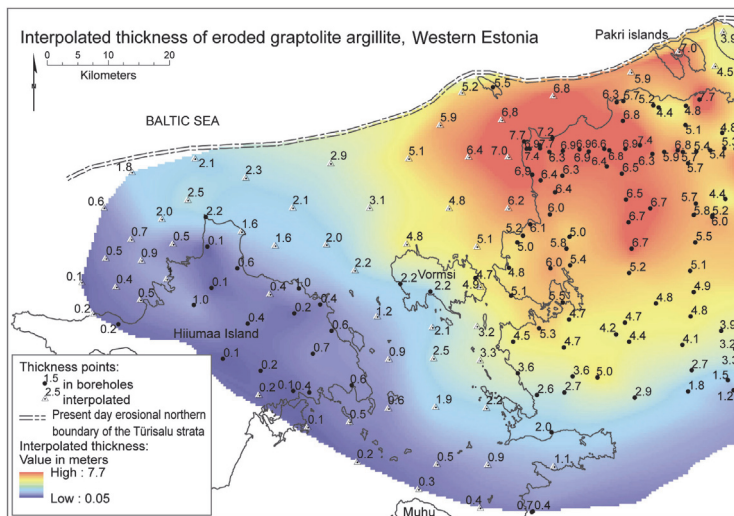
Fig. 3. Interpolated thickness grid of GA between Western Estonia and the islands.

gives about 18.93 billion tonnes (Figs. 2 and 3). This is an enormously large amount of material.

Very little is known about the timing and cause of erosion in Northern and Western Estonia. The most prominent feature of this erosion is the North Estonian Klint. One hypothesis which explains the klint formation is related to a large, old, possibly Late Cenozoic, river system [30, 31]. A vast amount of terrigenous sediments is known to exist in the North Sea with an area of 100,000 km^2 [32]. The Eridanos river system, which drained most of North and North-Western Europe, developed during the Late Cenozoic as a result of the simultaneous uplift of the Fennoscandian Shield and the accelerated subsidence in the North Sea Basin. The erosion of the area to the north of the present mainland of Estonia and Western Estonia is most likely attributable to the Pra-Neva River, the tributary of the Eridanos.

It is well known that the fluvial deposits of Miocene to Early Pleistocene Age in Germany and the Netherlands were transported to the delta of the Eridanos River System [33]. However, the exact provenance of this sedimentary material continues to be a subject of discussion. Some of the sand from the Fennoscandian crystalline rocks, Ordovician terrigenous material, erratics with well-defined Ordovician fossils, which are similar to those in Northern Estonia and the St. Petersburg region (Russia) [33], are known to exist within the sediments in the Eridanos fluvio-deltaic system in the North Sea area, the Netherlands and Germany. Most likely, the erosion of the Lower Paleozoic sections in Western Estonia, including graptolite argillite,

is related to those processes which generated the klint. The exact timing of those processes remains unknown, however, the original erosional processes were most likely active during the Late Miocene (some 20 to 5.332 million years ago) to Pliocene (5.332 to 2.588 million years ago). Some of the material may have been re-deposited during the Quaternary.

Knowing the volume and average chemical composition of the eroded graptolite argillite (Figs. 2 and 3), the amount of eroded, partly dissolved and redeposited metals can be calculated. Based on the extrapolated GA thickness and average metal contents in the drill cores from the most westerly part of Estonia, and from Vormsi and Hiiumaa islands, the total amount of uranium (elemental U) that has been eroded and re-deposited reaches 1.798 million tonnes (at an average content of 95 grams per tonne), zinc (Zn) 22.716 million tonnes (average 1200 g/t), lead (Pb) 6.625 million tonnes (average 350 g/t), molybdenum (Mo) 4.448 million tonnes (average 235 g/t) and vanadium (V) 13.251 million tonnes (average 700 g/t).

As for volume, the contribution of graptolite argillite from Western Estonia to the Eridanos sedimentary budget is not high, considering the overall 62,000 km^3 of sediments in the Southern North Sea Basin alone [32] versus 9,015 km^3 derived by erosion from Western Estonia. However, the metal contribution of GA to the overall Eridanos sedimentary budget is remarkable. The total amount of the elements that have now been re-deposited is extremely large. One can only imagine approximately 1.8 million tonnes of uranium and 13 million tonnes of vanadium incorporated into sediments somewhere below the Holocene sediments of the North Sea!

4. Estonian graptolite argillite as a metal resource

The vertical and lateral geochemical heterogeneity in GA has not been well understood, especially the scale of the heterogeneity and specific distribution pattern of elements. Recently, a study on vertical geochemical heterogeneity based on two cross-sections has showed distinctive differences between the eastern and western parts of GA [20]. The previous geochemical explorations [20] revealed that the studied sequences demonstrate pronounced vertical variations in U, V, Mo and Zn concentrations. The common distinctive feature of the sections is the occurrence of highest concentrations of the elements in the lower half of the section.

The distribution of V, Mo and Pb in the Estonian GA has been modeled in an earlier study [20] and the U distributions have been shown in Figure 4. The initial data were selected from the database of the Geological Survey of Estonia. This elemental concentration data represents the average concentrations in GA in the drill core. The central and western parts of the Eastern Zone show the highest concentrations for V and Mo, whereas V is also high in the southern part of the Eastern and Central Zones. Uranium shows the highest concentrations in the most easterly part of Estonia, while in Western

Estonia the concentrations show medium values and the lowest values are characteristic of the Central Zone (Fig. 4). The U distribution has not been modeled in the Estonian islands due to a small number of analyses (only 3 cores). The high concentrations in the south-western corner may be an artifact of the model, since there are only a few drill cores available and those show locally high contents of U. Generally, it can be concluded that the concentration of most of the metals (except Zn) is relatively low in the Central Zone of the GA area.

However, it is important to emphasize that the available chemical data is relatively unevenly distributed across the area and the present geochemical generalization is informative, and must be taken with caution. There is very little data on the southern margin of the GA area, so the concentrations may vary, but due to its limited thickness (less than 0.5 m); the total elemental amounts have not affected the calculations very much.

With respect to the standard values, such as PAAS and NASC, the Estonian GA is extremely rich in U and V. For example, the average U concentration in the Saka section (267 ppm) is a hundred times higher than the corresponding values for NASC. In case of V, there is a nine-fold difference between the concentrations in NASC and the average concentrations detected, for example, in the Saka section, in Eastern Estonia (190 ppm; [20]). In general, the U content of GA shows quite a strong positive correlation with the organic matter content, which most likely indicates early fixation via metal-organic complexes. At the same time, the correlation of P_2O_5 with other enriched trace elements, such as U, was not detected.

In general, the dominance of common marine redox-sensitive elements among the enriched metals in GA may favor a syngenetic enrichment as the major process of trace metal sequestration. The recent data [20] indicate that besides the elements, which are well known in the partitioning in the marine systems, the Estonian GA sporadically presents elevated levels of certain trace elements such as PGE and W, which are generally characterized by a
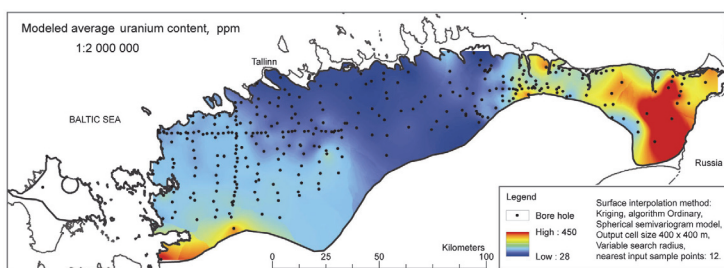

Fig. 4. Modeled uranium content in Estonian GA based on calculated average drill core analyses (data: Geological Survey of Estonia; www.maaamet.ee). Element concentration surface modeled by the Ordinary Kriging interpolation method.

very low abundance in the crust and modern marine sediments. The accumulation of such minor compounds in GA underlines the possible role of external input of metals into the sedimentary or diagenetic environment.

As average metal concentrations are very useful in indicating "poor" and "rich" deposits, the total content of a certain element depends on the thickness of the deposit layer. In order to calculate the total amount of the element/metal based on square meters, ESRI ArcGIS software was employed. The total amount of uranium, zinc and molybdenum in the Estonian GA is shown in Figure 5. This calculation is based: 1) on the element/metal grid which shows the element distribution in ppm (e.g. Fig. 4 for U); 2) on an interpolated grid of the GA thickness, in meters; 3) on an assumption that the average specific gravity of GA is 2.1 g/cm^3. As the element/metal and thickness grids were calculated using the cell size of 400 m × 400 m, the same cell size was used for the calculation of the total amount of element/metal.

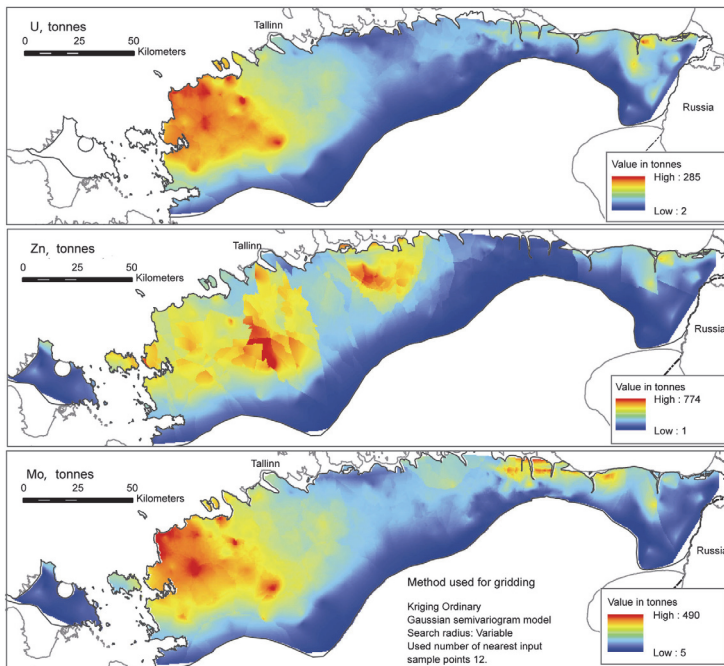Fig. 5. U, Zn and V tonnage (in tonnes) model in the 400 m × 400 m cell at the modeled thickness of graptolite argillite.

The U, Zn and Mo tonnage in the 400 m × 400 m cell (at the corresponding thickness of GA) is shown in Figure 5. These calculations allow for the provision of a more realistic total amount of metals in the Estonian GA (not just based on an average concentration value). The calculated amount of U is about 5.67 million tonnes (6.68 million tonnes as U_3O_8), Zn is 16.53 million tonnes (20.58 million tonnes as ZnO) and Mo is 12.76 million tonnes (19.15 million tonnes as MoO_3). The highest studied element amounts (Fig. 5) show a somewhat similar pattern – Western Estonia has the highest potential, especially for U and Mo. However, there are also distinctions between those elements. For example, the Central Zone, where the enrichment is the lowest, still shows high amounts of Zn. As an economic baseline, the pure metal market value can be calculated. The market value of these metals is high: about € 460 billion for uranium, € 30 billion for zinc and about € 350 billion for molybdenum, considering the average market prices in April 2013. It must be mentioned that this value does not encompass grade, economic viability assessment, market development trends, production cost or any other related cost but provides only some comparative resource value. At the moment, the Estonian GA may be classified as marginal to sub-marginal economic quantity. Moreover, since a simple, environmentally-friendly and economic technology has yet to be developed for the co-extraction of most of the enriched elements from GA, its economic value remains theoretical.

5. Conclusions

The occurrence of the Middle Cambrian to Upper Ordovician organic-rich black shale deposits in an extensive area of Baltoscandia has been known for a long time. Alum shale as well as Estonian graptolite argillite (GA) contains remarkably high concentrations of trace metals such as U, Mo, V and Ni, but may also be locally enriched with REE, Cd, Au, Sb, As and Pt.

The total estimated area (by ArcGIS software) of the Estonian GA on the mainland and islands is about 12,210 km², with the corresponding argillite volume of about 31.92 billion m³. The estimated eroded area between the West-Estonian islands is about 3,190 km² with the corresponding eroded material volume of 9.02 billion m³. Thus, the calculated total volume of Estonian GA (on the mainland and in the eroded part in Western Estonia) extends up to 40,935 km³. In order to calculate the tonnage of GA, the value of the specific gravity is needed. It is known [15] that the specific gravity of graptolite argillite varies to a great degree, mostly between 1.8 and 2.5 g/cm³. Assuming an average GA specific gravity of 2.1 g/cm³, the amount of GA is about 67 billion tonnes. The amount of possibly eroded/ dissolved material between the Estonian mainland and Hiiumaa Island is about 18.9 billion tonnes. This is an extremely large amount of material. Based on the extrapolated GA thickness and average metal contents in the

drill cores from the most westerly part of Estonia, Vormsi and Hiiumaa islands, the total amount of the uranium that has been eroded and redeposited/ dissolved reaches 1.798 million tonnes (at an average content of 95 grams per tonne), zinc (Zn) 22.716 million tonnes (average 1200 g/t), lead (Pb) 6.625 million tonnes (average 350 g/t), molybdenum (Mo) 4.448 million tonnes (average 235 g/t) and vanadium (V) 13.251 million tonnes (average 700 g/t).

The U, Zn and Mo tonnage is calculated in the cell of 400 m × 400 m (at the corresponding thickness of GA). These calculations allow us to provide a more realistic total amount of metals in the Estonian GA (based not just on an average concentration value). The calculated amount of U_3O_8 is about 6.68 million tonnes, ZnO is 20.58 million tonnes, and MoO_3 is 19.15 million tonnes. The highest studied element amounts (Fig. 5) show a somewhat similar pattern – Western Estonia has the highest potential, especially for U and Mo. However, there are also distinctions between those elements. For example, the Central Zone, where the enrichment is the lowest, still shows high amounts of Zn. However, since a simple, environmentally-friendly and economic technology has yet to be developed for the co-extraction of most of the enriched elements from GA, its economic value remains theoretical.

Acknowledgements

REFERENCES

1. Andersson, A., Dahlman, B., Gee, D. G., Snäll, S. *The Scandinavian Alum Shales*. Sveriges Geologiska Undersöknin,. 1985, **56**, 1–50.
2. Henningsmoen, G. Cambro-Silurian deposits of the Oslo region. In: *Geology of Norway* (Holtedahl, O., ed.). Norges geologiske undersmkelse, 1960, **208**, 130–150.
3. Poulsen, V. Cambro-Silurian Stratigraphy of Bornholm. *Medd. Dansk Geol. Foren.*, 1966, **16**, 117–137.
4. Männil, R. *Evolution of the Baltic Basin during the Ordovician*. Valgus, Tallinn, 1966, 200 pp (in Russian).
5. Szymanski, B. The Tremadoc and Arenig sediments in the Bialowieza area. *Pr. Inst. Geol.,* 1973, **69**, 1–92 (in Polish).
6. Baturin, G. N., Ilyin, A. V. Comparative geochemistry of shell phosphorites and Dictyonema shales of the Baltic. *Geochem. Int.*, 2013, **51**(1), 23–32.
7. Loog, A., Petersell, V. The distribution of microelements in Tremadoc grapto-litic argillite of Estonia. *Acta et Comm. Univer. Tartuensis,* Tartu, 1994, **972**, 57–75.

8. Hints, R., Hade, S., Soesoo, A., Voolma, M. Depositional framework of the East Baltic Tremadocian marginal black shale revisited. *GFF*, 2014, (in press).
9. Lindgreen, H., Drits, V. A., Sakharov, B. A., Salyn, A. L., Wrang, P., Dainyak, L. G. Illite-smectite structural changes during metamorphism in black Cambrian Alum shales from the Baltic area. *Am. Mineral.*, 2000, **85**(9), 1223–1238.
10. Sundblad, K., Gee, D. G. Occurrence of a uraniferous-vanadiniferous graphitic phyllite in the Köli Nappes of the Stekenjokk area, central Swedish Caledonides. *GFF*, 1985, **106**, 269–274.
11. Heinsalu, H., Bednarczyk, W. Tremadoc of the East European Platform: lithofacies and palaeogeography. *Proc. Acad. Sci. Estonian SSR. Geology,* 1997, **46**(2), 59–74.
12. Leventhal, J. S. Comparative geochemistry of metals and rare earth elements from the Cambrian alum shale and kolm of Sweden. *Special Publication of the International Association of Sedimentologists*, 1990, **11**, 203–215.
13. Petersell, V., Mineyev, D., Loog, A. Mineralogy and geochemistry of obolus sandstones and dictyonema shale of North Estonia. *Acta et Comm. Univer. Tartuensis,* Tartu, 1981, **561**, 30–49 (in Russian).
14. Thickpenny, A. The sedimentology of the Swedish Alum Shales. In: *Fine Grained Sediments: Deep Water Processes and Environments* (Stow, D. A. W., Piper, D. J. W., eds.). Spec. Publ., Geol. Soc., Blackwell Scientific Publications, Oxford, 1984, **15**, 511–526.
15. Petersell, V. Dictyonema argillite. In: *Geology and Mineral Resources of Estonia* (Raukas, A., Teedumäe, A., eds.). Estonian Academy Publishers, Tallinn, 1997, 313–326.
16. Veski, R., Palu, V. Investigation of Dictyonema oil shale and its natural and artificial transformation products by a vankrevelenogram. *Oil Shale,* 2003, **20**(3), 265–281.
17. Erdtmann, B.-D. The planktonic nema-bearing *Rhabdinopora flabelliformis* (Eichwald, 1980) versus benthonic root-bearing *Dictyonema Hall*, 1952. *Proc. Acad. Sci. Estonian SSR. Geology,* 1986, **35**(3), 109–114 (in Russian).
18. Pukkonen, E. & Rammo, M. Distribution of Molybdenum and Uranium in the Tremadoc Graptolitic Argillite (Dictyonema Shale) of North-Western Estonia. *Bull. Geol. Surv. Estonia*, 1992, **2**(1), 3–15.
19. Soesoo, A., Hade, S. Metalliferous organic-rich shales of Baltoscandia – a future resource or environmental/ecological problem. *Archiv Euro Eco*, 2012, **2**(1), 11–14.
20. Voolma, M., Soesoo, A., Hade, S., Hints, R., Kallaste, T. Geochemical heterogeneity of Estonian graptolite argillite. *Oil Shale*, 2013, **30**(3), 377–401.
21. Lippmaa, E., Maremäe, E. Uranium production from the local Dictyonema shale in North-East Estonia. *Oil Shale*, 2000, **17**(4), 387–394.
22. Kleesment, A., Kurvits, T. Mineralogy of Tremadoc graptolitic argillites of North Estonia. *Oil Shale,* 1987, **4**(2), 130–138 (in Russian).
23. Loog, A., Petersell, V. Authigenic siliceous minerals in the Tremadoc graptolitic argillite of Estonia. *Proc. Est. Acad. Sci. Geol.*, 1995, **44**(1), 26–32.
24. Soesoo, A., Hade, S. Black shale of Estonia: moving towards a Fennoscandian-Baltoscandian database. *Transactions of Karelian Research Centre, Russian Academy of Science*, 2014 (in press).

25. Baukov, S. S. General characteristics of dictyonema shale. In: *Geology of Coal and Oil Shale Deposits of the USSR*, Nedra, Moscow, 1968, **11**, 145–148 (in Russian).
26. Sibson, R. A brief description of natural neighbor interpolation. In: *Interpreting Multivariate Data* (Barnett, V., ed.). John Wiley, Chichester, 1981, 21–36.
27. Wahba, G. *Spline Models for Observational Data*. Society for Industrial and Applied Mathematics, Philadelphia, 1990, 162 pp.
28. Cressie, N. A. C. *Statistics for Spatial Data*. John Wiley & Sons, New York, 1991, 900 pp.
29. Estonian National Balance of Natural Resources, Year 2012. Located http://geoportaal.maaamet.ee/docs/koondbilanss_2012.pdf?t=20130614161639.
30. Suuroja, K. *Baltic Klint in North Estonia as a symbol of Estonian nature*. Ministry of Environment, Tallinn, 2006, 224 pp.
31. Soesoo, A. Miidel, A. *North Estonian Klint*. GeoGuide Baltoscandia, Tallinn, 2007, 28 pp.
32. Overeem, I., Weltje, G. J., Bishop-Kay, C., Kroonenberg, S. B. The Late Cenozoic Eridanos delta system in the Southern North Sea Basin: a climate signal in sediment supply? *Basin Res.*, 2001, **13**(3), 293–312.
33. Rhebergen, F. Ordovician sponges (Porifera) and other silicifications from Baltica in Neogene and Pleistocene fluvial deposits of the Netherlands and northern Germany. *Est. J. Earth Sci.*, 2009, **58**(1), 24–37.

PAPER IV

SOESOO, A., HADE, S. 2012. Metalliferrous organic-rich shales of Baltoscandia – a future resource or environmental/ecological problem? *Archiv Euro Eco*, **2(1)**, 11-14.
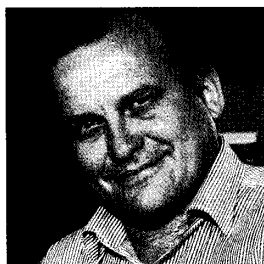
METALLIFEROUS ORGANIC-RICH SHALES OF BALTOSCANDIA — A FUTURE RESOURCE OR ENVIRONMENTAL/ECOLOGICAL PROBLEM?

PROF.
ALVAR SOESOO

SIGRID HADE

*Tallinn University of
Technology, Ehitajate tee 5,
Tallinn 19086, Estonia*

*alvar.soesoo@gmail.com
sigrid.hade@gmail.com*

ABSTRACT: Middle Cambrian to Late Ordovician black shales occupy large areas in Sweden, Norway, Estonia and Russia. They are commonly characterized by specific geochemical signature – they are high and very high in U, Mo, V, Zn, Pb and other metals and can be treated as metal ore and twofold energy source (including U and shale oil). These rocks have high scientific and probably significant economic value. At the same time, as it is historically known, the shale has major negative impact on the environment. The most known environmental problems are met in Estonia and Sweden, where the beds have historically been exploited for uranium production. In northern Estonia, graptolite argillite was removed during phosphorite mining causing thus pollution of soils and groundwater. Even if the Baltoscandian black shales possibly are an important future metal and oil reserve, there is very little done on the development of mining and ore processing technologies in order to meet elementary environmental requirement and secure natural species and public health in the area of production and outside.

KEYWORDS: sblack shale, graptolite argillite, metals, uranium, pollution, Estonia

Introduction

The occurrence of the Middle Cambrian to Late Ordovician organic-rich deposits in an extensive area of Sweden (alum shales; Andersson et al., 1985), Oslo region (Henningsmoen, 1960), Bornholm (Poulsen, 1966), Estonia and Russia (known as graptolite argillite, Dictyonema shale; Männil, 1966, and kukersite) and Poland (Szymanski, 1973) has been known for a long time (Fig. 1). As a possible westward continuation, the organic-rich black shales are known in the central part of the Scandinavian Caledonides - Norway (Stormer, 1941) and Sweden (Gee, 1981; Sundblad & Gee, 1984), where they represent metamorphosed pelites (phyllites) thrust onto the Baltoscandian Platform section during late Silurian and Devonian. In addition, Middle- to Late-Ordovician organic-rich oil shale — kukersite — is known in northern Estonia (Puura, 1986). Since the deposits are widespread, they are characterized by specific geochemical signature — except kukersite, they are high and very high in U, Mo, V, Zn, Pb and other metals and can be treated as metal ore and twofold energy source (including U and shale oil). These rocks have high scientific and significant economic value. At the same time, as historically known, the shale has major negative impact on the environment. The most known environmental problems are met in Estonia and Sweden.

Black shale as an ore resource

Alum shale as well as graptolite argillite contain remarkably high concentrations of trace metals such as U, Mo, V and Ni, but might also be locally enriched with respect to different REE, Cd, Au, Sb, As and Pt. The above beds have historically been exploited for uranium production in Sweden and Estonia. Besides, high content of potassium, sulfur and organic matter is characteristic of those beds. Kerogen in the black shales is of algal origin and the content of total organic carbon mostly stays between 10–25 wt% (Andersson et al., 1985). The mineral matter of the black shales is dominated by clay minerals illite-smectite and illite (Snäll, 1988). Distinctive for the black shales is the occurrence of high concentration of pyrite, which together with kerogen is thought to be the main carrier of rare elements.

As we know, alum shale and graptolite argillite form patches over extensive areas in the outskirts of Baltica palaeocontinent (Andersson et al., 1985). A possible spatial continuity towards the north are

graphitic phyllites, which form tectonically disrupted allochtonous and autochtonous Caledonian complexes in northern Sweden and Norway. The metal-enriched phyllites have shown to exhibit geochemical signatures similar to unmetamorphozed black shales of southern Baltoscandia (Sundblad & Gee, 1984). Despite a long history of exploration and exploitation of Baltoscandian black shales, the development of trace metal assemblages of the beds has remained controversial. Syndepositional accumulation of redox-sensitive metals under oxygen-depleted or anoxic conditions has generally been suggested as prominent mechanism for enrichment with rare metal compounds. Even less is known about their environmental impact in both situations — as a ground rock forming landscapes and as a product of mining and elemental processing.

Geological overview
of Estonian graptolite argillites

The Early Ordovician marine graptolite argillite (GA) underlies most of northern Estonia (Fig. 1). It is fine-grained, unmetamorphosed, horizontally lying organic-rich (8–20%) lithified clay belonging to the group of black shales of sapropelic origin (Raukas & Teedumäe, 1997, refs. therein). GA is characterized by high to very high concentrations of U (up to 1300 ppm), Mo, V, Ni and other heavy metals, and is rich in N, S and O. High concentrations of certain elements may be either potentially useful or hazardous. During the Soviet era, a total of 22 tons of U was produced in underground mine near Sillamäe.

According to the Estonian national natural resource register and WEC world overview (2007), Estonian GA resources are about 64 billion tons. GA calorific value ranges from 4.2–6.7 MJ/kg (Pukkonen & Rammo, 1992), the density is changeable varying from 1.8 to 2.5 g/cm³. Considering GA as a low-grade oil source, its potential reserves are about 2.1 billion tons. So the black shales are a low- to medium-grade solid fuel world-wide and are considered as a potential energetic reserve for future. At present, in Estonia GA is considered only as sub-marginal economic for ecological concerns and technological reasons.

Detailed geochemical changes across the GA unit are unknown. As an example of elemental distribution within the GA unit V, Mo and U distributions have been modeled in Figure 2. These data represent the calculated average concentration in the drill core. The central and western parts of the Eastern Zone show the highest concentrations for V and Mo, whereas V is also high in southern part of Eastern and Central zones. Generally, it can be concluded that the concentration of most of the metals is relatively low in the Central Zone (Fig. 2).

Some environmental concerns

The black shale utilisation in Sweden and Estonia is briefly summarised below.

In Sweden, the Cambrian and Lower Ordovician alum shale of Sweden has been known for more than 350 years. It was a source of potassium aluminium sulfate that was used in the leather tanning industry, for fixing colors in textiles, and as a pharmaceutical astringent. Mining the shales for alum began in 1637 in Skåne. The alum shale was also recognized as a source of fossil energy and, toward the end of the 1800s, attempts were made to extract and refine hydrocarbons (Andersson et al., 1985). Before and during World War II, alum shale was retorted for its oil, but production ceased in 1966 owing to the availability of cheaper supplies of crude petroleum. During this period, about 50 million tons of shale was mined at Kinnekulle in Västergötland and at Närke.

For uranium production, a pilot plant built at Kvarntorp produced more than 62 tons of uranium between 1950 and 1961. The highest uranium grades have been indicated at Ranstad, southern Sweden. The uranium-carrying horizon is 2.5 to 4.0 m thick with a grade varying between 250 to 325 ppm U. The total uranium content in the Randstad area is over 1 Mt of which it should be possible to recover at least 300 000 tons on a purely technical and economic basis. A small uranium mill was constructed at Ranstad and put on stream in 1965. The plant operated at reduced capacity for 3 years producing about 300 tons of yellowcake. Due to the low demand for uranium at that time, caused by delays in the nuclear power programmes, the plant was closed down in 1969. During the 1980s, production of uranium from high-grade deposits elsewhere in the world caused a drop in the world price of uranium to levels too low to profitably operate the Ranstad plant, and it was closed eventually in 1989 (Bergh, 1994).

Alum shale was also burned with limestone to manufacture "breeze blocks," a lightweight porous building block that was widely used in the Swedish construction industry. Production stopped when it was realized that the blocks were radioactive and emitted unacceptably large amounts of radon.

Just after World War II, due to the atomic bomb "competition", the Soviet Union started to look for uranium deposits. The nearest place where geologists had found large quantities of uranium ore was northeastern Estonia and the first Soviet uranium processing facility was started in a small Sillamäe town, eastern Estonia. The plant operated as a top-secret institution until 1991. It was privatized in 1997 and renamed as "AS Silmet". At the moment the plant produces rare
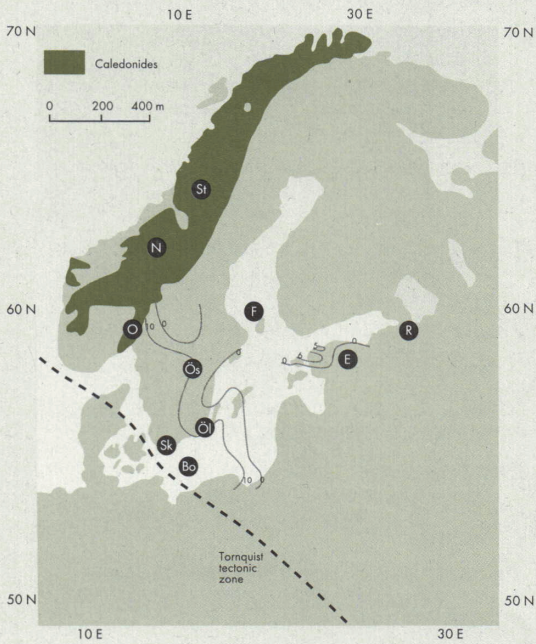
Fig. 1.
Organic-rich, Cambro-Ordovician shales of Balto-scandia. St – Stepenjokk; N – Nordaunevoll; O – Oslo; Ös – Östersund; Öl – Öland; Sk – Skane; Bo – Bornholm; E – Estonia; R – Russia
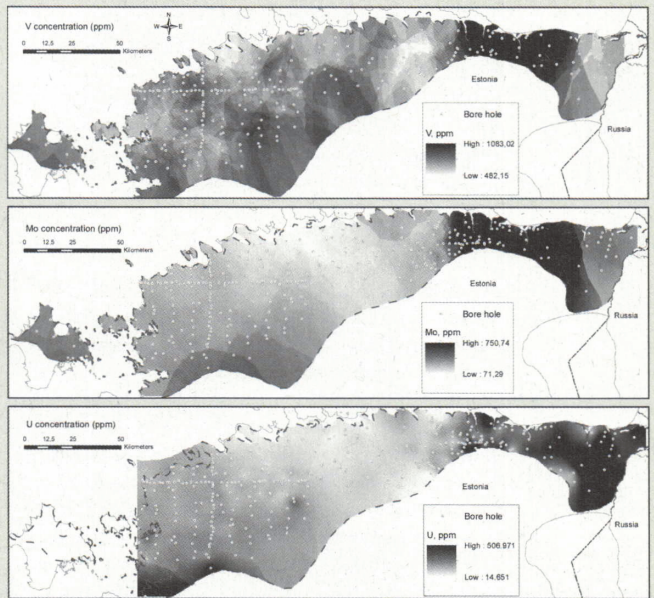
Fig. 2.
V, Mo and U concentrations in Estonian GA as modeled using calculated average drill core analyses. Element concentration surfaces were modeled by kriging method using spherical distances (ESRI ArcGIS)

metals, rare earth metals and their compounds, being the most important REE producer within the European Union.

Because GA is a co-product of phosphorite mining, the Maardu area near Tallinn is among the most polluted regions in Estonia. During the opencast mining of phosphorite the radioactive graptolite argillite with average uranium content of 50 to 130 ppm, maximum 300–450 ppm was deposited in waste dumps. In 1989, opencast mining at Maardu was carried out on more than 6 km^2. The mining and processing stopped in 1991. Today, waste hills at Maardu contain about 73 million tons of GA, which contains, as taken minimum content of 30 ppm U, totally as much as 2.19 million kg of U (Jüriado et al., 2012). This waste leaches into the surface and ground waters.

Under normal weathering conditions GA is easily oxidizing, and spontaneous combustion can happen. In some places at Maardu waste hills, the tempera-

tures in the heap occasionally exceeded 500° C. It is interesting that spontaneous combustion can occur in heaps that are both a few months as well as over 20 years old leading to the conclusion that some old heaps can still be dangerous. These processes lead to an annual leaching of 1500 tons of mineral matter per square kilometre of a waste dump and the waste water being discharged into the Maardu lake (Heinsalu, 1996). In 1990, at the average temperature of the heap, an estimated $520.3 \cdot 10^3$ tons of oxygen was spent on oxidizing the rocks buried in the heap. This equals to 6.6% of the annual oxygen output of Estonian forests during a 7-month vegetation period. The amount of gases emitted from burning shale was estimated as: $SO_2 — 10^4$ tons and $CO_2 — 73.3 \cdot 10^3$ tons (Pihlak, 2009). The effluent of the Maardu opencast mine and processing plant, which was directed into the Muuga Bay (Gulf of Finland) delivered up to 20.18 million m^3 of water with varying levels of polluting elements each

year. The amount of dissolved minerals delivered into the sea was estimated up to $38.4 \cdot 10^3$ tons annually (Pihlak, 2009; Jüriado et al., 2012).

GA is also a major source for radon (Rn) in Estonia. Very high radon concentrations up to 10 000 Bq/m^3 have been recorded at some natural outcrops of GA in the North Estonian Klint. Radon is highly radioactive and carcinogenic element causing mutations, especially lung cancer.
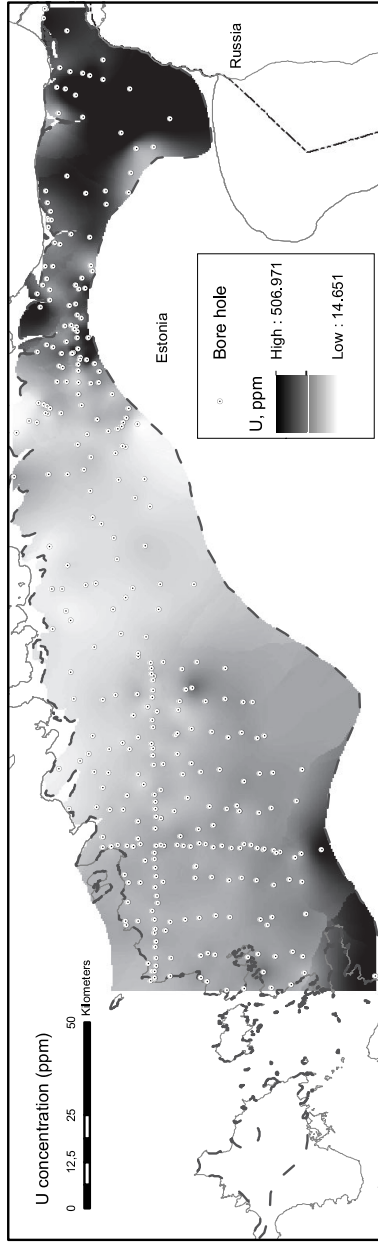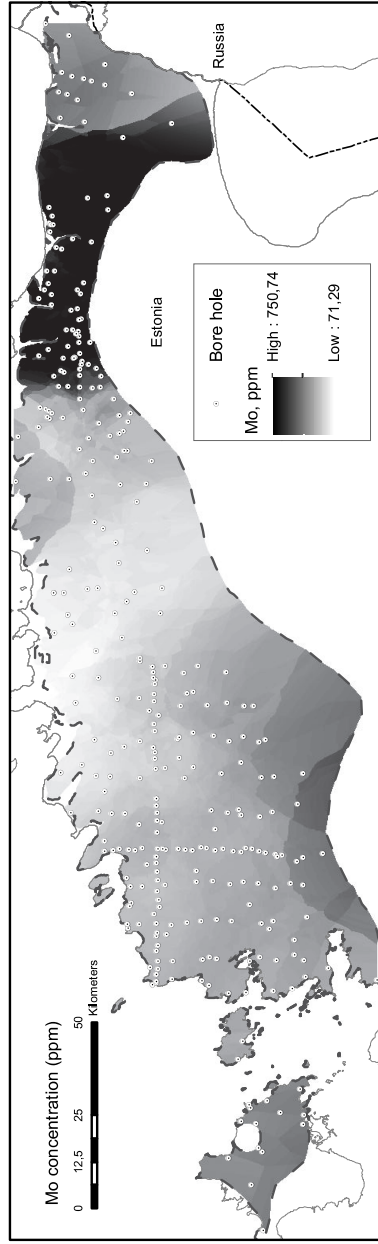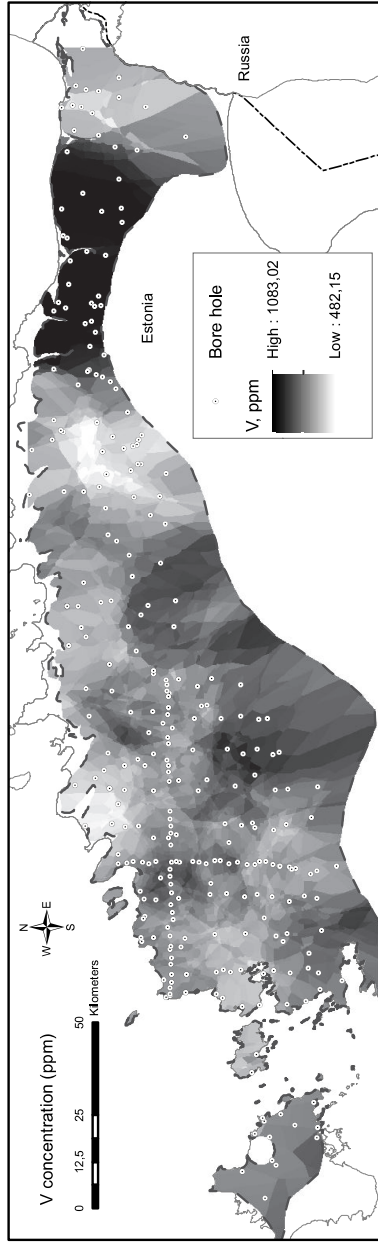
Conclusions

Middle Cambrian to Late Ordovician black shales occupy large areas in Sweden, Norway, Estonia and Russia. These shales are commonly characterized by specific geochemical signature — they are high and very high in U, Mo, V, Zn, Pb and other metals and can be treated as metal ore and twofold energy source (including U and shale oil). At the same time, it is historically known that the shale has major negative impact on the environment. The most known environmental problems are met in Estonia and Sweden, where the beds have historically been exploited for uranium (and oil & phosphorite) production. In northern Estonia, graptolite argillite was removed during phosphorite mining, causing thus pollution of soils and groundwater. The Baltoscandian black shales are important future metal and possibly oil reserve; however, there is too little done on the development of mining and ore processing technology to meet the elementary environmental needs and secure natural species and public health in the area of production and outside.

Acknowledgements

References

ANDERSSON, A., DAHLMAN, B., GEE, DG., SNÄLL, S. 1985. The Scandinavian Alum Shales. – Sveriges Geologiska Undersökning, 56, 1–50.

HEINSALU, A. 1996. Sediment Stratigraphy and Chemistry of Lake Maardu, Northern Estonia. – PACT 51. 163–173.

HENNINGSMOEN, G. 1960. Cambro-Silurian deposits of the Oslo region. In: Holtedahl (eds.). Geology of Norway. – Norges geologiske undersøkelse, 208, 130–150.

JÜRIADO, K., RAUKAS, A., PETERSELL, V., 2012. Alum shales causing radon risks on the example of Maardu area, North-Estonia. – Oil Shale, 29, 1, 76–84.

GEE, D. 1981. The Dictyonema-bearing phyllites at Nourdaunevoll, eastern Trondelag, Norway. – GFF, 61, 93–95.

MÄNNIL, R. 1966. Evolution of the Baltic basin during the Ordovician. – Valgus, Tallinn, 200 p. (in Russian).

PIHLAK, A.-T. 2009. On the history of investigation of self-burning processes and oxygen problems in Estonia. – Tallinn, Infotrükk, [in Estonian, with Russian summary].

POULSEN, V., 1966. Cambro-Silurian stratigraphy of Bornholm. – Meddelelser fra Dansk Geologisk Forening, 16, 117–137.

PUURA, V. 1986 (Eds). Geology of the Kukersite-bearing Beds of the Baltic Oil Shale Basin. – Tallinn: Valgus. (in Russian, English summary).

RAUKAS, A. & TEEDUMÄE, A. 1997 (Eds). Geology and mineral resources of Estonia. Estonian Academy Publishers, 436 p.

SNÄLL, S. 1988. Mineralogy and maturity of the alum shale south-central Jämtland, Sweden. – Sveriges Geologiska Undersökning, 81, 4, 1–46.

STÖRMER, L. 1941. Dictyonema shales outside the Oslo Region. – Norsk Geologisk Tidsskrift, 20, 161–170.

SUNDBLAD, K. & GEE, D. G. 1984. Occurrence of a uraniferous vanadiniferous graphitic phyllite in the Köli Nappes of the Stekenjokk area, central Swedish Caledonides. – GFF, 106, 269–274.

SZYMARISKI, B. 1973. Osady Tremadoku i Arenigu na obszarze Biatowieiy. – Institut Geologiczny, Prace, 69, 1–92.

WEC (World Energy Council) 2007. Information Energy Information Centre News and Events Publications Member Services. - http://www.worldenergy.org/wec-geis/publications

V concentration (ppm)

V, ppm
Bore hole
High : 1083,02
Low : 482,15

Estonia

Russia

0 12,5 25 50
Kilometers

Mo concentration (ppm)

Mo, ppm
Bore hole
High : 750,74
Low : 71,29

Estonia

Russia

0 12,5 25 50
Kilometers

U concentration (ppm)

U, ppm
Bore hole
High : 506.971
Low : 14.651

Estonia

Russia

0 12,5 25 50
Kilometers

PAPER V

SOESOO, A., HADE, S. 2014. Black shale of Estonia: moving towards a Fennoscandian-Baltoscandian database. *Transactions of Karelian Research Centre, Russian Academy of Science*, **1**, 103–114.

BLACK SHALE OF ESTONIA: MOVING TOWARDS A FENNOSCANDIAN-BALTOSCANDIAN DATABASE

A. Soesoo, S. Hade

Institute of Geology at Tallinn University of Technology

The occurrences of Cambro-Ordovician organic-rich black shale and their metamorphosed Precambrian and Lower Palaeozoic analogues have been known in Fennoscandia for a long time. These rocks show high concentrations of U, Mo, V, Zn, Pb, Ni and other metals. For example, Estonian uranium reserves have been estimated at 6.6 million tons (U_3O_8). Apart from commercial interest, there are environmental aspects related to black shale. Early mining in Sweden and Estonia caused significant damage to environment. Black shale emanates radon, and the weathering of shale releases harmful elements into the soil and groundwater. As the Fennoscandian and Baltoscandian black shale provides a large lithological and geochemical variety of shale and meta-shale, there is need for a new and updated assessment and re-evaluation of this resource. Our proposal is to feed geological, geochemical and environmental information into the Fennoscandian-Baltoscandian Black Shale Database (FBSD) with browser-based visualization possibilities. The database gathers data on both Paleozoic and Precambrian rocks, and includes shale stratigraphy, resource, metal/element distribution, environmental impact assessment, soil and groundwater impact, etc. Some visualizations have been presented using Estonian graptolite argillites as an example.

K e y   w o r d s: black shale, graptolite argillite, resource, Estonia, Fennoscandia, database.

А. Соесоо, С. Хаде. ЧЕРНЫЙ СЛАНЕЦ В ЭСТОНИИ: НА ПУТИ К СОЗДАНИЮ ФЕННОСКАНДИНАВСКО-БАЛТОСКАНДИНАВСКОЙ БАЗЫ ДАННЫХ

Проявления кембро-ордовикского обогащенного органическими веществами черного сланца и их метаморфизованные докембрийские и нижнепалеозойские аналоги давно известны в Фенноскандии. Для этих пород характерны высокие концентрации U, Mo, V, Zn, Pb, Ni и других металлов. К примеру, запасы урана в Эстонии оцениваются в 6,6 млн тонн (U_3O_8). Кроме коммерческого интереса с черным сланцем связаны и экологические проблемы. Ранняя добыча в Швеции и Эстонии нанесла серьезный вред окружающей среде. Черный сланец излучает радон, а при выветривании черного сланца высвобождаются вредные элементы, которые попадают в почву и грунтовые воды. Поскольку черный сланец Фенноскандии и Балтоскандии представляет собой сланцы и метасланцы с разнообразными литологическими и геохимическими характеристиками, необходимо уточнить его ресурсы. Мы предлагаем создать Базу данных по черному сланцу Фенноскандии-Балтоскандии с геологической, геохимической и экологической информацией. В эту базу данных заносятся данные по палеозойским и докембрийским породам, включая такие характеристики сланцев, как стратиграфия, ресурсы, распределение металлов/элементов, оценка воздействия на окружающую среду, влияние на почвы и грунтовые воды и т. д. Представлены некоторые визуализации на примере граптолитовых аргиллитов Эстонии.

К л ю ч е в ы е   с л о в а: черный сланец, граптолитовый аргиллит, ресурсы, Эстония, Фенноскандия, база данных.

Introduction

Shale is usually a fine grained sedimentary rock containing organic matter and silt and clay size mineral grains that have accumulated together. Shale is characterized by fissility – it breaks along thin laminae, parallel layering or bedding texture that is less than one centimeter in thickness. Black shale commonly forms in anoxic or low oxygen conditions and contains unoxidized carbon and iron sulfides such as pyrite. Minor amounts of authigenic carbonate minerals, either dispersed in cements or in concretions, are characteristic features of many black shale units. Most black shale is marine in nature and may have areal extents of thousands of square kilometers. It typically requires conditions that are conducive to the accumulation of large quantities of organic matter, as well as slow accumulation rates to prevent the dilution of the accumulating metals. Metals may be derived from seawater, either directly or via pre concentration in planktonic organisms. Unusual circulation patterns and volcanic ash deposition may enhance metal enrichments. There is currently no consensus on the source of metals and the genesis of black shale. It is plausible that several sources and mechanisms may be responsible in different black shale formations. Black shale is common in many Palaeozoic and Mesozoic strata worldwide including Fennoscandia and Baltoscandia. Black shale commonly contains abundant heavy and other metals. Its units may have beds enriched in metals by factors much greater than 50 for Ag, for example, and greater than 10 for Mo [Krauskopf, 1955]. Such increased concentrations of Ag, Mo, Zn, Ni, Cu, Cr, V, and less commonly Co, Se, and U are conspicuous features of only some black shale [Vine and Tourtelot, 1970]. There are black shales that are quite enriched in uranium, for example, the Estonian graptolite argillites and Swedish Alum shale are the main future resource of uranium for Europe.

Black shale as a metal resource

Organic carbon rich black shale has long been studied regarding the industrial interest in a variety of transition metals, especially Mo, Zn, Ni, Cu, Cr, V, Co, Pb, U, and Ag. These studies reveal a variety of metal sulfides in shale, and suggest that sulfide minerals are an integral part of the sediment diagenesis [e. g. Amstutz and Park, 1971; Vulimiri and Cheney, 1980; Hofmann, 1989; Schieber, 1991].

Besides these widespread, but low grade metal deposits, shale is also host to some of the world's largest economic deposits of copper, lead, and zinc. For example, the Kupferschiefer in Central Europe is probably one of the most well known occurrences. Mined since the Middle Ages, the mining in Germany continued until very recently [e.g. Jung and Knitschke, 1976], and still continues in Poland. Although generally very thin, the Upper Permian Kuperschiefer is a transgressive black shale deposit that extends from Poland to Britain and covers an area in excess of 600,000 km^2. Somewhat less extensive, and much less mined, black shale extends from the Syas River in Russia to Estonia, Sweden and to southern, central and northern Norway.

These occurrences of Middle Cambrian to Late Ordovician organic rich black shale deposits in an extensive area of Sweden [Alum shale; Andersson et al., 1985], the Oslo region [Henningsmoen, 1960], Bornholm [Poulsen, 1966], Estonia (known as graptolite argillite or "Dictyonema shale" [Männil, 1966], and kukersite as proper oil shale), Poland [Szymariski, 1973] and northwest Russia [Baturin and Ilyin, 2013] have been known for a long time. The Alum shale, as well as graptolite argillite, contains remarkably high concentrations of trace metals such as U, Mo, V and Ni, but may also be locally enriched with REE, Cd, Au, Sb, As, Pt [Voolma et al., 2013; Hade and Soesoo, submitted]. The beds have historically been exploited for local uranium production in Sweden and Estonia. Kerogen in the black shale is of algal origin and the content of total organic carbon is mostly between 10–25 wt % [Andersson et al., 1985]. The mineral matter of the black shale is dominated by clay minerals, illite smectite and illite [Pukkonen and Rammo, 1992; Lindgreen et al., 2000]. The high concentration of pyrite, which, together with kerogen, is thought to be the main carrier of some rare earth and other elements, is distinctive for black shale. The Alum shale and graptolite argillite form patches over extensive areas in the outskirts of the Baltica palaeocontinent [Andersson et al., 1985] – Baltoscandia and Fennoscandia. A possible spatial continuity of those complexes are the graphitic phyllites that are found in the tectonically disrupted allochtonous and autochtonous Caledonian complexes in central and northern Sweden and Norway [Sundblad and Gee, 1985]. The metal enriched phyllites exhibit geochemical signatures similar to the unmetamorphosed black shale of Baltoscandia [Sundblad and Gee, 1985]. These geochemical similarities suggest that organic rich mud might have accumulated over a wide geographic area and under fairly different depositional conditions – from pericratonic shallow marine settings to continental slope

environments. The black shale of Fennoscandia and the graptolite argillite (GA) of Estonia can thus be treated as metal ore and a twofold energy source (including U and shale oil); the rocks have a high scientific and significant economic value.

There are many known Paleozoic black shale deposits in various basins. The Silurian Zn Pb deposits of Howards Pass (Canada) are also located in graptolite shale and contain in excess of 100x106 metric tons of ore [Gustavson and Williams, 1981]. Devonian representatives are the well known Zn Pb deposits of Rammelsberg and Meggen in Germany and the Selwyn Basin Pb Zn deposits in the Yukon Territory (Canada) [Gardner and Hutcheon, 1985].

Some black shale is significantly enriched by noble metals, sometimes coupled with Mo and Ni bearing shale. For example, the Lower Cambrian black shale of southern China contains up to several hundred ppb's PGE's and Au in strata deposited as individual, metal rich sulfide layers, 2–15 cm thick [Grauch et al., 1991]. Some of these elements in the Fennoscandian Baltoscandian black shale may be of commercial value. In many Precambrian terrains metamorphosed sedimentary rocks, which were initially black shale, are known and also provide great economic interest.

Major base metal deposits in shale also occur in the Proterozoic of Australia, North America, and Africa. In Africa, the most prominent and best known are the deposits of the Zambian Copper Belt [Fleischer et al., 1976]. In Australia, there are several Pb Zn Ag deposits hosted in Proterozoic shale, such as Mt. Isa, Hilton, McArthur River, and Lady Loretta [Gustavson and Williams, 1981]. In North America, the known shale hosted mineral deposits of Proterozoic age include the White Pine copper deposit in Michigan and the Sullivan Pb Zn deposit in British Columbia [Gustavson and Williams, 1981].

The Fennoscandian Shield provides several good examples of metamorphosed metal rich black shale of the Precambrian age [Yudovich and Ketris, 1988; Arkimaa et al., 1999]. A few are in active mining operation, several in exploration stage and many waiting to be discovered and exploited. The Talvivaara mine in Finland, with more than one billion ton resource, has been in production since 2008, by Talvivaara Mining Company Plc, and is the first mining operation collectively recovering NiCoCuZn(Mn)(U) by bioheapleaching polymetallic black shale. In the Viken area, Sweden, Continental Precious Minerals Inc. has estimated the uranium resource to be 1.05 billion lbs. of U_3O_8 in Alum shale and large amount of other metals.

The Geological Survey of Finland has compiled a distribution map of Precambrian black shale in Finland, based on magnetic and apparent resistivity datasets [Arkimaa et al., 1999]. An extensive study of the Paleozoic Alum shale has previously been conducted in Sweden. The Geological Survey of Norway is compiling information about various aspects of black shale in the country. Russian scientists have also conducted drilling and studies of black shale (graptolite argillites) in the Leningrad oblast area. In Estonia, a compilation of existing and new geochemical studies has resulted in distribution maps of some elements and elemental resource calculation [see Hade and Soesoo, submitted; Voolma et al., 2013]. These results will be briefly presented here.

Apart from the commercial value of ore, there is another important aspect related to black sha le – the environmental one. It has been known for a long time that the early mining in Sweden and Estonia has caused significant damage to environment and human health. However, mining is not the only cause of environmental impact. On or near the surface sedimentary black shale emanates radon, weathering of shale releases harmful elements into the soil and groundwater, and so on. It is only recently that we have started comprehending all the possible negative impacts related to this type of organic and metal rich shale. It is also important to note that metamorphosed Precambrian black shale also has an environmental impact – even if it is not mined. This sulfide rich black shale weathers more easily and thus releases more harmful elements than most of types of rock in the Fennoscandian Shield. For example, a study of a small lake in a black shale area in Finland indicated that it has been acidified for 9,000 years already [Loukola Ruskeeniemi et al., 1998].

Since the Fennoscandian Shield and Paleozoic Baltoscandia provide a large variety of black shale, with different genetic characteristics and metal, sulfur and carbon occurrences, and different environmental aspects, there is a need for a new and updated assessment and re evaluation of this resource. Data should be gathered on both Paleozoic and Precambrian rocks and, at least, the following should be included: a) geographical/stratigraphical position and resource/reserve estimate, b) metal/element distribution, calorific value etc.; c) environmental and health impact assessment, soil and groundwater impact. The compiled data should be put in a database and visualized in geographical space, and made accessible to the public. Some black shale characteristics, in a format for the possible future database will be presented below, based on the Estonian graptolite argillite studies.

Overview of Estonian graptolite argillite (black shale)

Compared to the Fennoscandian sedimentary and metamorphic black shale, the geological position and stratigraphic characteristics of Estonian black shale are very simple. Therefore, Estonia may be a good example on which to base the future Fennoscandian-wide compilation.

Organic-rich Early Ordovician marine metalliferous black shale – graptolite argillite (GA) lies beneath most of northern Estonia (Fig. 1). Historically, it was called "Dictyonema shale", "Dictyonema argillite" or "alum shale." The word dictyonema came from the benthonic root-bearing Dictyonema abelliforme, which subsequently turned into planktonic nema-bearing Rhabdinopora abelliformis [Erdtmann, 1986]. Here the term graptolite argillite is used, while "Dictyonema shale" is still used in Russian literature.

The graptolite argillite is fine-grained, unmetamorphosed, (sub-)horizontally lying and undisturbed, organic-rich (8–20 %) lithified clay (Türisalu Formation), which is commonly 0.5 to 6 m thick and belongs to the group of black shale of sapropelic origin [Petersell, 1997; Voolma et al., 2013; Hade and Soesoo, submitted] (Fig 1, A). The graptolite argillite crops out in some places in Northern Estonia, in the klint area or in some narrow river valleys. Since the entire Estonian Lower Palaeozoic sedimentary section is inclined towards the south due to its geological position on the southern slope of Fennoscandian Shield [Soesoo et al., 2004], at the southwest end, the GA deposit lies at a depth of more than 250 meters (Fig. 1, B).

The Estonian GA is characterized by high to very high concentrations of U (up to 1200 ppm), Mo (1000 ppm), V (1600 ppm), Ni and other heavy metals, and is rich in N, S and O [Pukkonen and Rammo, 1992; Soesoo and Hade, 2012; Voolma et al., 2013]. High concentrations of certain elements may be potentially useful or hazardous. During the Soviet era, the GA was mined for uranium production at Sillamäe, in Northeast Estonia, between 1948 and 1952 [Veski and Palu, 2003]. A total of 22.5 tons of elemental uranium was produced from 272,000 tons of GA from an underground mine near Sillamäe. Between 1964 and 1991, approximately 73 million tons of GA was
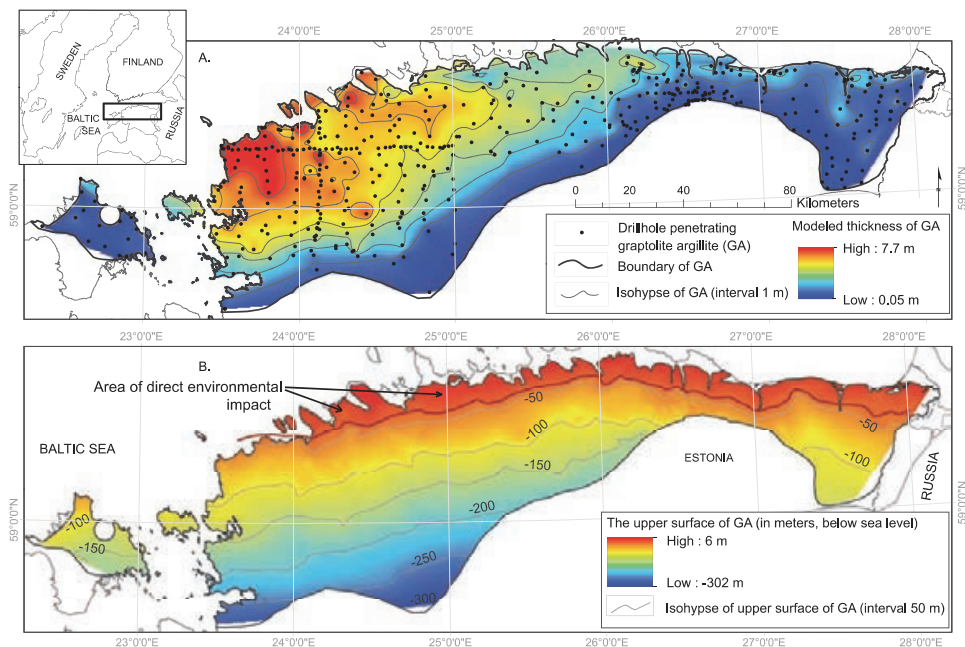

Fig. 1. A. Thickness map of the Estonian graptolite argillites and location of the drill holes penetrating argillite layers (black dots). The thickness of GA was modeled by ArcInfo 10.1, based on the studied drill holes. For creating the thickness grid, the Natural Neighbor interpolation method was used, and the grid cell size is 400 meters. B. The depth of graptolite argillite (upper surface). Due to the location in the southern margin of the Precambrian Fennoscandian Shield GA layer is dipping southwards following the regional trend. As GA crops out in Northern Estonia, direct environmental impacts result

mined from a covering layer of phosphorite ore at Maardu, near Tallinn. The GA was mixed up with other overlying deposits, such as carbonate rocks, sandstone, glauconite sandstone, and Quaternary sediments, and piled into waste heaps.

Although the reserves of GA surpass those of Estonian kukersite (oil shale), it is of a quality too poor for energy production. The GA calorific value ranges from 4.2–6.7 MJ/kg [Pukkonen and Rammo, 1992] and the Fischer Assay oil yield is 3–5 % (for Estonian kukersite, it is about 30–47 %, for example [Veski and Palu, 2003]). The moisture content of fresh GA ranges from 11.9 to 12.5 %, while average composition of the combustible part is: C – 67.6 %, H – 7.6 %, O – 18.5 %, N – 3.6 % and S – 2.6 % [Lippmaa and Maremäe, 2000]. However, considering it is a low grade oil source, its potential oil reserves are about 2.1 billion tons [Veski and Palu, 2003]. The Fennoscandian black shale together with Estonian GA is considered to be a potential energy reserve for the future.

The specific gravity of Estonian GA mostly varies between 1800 and 2500 kg/m^3 [Petersell, 1997]. The content of pyrite in GA is also highly variable, ranging from 1.5 % to 9.0 %, but concentrated between 2.4 % and 6 %. Pyrite forms fine crystalline disseminations, thin interlayers and concretions of different forms and sizes. The diameter of the concretions is usually 2–3 cm. Some concretions are complex in structure and contain crystals of galenite, sphalerite and calcite.

The mineral composition of GA is dominated by K feldspar, quartz and clay minerals. In the lateral, as well as vertical, dimension, the contents of the major rock forming minerals show slight, but pronounced variation patterns [Voolma et al., 2013]. It seems that a higher degree of sulphide mineralization within the GA is associated with the occurrence of silt interbeds. Those interbeds might also contain higher amount of other minor authigenic compounds typical of GA – phosphates (mainly apatite as biogenic detritus and nodules), carbonates (calcite and dolomite as cement and concretions), barite and glauconite. Organic matter, constituting about 15 % to 20 % of the GA, is sapropelic in origin [Pukkonen and Rammo, 1992] and rich in N, S and O. The ratio of C and H in OM is about 9. The concentration of S ranges between 2–6 %, of which 0.6–0.8 % is comprised of organic matter, ca. 0.3 % is sulphatic and the remaining part is sulphitic S [Petersell et al., 1981]. Based on previous geochemical exploration [Pukkonen and Rammo, 1992; Voolma et al., 2013], three geochemical zones have been distinguished in the Estonian GA – the Western, Central and Eastern zones. These zones differ mainly in the concentration of metals, but also in lithology.

Estonian graptolite argillite resources

Most of the geological information on the GA is obtained from basement mapping and exploration projects conducted by the Geological Survey of Estonia, which started in the 1950s. The vast amount of detailed information on the GA lithology and geochemistry was collected when Estonia's phosphorite resources were prospected in the 1980s. The previous estimates of the graptolite argillite reserves in Estonia range from 60 [Petersell, 1997] to 70 billion tons [Veski and Palu, 2003] and little is known about the calculation methods and the initial data (number of drill cores, etc.) that were used. Although practically no new data have been added during the last two decades, the GIS based methods now allow us to obtain better estimates of the total resource and metal distribution [see Hade and Soesoo, submitted]. The combined database of 468 drill cores [Estonian Geological Survey & Estonian Land Board database, see at www.maaamet.ee] has been used as the initial data. The estimated area of the Estonian GA on the mainland and islands is 12,212.64 km^2, with a corresponding volume of 31,919,259,960 m^3 [Hade and Soesoo, submitted]. For instance, Estonian oil shale – kukersite – occupies an area of 2.884 km^2, and its reserves (proven and probable) are about 5 billion tons [Kattai and Lokk, 1998]. In order to calculate the total weight of the GA, the value of the specific gravity (density) is required. It is known [Petersell, 1997] that the density of the graptolite argillite varies to a great degree, mostly between 1,800 and 2,500 kg/m^3. So, assuming an average density of 1,800 kg/m^3, the total mass of GA is about 57.45 billion tons, while in case of 2500 kg/m^3 the mass is 79.80 billion tons. Assuming the average density to be 2100 kg/m^3, the total weight of GA is about 67 billion tons, which is between the earlier estimates of 60 to 70 billion tons.

Metals in Estonian graptolite argillite

The vertical and lateral geochemical heterogeneity in the GA has not been well understood, especially the scale of the heterogeneity and specific distribution pattern of the elements. Recently, a study on vertical geochemical heterogeneity based on two cross sections has shown distinctive differences between the eastern and western part of the GA [Voolma et al., 2013]. The previous geochemical explorations revealed that the studied sequences demonstrate pronounced vertical variations in U, V, Mo, Zn and other element concentrations. The common distinctive feature
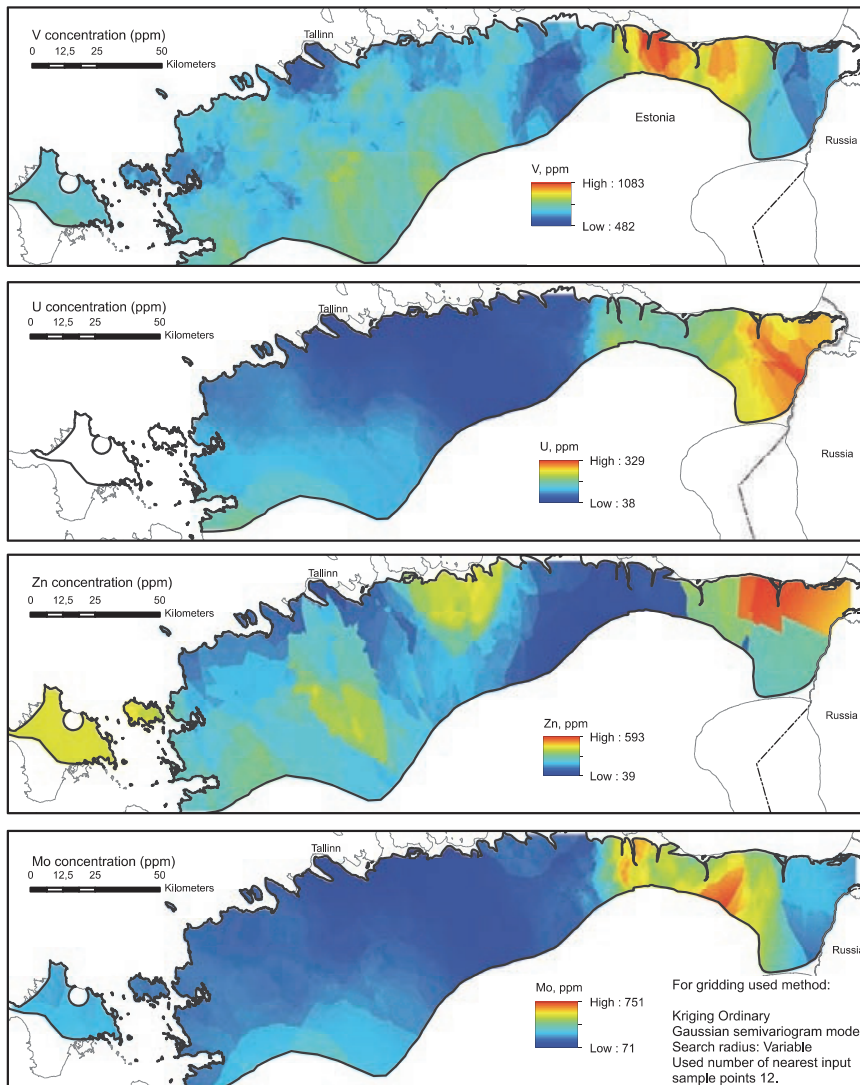
Fig. 2. Vanadium, uranium, zinc and molybdenum concentrations in the Estonian GA (in ppm) as modeled using calculated average drill core analyses. The element concentration surface was modeled with the Ordinary Kriging interpolation method using Gaussian semivariogram model (ESRI ArcInfo). Due to a small number of drill cores, U concentrations were not modeled for the western Estonian islands

of the sections is the occurrence of highest concentrations of the elements in the lower half of the section.

The distribution of U, Zn, Mo and V in the Estonian GA has been modeled and shown in Figure 2. The initial data were selected from the databases of the Geological Survey of Estonia and the Institute of Geology at TUT. These elemental concentration data represent the average concentrations in the GA in the drill core. The

central and western parts of the Eastern Zone show the highest concentrations for V and Mo, whereas V is also high in the southern part of the Eastern and Central Zones. Uranium shows the highest concentrations in the easternmost part of Estonia, while in Western Estonia the concentrations show medium values and the lowest values are characteristic of the Central Zone (Fig. 2). U distribution has not been modeled in the Estonian islands due to the small number of
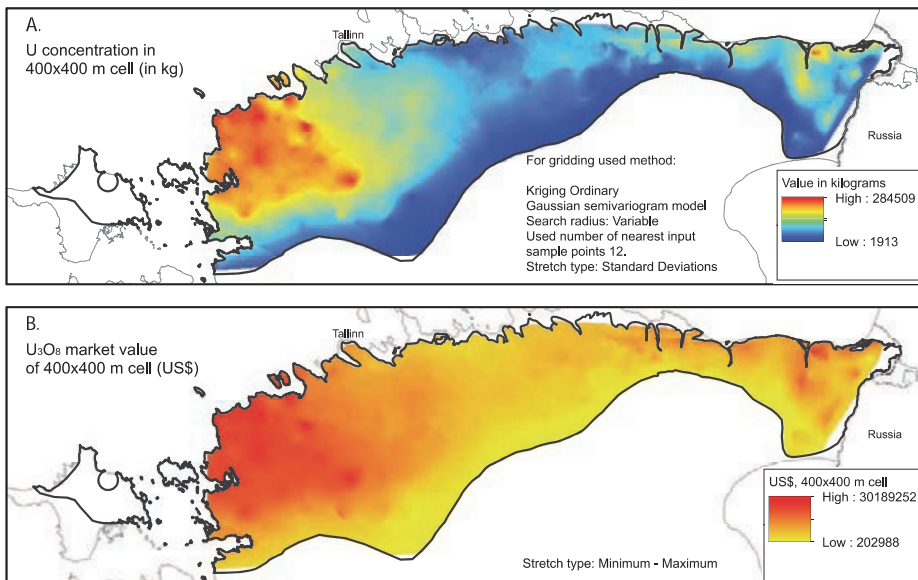
Fig. 3. A. Modeled uranium total concentrations (tonnage) in a cell of 400 m x 400 m at the thickness of the graptolite argillite. The speci c gravity of GA is set at 2100 kg/m^3. Note that the highest total uranium tonnage is observed in Western Estonia (up to 285 ton per cell), while elemental concentrations in ppm are the highest in Eastern Estonia. B. The market value of uranium oxide (U_3O_8) in a cell as calculated at 90 US$ per kilogram

analyses. The high co ncentrations in the southwest corner may be an artifact of the model, since there are only a few drill cores available and those show locally high contents of U. Generally, it can be concluded that the concentration of most of the metals (except Zn) is relatively low in the Central Zone of the GA area.

However, it is important to emphasize that the available chemical data are relatively unevenly distributed across the area and the present geochemical generalization is informative, but must be taken with caution. There is very little data on the southern margin of the GA area, so the concentrations may vary, but due to its limited thickness (less than 0.5 m); the total elemental amounts have not a ected the calculations very much.

With respect to the standard values, such as PAAS and NASC, the Estonian GA is extremely rich in U and V. For example, the average U concentration in the Saka section (267 ppm) is a hundred times higher than the corresponding values for NASC [Voolma et al., 2013]. In case of V, there is a nine-fold difference between the concentrations in NASC and the average concentrations detected, for example, in the Saka section, in Eastern Estonia (1,190 ppm [Voolma et al., 2013]). In general, the U content of GA shows quite a strong positive correlation with the

organic matter content, most likely indicating early fixation via metal-organic complexes. At the same time, no correlation of P_2O_5 with other enriched trace elements, such as U was detected.

As average metal concentrations are very useful in indicating "poor" and "rich" deposits, the total content of a certain element depends on the thickness of the deposit layer. In order to calculate the total amount of the element/metal based on square meters, ESRI ArcGIS software was employed. As an example, the total concentration (tonnage) of uranium in the Estonian GA is shown in Figure 3. This calculation is based: 1) on the element/metal grid which shows the element distribution in ppm (e. g. Fig. 2 for U); 2) on an interpolated grid of the GA thickness, in meters; 3) by assuming the average density of the GA to be 2,100 kg/m^3; 4) since the element/metal and thickness grids were calculated with the cell size of 400 x 400 meters, the same cell size was used for the calculation of the total amount of element/metal.

The results of U tonnage (A) and market values (B) within the cell of 400 m x 400 m (at the thickness of GA in the area) are shown in Figure 3. These calculations allow for the provision of a more realistic total amount for the metal in the Estonian GA (not just based on an average concentration value in ppm). The calculated total

weight of U is about 5.6656 million tons (6.6796 million tons as U_3O_8). Similarly, the calculations for some other elements are provided in the paper by Hade and Soesoo [submitted 05/2013]. Zn is as high as 16.5330 million tons (20.5802 million tons as ZnO) and Mo is 12.7616 million tons (19.1462 million tons as MoO_3). The highest studied element amounts show a somewhat similar pattern – Western Estonia has the highest potential, especially for U and Mo. However, there are also distinctions between those elements. For example, the Central Zone, where the enrichment is the lowest, still shows high amounts of Zn. The market value of these metals is high: about US\$ 460 billion for the uranium, US\$ 30 billion for the zinc and about US\$ 350 billion for the molybdenum, considering the average market prices in April 2013. However, since a simple, environment friendly and economical technology has yet to be developed for the co extraction of most of the enriched elements from GA, its economic value remains theoretical.

Health and environmental impact

Sedimentary, unmetamorphosed black shale has historically been used in Sweden and Estonia. In Sweden, the Cambrian and Lower Ordovician Alum shale has been known for more than 350 years. Mining the shale for alum began in 1630s in Sk ne. The Alum shale was also recognized as a source of fossil energy and, toward the end of the 1800s, attempts were made to extract and refine hydrocarbons [Andersson et al., 1985]. Before and during World War II, Alum shale was retorted for its oil, but production ceased in 1966 owing to the availability of cheaper supplies of crude petroleum. During this period, about 50 million tons of shale were mined at Kinnekulle and Närke in Sweden.

For uranium production, a pilot plant built at Kvarntorp, Sweden, produced more than 62 tons of uranium between 1950 and 1961. A small uranium mill was constructed at Ranstad and went on stream in 1965. The plant operated at reduced capacity for 3 years producing about 300 tons of yellowcake. The Alum shale was also burned with limestone to manufacture "breeze blocks," a lightweight porous building block that was widely used in the Swedish construction industry. Production stopped when it was realized that the blocks were radioactive and emitted unacceptably high amounts of radon.

Just after World War II, due to the atomic bomb "competition", the Soviet Union started looking for uranium deposits. The nearest place where geologists found large quantities of uranium ore (graptolite argillite) was in Northeast Estonia and the first Soviet uranium processing facility was started in a small town called Sillamäe. The plant operated as a top secret Soviet institution until 1991.

In addition, graptolite argillite is also a co product of phosphorite mining in Estonia, so the Maardu area near Tallinn is among the most polluted regions in Estonia [Jüriado et al., 2012]. During the opencast mining of phosphorite, radioactive GA with average uranium content of 50 to 130 ppm, and a maximum of 300–450 ppm, was deposited in waste dumps. It should be mentioned that the phosphorite in Estonia lies directly below the GA. In 1989, opencast mining at Maardu was carried out on more than 6 km^2. The mining and processing was discontinued in 1991. Today, waste hills in Maardu contain about 73 million tons of GA, which contains, with a minimum content of 30 ppm U, totally as much as 2.19 million kg of U [Jüriado et al., 2012]. This waste leaches into the surface water and groundwater.

Under normal weathering conditions GA is easily oxidizing, and spontaneous combustion can occur. In some places, for example at Maardu waste hills, in northern Estonia, the temperatures in the heap occasionally exceeded 500 °C. It is interesting to note that spontaneous combustion can occur in heaps that are a few months or over 20 years old, which leads us to the conclusion that some old heaps can still be dangerous. These processes lead to an annual leaching of 1,500 tons of mineral matter per square kilometer of a waste dump and the waste water being discharged into Lake Maardu. In 1990, at the average temperature of the heap, an estimated 520.3×10^3 tons of oxygen was spent on oxidizing the rocks buried in the heap. The amount of gases emitted from burning shale was estimated as $SO_2 - 10^4$ tons and $CO_2 - 73.3 \times 10^3$ tons [Pihlak, 2009]. The effluent of the Maardu opencast mine and processing plant, which was directed into Muuga Bay (Gulf of Finland) delivered up to 20.18 million m^3 of water with varying levels of polluting elements each year. The amount of dissolved minerals delivered into the sea was estimated at up to 38.4×10^3 tons annually [Pihlak, 2009; Jüriado et al., 2012].

GA, if lying on or near the surface, is also a major source for radon (Rn) in Estonia and elsewhere. Very high radon concentrations of up to 10 000 Bq/m^3 have been recorded at some natural outcrops of GA in the North Estonian Klint. Radon is a highly radioactive and carcinogenic element causing mutations, especially lung cancer.

In spite of the fact that the impact of black shale on a nation's health and biological environment is well recognized, little is being done

to quantify these impacts in a real and reliable way. Moreover, only a small number of measures are being taken to avoid direct contamination of soil and groundwater and direct and indirect influences on the local people. Sometimes, contaminated black shale industrial areas are used as a political instrument in decision making or for someone's commercial interest. In many cases, those decisions bring no real environmental improvement results.

There are areas in Estonia, Sweden and elsewhere in Fennoscandia where black shale forms the surfaces where humans live and conduct their everyday activities, thus directly influencing health and well being. For example, there are a number of towns in northern Estonia which are located in the area where graptolite argillite crops out, including the capital Tallinn, Paldiski, Kunda, Aseri and others. In Sweden, in the focus for the current interest in Alum shale mining is the Östersund area, where people have historically lived on the top of black shale. These influences need to be quantified and measures taken to minimize negative health and environmental impacts. However, as nations depend on mining and metal/electronics industries, the need for new resources cannot be neglected and a balance must be achieved between the nation's sustainable economic development, exploitation of black shale resources and public health. A new, modern, science based revision of black shale resources and related environments across Estonia – NW Russia – Sweden – Finland – Norway would definitely foster a better understanding of the problem, and help to create an industrially and environmentally sound expert model of the Fennoscandian and Baltoscandian black shale potential.

Moving towards a Fennoscandian Baltoscandian Black Shale Database

Creating regional, large scale, across border databases is not uncommon in geology. Geological maps are the best and oldest form of such information compilation, which extend across political borders and continents. An initiative group on the Fennoscandia Metallogenic Map and Database, which involves specialists from the geological surveys and other organizations in Finland, Norway, Russia and Sweden, has been active for more than a decade. The work has resulted in well compiled, cross border database and a digital map (see http://en.gtk.fi/informationservices/databases/fodd/index.html).

The Fennoscandian Ore Deposit Database (FODD) is a comprehensive numerical database that includes the metallic mines, deposits and significant occurrences in Fennoscandian Shield, which could be part of the geological information compilation and standardization, and be very useful for future metal ore discoveries. The first FODD metallogenic map was published in 2009. An updated version will be available in August 2013. This database contains information on about 1,700 (June, 2013) mines, deposits and significant occurrences in Fennoscandia. The map contains 168 major metallogenic areas, of which 46 are completely or partly in Finland, 40 in Norway, 41 in Russia, and 41 in Sweden. The map includes 24 areas that cross international border (http://en.gtk.fi/informationservices). The database and map contain information on the location, mining history, tonnage and commodity grades, with comments on data quality, geological setting, age, ore mineralogy, and types of mineralization, as well as genetic models and the primary sources of data.

This range of information is also important in "mapping" black shale. Our proposal is to compile the geological, geochemical and environmental information into the Fennoscandian Baltoscandian Black Shale Database (FBSD) with browser based visualization possibilities for thematic maps (Fig. 4).

1. The database should include both sedimentary and metamorphosed black shale from the Precambrian and Lower Paleozoic ages. There will be some overlapping with FODD data concerning some Precambrian ores which had formerly been black shale. However, compiling Fennoscandian Precambrian and Paleozoic black shale data according to a common standard may even add some understanding of sulphide ore geology, and especially environmental conditions.

2. The data structure should include: a) location; b) geological setting and structure, body/deposit size; c) age; d) major and trace element geochemistry, calorific values; e) ore mineralogy, style of mineralization; f) tonnage and commodity grades with a comment on data quality; g) genetic models; h) groundwater and surface geology/soil and hydro geological parameters; i) data on biological environment/harmful element assessment; j) infrastructure and population density; k) data source and l) mining history (Fig. 4).

3. The database should have GIS based, easily browserable thematic layers allowing for the assessment of specific impacts as well as metal/element concentrations, additional resource (oil, gas, etc.) potential assessment and more.
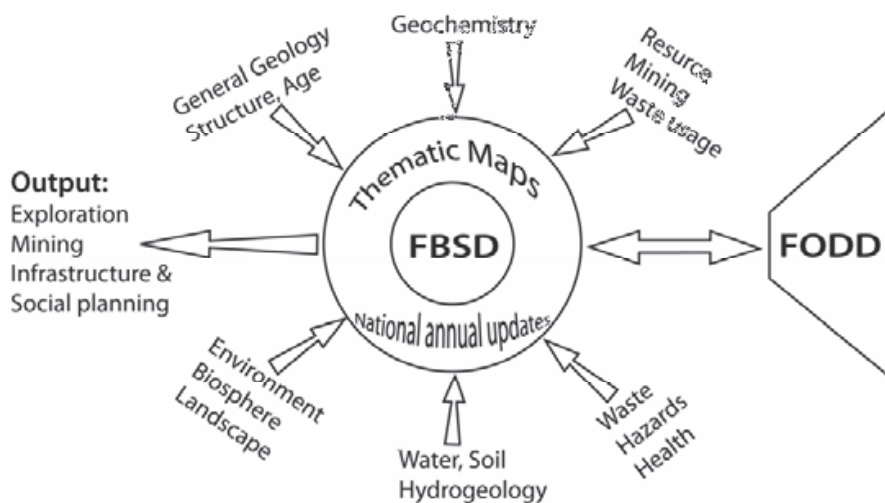
Fig. 4. A possible database (FBSD) structure, inputs and outputs of the Fennoscandian – Baltoscandian black shales database. Tight interaction with the Fennoscandian Ore Deposit Database (FODD) is envisaged

This database can then be used by a number of specialists and officials including mineral explorers and local government decision makers for preparing environmental impact assessments, as well as in infrastructure and social development planning. This information is also very useful for public health monitoring and development.

As far as the mineral resource part is concerned, the European Commission already took steps to improve the long term availability of raw materials through the implementation of the Raw Material Initiative in 2008. The Initiative lists fourteen economically important metals and minerals labeled as critical, that are subject to a higher risk of supply interruption (e.g. REE, PGE, Co, etc.). As some of these metals have been concentrated in black shale, black shale too could be under consideration as a source of some of the EU's critical metals in near future. Thus, the FBSD initiative could fulfill several requirements at the EU and national levels including resource, environment, public health and economy policies.

Conclusions

The occurrence of Middle Cambrian to Late Ordovician organic rich black shale deposits in an extensive area of Baltoscandia has been known for a long time. Alum shale, as well as Estonian graptolite argillite (GA), contain remarkably high concentrations of trace metals such as U, Mo, V and Ni, but may also be locally enriched with REE, Cd, Au, Sb, As and Pt. So do the Precambrian metamorphic analogues of shale in Fennoscandia, some of which are being actively mined. Apart from the commercial interest in ore, there is an environmental aspect related to black shale. Mining in Sweden and Estonia has caused significant damage to the environment. Close or near surface black shale emanates radon; weathering of shale releases harmful elements into the soil and groundwater. Some metamorphosed Precambrian black shale has an environmental impact, even without being mined. Since the Fennoscandian and Baltoscandian black shale provides a large lithological and geochemical variety of shale and meta shale, with different genetic characteristics and metal, sulfur and carbon occurrences, and different environmental aspects, there is need for a new and updated assessment and re evaluation of this resource.

Based on the principal structure of FODD initiative (The Fennoscandian Ore Deposit Database), our proposal is to compile cross border (Norway, Sweden, Finland, Estonia, Russia) geological, geochemical and environmental information on black shale into the Fennoscandian Baltoscandian Black Shale Database (FBSD) with browser based visualization possibilities that enable the creation of thematic maps.

The FBSD database should include both sedimentary and metamorphosed black shale of the Precambrian and Lower Paleozoic age. The data structure should include: a) location; b) geological setting and structure, body/deposit size; c) age; d) major and trace element

geochemistry, calorific values; e) ore mineralogy, style of mineralization; f) tonnage and commodity grades with a comment on data quality; g) genetic models; h) groundwater and surface geology/soil and hydro geological parameters; i) data on biological en vironment/harmful element assessment; j) infrastructure and population density; k) data source; l) mining history. Most importantly, the database should have a GIS based, simple, browser accessed module in order to select information and allow for the visualized assessment of specific parameters (e.g. distribution of element X) and impacts (release of hazardous element Y into soil) as well as social, medical and environmental impact assessments.

Some geological information, as well as thematic maps (black shale thickness and depth, elemental distribution, metal market value and reserve), have been presented using the Estonian graptolite argillite as an example. The total estimated area of Estonian GA on the mainland and islands is about 12,212.64 km^2, with corresponding argillite volume of about 31,919,259,960 m^3. Assuming an average GA density of 2,100 kg/m^3, the total weight of GA is about 67 billion tons. The calculated weight of U$_3$O$_8$ is about 6.6796 million tons; ZnO is 20.5802 million tons; and MoO$_3$ is 19.1462 million tons. The market value of these metals is high: about € 460 billion for the uranium, € 30 billion for the zinc and about € 350 billion for the molybdenum at the average market prices in April 2013. However, since a simple, environment friendly and economical technology has yet to be developed for the co extraction of most of the enriched elements from GA, its economic value remains theoretical.

References

Amstutz G. C., Park W. C. The paragenetic position of sulfides in the diagenetic recrystallization sequence // Soc. Mining Geol. 1971. Japan. Spec. Issue 3. P. 280–282.

Andersson A., Dahlman B., Gee D. G., Snäll S. The Scandinavian Alum Shales // Sveriges Geologiska Undersökning. 1985. Vol. 56. P. 1–50.

Arkimaa A., Hyvöne E., Lerssi J., Loukola Ruskeeniemi K., Vanne J. Compilation of maps of black shales in Finland: Applications for exploration and environmental studies // Ed. S. Autio. Geological Survey of Finland. 1999. Spec. Paper 27. P. 113–116.

Baturin N. G., Ilyin A. V. Comparative Geochemistry of Shell Phosphorites and Dictyonema Shales of the Baltic // Geochemistry International. 2013. Vol. 51, No. 1. P. 27–37.

Erdtmann B. D. The planktonic nema bearing Rhabdinopora flabelliformis versus benthonic root bearing Dictyonema Hall, 1952 // Proc. Acad. Sci. Estonian SSR. 1986. Vol. 35, No. 3. P. 109–114.

Fleischer V. D., Garlick W. G., Haldane R. Geology of the Zambian Copperbelt // Ed. K. H. Wolf. In: Handbook of Stata Bound and Stratiform Ore Deposits. 1976. Vol. 6. Elsevier, Amsterdam. P. 223–352.

Gardner H. D., Hutcheon I. Geochemistry, mineralogy, and geology of the Jason Pb Zn deposits, Macmillan Pass, Yukon, Canada // Economic Geology. 1985. Vol. 80. P. 1257–1276.

Grauch R. I., Coveney R. M. Jr., Murowchick J. B., Nansheng C. Black shales as hosts for unconventional Platinum Group Element resources? Examples from China and Yukon, Canada, and implications for U.S. resources // In: U.S.G.S. Research on Mineral Resources, 1991. Seventh Annual V. E. McKelvey Forum on Mineral and Energy Resources, Reno, Nevada. U.S.G.S. Circular 1062. P. 33.

Gustavson L. B., Williams N. Sediment hosted stratiform deposits of copper, lead, and zinc // Ed. B. J. Skinner. In: Seventy Fifth Anniversary Vol. The Economic Geology Publishing Co. Yale. 1981. P. 139–178.

Hade S., Soesoo A. Estonian graptolite argillites revisited: reserves and future resources // Oil Shale (submitted to Oil Shale, May, 2013)

Henningsmoen G. Cambro Silurian deposits of the Oslo region // Ed. A. Holtedahl. In: Geology of Norway. Norges geologiske undersmkelse. 1960. 208, P. 130–150.

Hofmann B. Erzmineralien in pal ozoischen, mesozoischen und terti ren Sedimenten der Nordschweiz und S dwestdeutschlands // Schweiz. Mineral. Petrogr. Mitt. 1989. 69. P. 345–357.

Jüriado K., Raukas A., Petersell, V. Alum shales causing radon risks on the example of Maardu area, North Estonia // Oil Shale. 2012. Vol. 29, No. 1. P. 76–84.

Jung W., Knitschke G. Kupferschiefer in the German Democratic Republic (GDR) with special reference to the Kupferschiefer deposit in the southeastern Harz foreland // Ed. K. H. Wolf. In: Handbook of Stata Bound and Stratiform Ore Deposits. 1976. Vol. 6. Elsevier, Amsterdam. P. 353–406.

Kattai V., Lokk U. Historical review of the kukersite oil shale exploration in Estonia // Oil Shale. 1998. 15. P. 102–110.

Krauskopf K. B. Sedimentary deposits of rare metals in Economic Geology // Ed. A. M. Bateman. Econ. Geol. 1955. 50th Anniversary. Vol. 1905–1955. P. 411–463.

Lindgreen H., Drits V. A., Sakharov B. A., Salyn A. L., Dainyak L. G. Illite smectite structural changes during diagenesis of Lower Paleozoic black Alum Shales from the Baltic area // American Mineralogist. 2000. Vol. 85, No. 9. P. 1223–1238.

Lippmaa E., Maremäe E. Uranium production from the local Dictyonema shale in North-East Estonia // Oil Shale. 2000. Vol. 17, No. 4. P. 387–394.

Loukola-Ruskeeniemi K., Uutela A., Tenhola M., Paukola T. Environmental impact of metalliferous black shales at Talvivaara in Finland, with indication of lake acidification 9000 years ago // Journal of Geochemical Exploration. 1998. 64. P. 395–407.

Männil R. Evolution of the Baltic basin during the Ordovician // Valgus, Tallinn. 1966. P. 1–200 (in Russian).

Petersell V., Mineyev D., Loog A. Mineralogy and geochemistry of obolus sandstones and dictyonema shale of North Estonia // Acta et Commentationes Universitatis Tartuensis, Tartu. 1981. Vol. 56. P. 30–49 (in Russian).

Petersell V. Dictyonema argillite // Eds. A. Raukas, A. Teedumäe. In: Geology and Mineral Resources of Estonia. Estonian Academy Publishers. Tallinn. 1997. P. 313–326.

Pihlak A.-T. On the history of investigation of self-burning processes and oxygen problems in Estonia // Tallinn, Infotrükk. 2009 [in Estonian, with Russian summary].

Poulsen V. Cambro-Silurian stratigraphy of Bornholm // Meddelelser fra Damk Geologisk Forening. 1966. Vol. 16. P. 117–137.

Pukkonen E., Rammo M. Distribution of Molybdenum and Uranium in the Tremadoc Graptolite Argillite (Dictyonema Shale) of North-Western Estonia // Bulletin of the Geological Survey of Estonia. 1992. Vol. 2, No. 1. P. 3–15.

Soesoo A., Hade S. Metalliferous organic-rich shales of Baltoscandia – a future resource or environmental/ecological problem // Archiv Euro Eco. 2012. Vol. 2. P. 11–14.

Soesoo A., Puura V., Kirs J., Petersell V., Niin M., All T. Outlines of the Precambrian basement of Estonia // Proceedings of the Estonian Academy of Sciences. Geology. 2004. Vol. 53, No. 3. P. 149–164.

Schieber J. The origin and economic potential of sandstone-hosted disseminated Pb-Zn mineralization in pyritic shale horizons of the Mid-Proterozoic Newland Formation, Montana, USA // Mineralium Deposita. 1991. 26. P. 290–297.

Sundblad K., Gee D. G. Occurrence of a uraniferous- vanadiniferous graphitic phyllite in the Kцli Nappes of the Stekenjokk area, central Swedish Caledonides // GFF. 1985. Vol. 106. P. 269–274.

Szymariski B. Osady Tremadoku i Arenigu na obszarze Biatowieiy // Institut Geologiczny, Prace. 1973. Vol. 69. P. 1–92.

Veski R., Palu E. Investigation of Dictyonema oil shale and its natural and artificial transformation products by a vankrevelenogram // Oil Shale. 2003. Vol. 20, No. 3. P. 265–281.

Vine J. D., Tourtelot, E. B. Geohemistry of Black Shale Deposits – A Summary Report // Economic Geology. 1970. Vol. 65. P. 253–272.

Voolma M., Soesoo A., Hade S., Hints R., Kallaste T. Geochemical heterogeneity of the Estonian graptolite argillite // Oil Shale. 2013. Vol. 30. P. 377–401.

Vulimiri M. R., Cheney E. S. Stratiform mineralization and origin of some of the vein deposits, Bunker Hill mine, Coeur d'Alene district, Idaho // Eds. M. L. Silberman, C. W. Field, A. L. Berry. In: Proceedings of the Symposium on Mineral Deposits of the Northwest - 1980. P. 248–260.

Юдович Я. Э., Кетрис М. П. Геохимия черных сланцев. Л.: Наука, 1988. 272 с.

СВЕДЕНИЯ ОБ АВТОРАХ:

Соесоо Алвар
проф. физической геологии,
зав. лаб. природных минеральных материалов
Институт геологии
Таллиннского технологического университета
Таллинн, Эстония
эл. почта: alvar.soesoo@gmail.com
тел.: +3725136994

Хаде Сигрид
научный сотрудник
Институт геологии
Таллиннского технологического университета
Таллинн, Эстония
эл. почта: sigrid.hade@gmail.com
тел.: +3725240219

Soesoo, Alvar
Institute of Geology at TUT
5 Ehitajate tee, Building IVC,
19086 Tallinn, ESTONIA
e-mail: alvar.soesoo@gmail.com
tel.: +3725136994

Hade, Sigrid
Institute of Geology at TUT
5 Ehitajate tee, Building IVC, 19086 Tallinn, Estonia
e-mail: sigrid.hade@gmail.com
tel.: +3725240219

PAPER VI

HADE, S., SOESOO, A. 2014b. Public perception in monitoring environmental conditions using GIS methods. *International Journal of Research in Earth and Environmental Sciences*, **1(3)**, 11 - 16.

PUBLIC PERCEPTION IN MONITORING ENVIRONMENTAL CONDITIONS USING GIS METHODS

Sigrid Hade[a] and Alvar Soesoo[b]

Tallinn University of Technology, Estonia
[a] E-mail: sigrid.hade@gmail.com
[b] E-mail: alvar.soesoo@gmail.com

ABSTRACT

Relationships between people and their environment have been examined in several scientific disciplines as in modern societies sustainable development and clean environmental usage is a key issue to support growing wealth and population numbers. A successful tool which allows matching qualitative and quantitative data with numerically immeasurable opinion of local people is called Public Participation Geographical Information System. We use this tool in Pakri peninsula, Estonia, to show how this method can be used in assessment of landscape changes, environmental pollution and recreational qualities of the area. The Pakri Peninsula was chosen for a pilot study because of its sensitive environment and very complex and ambiguous natural, cultural, military and social history, including major impacts on local landscapes during the two last centuries.

KEYWORDS: GIS methods, environmental protection, public participation, Pakri Peninsula, Estonia

INTRODUCTION

Environmental issues remain in focus of relationship between society and environment at present and in the future. Moreover, in modern societies sustainable development and clean environmental usage is a key issue to support growing wealth and population numbers. This in turn requires much better planning in landscape, natural resource and environment usage and better human population accommodation. The new approach should be able to grasp the relationship between a number of variables as a whole, taking into account the natural, historic, cultural, economic, and social factors, in conjunction with common human needs and environmental policies. A tool which allows matching qualitative and quantitative data with numerically immeasurable opinion of local people is called Public Participation Geographical Information System, or PPGIS (Sieber, 2006).

Relationships between people and their environment have been examined in several scientific disciplines in recent years in which the

concept of land use and better planning has become central. New aspects and research methods are constantly introduced, and an integrated approach which includes examining the interchange between natural, physical, culture-historical and social factors and considers the social implications in environmental planning, has gained popularity (Cosgrove & Daniels, 1988; Jones, 1991; Bender, 1993; Duncan & Ley, 1994; Hirsh & O'Hanlon, 1995; Olwig, 1996; Cinderby, 1999; Granö, 2001; Peil, 2005; Hade et al, 2005; Brown, 2006; Couper & Miller, 2008; Brown & Weber, 2011; Brown, 2012).

The initial idea behind PPGIS was empowerment and inclusion of marginalized populations, who have little voice in the public arena, through geographic technology education and participation. PPGIS uses and produces digital maps, satellite imagery, sketch maps, and many other spatial and visual tools to change geographic involvement and awareness on a local level. With worldwide development of Internet, the Internet-based PPGIS becomes an affordable and accessible GIS tool for public engagement in many key issues

of environmental planning. Here we present a case study about Pakri peninsula, Estonia, to show how PPGIS methods can be used in assessment of landscape changes, environmental pollution and recreational qualities of the area.

PUBLIC PARTICIPATION GEOGRAPHIC INFORMATION SYSTEM METHOD

The term Public Participation Geographical Information System (PPGIS) was conceived in 1996 at the meeting of the National Center for Geographic Information and Analysis (NCGIA) in the United States to describe how GIS technology could support public participation for a variety of applications with the goal of inclusion and empowerment of marginalized populations (Sieber, 2006). Since the 1990s, the range of PPGIS applications has been extensive, ranging from community and neighborhood planning to environmental and natural resource management to mapping traditional ecological knowledge of indigenous people or local society (see Dunn, 2007; Brown, 2005; Sawicki & Peterman, 2002 for a review of PPGIS applications and methods). However, the formal definition of PPGIS remains still nebulous (Tulloch, 2007) with use of the term PPGIS emerging in the United States, Australia and developed country contexts while the term participatory GIS or PGIS emerged from participatory planning approaches in rural areas of developing countries, the result of a spontaneous merger of Participatory Learning and Action (PLA) methods with geographic information technologies (see Rambaldi et al, 2006). PGIS is often used to promote the goals of nongovernmental organizations, grassroots groups, and community-based organizations that may oppose official government policy, especially as pertaining to the rights of indigenous/local peoples and the current distribution of wealth and political power. In contrast, PPGIS may be sanctioned by government agencies, especially in Western democratic countries, as more effective means to engage in public participation and community consultation in land-use planning and decision-making.

The public participation is a vital part of environmental planning. It is not only dealing with deliberate hearings, but also seeking and facilitating public involvement in planning topics and the decision-making process (Goodspeed, 2008). Effective participation is a two-way process that includes sending information out to the publics and getting back their ideas, concerns and thoughts. The resulting "map of public positions, attitudes and wishes" is a good base for democratic and scientifically settled planning activities.

How the method works? Mapping of landscape and environment values, pollution and other spatial attributes can be achieved using a number of different data collection methods: paper maps through mail surveys, electronic maps through the Internet, and structured interviews or facilitated group processes such as workshops. Each approach has its inherent strengths and weaknesses. Even though the paper GIS method is the simplest method for collecting landscape value information from the general public, it may be not the cheapest and fastest. Following the instructions provided with a paper map, participants place sticker dots (or use other markers) on a study area. The respondent's data on the maps are then digitized into a GIS. Structured interviews or facilitated group meetings can be done with either paper or electronic maps, but considerable human effort is required to set up the interviews or meetings. Electronic mapping via the Internet can have the shortest turnaround time but has the disadvantage of requiring prospective participants to have access to both a computer and the Internet. However, the internet questionnaire provides the participants an additional freedom of not disclosing his/her personality. The internet-based study can be implemented and completed using some digital map-based interface and data storing software. The Internet-based PPGIS method provides for rapid development and implementation of the studies at significantly reduced cost compared with a mail or workshop-based approach.

Once the spatial data are collected, the data can be analyzed using a variety of methods. The most useful starting point for analysis is to generate descriptive maps of topics under the questions (landscape values, special place locations, pollution etc.). The maps can be generated for each question/problem with different layers, if needed. The resulting maps can be analyzed by researchers and/or open for discussions by participants and other local society members for future elaborations and adequate decision-making. This is a good way to map the society's response to particular problems before the decisions are made.

The explosion in Internet mapping applications (including Google Maps and Google Earth) and virtual earth models has created an environment that should be favorable to the expansion of PPGIS methods in everyday life. However, the slow adoption of PPGIS methods by government agencies for regional and environmental planning does not appear technological but may reflect a lack of government commitment to public participation and two-directional consultation in general. The general lack of familiarity with PPGIS as a new consultation methodology and concerns with the accuracy and validity of lay knowledge in environmental decision processes serve to reinforce a propensity toward agency inertia.

THE PAKRI PENINSULA CASE STUDY

Pakri Peninsula was chosen for a pilot study because of its sensitive environment and very complex and ambiguous natural, cultural and social history, including major impacts on local landscapes during the two last centuries. Several projects have been launched on the Pakri peninsula in recent years, but there is still lack of reliable and unified understanding how the recent changes affect local perception (Hade et al, 2005).

Pakri peninsula is situated in the northwestern part of the Estonian mainland, Harjumaa County, between the Lahepere and Paldiski Bays of the Baltic Sea. The length of the peninsula is about 12 km, the width is 5 km, and the area in total is ca 35 km². Geologically, Pakri peninsula is a plateau which is bordered by the Ordovician and Cambrian limestone and sandstone outcrops. The highest part of the limestone cliff on the Cape Pakri is about 25 m above the sea level. The relief of the peninsula is flat, with some ice-edge formations, like ridges and moraines. The Quaternary cover is mainly gravel with thickness ranging from some centimeters to some meters. The Pakri peninsula is a colorful example of the northern coast of the North-Estonian Klint with its peculiar landscapes. The peninsula is edged by a klint escarpment, thus being one of the most remarkable klint sections of the entire Baltic Klint (Soesoo & Miidel, 2006). The northwestward rising limestone plateau of the klint peninsula is nearly 25 m high at the northern tip of the peninsula (Cape Pakri) and as high is the bordering escarpment. From west of Paldiski, up to Kersalu in the east (for 18 km in total), the klint

peninsula is bordered by a 2–24-m-high escarpment. Five separate coastal cliffs are differentiated here: Paldiski, Uuga, Pakerort, Leetse and Lahepere.

Historically, the deep and wind-sheltered Paldiski Bay has attracted seafarers already since the times of the Vikings. In the 17th century, the Swedes established a sea fortress. Peter the 1st planned to build a giant military port of Rogerwiek here. Construction of the port started in 1716. Despite the efforts of thousands of convicts, the planned 2-km-long giant facility was not completed and later the completed part was quite soon destroyed by autumn storms. In 1762, Catherine II renamed the sea fortress of Rogerwiek to Baltiiski Port. The precipices and hills preserved from the fortress at the northern edge of the town are popularly known as the Peter's Fortress or Muula Hills. After the town came into the possession of Estonians, it was renamed as Paldiski in 1920. In May 1940, civilians were deported from both the Pakri peninsula and Pakri Islands were to build Soviet military facilities here. In 1941, the area was occupied by the Germans, who burned down the town and the port at their withdrawal in 1944.

In the post-war period, the Pakri peninsula and Paldiski town were the military sites of the Soviet Army. In 1962, Paldiski became a Soviet Navy nuclear submarine training center. Two PWR type nuclear reactors, 70 and 90 MW in output power, were used for training in safe operations of the nuclear Delta and Echo class submarine propulsion systems. With two land-based nuclear reactors, and employing some 16,000 people, it was the largest such facility in the Soviet Union. Because of its military importance, the whole town was closed off with barbed wire until the last Russian warship left in August 1994. Apart from two submarine hull sections, several other pollution-related facilities existed on the site, including liquid waste storage and treatment facilities.

The initial study was carried out in 2003 and followed by second study in 2010. The geographical map based questionnaire was used in both as printed and web-based forms. People living in Paldiski town and on the Pakri peninsula were eligible to fill out the forms. Majority of local population preferred the web-based questionnaire.

After defining anonymously person's sex, education and age, the participant moved to a set of maps where by using the paintbrush tool (in web-based version) or color pencils (in paper version) he or she could give answers to the questions which included the following topics:
Where are located the most polluted areas in the peninsula? Where has the landscape changed most during the last decade in the peninsula? Which places do you prefer in the peninsula for recreational activities/free time?

Separate maps were painted according to person's knowledge and preferences. Then the printed maps were digitised. In the Adobe Flash Web-based interface the coordinates of painted sections were recorded and saved in MySQL backend database in the server with *php* scripts. By digitally summarizing all (answered) maps sheets, the resulting maps showed in colour grades the topical perception of local people (see Fig. 1).

Figure 1 exemplifies the local perception of the question/problem – "Where has the landscape changed most during the last decade in the peninsula?" As seen, the drastic changes happened before year 2000 and in early 2000, while 2010 results show already diminishing impact on the landscape (Fig. 1). This is also true for other environmental changes, including pollution. These results show that the major landscape change and environmental impact was related to the period when Soviet troops abandoned the area. However, the extent of environmental impact during the location of the Soviet military camp on the Pakri peninsula is unknown because the area was closed and no such studies were conducted. Likely, the period of 10 to 15 years is minimum time to get first results on land and environment rehabilitation and, thus, change the perception of local people.

CONCLUSIONS

Environmental issues remain in focus of relationship between society and environment. A new approach is needed to assess all social, ecological, economic and natural variables in community decision-making process. A tool which allows matching qualitative and quantitative data with numerically immeasurable opinion of local people is called Public Participation Geographical Information System, or PPGIS. Pakri peninsula was chosen for a pilot study because of its sensitive

environment and very complex and ambiguous natural, cultural and social history, including major impacts on local landscapes during the two last centuries. The initial study was carried out in 2003 and followed by a second stage in 2010. The geographical map based questionnaire was used in both printed and web-based forms. The results were summarized as colour-graded maps showing perception of local people in environmental pollution, landscape change and recreational domains. This is a suitable way to map the society's response to particular problems before making the local and regional decisions.

REFERENCES

1. **Bender B.** 1993 (Ed.). Landscape: politics and perspectives. - Oxford: Berg Publishers.
2. **Brown, G.** 2012. An empirical evaluation of the spatial accuracy of public participation GIS (PPGIS) data. - Applied Geography 34, 289-294. DOI:10.1016/j.apgeog.2011.12.004
3. **Brown, G., Weber, D.** 2011. Public Participation GIS: A New Method for Use in National Park Planning. - Landscape and Urban Planning, 102(1), 1-15.
4. **Brown, G. 2006.** Mapping Landscape Values and Development Preferences: A Method for Tourism and Residential Development Planning. - International Journal of Tourism Research, 8(2), 101-113.
5. **Brown, G.** 2005. Mapping Spatial Attributes in Survey Research for Natural Resource Management: Methods and Applications. - Society & Natural Resources, 18(1), 1-23.
6. **Cinderby S.** 1999. Geographic Information Systems for Participation: the future
7. of environmental GIS? - International Journal of Environment and Pollution 11(3), 304-31.

8.   **Cosgrove D., Daniels S.** 1988 (Eds.). The iconography of landscape: essays on the symbolic representation, design and use of past environments. - Cambridge: Cambridge University Press.

9.   **Couper M.P., Miller, P.V.** 2008. Web survey medhods introduction. – Public Opinion Quarterly, 72(5), 831-835.

10.   **Duncan J.S., Ley D.** 1993 (Eds.). Place/Culture/Representation. – London, New York: Routledge, 341 p.

11.   **Dunn, C.E.** 2007. Participatory GIS – A People's GIS? - Progress in Human Geography, 31(5), 616–637.

12.   **Goodspeed, R. C.** 2008. Citizen participation and Internet in urban planning (Master's thesis). - Retrieved from http://goodspeedupdate.com/wp-content/uploads/2008/11/goodspeedinternetparticipation.pdf

13.   **Granö O.** 2001. The archipelago coast as a transitional zone between land and open sea – the origins and development of a research tradition grounded in the natural environment. - Publicationes Instituti Geographici Universitatis Turkuensis, 164, 11- 25 (in Finnish).

14.   **Hade, S., Peil, T., Soesoo, A.** 2005. Maastikunägemus geoinfosüsteemi osana /Landscape as a part of geoinformation system/. - Estonian Social Science Online 3: Special Issue of the Estonian Social Science V Annual Conference. http://www.sotsioloogia.ee/esso3/15/sigrid_hade_tiina_peil.htm (in Estonian).

15.   **Hirsh E., O'Hanlon M.** 1995 (Eds.). The anthropology of landscape: perspectives on place and space. - Oxford: Clarendon Press.

16.   **Jones M.** 1991. The elusive reality of landscapes. Concepts and approaches in landscape research. - Norsk Geografisk Tidsskrift, 45, 229-44.

17.   **Olwig K.R.** 1996. Recovering the substantive nature of landscape. - Annals of

18.   the Association of American Geographers, 86(4), 630-53.

19.   **Peil, T.** 2005. Estonian heritage connection: people, past and place: The Pakri Peninsula. - International Journal of Heritage Studies, 11, 57-69.

20.   **Rambaldi G., Kwaku Kyem, A.P., Mbile, P., McCall, M., Weiner, D.** 2006. Participatory Spatial Information Management and Communication in Developing Countries, EJISDC, 25, 1, 1-9.

21.   **Sawicki, D.S., Peterman, D. R.** 2002. Surveying the Extent of PPGIS Practice in the United States. – In: W.J. Craig, T.M. Harris, and D.M. Weiner (Eds.), Community Participation and Geographic Information Systems, London: Taylor & Francis, 17-36.

22.   **Sieber, R.** 2006. Public Participation and Geographic Information Systems: A Literature Review and Framework. - Annals of the American Association of Geographers, 96/3, 491-507.

23.   **Soesoo, A., Miidel, A.** 2006. North Estonian klint. - Tallinn: Geoguide Baltoscandia, 32 p.

24.   **Tulloch, D.** 2007. Public Participation GIS (PPGIS). - In Encyclopedia of Geographic Information Science, SAGE Publications. http://www.sage-ereference.com/geoinfoscience/Article_n165.html
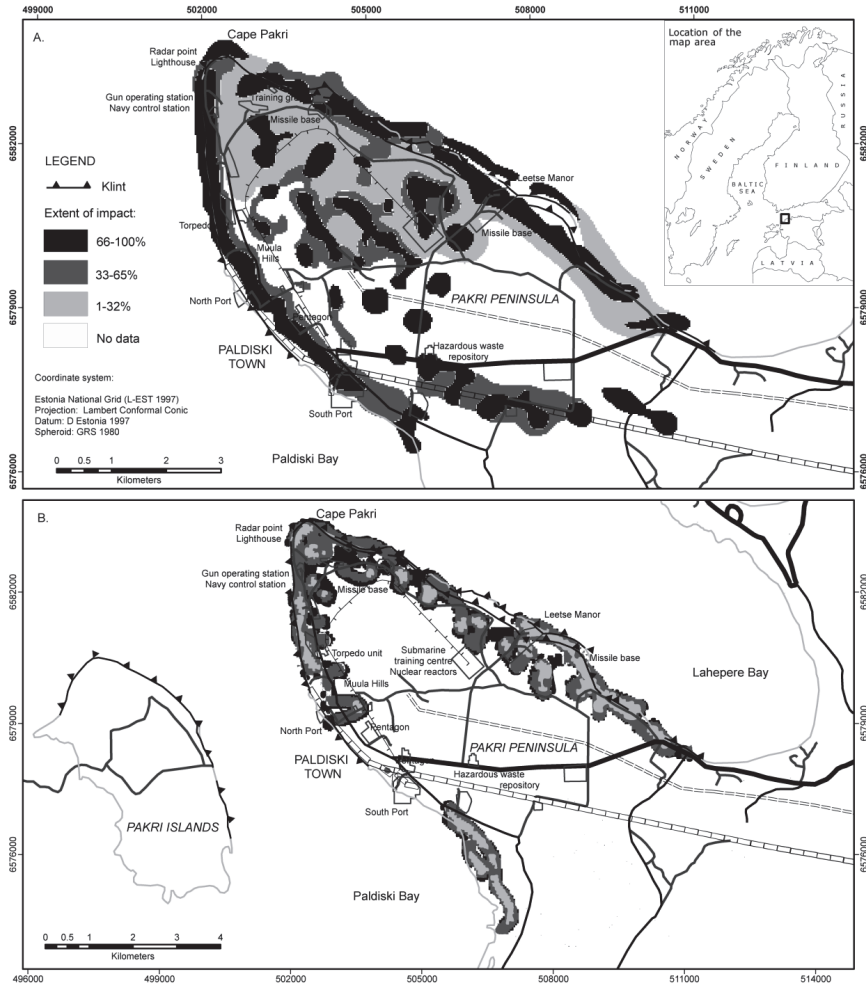
Figure 1. Resulting sketch-map of the public geographical map-based questionnaire showing local people perception to the question "Where has the landscape most changed during the last decade in the peninsula?" The study was conducted in 2003 (A) and repeated in 2010 (B). Previous Soviet military sites are shown (presently not operational).

DISSERTATIONS DEFENDED AT
TALLINN UNIVERSITY OF TECHNOLOGY ON
NATURAL AND EXACT SCIENCES

1. **Olav Kongas**. Nonlinear Dynamics in Modeling Cardiac Arrhytmias. 1998.
2. **Kalju Vanatalu**. Optimization of Processes of Microbial Biosynthesis of Isotopically Labeled Biomolecules and Their Complexes. 1999.
3. **Ahto Buldas**. An Algebraic Approach to the Structure of Graphs. 1999.
4. **Monika Drews**. A Metabolic Study of Insect Cells in Batch and Continuous Culture: Application of Chemostat and Turbidostat to the Production of Recombinant Proteins. 1999.
5. **Eola Valdre**. Endothelial-Specific Regulation of Vessel Formation: Role of Receptor Tyrosine Kinases. 2000.
6. **Kalju Lott**. Doping and Defect Thermodynamic Equilibrium in ZnS. 2000.
7. **Reet Koljak**. Novel Fatty Acid Dioxygenases from the Corals *Plexaura homomalla* and *Gersemia fruticosa.* 2001.
8. **Anne Paju**. Asymmetric oxidation of Prochiral and Racemic Ketones by Using Sharpless Catalyst. 2001.
9. **Marko Vendelin**. Cardiac Mechanoenergetics *in silico*. 2001.
10. **Pearu Peterson**. Multi-Soliton Interactions and the Inverse Problem of Wave Crest. 2001.
11. **Anne Menert**. Microcalorimetry of Anaerobic Digestion. 2001.
12. **Toomas Tiivel**. The Role of the Mitochondrial Outer Membrane in *in vivo* Regulation of Respiration in Normal Heart and Skeletal Muscle Cell. 2002.
13. **Olle Hints**. Ordovician Scolecodonts of Estonia and Neighbouring Areas: Taxonomy, Distribution, Palaeoecology, and Application. 2002.
14. **Jaak Nõlvak**. Chitinozoan Biostratigrapy in the Ordovician of Baltoscandia. 2002.
15. **Liivi Kluge**. On Algebraic Structure of Pre-Operad. 2002.
16. **Jaanus Lass**. Biosignal Interpretation: Study of Cardiac Arrhytmias and Electromagnetic Field Effects on Human Nervous System. 2002.
17. **Janek Peterson**. Synthesis, Structural Characterization and Modification of PAMAM Dendrimers. 2002.
18. **Merike Vaher**. Room Temperature Ionic Liquids as Background Electrolyte Additives in Capillary Electrophoresis. 2002.
19. **Valdek Mikli**. Electron Microscopy and Image Analysis Study of Powdered Hardmetal Materials and Optoelectronic Thin Films. 2003.
20. **Mart Viljus**. The Microstructure and Properties of Fine-Grained Cermets. 2003.
21. **Signe Kask**. Identification and Characterization of Dairy-Related *Lactobacillus.* 2003
22. **Tiiu-Mai Laht**. Influence of Microstructure of the Curd on Enzymatic and Microbiological Processes in Swiss-Type Cheese. 2003.

23. **Anne Kuusksalu**. 2–5A Synthetase in the Marine Sponge *Geodia cydonium*. 2003.

24. **Sergei Bereznev**. Solar Cells Based on Polycristalline Copper-Indium Chalcogenides and Conductive Polymers. 2003.

25. **Kadri Kriis**. Asymmetric Synthesis of C_2-Symmetric Bimorpholines and Their Application as Chiral Ligands in the Transfer Hydrogenation of Aromatic Ketones. 2004.

26. **Jekaterina Reut**. Polypyrrole Coatings on Conducting and Insulating Substracts. 2004.

27. **Sven Nõmm**. Realization and Identification of Discrete-Time Nonlinear Systems. 2004.

28. **Olga Kijatkina**. Deposition of Copper Indium Disulphide Films by Chemical Spray Pyrolysis. 2004.

29. **Gert Tamberg**. On Sampling Operators Defined by Rogosinski, Hann and Blackman Windows. 2004.

30. **Monika Übner**. Interaction of Humic Substances with Metal Cations. 2004.

31. **Kaarel Adamberg**. Growth Characteristics of Non-Starter Lactic Acid Bacteria from Cheese. 2004.

32. **Imre Vallikivi**. Lipase-Catalysed Reactions of Prostaglandins. 2004.

33. **Merike Peld**. Substituted Apatites as Sorbents for Heavy Metals. 2005.

34. **Vitali Syritski**. Study of Synthesis and Redox Switching of Polypyrrole and Poly(3,4-ethylenedioxythiophene) by Using *in-situ* Techniques. 2004.

35. **Lee Põllumaa**. Evaluation of Ecotoxicological Effects Related to Oil Shale Industry. 2004.

36. **Riina Aav**. Synthesis of 9,11-Secosterols Intermediates. 2005.

37. **Andres Braunbrück**. Wave Interaction in Weakly Inhomogeneous Materials. 2005.

38. **Robert Kitt**. Generalised Scale-Invariance in Financial Time Series. 2005.

39. **Juss Pavelson**. Mesoscale Physical Processes and the Related Impact on the Summer Nutrient Fields and Phytoplankton Blooms in the Western Gulf of Finland. 2005.

40. **Olari Ilison**. Solitons and Solitary Waves in Media with Higher Order Dispersive and Nonlinear Effects. 2005.

41. **Maksim Säkki**. Intermittency and Long-Range Structurization of Heart Rate. 2005.

42. **Enli Kiipli**. Modelling Seawater Chemistry of the East Baltic Basin in the Late Ordovician–Early Silurian. 2005.

43. **Igor Golovtsov**. Modification of Conductive Properties and Processability of Polyparaphenylene, Polypyrrole and polyaniline. 2005.

44. **Katrin Laos**. Interaction Between Furcellaran and the Globular Proteins (Bovine Serum Albumin β-Lactoglobulin). 2005.

45. **Arvo Mere**. Structural and Electrical Properties of Spray Deposited Copper Indium Disulphide Films for Solar Cells. 2006.

46. **Sille Ehala**. Development and Application of Various On- and Off-Line Analytical Methods for the Analysis of Bioactive Compounds. 2006.

47. **Maria Kulp**. Capillary Electrophoretic Monitoring of Biochemical Reaction Kinetics. 2006.

48. **Anu Aaspõllu.** Proteinases from *Vipera lebetina* Snake Venom Affecting Hemostasis. 2006.

49. **Lyudmila Chekulayeva**. Photosensitized Inactivation of Tumor Cells by Porphyrins and Chlorins. 2006.

50. **Merle Uudsemaa**. Quantum-Chemical Modeling of Solvated First Row Transition Metal Ions. 2006.

51. **Tagli Pitsi**. Nutrition Situation of Pre-School Children in Estonia from 1995 to 2004. 2006.

52. **Angela Ivask**. Luminescent Recombinant Sensor Bacteria for the Analysis of Bioavailable Heavy Metals. 2006.

53. **Tiina Lõugas**. Study on Physico-Chemical Properties and Some Bioactive Compounds of Sea Buckthorn (*Hippophae rhamnoides* L.). 2006.

54. **Kaja Kasemets**. Effect of Changing Environmental Conditions on the Fermentative Growth of *Saccharomyces cerevisae* S288C: Auxo-accelerostat Study. 2006.

55. **Ildar Nisamedtinov**. Application of ^{13}C and Fluorescence Labeling in Metabolic Studies of *Saccharomyces* spp. 2006.

56. **Alar Leibak**. On Additive Generalisation of Voronoï's Theory of Perfect Forms over Algebraic Number Fields. 2006.

57. **Andri Jagomägi**. Photoluminescence of Chalcopyrite Tellurides. 2006.

58. **Tõnu Martma**. Application of Carbon Isotopes to the Study of the Ordovician and Silurian of the Baltic. 2006.

59. **Marit Kauk**. Chemical Composition of $CuInSe_2$ Monograin Powders for Solar Cell Application. 2006.

60. **Julia Kois**. Electrochemical Deposition of $CuInSe_2$ Thin Films for Photovoltaic Applications. 2006.

61. **Ilona Oja Açik**. Sol-Gel Deposition of Titanium Dioxide Films. 2007.

62. **Tiia Anmann**. Integrated and Organized Cellular Bioenergetic Systems in Heart and Brain. 2007.

63. **Katrin Trummal**. Purification, Characterization and Specificity Studies of Metalloproteinases from *Vipera lebetina* Snake Venom. 2007.

64. **Gennadi Lessin**. Biochemical Definition of Coastal Zone Using Numerical Modeling and Measurement Data. 2007.

65. **Enno Pais**. Inverse problems to determine non-homogeneous degenerate memory kernels in heat flow. 2007.

66. **Maria Borissova**. Capillary Electrophoresis on Alkylimidazolium Salts. 2007.

67. **Karin Valmsen**. Prostaglandin Synthesis in the Coral *Plexaura homomalla*: Control of Prostaglandin Stereochemistry at Carbon 15 by Cyclooxygenases. 2007.

68. **Kristjan Piirimäe**. Long-Term Changes of Nutrient Fluxes in the Drainage Basin of the Gulf of Finland – Application of the PolFlow Model. 2007.

69. **Tatjana Dedova**. Chemical Spray Pyrolysis Deposition of Zinc Sulfide Thin Films and Zinc Oxide Nanostructured Layers. 2007.

70. **Katrin Tomson**. Production of Labelled Recombinant Proteins in Fed-Batch Systems in *Escherichia coli*. 2007.

71. **Cecilia Sarmiento**. Suppressors of RNA Silencing in Plants. 2008.

72. **Vilja Mardla**. Inhibition of Platelet Aggregation with Combination of Antiplatelet Agents. 2008.

73. **Maie Bachmann**. Effect of Modulated Microwave Radiation on Human Resting Electroencephalographic Signal. 2008.

74. **Dan Hüvonen**. Terahertz Spectroscopy of Low-Dimensional Spin Systems. 2008.

75. **Ly Villo**. Stereoselective Chemoenzymatic Synthesis of Deoxy Sugar Esters Involving *Candida antarctica* Lipase B. 2008.

76. **Johan Anton**. Technology of Integrated Photoelasticity for Residual Stress Measurement in Glass Articles of Axisymmetric Shape. 2008.

77. **Olga Volobujeva**. SEM Study of Selenization of Different Thin Metallic Films. 2008.

78. **Artur Jõgi**. Synthesis of 4'-Substituted 2,3'-dideoxynucleoside Analogues. 2008.

79. **Mario Kadastik**. Doubly Charged Higgs Boson Decays and Implications on Neutrino Physics. 2008.

80. **Fernando Pérez-Caballero**. Carbon Aerogels from 5-Methylresorcinol-Formaldehyde Gels. 2008.

81. **Sirje Vaask**. The Comparability, Reproducibility and Validity of Estonian Food Consumption Surveys. 2008.

82. **Anna Menaker**. Electrosynthesized Conducting Polymers, Polypyrrole and Poly(3,4-ethylenedioxythiophene), for Molecular Imprinting. 2009.

83. **Lauri Ilison**. Solitons and Solitary Waves in Hierarchical Korteweg-de Vries Type Systems. 2009.

84. **Kaia Ernits**. Study of In_2S_3 and ZnS Thin Films Deposited by Ultrasonic Spray Pyrolysis and Chemical Deposition. 2009.

85. **Veljo Sinivee**. Portable Spectrometer for Ionizing Radiation "Gammamapper". 2009.

86. **Jüri Virkepu**. On Lagrange Formalism for Lie Theory and Operadic Harmonic Oscillator in Low Dimensions. 2009.

87. **Marko Piirsoo**. Deciphering Molecular Basis of Schwann Cell Development. 2009.

88. **Kati Helmja**. Determination of Phenolic Compounds and Their Antioxidative Capability in Plant Extracts. 2010.

89. **Merike Sõmera**. Sobemoviruses: Genomic Organization, Potential for Recombination and Necessity of P1 in Systemic Infection. 2010.

90. **Kristjan Laes**. Preparation and Impedance Spectroscopy of Hybrid Structures Based on $CuIn_3Se_5$ Photoabsorber. 2010.

91. **Kristin Lippur**. Asymmetric Synthesis of 2,2'-Bimorpholine and its 5,5'-Substituted Derivatives. 2010.

92. **Merike Luman**. Dialysis Dose and Nutrition Assessment by an Optical Method. 2010.

93. **Mihhail Berezovski**. Numerical Simulation of Wave Propagation in Heterogeneous and Microstructured Materials. 2010.

94. **Tamara Aid-Pavlidis**. Structure and Regulation of BDNF Gene. 2010.

95. **Olga Bragina**. The Role of Sonic Hedgehog Pathway in Neuro- and Tumorigenesis. 2010.

96. **Merle Randrüüt**. Wave Propagation in Microstructured Solids: Solitary and Periodic Waves. 2010.

97. **Marju Laars**. Asymmetric Organocatalytic Michael and Aldol Reactions Mediated by Cyclic Amines. 2010.

98. **Maarja Grossberg**. Optical Properties of Multinary Semiconductor Compounds for Photovoltaic Applications. 2010.

99. **Alla Maloverjan**. Vertebrate Homologues of Drosophila Fused Kinase and Their Role in Sonic Hedgehog Signalling Pathway. 2010.

100. **Priit Pruunsild**. Neuronal Activity-Dependent Transcription Factors and Regulation of Human *BDNF* Gene. 2010.

101. **Tatjana Knjazeva**. New Approaches in Capillary Electrophoresis for Separation and Study of Proteins. 2011.

102. **Atanas Katerski**. Chemical Composition of Sprayed Copper Indium Disulfide Films for Nanostructured Solar Cells. 2011.

103. **Kristi Timmo.** Formation of Properties of $CuInSe_2$ and $Cu_2ZnSn(S,Se)_4$ Monograin Powders Synthesized in Molten KI. 2011.

104. **Kert Tamm**. Wave Propagation and Interaction in Mindlin-Type Microstructured Solids: Numerical Simulation. 2011.

105. **Adrian Popp**. Ordovician Proetid Trilobites in Baltoscandia and Germany. 2011.

106. **Ove Pärn**. Sea Ice Deformation Events in the Gulf of Finland and This Impact on Shipping. 2011.

107. **Germo Väli**. Numerical Experiments on Matter Transport in the Baltic Sea. 2011.

108. **Andrus Seiman**. Point-of-Care Analyser Based on Capillary Electrophoresis. 2011.

109. **Olga Katargina**. Tick-Borne Pathogens Circulating in Estonia (Tick-Borne Encephalitis Virus, *Anaplasma phagocytophilum*, *Babesia* Species): Their Prevalence and Genetic Characterization. 2011.

110. **Ingrid Sumeri**. The Study of Probiotic Bacteria in Human Gastrointestinal Tract Simulator. 2011.

111. **Kairit Zovo**. Functional Characterization of Cellular Copper Proteome. 2011.

112. **Natalja Makarytsheva**. Analysis of Organic Species in Sediments and Soil by High Performance Separation Methods. 2011.

113. **Monika Mortimer**. Evaluation of the Biological Effects of Engineered Nanoparticles on Unicellular Pro- and Eukaryotic Organisms. 2011.

114. **Kersti Tepp**. Molecular System Bioenergetics of Cardiac Cells: Quantitative Analysis of Structure-Function Relationship. 2011.

115. **Anna-Liisa Peikolainen**. Organic Aerogels Based on 5-Methylresorcinol. 2011.

116. **Leeli Amon**. Palaeoecological Reconstruction of Late-Glacial Vegetation Dynamics in Eastern Baltic Area: A View Based on Plant Macrofossil Analysis. 2011.

117. **Tanel Peets**. Dispersion Analysis of Wave Motion in Microstructured Solids. 2011.

118. **Liina Kaupmees**. Selenization of Molybdenum as Contact Material in Solar Cells. 2011.

119. **Allan Olspert**. Properties of VPg and Coat Protein of Sobemoviruses. 2011.

120. **Kadri Koppel**. Food Category Appraisal Using Sensory Methods. 2011.

121. **Jelena Gorbatšova**. Development of Methods for CE Analysis of Plant Phenolics and Vitamins. 2011.

122. **Karin Viipsi**. Impact of EDTA and Humic Substances on the Removal of Cd and Zn from Aqueous Solutions by Apatite. 2012.

123. **David Schryer**. Metabolic Flux Analysis of Compartmentalized Systems Using Dynamic Isotopologue Modeling. 2012.

124. **Ardo Illaste**. Analysis of Molecular Movements in Cardiac Myocytes. 2012.

125. **Indrek Reile**. 3-Alkylcyclopentane-1,2-Diones in Asymmetric Oxidation and Alkylation Reactions. 2012.

126. **Tatjana Tamberg**. Some Classes of Finite 2-Groups and Their Endomorphism Semigroups. 2012.

127. **Taavi Liblik**. Variability of Thermohaline Structure in the Gulf of Finland in Summer. 2012.

128. **Priidik Lagemaa**. Operational Forecasting in Estonian Marine Waters. 2012.

129. **Andrei Errapart**. Photoelastic Tomography in Linear and Non-linear Approximation. 2012.

130. **Külliki Krabbi**. Biochemical Diagnosis of Classical Galactosemia and Mucopolysaccharidoses in Estonia. 2012.

131. **Kristel Kaseleht**. Identification of Aroma Compounds in Food using SPME-GC/MS and GC-Olfactometry. 2012.

132. **Kristel Kodar**. Immunoglobulin G Glycosylation Profiling in Patients with Gastric Cancer. 2012.

133. **Kai Rosin**. Solar Radiation and Wind as Agents of the Formation of the Radiation Regime in Water Bodies. 2012.

134. **Ann Tiiman**. Interactions of Alzheimer's Amyloid-Beta Peptides with Zn(II) and Cu(II) Ions. 2012.

135. **Olga Gavrilova**. Application and Elaboration of Accounting Approaches for Sustainable Development. 2012.

136. **Olesja Bondarenko**. Development of Bacterial Biosensors and Human Stem Cell-Based *In Vitro* Assays for the Toxicological Profiling of Synthetic Nanoparticles. 2012.

137. **Katri Muska**. Study of Composition and Thermal Treatments of Quaternary Compounds for Monograin Layer Solar Cells. 2012.

138. **Ranno Nahku**. Validation of Critical Factors for the Quantitative Characterization of Bacterial Physiology in Accelerostat Cultures. 2012.

139. **Petri-Jaan Lahtvee**. Quantitative Omics-level Analysis of Growth Rate Dependent Energy Metabolism in *Lactococcus lactis*. 2012.

140. **Kerti Orumets**. Molecular Mechanisms Controlling Intracellular Glutathione Levels in Baker's Yeast *Saccharomyces cerevisiae* and its Random Mutagenized Gluthatione Over-Accumulating Isolate. 2012.

141. **Loreida Timberg**. Spice-Cured Sprats Ripening, Sensory Parameters Development, and Quality Indicators. 2012.

142. **Anna Mihhalevski**. Rye Sourdough Fermentation and Bread Stability. 2012.

143. **Liisa Arike**. Quantitative Proteomics of *Escherichia coli*: From Relative to Absolute Scale. 2012.

144. **Kairi Otto**. Deposition of In_2S_3 Thin Films by Chemical Spray Pyrolysis. 2012.

145. **Mari Sepp**. Functions of the Basic Helix-Loop-Helix Transcription Factor TCF4 in Health and Disease. 2012.

146. **Anna Suhhova**. Detection of the Effect of Weak Stressors on Human Resting Electroencephalographic Signal. 2012.

147. **Aram Kazarjan**. Development and Production of Extruded Food and Feed Products Containing Probiotic Microorganisms. 2012.

148. **Rivo Uiboupin**. Application of Remote Sensing Methods for the Investigation of Spatio-Temporal Variability of Sea Surface Temperature and Chlorophyll Fields in the Gulf of Finland. 2013.

149. **Tiina Kriščiunaite**. A Study of Milk Coagulability. 2013.

150. **Tuuli Levandi**. Comparative Study of Cereal Varieties by Analytical Separation Methods and Chemometrics. 2013.

151. **Natalja Kabanova**. Development of a Microcalorimetric Method for the Study of Fermentation Processes. 2013.

152. **Himani Khanduri**. Magnetic Properties of Functional Oxides. 2013.

153. **Julia Smirnova**. Investigation of Properties and Reaction Mechanisms of Redox-Active Proteins by ESI MS. 2013.

154. **Mervi Sepp**. Estimation of Diffusion Restrictions in Cardiomyocytes Using Kinetic Measurements. 2013.

155. **Kersti Jääger**. Differentiation and Heterogeneity of Mesenchymal Stem Cells. 2013.

156. **Victor Alari**. Multi-Scale Wind Wave Modeling in the Baltic Sea. 2013.

157. **Taavi Päll**. Studies of CD44 Hyaluronan Binding Domain as Novel Angiogenesis Inhibitor. 2013.

158. **Allan Niidu**. Synthesis of Cyclopentane and Tetrahydrofuran Derivatives. 2013.

159. **Julia Geller**. Detection and Genetic Characterization of *Borrelia* Species Circulating in Tick Population in Estonia. 2013.

160. **Irina Stulova**. The Effects of Milk Composition and Treatment on the Growth of Lactic Acid Bacteria. 2013.

161. **Jana Holmar**. Optical Method for Uric Acid Removal Assessment During Dialysis. 2013.

162. **Kerti Ausmees**. Synthesis of Heterobicyclo[3.2.0]heptane Derivatives *via* Multicomponent Cascade Reaction. 2013.

163. **Minna Varikmaa**. Structural and Functional Studies of Mitochondrial Respiration Regulation in Muscle Cells. 2013.

164. **Indrek Koppel**. Transcriptional Mechanisms of BDNF Gene Regulation. 2014.

165. **Kristjan Pilt**. Optical Pulse Wave Signal Analysis for Determination of Early Arterial Ageing in Diabetic Patients. 2014.

166. **Andres Anier**. Estimation of the Complexity of the Electroencephalogram for Brain Monitoring in Intensive Care. 2014.

167. **Toivo Kallaste**. Pyroclastic Sanidine in the Lower Palaeozoic Bentonites – A Tool for Regional Geological Correlations. 2014.

168. **Erki Kärber**. Properties of ZnO-nanorod/In_2S_3/$CuInS_2$ Solar Cell and the Constituent Layers Deposited by Chemical Spray Method. 2014.

169. **Julia Lehner**. Formation of Cu_2ZnSnS_4 and $Cu_2ZnSnSe_4$ by Chalcogenisation of Electrochemically Deposited Precursor Layers. 2014.

170. **Peep Pitk**. Protein- and Lipid-rich Solid Slaughterhouse Waste Anaerobic Co-digestion: Resource Analysis and Process Optimization. 2014.

171. **Kaspar Valgepea**. Absolute Quantitative Multi-omics Characterization of Specific Growth Rate-dependent Metabolism of *Escherichia coli*. 2014.